BAŞKENT UNIVERSITY
INSTITUTE OF SCIENCE
DEPARTMENT OF MOLECULAR BIOLOGY AND GENETICS
MASTER OF SCIENCE IN
MOLECULAR BIOLOGY AND GENETICS

DEVELOPMENT OF A SECOND-GENERATION MULTIEPITOPE HOMOLOGOUS VIRUS-LIKE PARTICLE (VLP)-BASED VACCINE CANDIDATE AGAINST SARS-CoV-2 ON A PLANT PLATFORM

BY

HALİS BATUHAN ÜNAL

MASTER OF SCIENCE THESIS

ANKARA – 2024

BAŞKENT UNIVERSITY
INSTITUTE OF SCIENCE
DEPARTMENT OF MOLECULAR BIOLOGY AND GENETICS
MASTER OF SCIENCE IN
MOLECULAR BIOLOGY AND GENETICS

DEVELOPMENT OF A SECOND-GENERATION MULTIEPITOPE HOMOLOGOUS VIRUS-LIKE PARTICLE (VLP)-BASED VACCINE CANDIDATE AGAINST SARS-CoV-2 ON A PLANT PLATFORM

BY

HALİS BATUHAN ÜNAL

MASTER OF SCIENCE THESIS

ADVISOR

ASSOC. PROF. DR. CEYHUN KAYIHAN

ANKARA – 2024

BAŞKENT UNIVERSITY
INSTITUTE OF SCIENCE

This study, which was prepared by Halis Batuhan Ünal, for the program of Master of Science with Thesis (English), has been approved in partial fulfillment of the requirements for the degree of Master of Science in Molecular Biology and Genetics Department by the following committee.

Date of Thesis Defense: 19/07/2024

Thesis Title: Development of a Second-Generation Multiepitope Homologous Virus-Like Particle (VLP)-Based Vaccine Candidate Against SARS-CoV-2 on a Plant Platform

Examining Committee Members	**Signature**
Prof. Dr. Aykut ÖZKUL, Ankara University	……
Prof. Dr. Füsun EYİDOĞAN, Başkent University	……
Assoc. Prof. Dr. Ceyhun KAYIHAN, Başkent University	……
Asst. Prof. Dr. Emre AKSOY, Middle East Technical University	……
Asst. Prof. Dr. Doğa Selin KAYIHAN, Başkent University	……

APPROVAL

Prof. Dr. Dilek ÇÖKELİLER SERDAROĞLU
Director, Institute of Science
Date : … / … / ……

BAŞKENT UNIVERSITY
INSTITUTE OF SCIENCE
YÜKSEK LİSANS TEZ ÇALIŞMASI ORİJİNALLİK RAPORU

Date: 19/08/2024

Öğrencinin Adı, Soyadı: Halis Batuhan ÜNAL

Öğrencinin Numarası: 22110086

Anabilim Dalı: Moleküler Biyoloji ve Genetik Anabilim Dalı

Programı: Moleküler Biyoloji ve Genetik Tezli Yüksek Lisans (İngilizce)

Danışmanın Unvanı/Adı, Soyadı: Doç. Dr. Ceyhun KAYIHAN

Yardımcı Danışmanın Unvanı/Adı, Soyadı: Dr. Öğr. Üyesi Doğa Selin KAYIHAN

Tez Başlığı: Development of a second-generation multiepitope homologous virus-like particle (VLP)-based vaccine candidate against SARS-CoV-2 on a plant platform

Yukarıda başlığı belirtilen Yüksek Lisans tez çalışmamın; Giriş, Ana Bölümler ve Sonuç Bölümünden oluşan, toplam 163 sayfalık kısmına ilişkin, 19/08/2024 tarihinde şahsım/tez danışmanım tarafından Turnitin adlı intihal tespit programından aşağıda belirtilen filtrelemeler uygulanarak alınmış olan orijinallik raporuna göre, tezimin benzerlik oranı %18'dur. Uygulanan filtrelemeler:

1. Kaynakça hariç

2. Alıntılar hariç

3. Beş (5) kelimeden daha az örtüşme içeren metin kısımları hariç

"Başkent Üniversitesi Enstitüleri Tez Çalışması Orijinallik Raporu Alınması ve Kullanılması Usul ve Esaslarını" inceledim ve bu uygulama esaslarında belirtilen azami benzerlik oranlarına tez çalışmamın herhangi bir intihal içermediğini; aksinin tespit edileceği muhtemel durumda doğabilecek her türlü hukuki sorumluluğu kabul ettiğimi ve yukarıda vermiş olduğum bilgilerin doğru olduğunu beyan ederim.

Öğrenci İmzası: …….

ONAY

Öğrenci Danışmanı

Assoc. Prof. Dr. Ceyhun KAYIHAN

Tarih: … / … / 20…

……..

To my lovely family and friends…

ACKNOWLEDGEMENTS

First of all, I would like to express my deepest gratitude to my supervisor Assoc. Prof. Dr. Ceyhun Kayıhan, who has helped me to take the most important steps to become a researcher since my undergraduate life and who has never withheld his support and guidance in this thesis. I would also like to express my endless gratitude to my co-supervisor Asst. Prof. Dr. Doğa Selin Kayıhan, who enabled me to take part in this project and informed me at every point of this project and did not withhold her support.

I would like to express my gratitude to Prof. Dr. Aykut Özkul from Ankara University, Faculty of Veterinary Medicine, Department of Virology for his consultancy and great contributions. I would also like to thank Dr. Alireza Hanifehnezhad for his participation and vast knowledge and Dr. Sıdıka Öztop for her valuable comments on the experimental parts.

I would like to thank Asst. Prof. Dr. Emre Aksoy from Middle East Technical University for his technical and practical support.

I would like to express my thanks to all my Başkent MBG professors (Prof. Dr. Füsun Eyidoğan, Assoc. Prof. Dr. Cem Erdoğan, Asst. Prof. Dr. Özge Erdemli, Asst. Prof. Dr. Çiğdem Akın Pekşen, Asst. Prof. Dr. Beyza Gökçınar Marpuç, Asst. Prof. Dr. Özge Akbulut Çalışkan and Asst. Prof. Dr. Aliye Ezgi Güleç Taşkıran, Dr. F. Şeyma Gökdemir) and research assistants (Zeynep Kavasoğlu, Berfin Doğa Koçkaya, Dilara Özden and Tuğçe Er), especially Prof. Dr. Özlem Darcansoy İşeri, the head of Department of Molecular Biology and Genetics, for their support from my undergraduate life to the end of my master's degree. And I would like to thank department secretary Esra Zeynep Bağcekoz for all her support.

I would like to thank my lab mate Oğuzhan Yaprak, who has been with me at every stage of my thesis from the beginning to the end, and who has never withheld his support. I would like to thank Neslihan Yaşar, Sedef Karagöz, Hikmet Yılmaz, Nihan Yurtseven, Buğra Can, and Oğuz Kaan Yaşar for their friendship and help in this study.

I would like to thank Buse Aydın and Öykü Irmak Dikkatli for their friendship and practical solution suggestions. Also, Efe Mıhçı, Buse Ceyda Öncel, Ece Odabaşı, Aslı Kürekçi, Yasemin Pazarçeviren, Yunus Emre Cavlak, Işıl Özdemir and Simay Pulak for their friendship and technical support.

I would like to thank our special project students Zeynep Can, Selen Dinge, Şevval İnan (TÜBİTAK STAR scholarship recipients), Erenay Aşık (TÜBİTAK STAR scholarship recipients), Güneş Davran, Duru Hayat Kılınçkaya and Rana Itır Onuş.

I would like to express my deepest gratitude to my family members, my grandfather Cemalettin Kocabaş, my grandmother Fatma Kocabaş, my mother Dilek Kocabaş, who have given me moral support and encouragement throughout my life. I am also grateful to my father Savaş Ünal for his support.

Finally, I would like to thank my colleague and girlfriend Ayşenur İnceyol for her endless support.

I would also like to thank TÜBİTAK for the BİDEB Scientist Support Scholarship.

ABSTRACT

Halis Batuhan ÜNAL

DEVELOPMENT OF A SECOND-GENERATION MULTIEPITOPE HOMOLOGOUS VIRUS LIKE PARTICLE (VLP)-BASED VACCINE CANDIDATE AGAINST SARS-CoV-2 ON A PLANT PLATFORM

Başkent University Graduate School of Natural and Applied Science
Department of Molecular Biology and Genetics
2024

The severe impact of the coronavirus disease 2019 (COVID-19) pandemic caused by severe acute respiratory syndrome coronavirus 2 (SARS-CoV-2) has been mitigated using a wide range of vaccines worldwide. However, the equitable distribution of COVID-19 vaccines remains challenging, particularly in developing and underdeveloped countries. Despite the great efforts to date in both the production and administration of COVID-19 vaccines against SARS-CoV-2, developing an accessible vaccine that can cross-neutralize emerging variants remains important. Therefore, in this thesis, we aimed to produce a virus-like particle (VLP)-based vaccine candidate containing all the structural proteins of SARS-CoV-2 in plant platform, as a cost-effective and fast expression system, that may exhibit a broad range of antigenicity with the highest similarity to the structure of SARS-CoV-2, and thus may protect against emerging variants.

Firstly, expression cassettes were designed for the genes encoding the structural proteins [spike (S), membrane (M), nucleocapsid (N), and envelope (E)] of SARS-CoV-2. To investigate the effect of cellular compartmentalization (endoplasmic reticulum; ER and chloroplast; chl) on the level of the expression products, different signal sequences were added. Following codon optimization, the gene cassettes were commercially synthesized. The gene cassettes were successfully cloned individually into a plant expression vector, pEAQ-HT. Each plasmid carrying the gene of interest (GOI) was transformed into *Agrobacterium tumefaciens* by electroporation. The leaves of approximately four-week-old *Nicotiana benthamiana* plants were co-infiltrated with *Agrobacterium tumefaciens* cells carrying these plasmids. As a control, leaves were infiltrated in parallel with pEAQ-HT-GFP containing *Agrobacterium* cells and visualized under ultraviolet light at 3-, 5-, and 7-days

post-infiltration. The expressions of the GOIs at mRNA level were determined by reverse-transcriptase polymerase chain reaction (RT-PCR). To demonstrate protein expression, total soluble proteins (TSPs) were isolated from the leaves and used for Western blot and ELISA analyses. Finally, VLPs were purified by double-layer sucrose cushion ultracentrifugation and analyzed by Western blot and ELISA using appropriate antibodies (anti-N and anti-S).

In this thesis, mRNA expressions of all the GOIs (S, S-chl, E, M N) were confirmed in the *Agrobacterium* co-infiltrated leaf samples. N protein was detected in both TSPs and the purified samples by Western blot and ELISA analyses. The expression of N protein was higher in ER-targeted samples (VLP-ER) than chloroplast-targeted samples (VLP-Chl) according to the Western blot band density and ELISA as well.

This study is the first demonstration of plant-based production of VLPs containing all structural proteins of SARS-CoV-2 and is considered an important step towards the development of a low-cost and scalable COVID-19 vaccine.

KEYWORDS: *Nicotiana benthamiana*, SARS-CoV-2, virus like particle (VLP), COVID-19 vaccine, transient expression

TÜBİTAK (Türkiye Bilimsel ve Teknik Araştırma Kurumu), Project Grand: 122Z123

ÖZET

Halis Batuhan ÜNAL

SARS-CoV-2 VİRÜSÜNE KARŞI İKİNCİ JENERASYON MULTİ-EPİTOPLU HOMOLOG VİRÜS BENZERİ PARÇACIK (VLP)-TEMELLİ AŞI ADAYININ BİTKİ PLATFORMUNDA GELİŞTİRİLMESİ

Başkent Üniversitesi Fen Bilimleri Enstitüsü
Moleküler Biyoloji ve Genetik Anabilim Dalı
2024

Ağır akut solunum yolu sendromu koronavirüs 2 (SARS-CoV-2)'nin neden olduğu koronavirüs hastalığı 2019 (COVID-19) pandemisinin ciddi etkisi, dünya çapında çok çeşitli aşıların kullanılmasıyla hafifletilmiştir. Bununla birlikte, COVID-19 aşılarının adil dağıtımı, özellikle gelişmekte olan ve az gelişmiş ülkelerde zor olmaya devam etmektedir. SARS-CoV-2'ye karşı COVID-19 aşılarının hem üretiminde hem de uygulanmasında bugüne kadar gösterilen büyük çabalara rağmen, ortaya çıkan varyantları çapraz nötralize edebilen erişilebilir bir aşı geliştirilmesi önemini korumaktadır. Bu sebeple bu tezde, SARS-CoV-2'nin tüm yapısal proteinlerini içererek SARS-CoV-2'nin yapısına en yüksek benzerlikle geniş bir antijenite yelpazesi sergileyebilecek ve böylece ortaya çıkan varyantlara karşı koruma sağlayabilecek virüs benzeri partikül (VLP) tabanlı bir aşı adayının uygun maliyetli ve hızlı bir ekspresyon sistemi olan bitki platformunda üretilmesi amaçlanmıştır.

İlk olarak, SARS-CoV-2'nin yapısal proteinlerini [spike (S), membran (M), nükleokapsid (N) ve zarf (E)] kodlayan genler için ekspresyon kasetleri tasarlanmıştır. Hücresel kompartmanlaşmanın (endoplazmik retikulum; ER ve kloroplast; chl) ifade ürünlerinin seviyesi üzerindeki etkisini araştırmak için farklı sinyal dizileri eklenmiştir. Kodon optimizasyonunu takiben, gen kasetleri ticari olarak sentezlenmiştir. Gen kasetleri, bir bitki ekspresyon vektörü olan pEAQ-HT'ye ayrı ayrı başarıyla klonlanmıştır. İlgilenilen geni (GOI) taşıyan her plazmid elektroporasyon yoluyla *Agrobacterium tumefaciens*'e aktarılmıştır. Yaklaşık dört haftalık *Nicotiana benthamiana* bitkilerinin yaprakları bu plazmidleri taşıyan *A. tumefaciens* hücreleri aracılığıyla infiltre edilmiştir. Kontrol olarak, yapraklar pEAQ-HT-GFP içeren *Agrobacterium* hücreleri ile paralel olarak infiltre edilmiş ve GFP ışıması 3, 5 ve 7 gün sonra ultraviyole ışık altında görüntülenmiştir. GOI'lerin mRNA düzeyindeki ifadeleri ters transkriptaz polimeraz zincir reaksiyonu (RT-PCR) ile

belirlenmiştir. Protein ifadesini göstermek için, toplam çözünür proteinler (TSP) yapraklardan izole edilmiş, Western blot ve ELISA analizleri için kullanılmıştır. Son olarak, VLP'ler çift katmanlı sükroz yastık ultrasantrifüjleme ile saflaştırılmış ve uygun antikorlar (anti-N ve anti-S) kullanılarak Western blot ve ELISA ile analiz edilmiştir.

Bu tezde *Agrobacterium* ko-infiltrasyonlu yaprak örneklerinde tüm GOI'lerin mRNA ekspresyonları doğrulanmıştır. N proteini hem TSP hem de saflaştırılmış örneklerde Western blot ve ELISA analizleri ile tespit edilmiştir. Western blot bant yoğunluğu ve ELISA sonucuna göre N proteininin ekspresyon seviyesinin ER'ye hedeflenmiş örneklerde (VLP-ER), kloroplasta hedeflenmiş örneklere (VLP-Chl) göre daha yüksek olduğu belirlenmiştir.

Bu çalışma, SARS-CoV-2'nin tüm yapısal proteinlerini içeren VLP'lerin bitki bazlı üretiminin ilk gösterilişidir ve düşük maliyetli ve ölçeklenebilir bir COVID-19 aşısının geliştirilmesine yönelik önemli bir adım olarak kabul edilmektedir.

ANAHTAR KELİMELER: *Nicotiana benthamiana***,** SARS-CoV-2, virüs benzeri partikül (VLP), COVID-19 aşısı, geçici ekspresyon

TÜBİTAK (Türkiye Bilimsel ve Teknik Araştırma Kurumu), Proje No: 122Z123

CONTENTS

Page

LIST OF TABLES

Page

LIST OF FIGURES

Page

LIST OF SYMBOLS AND ABBREVIATIONS

-	Negative
°C	Centigrade Celsius
+	Positive
Ab	Antibody
ACE2	angiotensin-converting enzyme 2
AdVac	Adenovirus Vaccine
APC	antigen-presenting cells
APS	Ammonium persulphate
ATP	Adenosine Triphosphate
B/IC	baculovirus/insect cell
BCA	Bicinchoninic acid
bp	Base Pair
BSA	Bovine Serum Albumin
C	Colony
CD4	Cluster of differentiation 4
cDNA	complementary Deoxyribonucleic Acid
Chl	Chloroplast
CHO cell	Chinese hamster ovary cell
COVID-19	Coronavirus Disease 19
CPMV-HT	Cowpea mosaic virus *hyper trans*
DARPA	Defense Advanced Research Projects Agency
DEPC	Diethyl Pyro carbonate
dH_2O	Distillated water
DNA	Deoxyribonucleic Acid
dNTPs	deoxyribonucleotides
dpi	day post infiltration
E	Envelope
EB	Elution Buffer
EDTA	Ethylenediaminetetraacetic acid
ELISA	Enzyme Linked Immunosorbent Assay
ER	Endoplasmic Reticulum
EV	Empty Vector
F	Forward
g	gravitational
Gb	Gigabase
GFP	Green Florescence Protein
GMO	Genetically modified organisms
GOI	Gene of Interest
HBV	Hepatitis B Virus
HCI	Hydrochloric acid
HEV	Hecolin for Hepatitis E
HF	High Fidelity
HRP	Horseradish Peroxidase
IFN	Interferon
IGV	Integrative Genome Viewer
KCl	Potassium chloride
kDa	kilodalton

L	Ladder
L	liter
LB	Luria-Bertani Broth
M	Membrane
METU	Middle East Technical University
mg	milligram
MHC-I	Major Histocompatibility Class I
min	minute
ml	milliliter
mM	millimolar
Mn	Manganese
mRNA	Messenger Ribonucleic Acid
MS	Murashige and Skoog
MTase	Methyltransferase
N	Nucleocapsid
N7-MTase	Guanine N7 Methyltransferase
NaCl	Sodium Chloride
NCBI	National Center for Biotechnology Information
NEB	New England Biolabs
ng	nanogram
NGS	Next Generation Sequencing
Nsp	Non-Structural Protein
NT	No Template
OD	Optical Density
ORF	Open Reading Frame
P	Plasmid
PBS	Phosphate Buffer Saline
PBST	Phosphate Buffer Saline with Tween-20
PCR	Polymerase Chain Reaction
pmol	picomole
pp1a	protein phosphatase 1
PTM	post-translational modification
PVDF	Polyvinylidene difluoride
R	Reverse
RBD	Ribosome Binding Domain
RNA	Ribonucleic Acid
rpm	Revolutions per minute
RT-PCR	Reverse-Transcription PCR
S	Spike
S-chl	Spike-chloroplast
S1	Subunit of SARS-CoV-2 Spike Protein
S2	Subunit of SARS-CoV-2 Spike Protein
SARS-CoV-2	Severe Acute Respiratory Syndrome Coronavirus-2
SDS-PAGE	Sodium Dodecyl Sulphate Polyacrylamide Gel Electrophoresis
sec	second
T-DNA	Transfer DNA
T4SS	type 4 secretion system
TBST	Tris Buffer Saline with Tween-20
TE	Tris-EDTA Buffer
TEMED	N,N,N’,N’ Tetramethylethylenediamine

Ti plasmid	Tumor inducer
Tm	Melting temperature
TM domain	Trans membrane domain
TMB	3,3',5,5' Tetramethylbenzidine
TMPRSS2	TM protease serine 2
TSP	Total Solable Protein
TUBITAK	Türkiye Bilimsel ve Teknik Araştırma Kurumu
U	Unit
UK	United Kingdom
USA	United States of America
UTR	Un-translated region
UV	Ultraviolet
VIGS	Virus-induced Gene Silencing
VIPs	VirE2-interacting proteins
Vir	virulence
VLP	Virus-like particle
VOC	variant of concern
VOI	variant of interest
VUM	variant under monitoring
WHO	World Health Organization
WT	Wild Type
YE medium	Yeast Extract Medium
µg	microgram
µl	microlit

1. INTRODUCTION

In late December 2019, the World Health Organization (WHO) received a report from the authorities in Wuhan, Hubei province, China, concerning an outbreak of pneumonia [1]. The symptoms were subsequently designated as severe acute respiratory syndrome coronavirus 2 (SARS-CoV-2) due to their resemblance to those observed in SARS-CoV-1. As the number of cases continued to rise globally, the outbreak was ultimately classified as a pandemic. The historical development of the SARS and MERS viruses demonstrates that local and regional pandemics have occurred intermittently around the globe. For this reason, scientists have conducted extensive research on the potential emergence of SARS-like viruses, which are readily capable of infecting human cells, in humans [2]. In light of the existing literature, the development of vaccine strategies against these viruses is not unexpected. These studies constituted a crucial point of reference for the development of the SARS-CoV-2 vaccine [3, 4].

Following the sequencing of the SARS-CoV-2 genome, a significant global race to develop a vaccine has commenced. A multitude of research teams have initiated the development of vaccines concurrently, employing a diverse array of vaccine platforms. A significant number of these vaccines were designed to target the protein of SARS-CoV-2 that interacts with angiotensin-converting enzyme 2 (ACE2) in host cells [5]. The rationale behind the development of many vaccines was that antibodies against the protein could block this interaction, thereby neutralizing the virus and providing protection. In March 2020, the initial phase I clinical trials commenced with alacrity, followed by phase II and phase III trials [6].

The large-scale distribution of vaccines commenced in December 2020 with the introduction of the Comirnaty mRNA vaccine, followed by the Spikevax mRNA vaccine and the Vaxzevria vectored vaccine. The interval between the initial phase I trials and the first approval ranged from two months (for Sputnik V, a viral vector) to 19 months (for Nuvaxovid, a recombinant spike). These disparate timeframes can be attributed to discrepancies in the stringency of regulatory frameworks, the configuration of clinical trial protocols, and the characteristics of the vaccine platform [7]. An alternative vaccine type is virus-like particles (VLPs), proteins that mimic the structure of the target virus but do not produce infectious viral particles [8], represented 4% of the vaccine candidates in clinical

development against COVID-19 according to landscape of WHO (last update on 30 March 2023).

The production of VLP-based vaccines against diseases such as COIVD-19 using plant expression systems shows considerable promise. The rapid production of plant expression systems is of great importance for the prompt response to pandemics. Furthermore, plant production offers significant advantages in terms of sustainability, as it is a cost-effective, environmentally friendly, and ethically neutral process. *Nicotiana benthamiana* is a preferred species for the production of VLP vaccines. Transient expression techniques allow for the isolation of VLPs produced in plants, which can then be used as vaccines [9, 10].

The use of plant based VLP vaccines is becoming an increasingly popular trend. These vaccines are widely used for many virus-borne diseases. Plant-based VLP vaccines are of great importance for public health. Especially after the COVID pandemic, their potential for use and production is gaining importance. Plant-based systems offer faster production compared to traditional methods. This flexibility enables rapid intervention in the early stages of a pandemic. VLPs effectively stimulate the immune system by mimicking the structures of the virus but are safe because they are not infectious. For rapidly mutating viruses such as COVID-19, plant production systems can quickly adapt to new variants. This ensures that the vaccine is updated and remains effective against the virus. The low cost of plant production systems makes vaccines more affordable. This increases access to the vaccine, especially in developing countries. Furthermore, thanks to large-scale production capacity, large quantities of vaccines can be produced and distributed worldwide. Such vaccines can be rapidly delivered to large segments of society and can control the spread of the virus by conferring widespread immunity [11]. Plant-based VLP vaccines also have the potential to provide a quick solution against new pandemics that may emerge in the future. Plant-based VLP vaccines are making significant contributions to public health by providing an effective, accessible, and sustainable solution to tackle global health crises such as COVID-19 [12].

In the industry, VBI Vaccines Inc.'s trivalent VLP vaccine, which is undergoing pre-clinical trials; Imophoron Ltd. and the Max Planck Center at Bristol University collaborated to produce the ADDomerTM multiepitope VLP vaccine; Medicago Inc.'s VLP vaccine, which is about to be completed of its clinical phase; and while there is not currently a VLP-

based SARS-CoV-2 vaccine that has been approved by the World Health Organization [13] and to be used, however; some working groups are creating vaccine candidates by using this platform. VLPs can be produced using various expression systems (yeast, bacteria, cell lines, plants, etc.). Each system has its own advantages and disadvantages. SARS-CoV-2 targeted VLPs in mammalian cell lines Vero E6 and HEK293 have been successfully produced in two recently completed COVID-19 vaccine development studies [14, 15]. However, in terms of producing material for clinical purposes, low protein yield, high production cost, long expression time and the possibility of cell lines carrying pathogens and infections may compromise mammalian expression systems.

Since the first production of HBV surface antigen in transgenic plants in the early 1990s, plant-based vaccines have been intensively studied. Following this research, correctly folded antigens for influenza, Ebola, rotavirus, norovirus, dengue, and many other infectious viruses have been produced by plant expression systems. In response to the 2003 SARS outbreak, oral vaccine candidates targeting the SARS-CoV S protein present in tobacco, tomato and lettuce plants have been developed [16, 17]. Numerous plant-based human papillomavirus (HPV) vaccine development studies have been published, but existing vaccines are expensive and of public health concern [18]. Most of these vaccines were derived from the tobacco species *Nicotiana benthamiana*, a model host in the field of plant-pathogen interactions and administered intramuscularly. Some were administered as edible vaccines, as mentioned above, while others were administered orally (such as potatoes and spinach). The first plant-based Newcastle disease agent approved by the US Department of Agriculture (USDA) was a vaccine for Newcastle disease virus (NDV) administered to chickens. The “Blue Angel” program, initiated by the US Defense Advanced Research Projects Agency (DARPA), prioritized plant-based influenza vaccine development as a potential rapid production technology during the 2009 H1N1 influenza virus pandemic [19, 20]. To prevent the COVID-19 pandemic, it developed the CoVLP vaccine candidate within 20 days of the SARS-CoV-2 genetic sequence being released.

Many plant-based vaccines have been tried to be produced and there are still many vaccines in the production phase. Considering the COVID-19 pandemic, there is a need for second and even third doses in existing vaccines, so there is a need for both many vaccines and second-generation vaccines due to developing variants [21]. In addition, SARS-CoV-2 virus is expected to evolve into a seasonal pathogen like influenza over time. This again

necessitates a continuous immunization program. In this direction, the objective of this thesis was to develop a VLP vaccine candidate containing all the structural proteins (S, N, E, M) of SARS-CoV-2 against COVID-19 by transient expression the *N. benthamiana* plant via *Agrobacterium*. the development of a domestic and plant-based VLP vaccine candidate targeting all structural proteins of SARS-CoV-2 virus against COVID-19 disease and the pathway that provides the highest efficiency by testing 2 different localization types (endoplasmic reticulum and chloroplast) at the cell level in the expression system were aimed. This plant-based system has the potential to provide vaccines in large quantities at a lower cost than traditional methods. Especially when it comes to a disease that emerges as a pandemic and affects people all over the world, an ideal vaccine candidate to be developed will be highly protective against the disease, reliable, cost-effective, and also quickly produced and available on a large scale.

2. LITERATURE

2.1. Nicotiana benthamiana

Nicotiana benthamiana, a plant species originating from Australia, is closely related to *Nicotiana tabacum*. It has 19 chromosomes with an estimated genome of 3 Gb and belongs to the Solanaceae family [22, 23, 24]. *N. benthamiana* is the most frequently used experimental organism in plant biotechnology, molecular plant biology, and molecular farming for plant-based production of many secondary metabolites and vaccines. Furthermore, *N. benthamiana* is becoming increasingly popular, especially in plant-based systems for protein expression and purification, due to its high genetic transformation and regeneration efficiency [25]. It is known to be particularly advantageous to produce biopharmaceuticals due to its rapid growth rate and ability to express heterologous gene sequences [26]. Optimized procedures are generally used for the transient expression of recombinant proteins in *N. benthamiana*, which include infiltration of leaf tissue with *Agrobacteria* harboring a DNA transgene for the protein of interest. There are also studies in the literature indicating the production of various therapeutic and diagnostic proteins, including antibodies, viral antigens, and other proteins of potential clinical value, in agroinfiltrated *N. benthamiana* plants [27].

2.2. COVID-19 Pandemic and SARS-CoV-2

COVID-19 (Coronavirus disease 19) caused by the SARS-CoV-2 (Severe Acute Respiratory Syndrome Coronavirus-2) virus, emerged as a "novel coronavirus" in late 2019, was declared pandemic by the World Health Organization (WHO) on March 11th, 2020. To date, according to WHO (2024) 775645882 cases, and 7051876 deaths were confirmed worldwide [28]. In Türkiye, while the total number of reported cases is over 17 million, the total number of deaths has exceeded 102 thousand [29].

SARS-CoV-2 is a Positive-sense single-stranded RNA virus in the Coronaviridae family. Like other Coronaviridae viruses, it can cause non-fatal illnesses such as the common cold beside more severe diseases. SARS-CoV-2 is the seventh strain of this family known to infect humans, other strains are 229E, NL63, OC43, HKU1, MERS-CoV and the original SARS-CoV.

Like all coronaviruses, SARS-CoV-2 has four structural proteins (Figure 2. 1) known as spike (S), envelope (E), membrane (M), and nucleocapsid (N) and has a genome of approximately 30 kb encoding 14 open reading frames (ORFs). The S, E and M are located on the outer membrane of the SARS-CoV-2 virus, and form the viral envelope, while the N protein is attached to the RNA genome of the virus. Furthermore, SARS-CoV-2 has many kinds of proteins which could be categorized into three titles (structural proteins, non-structural proteins and accessory proteins) (Table 2. 1).

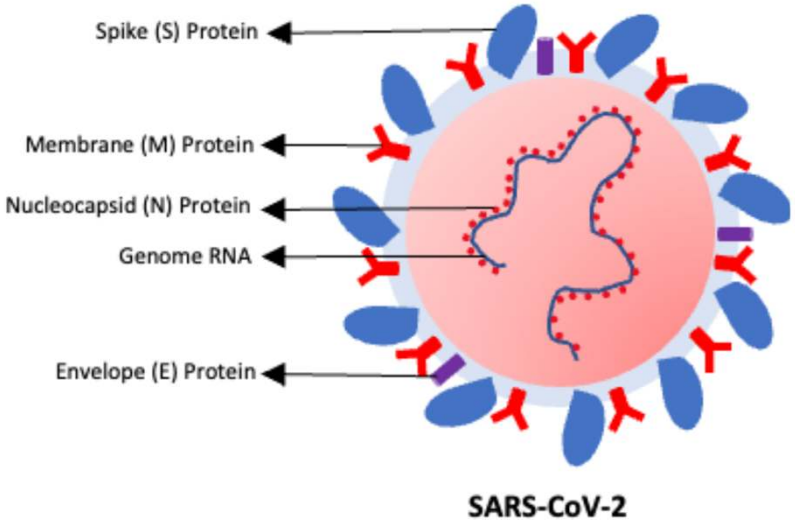

Figure 2. 1. Schematic representation of the structural proteins of SARS-CoV-2. Created with PowerPoint.

Table 2. 1. The functions of all SARS-CoV-2 proteins

Structural Proteins	**Functions**	**Reference**
Envelope	Has a vital part in pathogenesis, viral assembly and release.	[30, 31]
Membrane	Interacts with other viral structural proteins, easing the molecular assembly of virus particles.	[30, 31]
Nucleocapsid	Organizes and protects the virus genome, easing virion assembly, increasing virus transcription efficiency.	[30, 31]
Spike	Determinate of host immune response and implicates viral pathogenesis by the stimulation of the endoplasmic reticulum stress response, and binding to a host cell receptor prior to combining.	[30, 31]

Non-Structural Proteins	Functions	
Nsp1	Hinders host translation and degrades host mRNAs, expresses effective viral gene in infected cells.	[32, 33]
Nsp2	Associates with PHB1 and PHB2 complexes on the host proteins, contributing to mitochondrial biogenesis	[32]
Nsp3	Detaches Nsp1 and Nsp2 from polyproteins, links other viral Nsps and RNA to create a replication/transcription complex, and releases tags from old proteins set for elimination.	[32, 176]
Nsp4	Nucleates and attaches viral replication complexes on double-membrane vesicles present within the cytoplasm.	[32, 34]
Nsp5	Cuts at numerous different sites to provide mature and intermediate Nsps.	[32]
Nsp6	Promotes ER-derived autophagosomes production and double-membrane vesicles.	[32]
Nsp7	Dimerizes and engages with other Nsps.	[32]
Nsp8	Newly initiates replication and is believed to function as primase.	[32]
Nsp9	Thought bind to helicase by presenting oligosaccharide/oligonucleotide binding fold.	[32]
Nsp10	Promotes Nsp16 to carry out SAM-dependent MTase activity.	[32]
Nsp11	Unknown	[32]
Nsp12	Produces a viral replication complex alongside other Nsps, and methylation.	[32]
Nsp13	ATP-binding helicase core domain, contains a zinc-binding domain participating in replication and transcription, unwinds the double strands in a 5’-3’ direction using nucleotide hydrolysis energy.	[32]

Nsp14	Has exoribonuclease domain in a 3'-5' direction for proofreading against fatal mutagenesis and N7-MTase for mRNA capping.	[32]
Nsp15	Cleaves 3'uridine through Mn-dependent endoribonuclease activity for antiviral defense.	[32]
Nsp16	Assembles mRNA cap 2'-O-ribose methylation to the viral mRNAs' 5'-cap through MTase.	[32]
Accessory Proteins	**Functions**	
ORF3a	Associates with structural proteins, form ion channel in the host cell membrane, provides virus detachment, apoptosis, and pathogenesis.	[35, 36]
ORF3b	Stimulates apoptosis and necrosis and impedes antiviral innate immune response.	[35, 36]
ORF6	Inhibits IFN formation and signaling, downregulates protein expression through the blockage of mRNAs' nuclear export.	[35]
ORF7a	Stimulates apoptosis, suppress the synthesis of cellular protein and interrupts cell cycle at the G0/G1 phase.	[35, 36]
ORF7b	Thought to intervene with cellular processes and protein activity.	[35, 36]
ORF8	Increases replication; connects with MHC-I, moderating their degradation in cell culture and assisting immune evasion, and other structural proteins.	[35]
ORF9a	According to some sources ORF9b is known as ORF9a or ORF9b, however, ORF9b is the common name.	[35]
ORF9b	Cooperates with adaptor proteins, inhibiting IFN-1 mediates antiviral response, and Nsps and fuses into mature virions.	[35]
ORF9c	Weakens cell antiviral response.	[35, 36]
ORF10	Though to modulate immune functions	[35]

E protein, the smallest structural protein of SARS-CoV-2, consists of 75 amino acids and is called viroporin [37]. E protein is a multifunctional protein that plays an important role in both the virulence phases of the SARS-CoV-2 life cycle and mediates host immune responses after the virus has infected the host [38]. This protein consists of two basic domains, the N-terminal transmembrane domain, and C-terminal domain [37, 39]. Structurally, the N-terminal transmembrane domain forms a pentameric ion channel, whereas the C-terminal domain is not well known because it is unstable [40, 41].

M protein, one of the structural proteins of SARS-CoV-2, is predicted to have three transmembrane motifs and consists of 222 amino acids [42]. M protein is one of the most immunogenic proteins with S protein and is involved in the maturation of the N-glycosylation of S protein with E protein [43, 59]. Together, S and E proteins also contribute optimally to the production of SARS-CoV-2 virus-like particles [43].

N protein consists of 419 amino acids and two conserved regions: N-terminal and C-terminal domain [44, 45]. The N-terminal region of N protein is involved in RNA binding, while the C-terminal region is involved in dimerization as well as RNA binding [46]. This protein is more immunogenic than other structural proteins, and its expression increases when the virus infects the host [47, 48].

S protein, the largest structural protein of SARS-CoV-2, consists of 1273 amino acids, signal peptide, S1 subunit, and S2 subunit. S1 and S2 regions are involved in receptor binding [49]. The S1 subunit contains the N-terminal region and receptor binding site, while the S2 subunit contains the fusion peptide, heptapeptide repeat sequence 1, heptapeptide repeat sequence 2, TM domain and cytoplasmic domain [49]. SARS-Cov-2 virus has many glycosylated S proteins on its surface. It binds to the angiotensin-converting enzyme 2 (ACE2) receptor of the host cell, whereby S protein is activated by TM protease serine 2 (TMPRSS2), allowing the virus to enter the host cell [50].

2.3. Life Cycle of SARS-CoV-2

SARS-CoV-2 invades goblet cells via the respiratory tract and the S protein of SARS-CoV-2 binds to the host cell receptor hACE2, causing conformational changes. After entering the cell, the coronavirus expresses its genomic RNAs inside the cell to replicate viral replicase protease enzymes (pp1a and 1ab) and viral fragments encoded by the virus. The mRNA fragments that enter the cell via viral polymerases are transcribed to form the structural proteins of SARS-CoV-2. Three of the four structural proteins (E, M and S) are localized between the membranes of the endoplasmic reticulum (ER) and Golgi organelles, while the N protein forms a complex with the viral genome of SARS-CoV-2 in the cytoplasm. The intracellularly assembled structural proteins are then released from the infected host cell by exocytosis (Figure 2. 2) [5, 51].

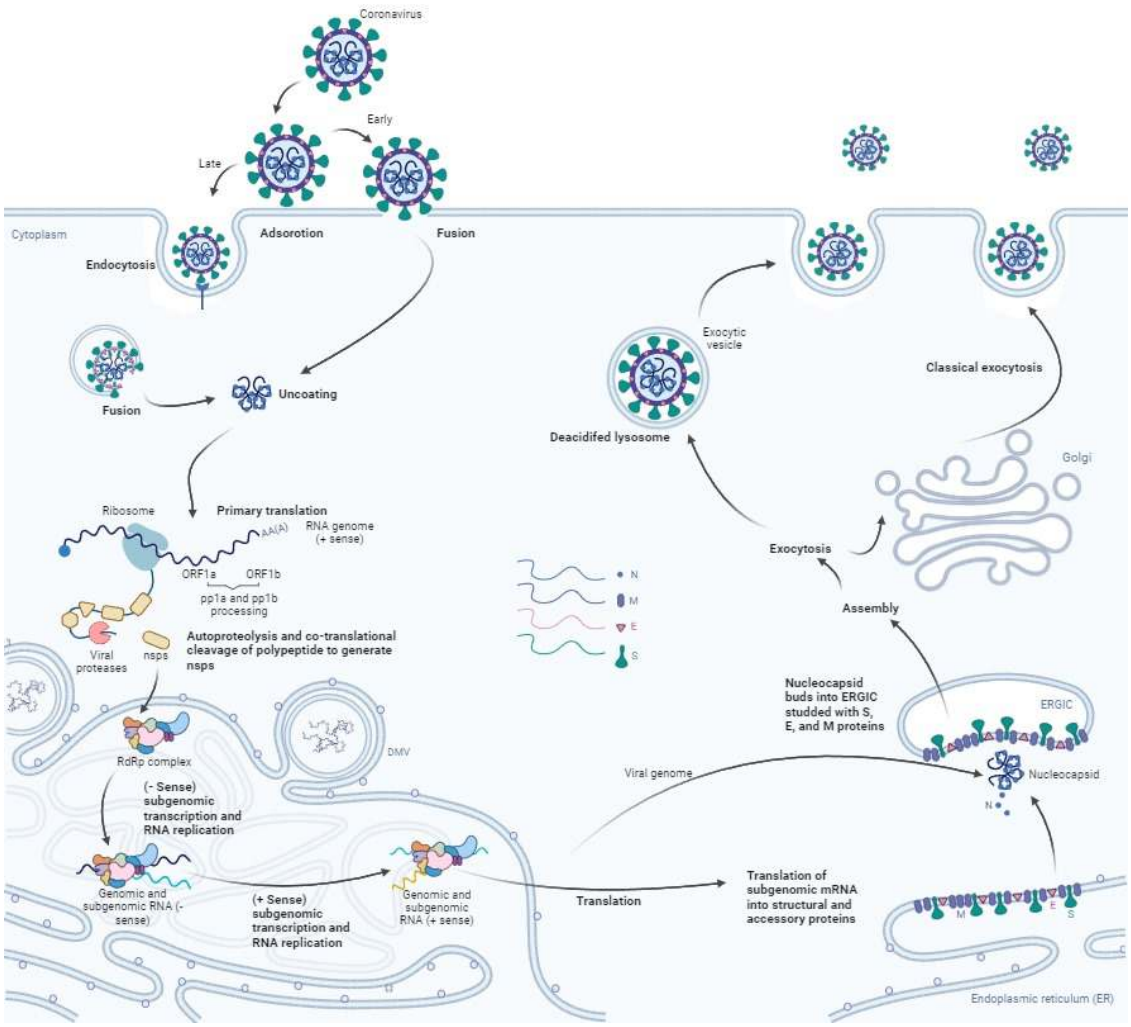

Figure 2. 2. Schematic representation of the life cycle of SARS-CoV-2 within the host cell. Created with BioRender.com

2.4. Evolution of SARS-CoV-2

Currently, there are several distinct variants of the SARS-CoV2. According to the classification of WHO over SARS-CoV2 variants, there are three main categories as variant of concern (VOC), variant of interest (VOI), and variant under monitoring (VUM). VOCs are defined by the Centers for Disease Control and Prevention (CDC) as the variants having enhanced virulence, transmission, and level of severity of the symptoms. These types of variants also have lower efficacy of antibody neutralization, treatments, protection, and diagnosis. On the other hand, the variants having mutations alter the specificity of the receptor binding causing to increased transmission, evading the immune response, and reducing the accuracy of current diagnosis are classified as VOIs. VUMs are defined as the variants with genetic alterations that are thought to influence the characteristic properties of the virus and initial signs of having a growth advantage compared to other variants. However, the effect of these genetic alterations on the virus' behavior and spread is still uncertain. Therefore, it is necessary to closely monitor and reassess this variant until more evidence becomes available. There are several mutants of SARS-CoV-2 until omicron variant were given in the Figure 2. 3

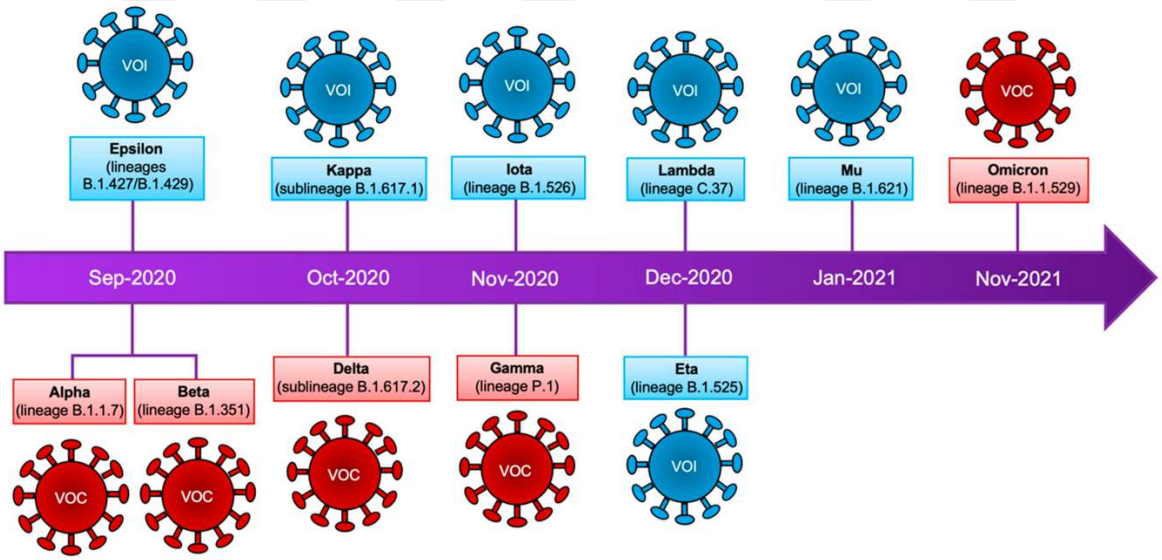

Figure 2. 3. Chronological order of emerging variants with lineage until the Omicron variant of SARS-CoV-2. VOI: variant of interest, VOC: variants of concern [52].

2.4.1. Alpha Variant

Alpha variant (lineage B.1.1.7) first appeared in the UK in September 2020. It differs from the original virus with mutations at locations Q493N and Q498Y in the S protein, which increases its binding affinity to the ACE2 receptor [53]. Reductions in neutralizing antibodies and plasma recovery in vaccinated patients are tightly linked to mutations in the S protein's S1 subunit [54]. Comirnaty vaccine (Pfizer/BioNTech) recipients who received two doses had 89% effectiveness against this variant [55].

2.4.2. Beta Variant

In September 2020, a lineage known as B.1.351 was found as a Beta variant in South Africa [56]. This variation of SARS-CoV-2 has nine mutations in the S protein, compared to the wild-type strain [57]. Three of these mutations (K417N, E484K, and N501Y), are situated in the RBD domain and boost the binding affinity to the ACE2 receptor by almost 19 times [57]. This variation leads to a greater increase in the disease's infectiousness and dissemination [55]. Research indicates that the efficacies of Comirnaty, Nuvaxovid and, Vaxzevria were 75%, 86%, and 10%, respectively [58].

2.4.3. Gamma Variant

S protein has 12 mutations in the gamma variation (P.1 lineage), discovered in Brazil and Japan in November 2020 [60, 61]. The Gamma variant decreases the efficacy of monoclonal antibodies and has significant effects on the virus's ability to propagate and infect others [62]. Against this variant, the two-dose Comirnaty and Vaxzevria vaccines have about 50% reduction in efficacy, while the CoronaVac vaccine has an around 40% reduction in efficacy [63]. Additionally, the Spikevax vaccine's protection diminishes a little slightly [64].

2.4.4. Delta Variant

S protein contains eleven mutations in the Delta variant (sub-lineage B.1.617.2) which was discovered in India in October 2020 [60]. It is thought to be the most hazardous variant until now. This variation is deficient in mutations in the S protein's RBD domain, which is linked to antibodies' ability to evade neutralizing action. At the same time, S protein binding

to ACE2 was not enhanced and certain monoclonal antibodies were unable to bind due to alterations in RBD [65]. The S protein's affinity for ACE2 receptors was enhanced by the N501Y mutation in the alpha, beta, and gamma forms, making it easier for the virus to adhere to and enter the host cell [66]. It was found that the delta form, containing ten mutations in the S protein, was less sensitive to neutralization by anti-NTD (N-terminal region) and anti-RBD [66]. The efficacies of the Comirnaty vaccine (Pfizer/BioNTech) and Vaxzevria vaccine against the delta variant were 88% and 67%, respectively [67].

2.4.5. Epsilon Variant

In September 2020, an epsilon variant (B.1.427 and B.1.429 lineages) was discovered in California, USA [60]. It is characterized by mutations in the W152C and S131; mutations in the S protein [68]. The L452R mutation raises the virus's affinity for ACE2, and these mutations boost the variant's infectivity [69].

2.4.6. Eta Variant

The Eta variant, also known as lineage B.1.525, was discovered in December 2020 and consists of 6 mutations and 3 deletions unique to the S protein [60]. It was shown that Eta variation led to an increase in infection and a decrease in the potency of neutralizing antibodies [70]. Some of these mutations increase the quantity of infected cells expressing ACE2 [71]. Positive outcomes against this variation have been documented with the Comirnaty vaccine (Pfizer/BioNTech) [72].

2.4.7. Iota Variant

The Iota variant (B.1.526) first appeared in New York in November 2020 [61]. The Iota variant has two significant mutations E484K mutation in the S protein is one of these mutations that enables the virus to evade detection by antibodies [73]. S477N mutation allows the virus to attach to the host cell more securely.

2.4.8. Kappa Variant

The Kappa variant (sub-lineage B.1.617.1), first identified in India in October 2020, is considered the ancestor of the delta variant [60]. The RBD region has six alterations, and

the E484Q mutation increases ACE2 affinity [74]. Neutralization of antibodies decreased in those vaccinated with Comirnaty and Spikevax [75].

2.4.9. Lambda Variant

The Lambda variant (C.37 lineage), discovered in Peru in December 2020, contains seven amino acid deletions in the N-terminal region and six mutations in the S protein [61]. These mutations and amino acid deletions are associated with increased viral infection and resistance to increased neutralization activity [76]. Decreased neutralizing activity has been indicated in those who were vaccinated with Comirnaty and Spikevax [76].

2.4.10. Mu Variant

Mu variant (B.1.621 lineage) with nine mutations on S protein, was first identified in Colombia in January 2021 [60]. According to WHO data, Ecuador and Colombia have significant infection rates caused by the Mu strain, which affects 0.1% of the global population [60]. Vaccine efficiency has declined among those who had Comirnaty vaccine. [77].

2.4.11. Omicron Variant

On November 11, 2021, the Omicron variant (lineage B.1.1.529) was discovered in Africa. It includes more than 30 mutations in the S protein, and 15 of them are found in the RBD domain. Antibodies by escaping from as in Delta and Alpha variants the B.1.1.529 lineage has given rise to sub-lineages. Despite increased mutation, increased infection, and antibody escape, it was concluded that pathogenicity was lower than in the Delta variants. It suggests that the Omicron variant is more contagious because it can escape from the humoral immune system in those who were vaccinated. The effectiveness of the available vaccinations was significantly reduced by the omicron variant. When the efficacy of Comirnaty, Spikevax and Vaxzevria vaccines against omicron infection was examined, it was determined that 2 doses of COVID-19 vaccine had no protection effect, while a 3rd dose mRNA vaccine protected only 37% [78].

2.5. Current COVID-19 vaccines and vaccine platforms

2.5.1. COVID-19 vaccines approved by WHO

Before approvement of a vaccine, clinical trials take a long time under normal conditions. However, in December 2020, vaccine candidates emerged shortly after the COVID-19 case in Wuhan, China. First COVID-19 vaccine was approved after a short time (approximately one year). 12 vaccines were approved by WHO (Table 2. 2).

Table 2. 2. Current vaccines approved by WHO

Vaccines	Produced by	Produced Vaccine Platform	Implemented by	Approved by
Nuvaxovid	Novavax	Protein Subunit	14 countries	40 counties
COVOVAX	Serum Institute of India	Protein Subunit	3 countries	6 countries
SKYCovione	SK Bioscience Co Ltd	Protein Subunit	6 countries	1 country
Spikevax	Moderna	RNA	24 countries	88 countries
Comirnaty	Pfizer/BioNTech	RNA	31 countries	149 countries
Convidecia	CanSino	Non-Replicating Viral Vector	6 countries	10 countries
Jcovden	Janssen (Johnson & Johnson)	Non-Replicating Viral Vector	25 countries	113 countries
Vaxzevria	Oxford / AstraZeneca	Non-Replicating Viral Vector	34 countries	149 countries
Covishield	Serum Institute of India	Non-Replicating Viral Vector	1 country	49 countries
Covaxin	Bharat Biotech	Inactivated	2 countries	14 countries
Covilo	Sinopharm (Beijing)	Inactivated	18 countries	93 countries
CoronaVac	Sinovac	Inactivated	10 countries	56 countries

2.5.1.1. Nuvaxovid and COVOVAX

Nuvaxovid (NVX-CoV2373) is a nanoparticle vaccine with a recombinant spike protein. COCOVAX has the same formulation with Nuvaxovid. It is the first recombinant protein-based vaccine approved in the European Union and Great Britain and the first covid-19 vaccine combined with an adjuvant [79]. The Nuvaxovid vaccine differs from existing vaccines in that it is a variant of the Nuvaxovid vaccine due to many mutations in the spike protein and that SARS-CoV-2 endemically causes different pathogenicity [79, 80]. In the production of this vaccine, the recombinant spike protein was produced in a baculovirus, and two proline amino acids were modified to stabilize the spike protein. The recombinant spike protein was produced by introducing the produced spike protein into Sf9 moth cells with baculovirus and spike proteins in trimeric form were collected from the moth cells. It was then combined with Matrix-M adjuvant to form Nuvaxovid [80]. According to WHO data, it is a Covid-19 vaccine accepted by 40 countries and implemented by 14 countries [81].

2.5.1.2. SKYCovione

SKYCovione is the first Covid19 vaccine designed by Korea. It has nanoparticles containing fragments of the Spike protein of SARS-CoV-2. When administered to the patient, the Spike protein fragments trigger an immune response in the patient and trigger antibody production. According to WHO data, SKYCovione is a Covid-19 vaccine approved only by the Republic of Korea and implemented in 6 countries. [81, 82]

2.5.1.3. Spikevax

Spikevax vaccine is an RNA vaccine that uses a nucleoside-modified mRNA (modRNA) expressing the spike protein of SARS-CoV-2 [83]. In addition to the Spikevax vaccine, bivalent forms of this vaccine have been created. One of the bivalent forms, Spikevax Bivalent Zero/Omicron, is used as a booster dose in patients older than 18 years of age, while the other bivalent form, Omicron, has been used against the BA.4/BA.5 variant [84, 85]. It has been observed that the effect of this vaccine is reduced in the presence of the delta variant. According to WHO data, it is a vaccine accepted by 88 countries and implemented by 24 countries.

2.5.1.4. Comirnaty

Comirnaty vaccine is a Covid-19 mRNA-based vaccine produced in partnership with BioNTech and Pfizer. It is encapsulated in lipid nanoparticles using modRNA expressing the mutated form of Spike protein, one of the structural proteins of SARS-CoV-2 [86]. Nanoparticles are administered to the patient intramuscularly and the encapsulated mRNA structure settles into the cell. The mRNA inside the cell is converted into protein by ribosomes. Immune response is generated against the spike protein recognized by immune cells [87]. Bivalent Comirnaty vaccines (BA.1 and BA.4/BA.5) were administered as booster doses after a while [88]. According to WHO data, Comirnaty is a vaccine accepted by 149 countries and implemented by 31 countries.

2.5.1.5. Convidecia

The full spike glycoprotein of the SARS-CoV-2 virus was contained in the E1/E3 deleted Ad5-based vector used to create the Convidecia vaccine [89]. In further pre-clinical testing, the virus was shown to replicate in the upper respiratory tract but not in the lung [90]. Because of this, even though it protects the upper respiratory tract, it has been shown to have little protective effect in people with asthma [90]. According to WHO data, Convidecia is a vaccine accepted by 10 countries and implemented by 6 countries.

2.5.1.6. Jcovden

Johnson & Johnson used AdVac technology, which was also utilized in the creation of the Ebola vaccine, to design the Jcovden vaccine. The naturally occurring Adenovirus type 26 virus is a vector for viruses and causes symptoms similar to a cold [91]. To elicit an immunological response, the human host and the Adenovirus type 26 virus were exposed to the SARS-CoV-2 Spike protein [92]. According to WHO data, Jcovden is a vaccine accepted by 113 countries and implemented by 23 countries.

2.5.1.7. Vaxzevria and Covishield

Vaxzevria and Covishield, also known as the Vaxzevria vaccine, is a monovalent vaccine consisting of a single recombinant, replication-deficient chimpanzee adenovirus (ChAdOx1) vector encoding the S glycoprotein of SARS-CoV-2 [93]. The SARS-CoV-2 S

protein in the vaccine is expressed in the trimeric pre-fusion conformation; after administration, the S glycoprotein of SARS-CoV-2 is locally expressed, stimulating neutralizing antibody and cellular immune responses, which may contribute to protection against COVID-19 [94]. According to WHO data, while Vaxzevria is a vaccine accepted by 149 countries and implemented by 34 countries, Covishiled is a vaccine accepted by 49 countries and implemented by only 1 country.

2.5.1.8. Covaxin

Covaxin, also known as BBV12, produced by using Whole-Virion Inactivated Vero Cell, involves isolation of the Sars-CoV-2 strain directly from patients, followed by inactivation of the virus by using chemicals, purified and then used to stimulate an immune response against covid-19 [95]. According to WHO data, Covaxin is a vaccine accepted by 14 countries and implemented by 2 countries.

2.5.1.9. Covilo

Covilo, also known as BIBP vaccine, is similar to Covaxin and CoronaVac. It is a type of inactivated virus but different from other inactivated viruses. The inactivation process involves using beta-propiolactone, which prevents the virus from binding to its genetic material while providing an intact structure. The virus is then formulated using aluminum hydroxide to improve the stimulation of the immune response [96]. According to WHO data, Covilo is a vaccine accepted by 93 countries and implemented by 18 countries.

2.5.1.10. CoronaVac

The CN2 viral strain was grown in Vero cells for the purpose of creating the CoronaVac vaccine, and the viruses were eradicated using substances known as beta-propiolactone [97, 98]. The Sinovac company then released the vaccine after adding an adjuvant made of aluminum to make it possible to deliver it [98]. It was shown that there were strong immune reactions to the Delta variant [99]. According to WHO data, CoronavaC is a vaccine accepted by 56 countries and implemented by 10 countries.

2.5.2. Vaccine Platforms

Many vaccines can be developed using different platforms. These vaccine platforms are called traditional and next-generation vaccine platforms. While traditional vaccine platforms include inactivated and live-attenuated vaccines, next-generation vaccine platforms include replicating viral vectors, non-replicating viral vectors, nucleic acid-based (DNA and RNA), protein subunit, and virus-like particles (VLPs) vaccines.

2.5.2.1. Inactive Vaccine

Inactivated vaccines are a subtype produced by using heat or phenols to destroy the genetic material of the virus. The viral genome in such vaccines is not able to replicate but is recognized by the host, and antibodies are produced against them by the host. It is easier to prepare than other vaccines, but as a disadvantage, the production phase is slow and it is difficult to produce at high scales [100, 101].

2.5.2.2. Live-Attenuated Vaccine

In this platform, the virulence of the virus is reduced without killing it. The virus by propagating it until it reaches a non-disease-causing level. These vaccines have advantages, such as providing long-term immunity, being used for many vaccines, and not requiring adjuvants. However, it contains the entire virus and is expensive to produce [101, 102].

2.5.2.3. Viral Vector Vaccine

Viral vector vaccines, one of the new generation vaccine methods, are type of vaccines that use the antigen-encoding part of the protein or genetic material of the virus as a viral vector to provide immunity. Viral vector vaccines can be divided into two groups. One is replicative viral vector vaccines that have not lost their ability to replicate and can self-reproduce in infected cells [103]. The other is non-replicative viral vector vaccines that do not replicate in infected cells [103]. High levels of cellular and humoral immunity can be obtained from viral vector vaccines, but their large-scale manufacturing is restricted, and future responses to the dosage may be adversely affected by immunity to the vector. [104].

2.5.2.4. Nucleic acid vaccine

By the host whose nucleic acid vaccines, it based on DNA or RNA that will be expressed into the immune system will use to make antibodies. Although DNA vaccines are easily designed and can be produced quickly, there are drawbacks including the incorporation of the genetic material into the host genome, the requirement for adjuvants to boost the immune response, and the high cost of the equipment needed for gene delivery techniques [105, 106].

mRNA vaccines are responsible for immunizing the host by encoding the antigen required after the mRNA molecule enters the host's immune cells. RNA vaccines are easy to manufacture and design and have no infection properties. However, RNA vaccines need to be encapsulated because they are unstable under physiological conditions. They are also expensive to produce and have extreme storage conditions [107].

2.5.2.5. Protein Subunit Vaccine

Protein subunit vaccines are vaccine systems that contain all or part of the isolated and purified antigen-producing proteins of the virus is one of the reasons for. While its reliability due to its low side effects high applicability of this vaccine type, the need for adjuvants multiple doses are disadvantages [108].

2.5.2.6. Virus-Like Particle (VLP) Vaccine

Virus-like particles are derived from viruses and made up of some self-assembling structural compartments of a virus particle. So that, they are able to mimic the structure of SARS-CoV-2 without infecting the host since none of these structural proteins contain the genetic material of this virus. When compared to other vaccine types, VLPs are safer due to their lacking infectivity. Once within the body, 20–200 nm-diameter VLPs can quickly diffuse into lymph nodes where they interact directly with antigen-presenting cells (APCs) to trigger both enduring cellular and humoral response [109]. Furthermore, B cells can be stimulated to produce antibodies by cross-linking the multimeric epitopes on VLPs to B cell receptors; in certain cases, this can happen even in the absence of CD4+ T cells. Adjuvants have not been used in many VLP vaccination platforms because of this robust immune

response. Hence, VLPs are now a commonly utilized vaccine platform in the field of vaccine manufacturing because of their unique characteristics. [110]

Although the WHO have approved a VLP-based SARS-CoV-2 vaccine yet some research groups have developed vaccine candidates using this platform. In our country, preclinical examinations of VLP based vaccine candidate targeting four structural proteins [S, N, M and E] of SARS-CoV-2 were successfully completed [15]. In the industrial field, VLP vaccine candidates approved by WHO include the trivalent VLP vaccine of VBI vaccines Inc. in pre-clinical trials, the ADDomerTM multiepitope VLP vaccine produced in collaboration with Imophoron Ltd and the Max Planck Center of Bristol University. There are already licensed VLP vaccines available for human use, targeting various disease agents and in clinical use (Recombivax HB and Engerix-B for Hepatits B Virus (HBV), Gardasil, Cervarix and Gardasil-9 for Human Papilloma Virus (HPV), Hecolin for Hepatitis E Virus (HEV)) [20].

2.6. Expression System for VLPs

VLPs can be produced by different expression systems (bacteria, yeast, cell lines, baculovirus/insect cell (B/IC), and plants), each has its own advantages and disadvantages (Table 2. 3).

Table 2. 3. Advantages and disadvantages of VLP expression systems.

VLP Expression System	Advantages	Disadvantages
Bacterial System	- Fast growth rate. -Simple to operate. -It is possible to generate recombinant proteins in less than a day.	- Incapacity to carry out the PTM required for appropriate VLP assembly, such as glycosylation. - The existence of bacterial endotoxins that need to be eliminated after production.
Yeast System	- Commonly used for commercial VLP production. - Able to undergo certain post-translational changes.	- The majority of glycosylation is restricted to variable high mannose glycoforms, which are not ideal for VLP assembly.

Insect System	- Used in the commercial manufacture of vaccines such as HPV. -Capable of more complex post-translational modifications than bacterial systems.	-The simple PTM, like a high mannose glycosylation level. - One potential drawback may be the coproduction of baculovirus particles.
Mammalian Cell System	- Most suitable for authentic PTMs and correct VLP assembly. - Produces VLPs with correct glycosylation patterns.	- Significant capital investment required. - High production costs. - Risk of spreading pathogens to humans. - Challenges in scalability due to the requirement for specialized facilities.
Plant System	- Creates VLPs with the proper glycosylation patterns appropriate eukaryotic modification and VLP construction. - Inexpensive and highly scalable. - Limited threat of unexpected infections in humans. - Inexpensive large-scale growth.	- Production processes were slow, and yields were low in the early systems. - Regulatory obstacles, such as FDA approval need to be completely overcome.

2.6.1. Bacteria system

One of the VLP expression systems frequently used to produce recombinant proteins is the bacterial system, which frequently uses strains that have been thoroughly studied. Nevertheless, this system is unsuitable for enveloped VLP production since it lacks PTM (post-translational modification) and disulfide bond formation. In this system, *Escherichia coli* is the most favored bacterial strain. Although *E. coli* is typically used to make small proteins, PTM prevents the production of large proteins. [111, 112]

2.6.2. Yeast system

Similar to bacterial cells, yeast cells are employed for the expression of recombinant proteins and the synthesis of VLP. *Saccharomyces cerevisiae* and *Pichia pastoris* strains are the most commonly used strains in yeast expression systems. These strains may produce complicated proteins than *E. coli*. The bacteria of the vectors must first be prepared in their cells before being delivered into the yeast cells in order to accomplish expression in those

cells. While the yeast expression system can provide some post-translational modifications, it is still insufficient to produce complex proteins. In addition, yeast expression systems are less advantageous than bacterial ones due to factors like high amounts of mannose glycosylation, plasmid loss, and relatively poor protein production. [20, 113]

2.6.3. Insect system

One of the most popular expression methods for producing enveloped and non-enveloped VLPs is the Baculovirus / Insect cells (B/IC) VLP expression system. Its large-scale cultivation capability as well as rapid growth makes it a popular option for VLP production. Furthermore, this system is a good platform to produce multi-protein VLPs with complex post-translational modifications and offers comparatively more efficient protein expression than bacterial and yeast systems. However, their N-glycosylation characteristics are still rather simple when compared to glycoproteins expressed by mammalian cells [20]. However, even though baculoviruses are not harmful to humans, they nonetheless have a risk for environment and must be inactivated before preparation of vaccines. The immunogenicity of VLP can be harmed by the inactivation process. Furthermore, because of similar morphologies, baculovirus particles and VLPs may be confused in purification steps. [110]

2.6.4. Mammalian system

Both enveloped and non-enveloped VLPs can be produced using animal cell expression systems which continue to be attractive and valuable platforms. Because animal cell expression platforms can produce the exact and complex PTM needed for correct protein folding, they are highly effective methods to produce recombinant proteins. For the generation of VLP, the mammalian cell lines CHO, Vero E6, and HEK293 are commonly utilized. Mammalian expression methods, however, may be less advantageous in terms of clinical use due to the factors such as low protein yield, high production costs, extended-expression times, and the potential of cell lines to become infected with mammalian pathogens. [20, 114]

2.6.5. Plant system

Plant expression systems offer high expression levels of soluble proteins. Many proteins and antibodies needed in the pharmaceutical sector may be generated at high rates from plants [115, 116, 117].

Viral glycoproteins must be correctly folded, and this requires N-glycosylation. Plant cells have the benefit of displaying a single glycosylation pattern, in contrast to the majority of glycoproteins produced by mammalian cells, which have varied glycosylation pattern. These glycosylated antigens function as adjuvants and aid in antigen capture by attaching to sugar-specific APC cell surface receptors because they include plant-specific N-glycans [118]. Glycoengineering technology can also be used to manipulate the glycosylation characteristics of plant lines in order to create humanized plant lines [119]. Another advantageous feature of plants is that edible vaccines can be produced using rice, potatoes, or lettuce etc. [120, 121, 122]. Such vaccines can be used directly without need for steps such as purification of the antigen which reduces cost and labor [119]. VLPs self-assemble in the host plant [123].

2.7. *Agrobacterium*-mediated gene expression system

2.7.1. Stable gene expression

A plant pathogen called *Agrobacterium tumefaciens* naturally has a tumor inducer (Ti) plasmid (Figure 2. 5) and leads to crown gall disease by transferring a DNA fragment [124]. T-DNA is transported from bacterial cells to plant cells by cooperation of virulence (vir) genes [125].

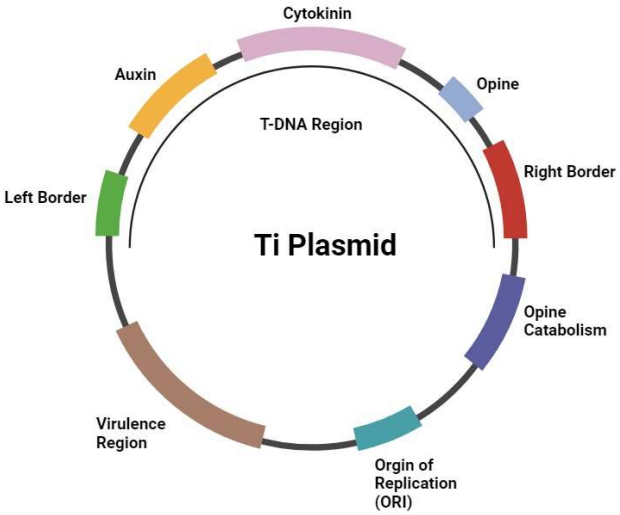

Figure 2. 4. Schematic representation of Ti plasmid. Created with BioRender.com

Acetosyringone (3,5-dimethoxyacetophenone) is the first phenolic chemical shown to activate viral genes in bacteria and start T-DNA transfer in the absence and presence of the plant [126, 127]. Acetosyringone is only produced when dicot plants are injured. Monocot plants do not produce acetosyringone. VirA and VirG proteins are two components acting as antenna in the periplasm and are generally involved in signal transduction. VirA protein senses the presence of acetosyringone, the phenolic compound produced by plant at the time of injury and vir genes are expressed [128]. Upon binding the phenolic compound to VirA, VirA is auto-phosphorylated and phosphorylates VirG protein to activate VirG protein [129]. In addition to the activating effect of phenols, other signals emitted by plants and monosaccharides also play a role in activating vir genes [130, 131]. Only monosaccharides have a very low activating ability, thus enhancing the effect of phenolic compounds such as acetosyringone. In addition, low pH and low phosphate concentration can activate vir genes directly through VirA and ChvE and ChvG proteins on the cell membrane [130, 132, 133] (Figure 2. 6).

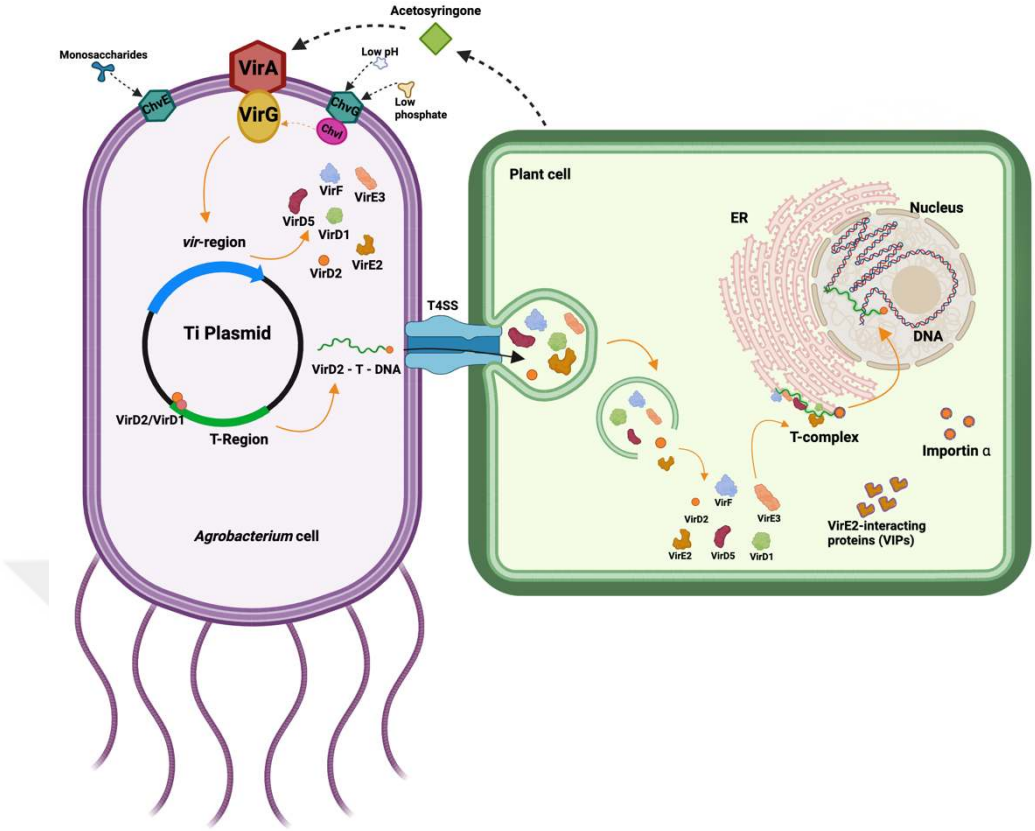

Figure 2. 5. Schematic representation of *Agrobacterium*-mediated transformation. Created with BioRender.com

During the attachment of bacterial cells to plant cells, cellulose fibrils and cyclic glucans are synthesized by the bacteria, forming a biofilm structure in which the bacteria can attach to the plant [134, 135]. This structure is important for the virulence of most plant bacteria. The passage of T-DNA and proteins into the host plant cell is mediated by the bacterial type 4 secretion system (T4SS) and 11 genes encoded by VirD2 and VirB [136]. The T4SS system is 2nm in diameter and mechanically perforates the cell wall of the host plant cell and is involved in the passage of ssDNA and folded proteins into the host plant cell [137]. For T-DNA to pass into the host plant cell, VirD2 (a component of bacterial endonuclease) must bind covalently to the 5' end of the T-DNA [138, 139]. The VirD2 protein has two nuclear localization signals, a monopartite amino terminal, and a bipartite carboxyl terminal [140] which is necessary for T-DNA transport [141]. VirD2 carries T-DNA through the T4SS to the host plant cell. Plant importin α, VirE2, and VirE2-interacting proteins (VIPs) interact with T-DNA within the host plant cell to facilitate its transport into the nucleus [142, 143].

Stable gene transfer to plant cells is achieved by two methods which are nuclear and chloroplast. In nuclear gene transformation, methods of gene transformation into *A. tumefaciens* cells include electroporation, microinjection, and polyethylene glycol. First of all, oncogenes in the T-DNA must be removed to make pathogenic *A. tumefaciens* nonpathogenic (disarmed) [144, 145]. Genetically modified Ti plasmids of disarmed *A. tumefaciens* strains have been used to transfer genes to many plant species and increase their productivity. With stable transformation, the plant must carry the gene transferred from generation to generation. The formation of a whole plant using cells or tissues with stable gene expression requires long-term plant tissue culture studies. Stable transformation is a lengthy process that often requires established tissue culture techniques to stimulate whole plant growth from transformed cells or tissues [146]. This method has the disadvantages of compromising the molecular integrity of the transferred DNA, the formation of chimeric plants and epigenetic silencing [147, 148].

Another method, the chloroplast-targeted method, can be used in various tissues of various plant species. Gold or tungsten-coated DNA is delivered to plant tissues with a particle gun to enter the plant cell [147, 149]. The transformed plant tissues are then allowed to grow in appropriate antibiotic media. The chloroplast-targeted method has advantages over the nuclear-targeted method such as ease of manipulation, high expression level and recombinant protein production with optimum yield [150].

2.7.2. Transient gene expression

While stable transformation was the approach to produce recombinant proteins in plants until the early 2000s, significant results were obtained with transient transformation as a result of modifications in the design and expression system of recombinant plant vectors. Transient transformation is defined as inserting DNA into plant cells without incorporating transgenes into the genome. In other words, integrating foreign DNA into plant cell is not stable when plant tissues undergo transient transformation. This technique enables the quick and simple testing of novel structures and promoters, which is crucial for plants that are challenging to transform and have a slow regeneration rate. Furthermore, by expressing protein derivatives with fluorescent tags and producing proteins in particular plant organs, these transient expression techniques enable accurate assessments of protein localization. Moreover, quick, and high-level recombinant protein expression is a benefit of transient

expression methods utilizing virus-based carriers [151]. In vivo stable transformation is most commonly achieved via infiltration of *Agrobacterium*, which was first discovered in *N. benthamiana* leaves [152]. *Agrobacterium*-mediated transient transformation of plants is a method that is frequently employed for the functional testing of genes since it may quickly induce high-level expression of target genes. This technology is powerful for studying the function of plant genes without the need for a genetic transformation system because, unlike stable transformation, it does not require regeneration of the transformed cell, has no effect on the stability of the host genome, is independent of the position effects of the T-DNA integration sites, and allows for the processing of large numbers of plants as well as multiple gene transient expression on a single leaf [153]. Moreover, in the transgenic plant approach, the transgenic expression system provides the final product in a period of one or several years after integration into the genome, whereas with the transient expression system without genome integration, the target protein can be obtained in a week. Public concerns about the transgenic plant approach and obtaining expression products in a very short time with transient expression have led heterologous plant expression studies, especially in the last 20 years, to focus on transient transformation (without genome integration / non-GMO) method [154, 19]. As an example of these studies, Maclean et al. [155] transiently expressed the human papillomavirus (HPV)-16 L1 capsid protein in *N. benthamiana* leaves by targeting chloroplast, endoplasmic reticulum, and cytoplasm. Among them, the highest transient expression of L1 was achieved in chloroplasts. When compared to cell-based VLPs, plant-based production of L1 exhibited significantly lower immunogenicity in mice. They suggested that this methodology of transient expression of recombinant proteins in plants has a great promise. In another study, Zahin et al. [156] stated that the same HPV-16 L1 protein was efficiently and transiently expressed in chloroplasts. They tested three different constructs, and the most efficient one was TPL1F. And the VLPs were purified from *N. benthamiana* leaves successfully via size exclusion chromatography and cesium chloride density gradient chromatography. When all factors considered, they suggested that this transient expression of chloroplast-targeted L1 protein in tobacco has a promise for the development of an affordable and effective HPV-16 L1 VLP vaccine. In addition to these studies, Pyrski et al. [157] used the same strategy against chronic hepatitis B (CHB) in order to produce its core antigen (HBcAg) in tobacco plant. After the production of HBcAg, they developed a transgenic lettuce producing the antigen for oral vaccination. They showed that orally immunizing the mice provided additional protection with the injection against CHB

and the mice exhibited an immune response. Their study offers a possible novel therapy for CHB.

2.8. pEAQ vector series

The combination of *Agrobacterium*-based transformation method and virus-based vectors enables the efficient transient expression system of the pEAQ vector series to be used in plants. Cowpea mosaic virus *hyper trans* CPMV-HT, a deleted derivative of cowpea CPMV RNA-2, is used to produce proteins at high efficiency and speed without viral replication [158, 159]. The expression vector pEAQ-HT (Figure 2. 7) combines pEAQ vector and CPMV-HT is a vector designed for both high-level and transient expression, facilitating the insertion of desired sequences between 5'UTR and 3'UTR into the plant [158, 160, 161]. Furthermore, this system has many advantages over other systems, such as expression of multiple genes in the same tissue, fewer biological limitations, and no genetic drift in replication [162]. All pEAQ vectors contain a 5.2 kb backbone, oriV, colE1 (origin of replication), trfA (for plasmid replication) and nptIII (kanamycin resistance gene). Cloning and expression diversity show that the diversity of the T-DNA region varies depending on the presence or absence of P19 (gene silencing suppressor) and NPTII (eukaryotic kanamycin resistance gene).

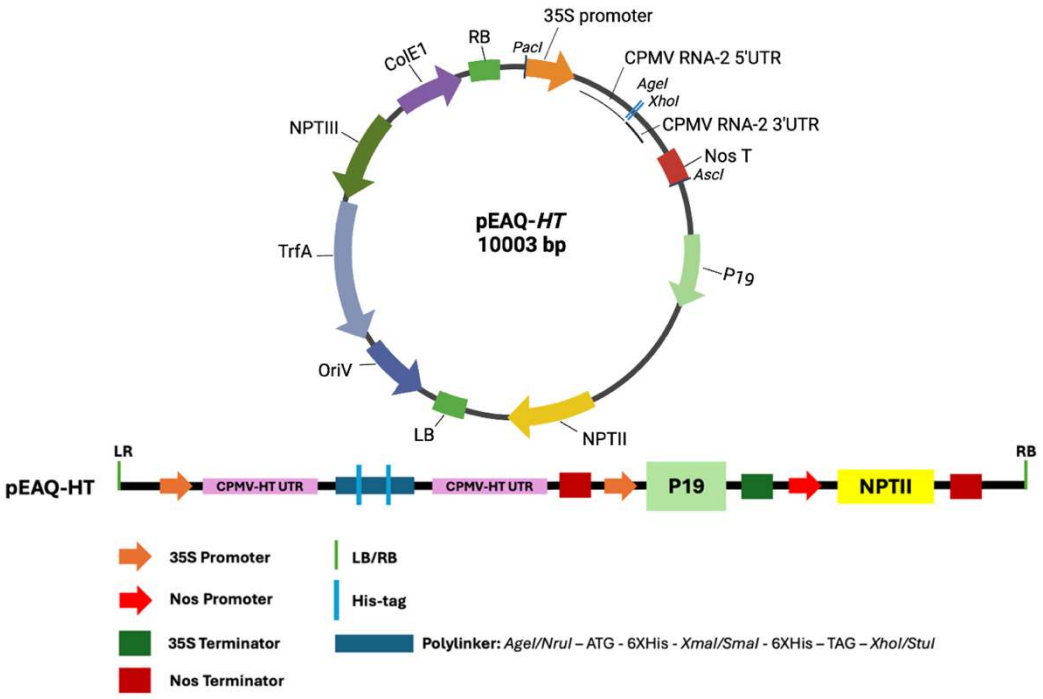

Figure 2. 6. Schematic representation of pEAQ-HT vector (Created with Biorender.com).

CPMV consists of 6kb RNA-1 and 3.5kb RNA-2 molecules and a single long open reading frame. The RNA-1 molecule encodes the viral the replication machinery and the 24K protease, enabling the release of the RNA-1 molecule with 24K activity. The RNA-2 molecule is dependent on the RNA-1 molecule and encodes viral sheath proteins and movement proteins [163].

3. MATERIALS AND METHOD

3.1. Plant Material

The seeds of *Nicotiana benthamiana* were obtained from Prof. Dr. Musa Kavas (Ondokuz Mayıs University, Samsun). Surface sterilization was carried out before the seeds were taken to medium culture. Firstly, the seeds were washed with 300 µl of 30 % $NaOCl^-$ (v/v) and then rinsed 3 times with 300 µl of ultrapure water. Surface-sterilized seeds were transferred in petri dishes containing ½ MS medium and kept at 4 ºC for 1 day. Seeds were germinated and led grow in growth chamber providing photoperiod of 24 ±2 ºC, 300 $\mu mol.m^{-2}.s^{-1}$, 70 % humidity and 16/8 hours (light/dark) photoperiod. Germinated *N. benthamiana* plantlets were sub-cultured after 21 days and allowed to grow under the same conditions for 30 days. Then, the plants were transferred to the soil in the Middle East Technical University (METU) greenhouse. For acclimatization, the plants were covered with nylon, after 3 days nylons were pierced, and removed at the end of 1 week. Finally, at the end of 2 months, new seeds were harvested and used to obtain the plant material for transient expression experiments.

3.2. Preparation of the plant transformation system

3.2.1. pEAQ vector series

3.2.1.1. Transformation of competent cells with pEAQ vector

The pEAQ vectors (pEAQ-HT and pEAQ-HT-GFP) were obtained from Leaf Expression Systems (UK) (Figure 3. 1). Firstly, vectors were first transferred to competent cells (NEB 10-beta Competent *E. coli* High Efficiency).

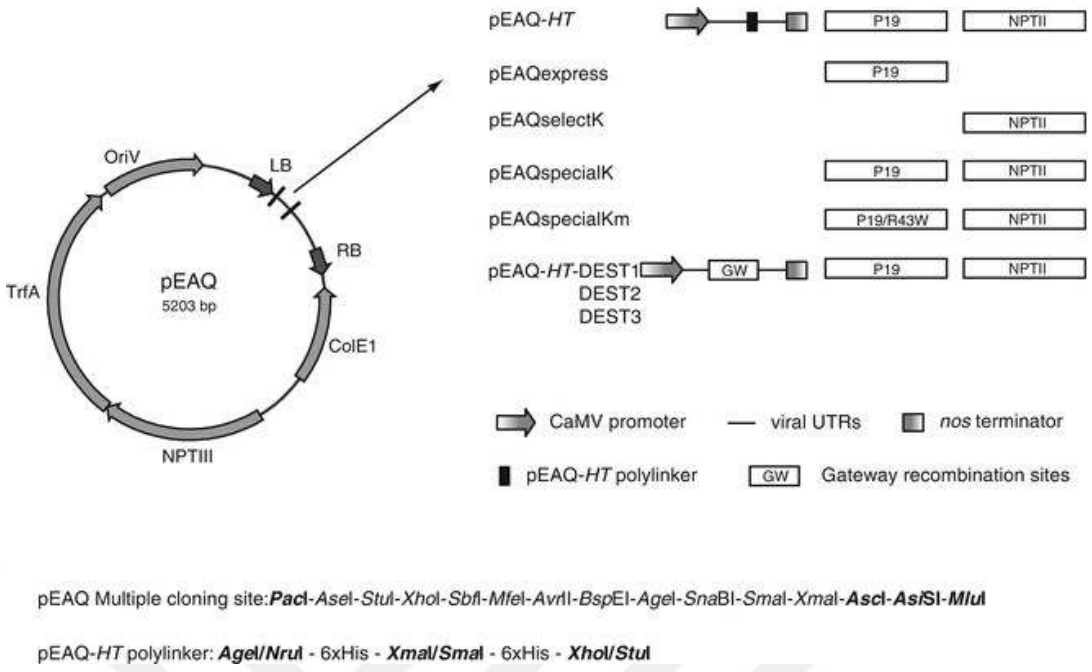

Figure 3. 1. Schematic image of pEAQ vector series.

The competent *E. coli* cells were taken from -80 °C onto the ice, and after thawing, 50 µl cells were transferred into a 1.5 ml Eppendorf tube. After adding 1 µl of vector to the bacteria, the tube was gently tapped 4-5 times and then incubated on ice for 30 min. After incubation, the cells were immersed in a water bath at 42 ºC and kept for 30 s, then quickly transferred to ice, and kept there for 5 min. Then, 950 µl of NEB 10-beta/Stable Outgrowth Medium at room temperature was added to it and incubated at 37 ºC for 60 min at 250 rpm. After incubation, 100 µl bacteria were inoculated directly or 10-fold diluted into petri dishes containing LB (Luria-Bertani) agar with kanamycin (50mg/L). Following over-night incubation at 37 ºC, positive colonies were selected by using colony-PCR.

3.2.1.2. Colony Polymerase Chain Reaction (PCR)

Colony PCR was performed to screen bacterial cells transferred with pEAQ-HT and pEAQ-GFP. 8-10 colonies were taken with a sterile toothpick and dissolved in 30 µl ultra-pure water and used as a template in the PCR reaction. The chemicals used in PCR and their concentrations are given in Table 3. 1. Annealing temperature was adjusted to be 2-3 ºC below Tm of the primers (Table 3. 2). Ultra-pure water was used as negative control, and the relevant plasmids were (diluted 10-fold) used as positive control. The primers targeting

p19 and NPTII were designed using the primer-BLAST program in the NCBI database and synthesized by Oligomer Biotechnology. The sequence information of the primers and the expected sizes of the amplification products are given in Table 3. 3.

Table 3. 1. PCR reaction components

Chemicals	**Stock Concentration**	**Final Concentration**	**Volume (µL)**
Gene Specific Primer F	10 µM	0.4 µM	1
Gene Specific Primer R	10 µM	0.4 µM	1
Dream Taq Buffer (including 2mM MgCl2)	10 X	1 X	2.5
dNTP	2.5 mM	0.2 µM	2
Dream Taq DNA polymerase	5 Unit/µl	0.1 U/µl	0.5
UPW			16
Template			2
Total			**25**

Table 3. 2. Colony PCR thermal cycler conditions

	Temperature (°C)	**Time**	**Number of Cycle**
Initial Denaturation	95	3 min	1
Denaturation	95	30 sec	35
Annealing	56	30 sec	
Extinction	72	1 min	
Final Extension	72	5 min	1

Table 3. 3. P19 and NPTII primers

Name of Primer	Direction	Sequence (5'->3')	Expected Amplicon Size
P19_F	Forward	GGAAACGACGCTAGGGAACA	231
P19_R	Reverse	CAGTGAAGCTTCCGTCCTGT	
NPTIII_F	Forward	AAGGGACTGGCTGCTATTGG	468
NPTIII_R	Reverse	TAAAGCACGAGGAAGCGGTC	

3.2.1.3. Plasmid isolation from bacteria

Positive colonies from 3.2.1.2 were inoculated into liquid LB medium with antibiotics (100 mg/L Kanamycin) and grown at 37 °C for 16 hours. The Monarch™ Plasmid Miniprep Kit (NEB, T1010) was used for plasmid isolation and the instructions given in the kit were followed. Accordingly, 1.5 ml of bacterial culture was precipitated by centrifugation at 16000 *g* for 30 s, and the supernatant was removed. 200 µl of B1 solution was added on the pellet and pipetting was done to dissolve the pellet. 200 µl of B2 was added on it and the tube was slightly inverted 5-6 times and kept at room temperature for 1 min. Then, 400 µl of B3 solution was added, the tube was gently inverted 5-6 times and kept at room temperature for 2 min. After the tubes were centrifuged at 16000 *g* for 5 min, the supernatants were transferred into the tube. Then, after centrifugation at 16000 *g* for 1 min, the collection tube was removed and replaced with a new one, and 200 µl of Washing Solution-1 (WB1) was added to the filter tube and centrifuged at 16000 *g* for 1 min. After centrifugation, 400 µl of Washing Solution-2 (WB2) was added to the filter tube and centrifuged at 16000 *g* for 1 min. The filtered tube was taken into a clean collection tube, 30 µl of Elution Buffer (EB) was added, and the plasmid solution was obtained by centrifuging at 16000 *g* for 1 min. Concentrations and purity of plasmids were measured on the NanoDrop (DeNovix, DS-11) instrument. It was then run on a 1.5 % Agarose gel to monitor the integrity of the plasmids. Finally, PCR was conducted by using isolated template and the respective primers as previously mentioned in 3.2.1.2. Amplification products were observed on the SYNGENE / GBOX-Chemi-XRQ imaging device after running on agarose gel.

3.2.2. Preparation of gene cassettes

The designs of the gene cassettes for VLP-ER (ER-targeted) and VLP-Chl (chloroplast targeted) were overviewed in Figure 3. 2. and explained in detail in the following sub-sections.

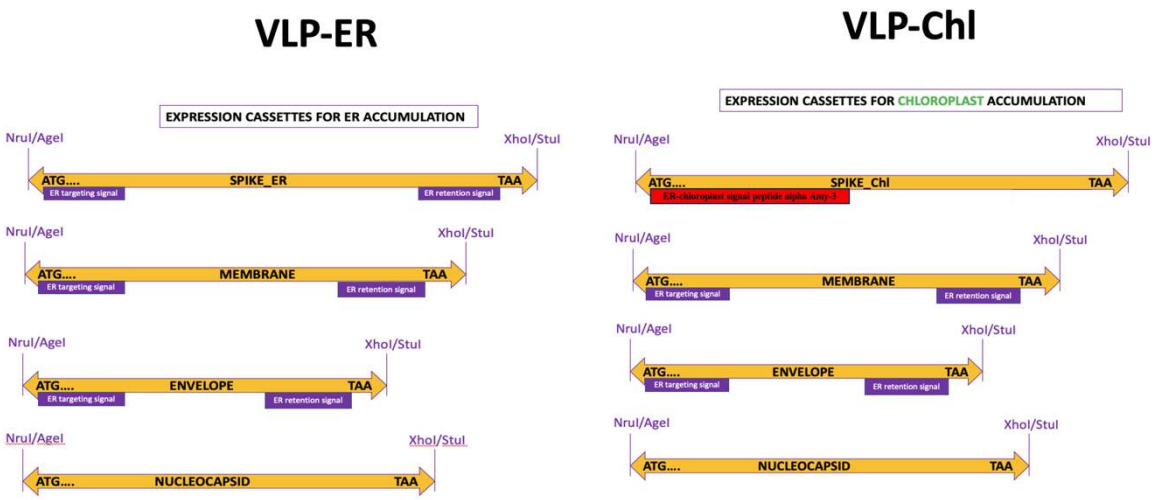

Figure 3. 2. General overview of the gene cassette designs for VLP-ER (ER-targeted) and VLP-Chl (chloroplast targeted). NruI/AgeI and XhoI/StuI: restriction enzymes, ATG: start codon, TAA: stop codon.

3.2.2.1. Envelop (E) gene

The E gene was designed based on the genome information of the Omicron variant in the NCBI database (GenBank OM287553), and codon optimization was carried out according to the *Nicotiana tabacum* via the EMBOSS program [164]. A few modifications were made while designing the gene cassette: restriction enzyme cutting sites (accggt for AgeI and ctcgag for XhoI, respectively) were added to the 5' and 3' ends of the gene. "Murine leader ER targeting signal" was added to the 5' end of the E gene and "SEKDEL ER retention signal" was added to the 3' end. The designed gene cassette was translated into amino acid sequence and analyzed for target signal with the 'TargetP' program. Accordingly, peaks occurred in the expected regions in the sequence of the E gene. The gene cassettes were synthesized synthetically by Eurofins.

3.2.2.1.1. Transformation of the plasmid harboring E gene cassette to competent cells

The synthesized cassette was obtained in the lyophilized plasmid (pEX-A128-E, 1.4 µg) which was dissolved in 140 µl of TE Buffer (10 mM Tris, 1 mM EDTA, pH: 8) and then was transferred to competent cells (NEB, 10-beta Competent *E. coli* High Efficiency) as described in 3.2.1.1. The cells were inoculated to LB agar medium with ampicillin (100 mg/L). Colony PCR was performed to screen bacteria transformed with pEX-A128-E as described in 3.2.1.2.

Table 3. 4. E primers.

Name of Primer	Direction	Sequence (5'->3')	Expected Amplicon Size
E-gene_F	Forward	ACCGGTATGGGATGGTCTTG	318
E-gene_R	Reverse	CCGCTCGAGCGGTTAAAG	
E-in_F	Forward	TGCTTTTGTTGTTTTTCTTCTTG	181
E-in_R	Reverse	AAGCTCATCCTTCTCAGAAACAA	
E-yeni_F	Forward	ATCGGACCGGTATGGGATGG	

Positive colonies for pEX-A128-E were inoculated into liquid LB medium with antibiotics (100mg/L Ampicillin) and grown at 37 °C for 16 hours. The Monarch™ Plasmid Miniprep Kit (NEB, T1010) was used for plasmid isolation and the instructions outlined in 3.2.1.3 were followed. After measuring the concentrations and purity of the plasmids in the NanoDrop (DeNovix, DS-11) device, they were also run on a 1.5% Agarose gel to observe their integrity. Finally, PCR was conducted with condition stated at Table 3. 1 and Table 3. 2.

3.2.2.2. Membrane (M) gene

The M gene was designed based on the genome information of the Omicron variant in the NCBI database (GenBank OM287553), and codon optimization was carried out according to the *Nicotiana tabacum* plant via the EMBOSS program [164]. A few modifications were made while designing the gene cassette: restriction enzyme cutting sites

(accggt for AgeI and ctcgag for XhoI, respectively) were added to the 5' and 3' ends of the gene. "Murine leader ER targeting signal" was added to the 5' end of the M gene and "SEKDEL ER retention signal" was added to the 3' end. The designed gene cassette was translated into amino acid sequence and analyzed for target signal with the 'TargetP' program. Accordingly, peaks occurred in the expected regions in the sequence of the M gene. The gene cassettes were synthesized synthetically by Eurofins.

3.2.2.2.1. Transformation of the plasmid harboring M gene cassette to competent cells

The synthesized cassette was obtained in the lyophilized plasmid (pEX-A128-M, 3 µg) which was dissolved in 140 µl of TE Buffer (10 mM Tris, 1 mM EDTA, pH: 8) and then was transferred to competent cells (NEB, 10-beta Competent *E. coli* High Efficiency) as described in 3.2.1.1. The cells were inoculated to LB agar medium with ampicillin (100 mg/L). Colony PCR was performed to screen bacteria transformed with pEX-A128-M as described in 3.2.1.2.

Table 3. 5. M primers

Name of Primer	Direction	Sequence (5'->3')	Expected Amplicon Size
M-gene_F	Forward	ACCGGTATGGGATGGTCTTGT	759
M-gene_R	Reverse	CCGCTCGAGCGGTTAAAGCT	
M-in_F	Forward	TGCTACTGGAGTTCATTCTGCT	195
M-in_R	Reverse	ACTGGCCAAAGAAGCCAAAGA	

Positive colonies for pEX-A128-M were inoculated into liquid LB medium with antibiotics (100mg/L Ampicillin) and grown at 37 °C for 16 hours. The Monarch™ Plasmid Miniprep Kit (NEB, T1010) was used for plasmid isolation and the instructions outlined in 3.2.1.3 were followed. After measuring the concentrations and purity of the plasmids in the NanoDrop (DeNovix, DS-11) device, they were also run on a 1.5% Agarose gel to observe their integrity. Finally, PCR was conducted with condition stated at Table 3. 1 and Table 3. 2.

3.2.2.3. Nucleocapsid (N) gene

The N gene was designed based on the genome information of the Omicron variant in the NCBI database (GenBank OM287553), and codon optimization was carried out according to the *Nicotiana tabacum* plant via the EMBOSS program [164]. A few modifications were made while designing the gene cassette: restriction enzyme cutting sites (accggt for AgeI and ctcgag for XhoI, respectively) were added to the 5' and 3' ends of the gene. No signal was added to N gene. The designed gene cassette was translated into amino acid sequence and analyzed for target signal with the 'TargetP' program. Accordingly, peaks occurred in the expected regions in the sequence of the N gene. The gene cassettes were synthesized synthetically by Eurofins.

3.2.2.3.1. Transformation of the plasmid harboring N gene cassette to competent cells

The synthesized cassette was obtained in the lyophilized plasmid (pEX-A128-N, 1.4 µg) which was dissolved in 140 µl of TE Buffer (10 mM Tris, 1 mM EDTA, pH: 8) and then was transferred to competent cells (NEB, 10-beta Competent *E. coli* High Efficiency) as described in 3.2.1.1. The cells were inoculated to LB agar medium with ampicillin (100 mg/L). Colony PCR was performed to screen bacteria transformed with pEX-A128-N as described in 3.2.1.2.

Table 3. 6. N primers

Name of Primer	Direction	Sequence (5'->3')	Expected Amplicon Size
N-gene_F	Forward	ACCGGTATGTCTGATAATGGAC	306
N-gene_R	Reverse	CCGCTCGAGCGGTTAAG	
N-in_F	Forward	GCATTGGCCACAAATTGCTC	1269
N-in_R	Reverse	TCAAGATCAGCAGCTGGAAGA	

Positive colonies for pEX-A128-N were inoculated into liquid LB medium with antibiotics (100mg/L Ampicillin) and grown at 37 °C for 16 hours. The Monarch™ Plasmid Miniprep Kit (NEB, T1010) was used for plasmid isolation and the instructions outlined in

3.2.1.3 were followed. After measuring the concentrations and purity of the plasmids in the NanoDrop (DeNovix, DS-11) device, they were also run on a 1.5% Agarose gel to observe their integrity. Finally, PCR was conducted with condition stated at Table 3. 1 and Table 3. 2.

3.2.2.4. Spike (S) gene and Spike-chloroplast (S-chl)

The design of the S gene was based on the genome information of the Omicron variant in the NCBI database (GenBank OM287553), and codon optimization was carried out according to the *Nicotiana tabacum* plant through the EMBOSS program [164]. A number of modifications were made to the gene designs: restriction enzyme cutting sites (accggt for AgeI and ctcgag for XhoI, respectively) were added to the 5' and 3' ends of the gene. The natural signal peptide at the 5' end of the ER-targeting S gene was replaced with the "Murine leader ER targeting signal" sequence [165], and the signal at the 3' end was replaced with the sequence "SEKDEL ER retention signal". To increase the possibility of spike trimerization, the "GCN4p-II Trimerization domain" sequence was added to the 3' end before the signal, and then the "TEV protease cleavage site" sequence was added to remove it. Two proline changes (S-2P: K983P and V984P) were made to ensure the stabilization of the prefusion conformation of the S protein [166], and R679G, R680S, R682S changes were made in the S1/S2 cut region to increase stability [9]. In order to direct the assembled VLPs to chloroplast S-chl gene cassette was designed, where ER retention signal was removed, and ER-targeting signal was replaced with αAmy3 signal peptide of rice (*Oryza sativa*) α-amylase [167]. The designed gene cassettes were translated into amino acid sequence and analyzed for target signal with the TargetP program. Peaks were formed in the expected regions in the S sequences. Following the completion of the design, the genes were synthesized synthetically by Eurofins.

3.2.2.4.1. Transformation of the plasmid harboring Spike (S) and Spike-chloroplast (S-chl) gene cassette to competent cells

The synthesized cassette was obtained in the lyophilized plasmid (pUC57-S and pUC57-S-chl, 4 µg) which was dissolved in 400 µl of TE Buffer (10 mM Tris, 1 mM EDTA, pH: 8) and then was transferred to competent cells (NEB, 10-beta Competent *E. coli* High Efficiency) as described in 3.2.1.1. The cells were inoculated to LB agar medium with

ampicillin (100 mg/L). Colony PCR was performed to screen bacteria transformed with pEX-A128-E as described in 3.2.1.2.

Table 3. 7. S and S-chl primers

Name of Primer	Direction	Sequence (5'->3')	Expected Amplicon Size
S-gene_F	Forward	ATCGGACCGGTATGGGATGG	3980
S-gene_R	Reverse	CCGCTCGAGCGGTTAAAGCT	
S-in_F	Forward	TGCTTGGGTGATATTGCTGC	658
S-in_R	Reverse	CATGTGGAGCAGATTGTGGA	
S-chl-gene_F	Forward	ATCGCACCGGTATGAAGAAT	3999
S-chl-gene_R	Reverse	CCGCTCGAGCGGTTATCTTT	

Positive colonies for pUC57-S and pUC57-S-chl were inoculated into liquid LB medium with antibiotics (100mg/L Ampicillin) and grown at 37 °C for 16 hours. The Monarch™ Plasmid Miniprep Kit (NEB, T1010) was used for plasmid isolation and the instructions outlined in 3.2.1.3 were followed. After measuring the concentrations and purity of the plasmids in the NanoDrop (DeNovix, DS-11) device, they were also run on a 1.5% Agarose gel to observe their integrity. Finally, PCR was conducted with condition stated at Table 3. 1 and Table 3. 2.

3.2.3. Cloning of gene of interests (GOIs) into plant expression vector

3.2.3.1. Cloning E gene into pEAQ-HT vector

In order to clone the E gene expression cassette into the pEAQ-HT plasmid, the E gene was amplified by Q5 High-Fidelity DNA Polymerase (NEB, M0491S) using E-YENİ_F and E-gene_R primers. The chemicals used in PCR and their concentrations are given in Table 3. 8. Ultra-pure water was used as negative control. 'NEB Tm Calculator (https//tmcalculator.neb.com/#!/main#!%2F)' program was used to calculate the annealing temperature (Table 3. 9). The amplification products were observed on the imaging device after running on the agarose gel.

Table 3. 8. PCR protocol for amplifying E-gene with Q5 High-Fidelity DNA Polymerase.

Chemicals	Stock Concentration	Final Concentration	Volume (µL)
Gene Specific Primer F	10 µM	0.5 µM	2.5
Gene Specific Primer R	10 µM	0.5 µM	2.5
Q5 Reaction Buffer	5 X	1 X	10
dNTP	10 mM	0.2 µM	1
Q5 High-Fidelity DNA Polymerase	2 Unit/µl	0.02 U/µl	0.5
UPW			31.5
Template			2
Total			**50**

Table 3. 9. Thermal cycler condition for amplifying E-gene by using Q5 High-Fidelity DNA Polymerase.

	Temperature (°C)	Time	Number of Cycle
Preheated	98	30 sec	
Denaturation	98	10 sec	
Annealing	63	20 sec	30
Extinction	72	30 sec	
Final Extension	72	3 min	1

Magnetic beads (MAGBIO, HighPrepTM PCR Clean-up System) were used to purify PCR products. Accordingly, magnetic beads, 1.8-fold the volume, were added at 1ç8 times the volume to the PCR product, and incubated for 5 min. Then, the magnetic beads were separated on the magnetic separator rack. The separated liquid was removed without moving the PCR product over the magnetic separator rack. Magnetic beads were first washed with 200 µl of 80 % ethanol for 5 min. After, ethanol was removed, PCR products were removed from the magnetic separator rack and dissolved with 30 µl Elution Buffer for 5 min. The concentration of the purified PCR product was measured on the Qubit (Qubit 3.0 Fluorometer).

The purified E gene PCR product was digested by the "Double Digestion" method. Double digestion reaction mixture (for 1X) containing 35.3 µl of distilled water, 5 µl of rCutSmart Buffer (10X), 0.5 µl of 7 µl of purified E gene PCR product (1 µg) was prepared and incubated for 30 min at 37 °C and 20 min at 65 °C for digestion. Following incubation, the reaction tube was placed on ice. Double digestion reaction mixture for pEAQ-HT plasmid (for 1X); 40.4 µl of distilled water, 5 µl of rCutSmart Buffer (10 X), 0.5 µl of XhoI restriction enzyme (NEB, R0146S, 20 U/µl), 0.5 µl of AgeI-HF restriction enzyme (NEB, R3552S, 20 U/µl) and 3.5 µl plasmid (1 µg). Plasmid digestion was conducted by incubation for 30 min at 37 °C and 20 min at 65°C. In order to dephosphorylate the digested plasmid, 1 µl Quick CIP (NEB, M0525S) was added for dephosphorylation and after incubation for 30 min at 37 °C. The reaction was stopped by keeping it at 80 °C for 2 min. The digested E gene product and pEAQ-HT plasmid were purified with magnetic beads as described before, and their concentrations were measured in the Qubit device.

https//nebiocalculator.neb.com/#!/ligation program was used for the ligation of the double digested E gene and the pEAQ-HT plasmid. The chemicals and their volumes used in ligation of E and pEAQ-HT vector are given in Table 3. 10.

Table 3. 10. Ligation protocols for pEAQ-HT and E-gene.

Ligation for 1:7 Ratio		**Ligation for 1:10 Ratio**	
Chemicals	**Volume (µl)**	**Chemicals**	**Volume (µl)**
T4 Buffer	2	T4 Buffer	2
T4 DNA Enzyme	1	T4 DNA Enzyme	1
Insert (0.14 pmol, 13.97 ng)	0.6	Insert (0.2 pmol, 19.96 ng)	0.9
Plasmid (0.02 pmol, 123.6 ng)	5.2	Plasmid (0.02 pmol, 123.6 ng)	5.2
UPW	11.2	UPW	10.9
Total	**20**	**Total**	**20**

Ligation was performed with 16 hours incubation at 16 °C for 16 hours and at 65 °C for 10 min. The reaction was stopped at +4 °C. After ligation, the products were first transferred to competent cells (NEB, 10-beta Competent *E. coli* High Efficiency) as described in 3.2.1.1. In order to validate both insertion and orientation of the E gene. Colony-

PCR was performed with insert specific (E-in) and orientation primers (HT-5UTR_F and E-in R) as described in 3.2.2.1.1.

In order to perform plasmid isolation, selected colonies were inoculated in liquid LB medium with antibiotics (50 mg/L kanamycin) and grown at 37 °C for 16 hours. Monarch™ Plasmid Miniprep Kit (NEB, T1010) was used for plasmid isolation and the instructions in the kit were applied as described in 3.2.1.3. After the concentrations and purities of the plasmids were measured on the NanoDrop (DeNovix, DS-11) device, they were also run on agarose gel. Confirmed plasmids were amplified by PCR under the previously stated conditions using the relevant primers, and the amplification products were observed on the imaging device after running on 1 % agarose gel.

The final plasmid named as pEAQ-HT-E was sent to the INTERGEN Genetics and Rare Diseases Diagnostic Center for sequencing and sequence analysis. As a result of the sequencing, Egene.fasta, Egene.bam, Egene.bam.bai files were received, and the sequence of the E gene was obtained using the Integrative Genome Viewer (IGV) application. This sequence was aligned with the original construct using the Cluster Omega (https//ebi.ac.uk/Tools/msa/clustalo/) program.

3.2.3.2. Cloning M gene into pEAQ-HT vector

In order to clone the M gene expression cassette into the pEAQ-HT plasmid, the M gene was amplified by Q5 High-Fidelity DNA Polymerase (NEB, M0491S) using E-YENİ_F and M-gene_R primers. The chemicals used in PCR and their concentrations are given in Table 3. 11. Ultra-pure water was used as negative control. 'NEB Tm Calculator (https//tmcalculator.neb.com/#!/main#!%2F)' program was used to calculate the annealing temperature (Table 3. 12). The amplification products were observed on the imaging device after running on the agarose gel.

Table 3. 11. PCR protocol for amplifying M-gene with Q5 High-Fidelity DNA Polymerase.

Chemicals	Stock Concentration	Final Concentration	Volume (µL)
Gene Specific Primer F	10 µM	0.5 µM	2.5
Gene Specific Primer R	10 µM	0.5 µM	2.5
Q5 Reaction Buffer	5 X	1 X	10
dNTP	10 mM	0.2 µM	1
Q5 High-Fidelity DNA Polymerase	2 Unit/µl	0.02 U / µl	0.5
UPW			31.5
Template			2
Total			**50**

Table 3. 12. Thermal cycler condition for amplifying M-gene by using Q5 High-Fidelity DNA Polymerase.

	Temperature (°C)	Time	Number of Cycle
Preheated	98	30 sec	
Denaturation	98	10 sec	
Annealing	70	20 sec	30
Extinction	72	30 sec	
Final Extension	72	3 min	1

Magnetic beads were used to purify PCR products as described in 3.2.3.1.1 The concentration of the purified PCR product was measured on the NanoDrop (DeNovix, DS-11).

The purified M gene PCR product was digested by the “Double Digestion” method. Double digestion reaction mixture (for 1X) containing 34 µl of distilled water, 5 µl of rCutSmart Buffer (10X), 0.5 µl of 10 µl of purified M gene PCR product (1 µg) was prepared and incubated for 30 min at 37 °C and 20 min at 65 °C for digestion. Following incubation, the reaction tube was placed on ice. Double digestion reaction mixture for pEAQ-HT plasmid (for 1X); 40.5 µl of distilled water, 5 µl of rCutSmart Buffer (10 X), 0.5 µl of XhoI

restriction enzyme (NEB, R0146S, 20U/µl), 0.5 µl of AgeI-HF restriction enzyme (NEB, R3552S, 20 U/µl) and 3.5 µl plasmid (1 µg). Plasmid digestion was conducted by incubation for 30 min at 37 °C and 20 min at 65 °C. In order to dephosphorylate the digested plasmid, 1 µl Quick CIP (NEB, M0525S) was added for dephosphorylation and after incubation for 30 min at 37 °C. The reaction was stopped by keeping it at 80 °C for 2 min. The digested M gene product and pEAQ-HT plasmid were purified with magnetic beads as described before, and their concentrations were measured in the Qubit device.

https//nebiocalculator.neb.com/#!/ligation program was used for the ligation of the double digested M gene and the pEAQ-HT plasmid. The chemicals and their volumes used in ligation of M and pEAQ-HT vector are given in Table 3. 13.

Table 3. 13. Ligation protocols for pEAQ-HT and M-gene.

Ligation for 1:5 Ratio		**Ligation for 1:7 Ratio**	
Chemicals	**Volume (µl)**	**Chemicals**	**Volume (µl)**
T4 Buffer	2	T4 Buffer	2
T4 DNA Enzyme	1	T4 DNA Enzyme	1
Insert (0.1 pmol, 47.35 ng)	1.2	Insert (0.14 pmol, 66.3 ng)	1.7
Plasmid (0.02 pmol, 123.6 ng)	3.85	Plasmid (0.02 pmol, 123.6 ng)	3.85
UPW	11.95	UPW	11.5
Total	**20**	**Total**	**20**

Ligation was performed with 16 hours incubation at 16 °C for 16 hours and at 65 °C for 10 min. The reaction was stopped at +4 °C. After ligation, the products were first transferred to competent cells (NEB, 10-beta Competent *E. coli* High Efficiency) as described in 3.2.1.1. In order to validate both insertion and orientation of the M gene. Colony-PCR was performed with insert specific (M-in) and orientation primers (HT-5UTR_F and M-in R) as described in 3.2.2.1.1.

In order to perform plasmid isolation, selected colonies were inoculated in liquid LB medium with antibiotics (50 mg/L kanamycin) and grown at 37°C for 16 hours. Monarch™ Plasmid Miniprep Kit (NEB, T1010) was used for plasmid isolation and the instructions in the kit were applied as described in 3.2.1.3. After the concentrations and purities of the

plasmids were measured on the NanoDrop (DeNovix, DS-11) device, they were also run on agarose gel. Confirmed plasmids were amplified by PCR under the previously stated conditions using the relevant primers and the amplification products were observed on the imaging device after running on 1 % agarose gel.

The final plasmid named as pEAQ-HT-M was sent to the INTERGEN Genetics and Rare Diseases Diagnostic Center for sequencing and sequence analysis. As a result of the sequencing, Mgene.fasta, Mgene.bam, Mgene.bam.bai files were received, and the sequence of the M gene was obtained using the Integrative Genome Viewer (IGV) application. This sequence was aligned with the original construct using the Cluster Omega (https//ebi.ac.uk/Tools/msa/clustalo/) program.

3.2.3.2.1. Cloning N gene into pEAQ-HT vector

In order to clone the N gene expression cassette into the pEAQ-HT plasmid, the N gene was amplified by Q5 High-Fidelity DNA Polymerase (NEB, M0491S) using N-YENİ2_F and N-gene_R primers. The chemicals used in PCR and their concentrations are given in Table 3. 14. Ultra-pure water was used as negative control. 'NEB Tm Calculator (https//tmcalculator.neb.com/#!/main#!%2F)' program was used to calculate the annealing temperature (Table 3. 15). The amplification products were observed on the imaging device after running on the agarose gel.

Table 3. 14. PCR protocol for amplifying N-gene with Q5 High-Fidelity DNA Polymerase.

Chemicals	**Stock Concentration**	**Final Concentration**	**Volume (µL)**
Gene Specific Primer F	10 µM	0.5 µM	2.5
Gene Specific Primer R	10 µM	0.5 µM	2.5
Q5 Reaction Buffer	5 X	1 X	10
dNTP	10 mM	0.2 µM	1
Q5 High-Fidelity DNA Polymerase	2 Unit/µl	0.02 U/µl	0.5
UPW			31.5
Template			2
Total			**50**

Table 3. 15. Thermal cycler condition for amplifying N-gene by using Q5 High-Fidelity DNA Polymerase.

	Temperature (°C)	**Time**	**Number of Cycle**
Preheated	98	30 sec	
Denaturation	98	10 sec	
Annealing	64	20 sec	30
Extinction	72	30 sec	
Final Extension	72	3 min	1

Magnetic beads were used to purify PCR products as described in 3.2.3.1.1. The concentration of the purified PCR product was measured on the NanoDrop (DeNovix, DS-11).

The purified N gene PCR product was digested by the "Double Digestion" method. Double digestion reaction mixture (for 1X) containing 27.92 µl of distilled water, 5 µl of rCutSmart Buffer (10X), 0.5 µl of 10 µl of purified N gene PCR product (1 µg) was prepared and incubated for 30 min at 37 °C and 20 min at 65 °C for digestion. Following incubation, the reaction tube was placed on ice. Double digestion reaction mixture for pEAQ-HT plasmid (for 1X); 40.5 µl of distilled water, 5 µl of rCutSmart Buffer (10 X), 0.5 µl of XhoI restriction enzyme (NEB, R0146S, 20U/µl), 0.5 µl of AgeI-HF restriction enzyme (NEB, R3552S, 20 U/µl) and 3.5 µl plasmid (1 µg). Plasmid digestion was conducted by incubation for 30 min at 37 °C and 20 min at 65 °C. In order to dephosphorylate the digested plasmid, 1 µl Quick CIP (NEB, M0525S) was added for dephosphorylation and after incubation for 30 min at 37 °C. The reaction was stopped by keeping it at 80 °C for 2 min. The digested N gene product and pEAQ-HT plasmid were purified with magnetic beads as described before, and their concentrations were measured in the Qubit device.

https//nebiocalculator.neb.com/#!/ligation program was used for the ligation of the double digested N gene and the pEAQ-HT plasmid. The chemicals and their volumes used in ligation of N and pEAQ-HT vector are given in Table 3. 16.

Table 3. 16. Ligation protocols for pEAQ-HT and N-gene.

Ligation for 1:3 Ratio		**Ligation for 1:5 Ratio**	
Chemicals	**Volume (µl)**	**Chemicals**	**Volume (µl)**
T4 Buffer	2	T4 Buffer	2
T4 DNA Enzyme	1	T4 DNA Enzyme	1
Insert (0.06 pmol, 46.38 ng)	1.44	Insert (0.1 pmol, 77.31 ng)	2.4
Plasmid (0.02pmol, 123.6 ng)	3.85	Plasmid (0.02pmol, 123.6 ng)	3.85
UPW	11.75	UPW	10.8
Total	**20**	**Total**	**20**

Ligation was performed with 16 hours incubation at 16 °C for 16 hours and at 65 °C for 10 min. The reaction was stopped at +4 °C. After ligation, the products were first transferred to competent cells (NEB, 10-beta Competent *E. coli* High Efficiency) as described in 3.2.1.1. In order to validate both insertion and orientation of the N gene. Colony-PCR was performed with insert specific (N-in) and orientation primers (HT-5UTR_F and N-in R) as described in 3.2.2.1.1.

In order to perform plasmid isolation, selected colonies were inoculated in liquid LB medium with antibiotics (50 mg/L kanamycin) and grown at 37°C for 16 hours. Monarch™ Plasmid Miniprep Kit (NEB, T1010) was used for plasmid isolation and the instructions in the kit were applied as described in 3.2.1.3. After the concentrations and purities of the plasmids were measured on the NanoDrop (DeNovix, DS-11) device, they were also run on agarose gel. Confirmed plasmids were amplified by PCR under the previously stated conditions using the relevant primers, and the amplification products were observed on the imaging device after running on 1 % agarose gel.

The final plasmid named as pEAQ-HT-N was sent to the INTERGEN Genetics and Rare Diseases Diagnostic Center for sequencing and sequence analysis. As a result of the sequencing, Ngene.fasta, Ngene.bam, Ngene.bam.bai files were received, and the sequence of the N gene was obtained using the Integrative Genome Viewer (IGV) application. This sequence was aligned with the original construct using the Cluster Omega (https//ebi.ac.uk/Tools/msa/clustalo/) program.

3.2.3.2.2. Cloning S gene into pEAQ-HT vector

In order to clone the S gene expression cassette into the pEAQ-HT plasmid, the S gene was amplified by Q5 High-Fidelity DNA Polymerase (NEB, M0491S) using S-gene_F and S-gene_R primers. The chemicals used in PCR and their concentrations are given in Table 3. 17. Ultra-pure water was used as negative control. 'NEB Tm Calculator (https//tmcalculator.neb.com/#!/main#!%2F)' program was used to calculate the annealing temperature (Table 3. 18). The amplification products were observed on the imaging device after running on the agarose gel.

Table 3. 17. PCR protocol for amplifying S-gene with Q5 High-Fidelity DNA Polymerase.

Chemicals	**Stock Concentration**	**Final Concentration**	**Volume (µL)**
Gene Specific Primer F	10 µM	0.5 µM	2.5
Gene Specific Primer R	10 µM	0.5 µM	2.5
Q5 Reaction Buffer	5 X	1 X	10
dNTP	10 mM	0.2 µM	1
Q5 High-Fidelity DNA Polymerase	2 Unit/µl	0.02 U/ µl	0.5
UPW			31.5
Template			2
Total			**50**

Table 3. 18. Thermal cycler condition for amplifying S-gene by using Q5 High-Fidelity DNA Polymerase.

	Temperature (°C)	**Time**	**Number of Cycle**
Preheated	98	30 sec	
Denaturation	98	10 sec	
Annealing	70	20 sec	30
Extinction	72	2 min	
Final Extension	72	3 min	1

Magnetic beads were used to purify PCR products as described in 3.2.3.1.1 The concentration of the purified PCR product was measured on the NanoDrop (DeNovix, DS-11).

The purified S gene PCR product was digested by the "Double Digestion" method. Double digestion reaction mixture (for 1X) containing 38.87 µl of distilled water, 5 µl of rCutSmart Buffer (10X), 0.5 µl of 5.13 µl of purified S gene PCR product (1 µg) was prepared and incubated for 30 min at 37 °C and 20 min at 65 °C for digestion. Following incubation, the reaction tube was placed on ice. Double digestion reaction mixture for pEAQ-HT plasmid (for 1X); 40.5 µl of distilled water, 5 µl of rCutSmart Buffer (10 X), 0.5 µl of XhoI restriction enzyme (NEB, R0146S, 20U/µl), 0.5 µl of AgeI-HF restriction enzyme (NEB, R3552S, 20 U/µl) and 3.5 µl plasmid (1 µg). Plasmid digestion was conducted by incubation for 30 min at 37 °C and 20 min at 65 °C. In order to dephosphorylate the digested plasmid, 1 µl Quick CIP (NEB, M0525S) was added for dephosphorylation and after incubation for 30 min at 37 °C. The reaction was stopped by keeping it at 80 °C for 2 min. The digested S gene product and pEAQ-HT plasmid were purified with magnetic beads as described before, and their concentrations were measured in the Qubit device.

https//nebiocalculator.neb.com/#!/ligation program was used for the ligation of the double digested S gene and the pEAQ-HT plasmid. The chemicals and their volumes used in ligation of S and pEAQ-HT vector are given in Table 3. 19.

Table 3. 19. Ligation protocol for pEAQ-HT and S-gene.

Ligation for 1:3 Ratio	
Chemicals	**Volume (µl)**
T4 Buffer	2
T4 DNA Enzyme	1
Insert (0.06 pmol, 46.38 ng)	1.44
Plasmid (0.02pmol, 123.6 ng)	3.85
UPW	11.75
Total	**20**

Ligation was performed with 16 hours incubation at 16°C for 16 hours and at 65 °C for 10 min. The reaction was stopped at +4 °C. After ligation, the products were first transferred to competent cells (NEB, 10-beta Competent *E. coli* High Efficiency) as described in 3.2.1.1. In order to validate both insertion and orientation of the S gene. Colony-PCR was performed with insert specific (S-in) and orientation primers (HT-5UTR_F and S-in R) as described in 3.2.2.1.1.

In order to perform plasmid isolation, selected colonies were inoculated in liquid LB medium with antibiotics (50 mg/L kanamycin) and grown at 37°C for 16 hours. Monarch™ Plasmid Miniprep Kit (NEB, T1010) was used for plasmid isolation and the instructions in the kit were applied as described in 3.2.1.3. After the concentrations and purities of the plasmids were measured on the NanoDrop (DeNovix, DS-11) device, they were also run on agarose gel. Confirmed plasmids were amplified by PCR under the previously stated conditions using the relevant primers and the amplification products were observed on the imaging device after running on 1 % agarose gel.

The final plasmid named as pEAQ-HT-S was sent to the INTERGEN Genetics and Rare Diseases Diagnostic Center for sequencing and sequence analysis. As a result of the sequencing, Sgene.fasta, Sgene.bam, Sgene.bam.bai files were received, and the sequence of the S gene was obtained using the Integrative Genome Viewer (IGV) application. This sequence was aligned with the original construct using the Cluster Omega (https//ebi.ac.uk/Tools/msa/clustalo/) program.

3.2.3.2.3. Cloning S-chl gene into pEAQ-HT vector

In order to clone the S-chl gene expression cassette into the pEAQ-HT plasmid, the S-chl gene was amplified by Q5 High-Fidelity DNA Polymerase (NEB, M0491S) using S-chl-gene_F and S-chl-gene_R primers. The chemicals used in PCR and their concentrations are given in Table 3. 20. Ultra-pure water was used as negative control. 'NEB Tm Calculator (https//tmcalculator.neb.com/#!/main#!%2F)' program was used to calculate the annealing temperature (Table 3. 21). The amplification products were observed on the imaging device after running on the agarose gel.

Table 3. 20. PCR protocol for amplifying S-chl-gene with Q5 High-Fidelity DNA Polymerase.

Chemicals	Stock Concentration	Final Concentration	Volume (µL)
Gene Specific Primer F	10 µM	0.5 µM	2.5
Gene Specific Primer R	10 µM	0.5 µM	2.5
Q5 Reaction Buffer	5X	1 X	10
dNTP	10 mM	0.2 µM	1
Q5 High-Fidelity DNA Polymerase	2 Unit/µl	0.02 U/µl	0.5
UPW			31.5
Template			2
Total			**50**

Table 3. 21. Thermal cycler condition for amplifying S-chl-gene by using Q5 High-Fidelity DNA Polymerase.

	Temperature (°C)	Time	Number of Cycle
Preheated	98	30 sec	
Denaturation	98	10 sec	
Annealing	65	20 sec	30
Extinction	72	2 min	
Final Extension	72	3 min	1

Magnetic beads were used to purify PCR products as described in 3.2.3.1.1 The concentration of the purified PCR product was measured on the NanoDrop (DeNovix, DS-11).

The purified S-chl gene PCR product was digested by the “Double Digestion” method. Double digestion reaction mixture (for 1X) containing 28.62 µl of distilled water, 5 µl of rCutSmart Buffer (10X), 0.5 µl of 15.38 µl of purified S-chl gene PCR product (1 µg) was prepared and incubated for 30 min at 37 ^{o}C and 20 min at 65 ^{o}C for digestion. Following incubation, the reaction tube was placed on ice. Double digestion reaction mixture for pEAQ-HT plasmid (for 1X); 40.5 µl of distilled water, 5 µl of rCutSmart Buffer (10 X), 0.5

µl of XhoI restriction enzyme (NEB, R0146S, 20U/µl), 0.5 µl of AgeI-HF restriction enzyme (NEB, R3552S, 20 U/µl) and 3.5 µl plasmid (1 µg). Plasmid digestion was conducted by incubation for 30 min at 37 ºC and 20 min at 65ºC. In order to dephosphorylate the digested plasmid, 1 µl Quick CIP (NEB, M0525S) was added for dephosphorylation and after incubation for 30 min at 37 ºC. The reaction was stopped by keeping it at 80 ºC for 2 min. The digested S-chl gene product and pEAQ-HT plasmid were purified with magnetic beads as described before, and their concentrations were measured in the Qubit device.

https//nebiocalculator.neb.com/#!/ligation program was used for the ligation of the double digested S-chl gene and the pEAQ-HT plasmid. The chemicals and their volumes used in ligation of S-chl and pEAQ-HT vector are given in Table 3. 22.

Table 3. 22. Ligation protocol for pEAQ-HT and S-chl-gene.

Ligation for 1:3 Ratio	
Chemicals	**Volume (µl)**
T4 Buffer	2
T4 DNA Enzyme	1
Insert (0.06 pmol, 147.8 ng)	5.68
Plasmid (0.02pmol, 123.6 ng)	3.85
UPW	7.46
Total	**20**

Ligation was performed with 16 hours incubation at 16ºC for 16 hours and at 65 ºC for 10 min. The reaction was stopped at +4 ºC. After ligation, the products were first transferred to competent cells (NEB, 10-beta Competent *E. coli* High Efficiency) as described in 3.2.1.1. In order to validate both insertion and orientation of the S-chl gene. Colony-PCR was performed with insert specific (S-in) and orientation primers (HT-5UTR_F and S-in R) as described in 3.2.2.1.1.

In order to perform plasmid isolation, selected colonies were inoculated in liquid LB medium with antibiotics (50 mg/L kanamycin) and grown at 37°C for 16 hours. Monarch™ Plasmid Miniprep Kit (NEB, T1010) was used for plasmid isolation and the instructions in the kit were applied as described in 3.2.1.3. After the concentrations and purities of the plasmids were measured on the NanoDrop (DeNovix, DS-11) device, they were also run on

agarose gel. Confirmed plasmids were amplified by PCR under the previously stated conditions using the relevant primers and the amplification products were observed on the imaging device after running on 1 % agarose gel.

The final plasmid named as pEAQ-HT-S-chl was sent to the INTERGEN Genetics and Rare Diseases Diagnostic Center for sequencing and sequence analysis. As a result of the sequencing, Schlgene.fasta, Schlgene.bam, Schlgene.bam.bai files were received, and the sequence of the S-chl gene was obtained using the Integrative Genome Viewer (IGV) application. This sequence was aligned with the original construct using the Cluster Omega (https//ebi.ac.uk/Tools/msa/clustalo/) program.

3.2.4. Transformation of *Agrobacterium tumefaciens* with plant expression vector

3.2.4.1. Preparation of *Agrobacterium* competent cells

A. tumefaciens LBA4404 (Goldbio, CC-220) strain used for expression studies in this thesis. For this purpose, competent *Agrobacterium* cells were prepared. Firstly, 975 µl Recovery Media (GoldBio) was added to 25 µl bacterial sample taken from the LBA4404 strain and allowed to grow at 200 rpm at 28 °C for 3 hours. Then, 200 µl of bacterial solution was added to LB Agar (streptomycin and rifampicin) medium with glass beads and allowed to grow at 200 rpm at 28℃ for 3 hours. 5 ml liquid YE medium (for 1L: 1 g Yeast Extract, 13.5 g Nutrient Broth, 0.493 g $MgSO_4.7H_2O$, 5 g sucrose and pH: 7) containing streptomycin (50 mg/L) and rifampicin (25 mg/L) antibiotics selected from the growing bacterial colonies, incubated overnight at 200 rpm at 28℃. To prepare competent cells, 100 µl of the bacteria measured as OD550: 0.9477 was inoculated into 40 ml of liquid YE medium containing Step50 antibiotic into 250 ml flask and incubated overnight at 200 rpm at 28℃ to grow. Cells with OD550: 1.1828 were pelleted at 3500 *g* at 4℃ for 5 min and then the supernatant was removed. The pellet was thawed on ice with 10 ml of pre-cooled 10 % sterile glycerol solution and centrifuged again at 3500 *g* at 4℃ for 5 min and the upper phase was removed again. After this process was repeated once more, the pellet was dissolved with 2 ml of 10 % sterile glycerol and 100 µl aliquots were transferred into pre-chilled Eppendorf tubes. Then, competent *Agrobacterium* cells were removed to be stored at -80℃.

3.2.4.2. Transformation of *Agrobacterium* with pEAQ-HT-GOI plasmid

Competent LBA4404 cells were first transferred from -80 °C to dry ice and thawed on ice before electroporation. Electroporator (Gune Pulser Xcell Electroporator, Ankara University Biotechnology Institute) was set as given in Table 3. 23. Then, 1 µl of pEAQ-HT plasmid (1 ng) was added onto 25 µl of competent cells and transferred to the pre-cooled electroporator cuvette without leaving any bubbles and placed in the electroporator. After electroporation, 975 µl Recovery Media (GoldBio) was quickly added to the cells and the cells were allowed to grow at 200 rpm at 28 °C (NÜVE, EN 500) for 3 hours. At the end of the incubation, 100 µl of the cells were spread directly and concentrated into selective LB agar medium (Rif25, Strep50, Kan50). They were left to incubate for 2-3 days at 28 °C.

After incubation of transformant bacteria, 2 colonies were selected from the colonies that grew for 3 days at 28 ºC in selective medium containing Rif25, Strep50 and Kan50), were taken with a sterile toothpick and dissolved in 30 µl ultra-pure water. Colony-PCR was performed as described in Table 3. 1 and Table 3. 2 with insert-specific primers targeting the gene, and amplicons were run on 1 % Agarose gel.

Table 3. 23. Electroporation conditions

Electroporator	**Settings**	
Gene Pulser II Electroporator	**Voltage (V)**	1200
	Capacitance ()	3.0
	Resistance (Ω)	200

To perform plasmid isolation, selected colonies were inoculated in liquid YE medium with antibiotics (Rif25, Strep50 and Kan50) and grown at 28°C for 24 hours. Monarch™ Plasmid Miniprep Kit (NEB, T1010) was used for plasmid isolation and the instructions in the kit were applied as described in 3.2.1.3. After the concentrations and purities of the plasmids were measured on the NanoDrop (DeNovix, DS-11) device, they were also run on 1 % agarose gel.

3.2.5. Agro-infiltration to *N. benthamiana* leaves

3.2.5.1. Agro-infiltration

Agrobacterium cells harboring relevant plasmid were cultured in liquid YE medium containing Rif25, Strep50 and Kan50 antibiotics. Agroinfiltration solution was prepared by using MMA (100 mM MES, 100mM $MgCl_2$, 100mM Acetosyringone) infiltration medium with bacterial culture with an OD_{600} value exceeding 2, which adjusted to a final value of 0.4 [159]. After left for 1-3 hours at room temperature, the agroinfiltration solution was infiltrated into 6–8-week-old *N. benthamiana* leaves with the help of a 1 ml needleless syringe. Samples were collected from plants 3-5-7-day post infiltration leaves (dpi). Two leaf samples were taken per day and stored at -80 °C. GFP expression in leaves infiltrated with *Agrobacterium*-pEAQ-HT-GFP was visualized at 366 nm using the 'UV Cabinet 4' in parallel.

3.2.5.2. Co-infiltration of *Agrobacterium tumefaciens*

To obtain SARS-CoV-2 VLP in plant tissue, it was aimed to co-infiltrate 4 different *Agrobacterium* cultures containing 4 different structural genes into *N. benthamiana* leaves for VLP-ER (Agro_pEAQ-HT-E, Agro_pEAQ-HT- M, Agro_pEAQ-HT-N, Agro_pEAQ-HT-S) and VLP-Chl (Agro_pEAQ-HT-E, Agro_pEAQ-HT- M, Agro_pEAQ-HT-N, Agro_pEAQ-HT-S-chl).

Each bacterium was mixed to a final OD_{600}: 0.4. For VLP-ER 100 µl of each glycerol stock LBA4404 bacteria (containing pEAQ-HT-E, pEAQ-HT-N, pEAQ-HT-M and pEAQ-HT-S plasmids) were added into 25 ml of liquid YE with the necessary antibiotics (50 mg/L kanamycin, 50 mg/L streptomycin, 25 mg/L rifampicin) at 250 rpm at 28 °C in separate 250 ml flasks until the OD_{600} value reached 2. For VLP-Chl, bacteria (containing pEAQ-HT-E, pEAQ-HT-N, pEAQ-HT-M and pEAQ-HT-S-chl plasmids) were prepared in the same way. To obtain an OD_{600} value of 1.6 the bacteria were centrifuged at 4000 *g* for 10 min at room temperature, then the supernatant was carefully removed with a pipette and the bacterial pellet was dissolved with 3 ml of freshly prepared MMA solution. To obtain VLP-ER and VLP-Chl co-infiltration solutions, 3 ml of each 4 bacteria solutions were mixed as for making a final OD_{600} 0.4 in a total volume of 12 ml. After the co-infiltration solution mixture

was kept at room temperature for 1 hour, it was infiltrated into leaves of 6–8-week-old plant leaves with the help of a needleless syringe. All samples were collected from two biological replicates each containing two technical replicates. Leaf samples were collected 3-5-7 dpi and stored at -80 °C after freezing with liquid nitrogen for the further use.

3.2.6. RNA Isolation and Reverse-Transcription PCR (RT-PCR)

Total RNAs were isolated from agro-infiltrated leaves of *N. benhtamiana*. DEPC-treated water (1ml DEPC in 1L dH2O) was prepared in a hood. After DEPC was added to the water, it was shaken until it foamed well and added into the mortars with the pestles inside and were kept in the hood overnight. The water in the mortars was poured out and the mortars and pestles were wrapped separately with aluminum foil and autoclaved. The mortars and pestles to be used for isolation were cooled with liquid nitrogen and the samples were thoroughly ground with the help of liquid nitrogen.

The samples were collected into pre-cooled 1.5 ml eppendorf tubes (up to approximately 0.3 ml) and were stored in liquid nitrogen in an eppendorf until all samples were grinded. 1 ml of Trizol (Ambion) was added on the samples and vortexed rapidly for 15 min. After vortexing, the samples were centrifuged at 21000 g (highest g) for 5 min at room temperature. After centrifugation, 900 µl of the supernatant (without touching the pellet) was transferred into a new 1.5 ml ependorf tube and 180 µl of Chloroform was added. After vortexing for 15 sec, it was incubated at room temperature for 3 min. After centrifugation at 21000 *g* for 15 min at +4 ^{o}C, 400 µl of the supernatant was taken into a new 1.5 ml ependorf tube without touching the other phases. 400 µl cooled isopropanol was added to the supernatant and incubated at room temperature for 10 min. The supernatant was then removed after centrifugation at 21000 *g* for 10 min at room temperature. Pellet was washed with 75 % cooled Ethanol and kept at room temperature for 3 min. Ethanol was removed by centrifugation at 21000 *g* for 5 min at room temperature. The pellet was centrifuged once more for 15 sec to remove the remaining ethanol and allowed to dry for a while in the laminar flow. The pellet was resolved with 50 µl of autoclaved DEPC water kand the concentration and purity of RNAs were measured following incubation at 65 ^{o}C for 15 min.

Table 3. 24. Preparation of RNA mix

RNA MIX	Volume (µl)
Total RNA (0.1 ng -5 µg)	A
Primer Oligo dT	1
Nuclease Free Water	B
Total	12 (A + 1 + B)

The amount of RNA for cDNA conversion was calculated between 500 ng – 1 µg and RNA MIX was prepared as shown in Table 3. 26. The reagents in Table 3. 27 were prepared as master mix and aliquoted as 8 µl according to the number of samples. 12 µl of RNA MIX was added to the aliquot. Thermal cycler was set at 42 ºC for 60 min, 70 ºC for 5 min and hold at +4 ºC.

Table 3. 25. Preparation of RT-PCR master mix

Reagents	Stock	1 X (µl)
dNTP	10 mM	2
Reaction Buffer	5 X	4
RiboLock RNase Inhibitor	20 Units/µl	1
ReverseAid M-MuLV RT	200 Units/µl	1
RNA MIX		12
Total		20

3.2.7. Total Protein Isolation and quantification from transfected *N. benthamiana* leaves

Fresh leaf samples (3-5-7 dpi) were weighed and ground in a mortar and pestle with three volumes of TEN Buffer (10 mM Tris-HCl, 1 mM EDTA, 1 M NaCl, pH:7.4). Homogenized samples were centrifuged at 16000 g at 4 °C for 10 min and the supernatants were aliquoted as 100 µl. They were stored at -80 °C for further studies.

Pierce™ BCA Assay (Thermo Fisher Scientific) was performed to quantitate proteins from isolated samples. BSA Standards were prepared as shown in Table 3. 24.

Table 3. 26. BSA standard preparation for BCA Assay

Tube	Diluent Volume	Volume and BSA Source	Final BSA Concentration (mg)
A	0	300 µl of stock	2000
B	125	375 µl of stock	1500
C	325	325 µl of stock	100
D	175	175 µl of B tube	750
E	325	325 µl of C tube	500
F	325	325 µl of E tube	250
G	325	325 µl of F tube	125

Working Solution was prepared by taking the Reagent A and Reagent B solutions in the kit in a ratio of 50:1 (1 ml of Reagent A, 20 µl of Reagent B). The prepared Working Solution was taken to ice. For protein samples and BSA standards of unknown amounts, 40 µl of Working Solution was added into a new 0.5 ml Eppendorf tube, along with 2 µl each of the relevant protein and prepared BSA standards. The tubes containing the Working Solution and samples were incubated in the dark at 37 °C for 30 min. Concentrations of samples were measured by Thermo Nanodrop One. The 'Protein' tab was selected from the main screen and then 'Protein BCA' was selected. In particular, the number of replicates for each standard was determined as 2. 'Final BSA Standards (µg/ml)' are written from smallest to largest (0.125 for G, 0.250 for F, 0.500 for E, 0.750 for D, 1 for C, 1.5 for B and 2 for A). 'Curve Type' to 'Linear' was selected as the settings recommended by the kit manual. 2 µl of TEN Buffer was loaded as a blank. Each standard (from smallest to largest) was loaded with 2 µl in duplicate and read. After the standard measurements were completed, 2 µl of each sample was loaded into the NanoDrop (DeNovix, DS-11) device, and the results were noted. Samples with an 'out of range' warning were diluted and reloaded. Sample concentration was calculated by the following equation:

Concentration of the sample (µg/ml) = [Absorbance Value Measured on the Device (mg/ml)] x (Dilution Factor) x 1000

3.2.8. Protein Extraction and Purification

Fresh weight of infiltrated *N. benthamiana* leaves were measured 3-5-7 dpi and homogenized. In a mortar and pestle with 3 volumes TEN Buffer (10 mM Tris-HCl, 1 mM EDTA, 1 M NaCl, pH:7.4). Samples were centrifuged at 16000 *g* for 10 min at +4 °C. The supernatants were then collected and stored at -80 °C. To obtain high amounts of protein and purify the proteins, 15 g infiltrated leaves were homogenized in a mortar with 45 ml TEN Buffer. The homogenized samples were filtered through a double layer of Mirachloth (Merck) on ice. They were then centrifuged at 1580 *g* for 30 min at +5 °C and then the supernatant was passed through a 0.45 µm syringe filter. Then 29 ml protein extract were added dropwise into the ultracentrifuge tube containing double layer sucrose cushion with a syringe from the bottom to the top. 2 ml of 70 % sucrose solution, 6 ml of 25 % sucrose solution were prepared with PBS. If the volume of protein extracted was too less, PBS was added on top. The samples were ultracentrifuged at 167000 *g* for 3 hours at +4 °C. After centrifugation, samples were collected from the bottom of the tube (70 %, interface between 70 % and 25 %, interface between 25 % and protein extract and protein extract) with a syringe. The collected samples were stored at -20 °C for further studies. For the preparation of PD-10 desalting column (Cytiva), the top cap was cut and the storage liquid inside was removed by centrifugation at 2000 rpm for 2 min. The column was washed four times with PBS by centrifugation at 2000 rpm for 2 min. Maximum 2.5 ml of samples were loaded onto column. The prepared samples were added to the PD-10 Desalting column (Cytiva) and were eluted with 3.5 ml elution buffer (calculated according to graph in Figure 3. 3).

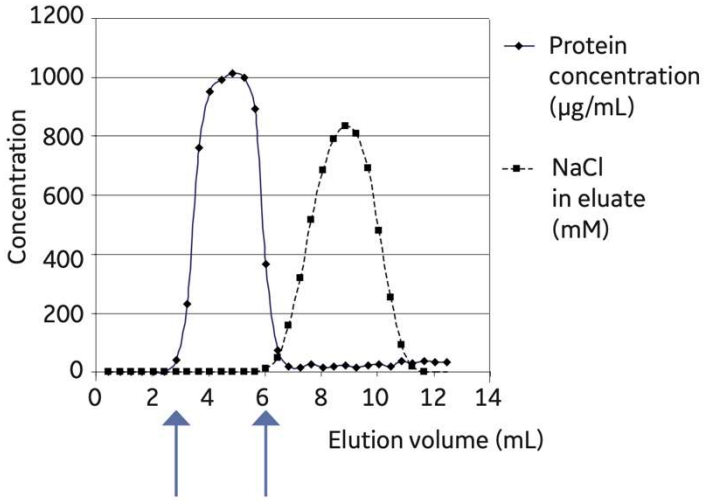

Figure 3. 3. Elution buffer amount used correlated with the amount of protein in PD-10 Desalting column.

After centrifugation at 2000 rpm for 2 min at room temperature, the samples were passed through a 0.22 µm syringe filter. The obtained samples were passed through the next step, OptiPrep Density Gradient Medium. The medium was added dropwise into the ultra-centrifuge tube containing OptiPrep Density Gradient Medium (30 %, 24 %, 16 % and 12 %) from the bottom to the top with the help of a syringe. At the top, 2.5 ml of filtered sample was added. After filling the empty spaces on the prepared tubes with PBS, ultracentrifugation was performed at 260000 *g* (50200 rpm) +4 °C for 2.5 hours. After centrifugation, samples were collected from six region of tube and stored at -20 °C for further studies.

3.2.9. SDS-PAGE and Western Blotting

SDS-PAGE and Western Blot methods were used to detect the samples. Separating Gel and Stacking Gel were prepared according to the Table 3. 25.

Table 3. 27. SDS-PAGE gel preparation protocol for different ratio of separating gels.

	Separating Gel (ml) (2X)			**Stacking Gel (ml) (2X)**
	%10	%12	%20	%4
Gel Solution (30 % Acrylamide, 2 % Bisacrylamide)	6.6	8	13.2	0.650
dH_2O	8	6.6	1.4	3.2

1.5 M Tris-HCl, pH: 8.8	5	5	5	-
0.5 M Tris-HCl, pH: 6.8	-	-	-	1.250
10 % SDS (w/v)	0.2	0.2	0.2	0.05
10 % APS (w/v)	0.2	0.2	0.2	0.05
TEMED	0.02	0.02	0.02	0.005

Separating gel was poured between two 1 mm glasses and isopropanol was added on it for solidification. After solidification of separating gel, isopropanol was removed and stacking gel was poured onto solidified separating gel and appropriate comb was placed. The solidified gels were wrapped in a wet napkin and stored at +4 ºC. Solidified gels were placed into SDS tank and Running Buffer (1 X) was added. Samples were mixed with 4 X Lammeli Buffer to a final volume of 1 X, and the proteins were denaturated at 95 ºC for 1 min. Denaturated samples were loaded into the wells and run at 110 V for 1 hour.

The gel between the 1mm glass was slowly removed and placed in 1 X Transfer Buffer. The PVDF membrane was cut to the appropriate size for the gel and activated in Methanol for 1 min and then placed in 1 X Transfer Buffer. On the Semi-dry blot system (Hoefer), two Whatmann papers, PVDF membrane, gel and two Whatmann papers were arranged on the cathode (+) surface, respectively, and the anode (-) was covered on the surface. After the transfer process was carried out for 1 hour at 18 V, the membrane was washed 2 times for 7 min each on a shaker with TBST (for 20 X TBS: 50 mM Tris, 300 mM NaCl, 4 mM KCl, pH: 7.4, 1 X TBST including 0.1 % Tween-20). Then, the membrane was blocked with 5 % Milk Powder (in TBST, filtrated with coarse filter) on the shaker for 1 hour. After blocking, the membrane was washed 3 times for 10 min with TBST. Primary Antibody [(Rabbit anti-SARS-CoV-2 Envelope Protein Polyclonal antibody: ProteinTech, 28904-1-AP, 1:1000), (SARS-CoV-2 Nucleocapsid Phosphoprotein Polyclonal antibody: ProteinTech, 28769-1AP, 1:1000), SARS-CoV-2 Membrane Glycoprotein Polyclonal antibody: ProteinTech, 28882-1AP, 1:1000), Anti-Sars-CoV-2 S1/RBD, monoclonal antibody: TUBITAK, GEN245, 1:1000)] dilution was prepared with 5 % Milk Powder in TBST. It was added onto the membrane and incubated on a shaker at room temperature for 1 hours. Primary antibody was collected from membrane. Secondary antibody [(HRP-conjugated Affinipure Goat Anti-Rabbit IgG(H+L): ProteinTech, SA00001-2, 1:2000), (Anti-mouse IgG, HRP-linked Antibody: Cell Signaling, 7076, 1:2000)] was prepared with 5 % Milk Powder in TBST and

incubated 1 hour at room temperature. The membrane was incubated with secondary antibody for 1 hour on the strainer. The membrane was washed with TBST 3 times for 10 min each. Then, 1 ml of HRP Substrate (Merck, Immobilon Crescendo Western HRP Substrate) was added to the membrane in the dark and incubated for 1 min at room temperature and then gel was imaged on SYNGENE / GBOX-Chemi-XRQ.

3.2.10. ELISA

ELISA was performed for quantitative measurement of isolated proteins and VLP samples (VLP-ER and VLP-Chl). 50 µl of 50 ng/µl samples were loaded into a 96-well plate with 2 replicates each and 50 µl of PBS was added on to it at a dilution of 1:2 and coated overnight at +4 ^{o}C. The liquid was poured out and the plate was washed 3 times with PBST (PBS containing 0.05 % Tween-20). Then 200 µl of 1 % BSA (in PBST) was loaded to each well and blocked for 2 hours at room temperature. Then the BSA solution was poured, and the plate was washed 3 times with PBST and 100 µl of primary antibody (in PBST containing 1 % BSA) was added to each well. The primary antibody was incubated at room temperature for 1 hour, then removed and the plate was washed 3 times with PBST. Secondary antibody was then prepared in PBST containing 1 % BSA and added at 100 µl per well. The secondary antibody was incubated at room temperature in the dark for 1 hour, then removed and the wells were washed 4 times with PBST. Then 50 µl TMB Substrate was added per well and incubated in the dark at room temperature for 20 min. Stop Solution was added without removing the substrate and measured at 450 nm in 30 min on microplate reader (Thermo Scientific, Multiskan Go).

SARS-CoV-2 total soluble protein isolated for standard measurement was used as a positive control. SARS-CoV-2 protein was loaded into a 96-well plate at different concentrations of 50 µl with different antibody conditions and the standard curve was plotted.

3.3. Statistical analysis

Plant samples were chosen at random for the experiments in this study, and the SPSS statistical program was utilized to compare the effects of the various treatments. Analysis of variance (ANOVA) was used to confirm the validity of the findings and the variability of

the data. To ascertain the differences between treatments with $p<0.05$, the significant least significant difference test (LSD) was also used (n=2).

4. RESULTS

4.1. Preparation of plant material

Various methods were tried to obtain sufficient numbers of seeds to be used in studies and to determine the most suitable conditions for growing plants (Table 4.1).

Table 4. 1. Optimization of growing up *N. benthamiana* and obtaining its seeds

Method	Surface Sterilization	Germination Medium / Time	Transferring into soil / Subculturing	Total time for obtaining seeds	Greenhouse
1	Yes	Culture / 3 days	1 / 51 days	3.6 month	METU
2	Yes	Soil / No	No	No	METU
3	No	Soil / 7 days	No	4.4 month	METU
4	Yes	Culture / 3 days	No	4.2 month	Başkent University

In the first method, the germinated *N. benthamiana* seedlings were subcultured after 21 days and allowed to grow under the same conditions for 30 days. Then, the plantlets were transferred from *in vitro* conditions to the soil in the Middle East Technical University (METU) greenhouse. Flowering was observed 40 days after the plants were transferred to the soil, and seeds were obtained approximately 45 days after flowering. In the second method, the seeds were vernalized for 1 day and transferred directly to the soil in the METU greenhouse. However, germination did not occur under these conditions. In the third method, the seeds were directly (without surface sterilization) into the soil in the METU greenhouse. On the tenth day the seeds started to germinate, and plants were bloomed approximately following 60 days. The seeds were obtained approximately 50 days after flowering. As the fourth method, the germinated *N. benthamiana* plantlets were transferred to the soil in the Başkent University greenhouse after 30 days. Acclimatization was performed as described previously. Flowering was observed approximately 30 days after the plants were transferred to the soil. Seeds were harvested from plants approximately 60 days after flowering. The

most effective way and the shortest time to obtain seed were observed in the first method which was chosen to be used in the Başkent University greenhouse. Different growth stages of *N. benthamiana* plants were given in Figure 4.1.

Figure 4. 1: Different growth of *N. benthamiana* A) 3-week-old seedlings germinated and grown on 1/2 MS medium, B) 3-week-old plantlets after the first subculture on 1/2 MS medium, C) 9-week-old plants after transfer to soil in the METU greenhouse D) 6-week-old plants transferred to soil in greenhouse at the Başkent University.

4.2. Preparation of plant transformation vector

Plant expression vector pEAQ-HT was transferred to *E. coli* 10-Beta competent cells. The presence of the plasmid was validated by colony Polymerase Chain Reaction (PCR) by using primers p19 and nptII targeting on the backbone into pEAQ-HT vector. The colony-PCR result of 10 colonies grown on kanamycin selective medium was shown in Figure 4. 2. As a result of PCR performed with the p19 primer pair, the expected 231 bp size bands were

observed for the 1, 2, 3, 5, 6, 7, 9 and 10th colonies. As a result of PCR performed with the nptII primer pair, the expected 468 bp size bands were observed in colonies 1, 2, 3, 4, 5, 6, 7, 9 and 10th.

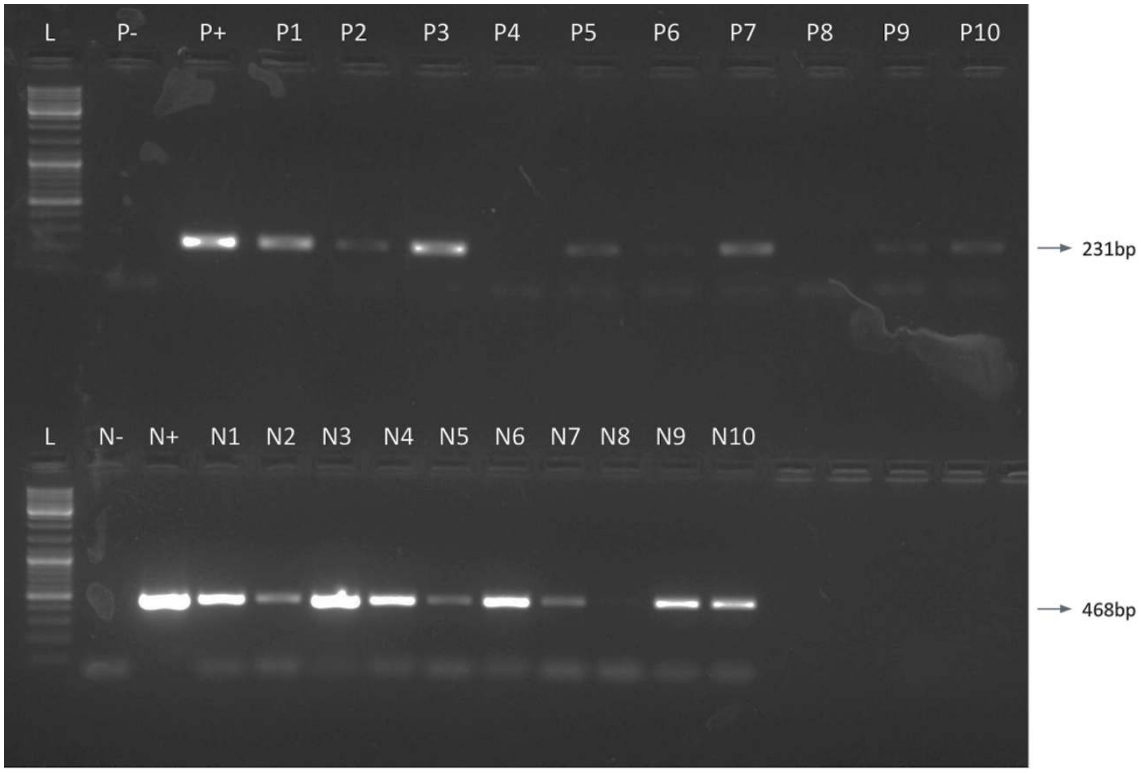

Figure 4. 2: Colony PCR results for pEAQ-HT vector L: Ladder (SMO331), +: positive control, -: negative control, P: p19, N: nptII

Colony-1 and colony-3 were selected for plasmid isolation and were grown in LB containing 50 mg/L kanamycin. Concentrations and purities of the plasmids were measured by NanoDrop (DeNovix, DS-11) (Table 4. 2) and integrities of the plasmids were visualized by agarose gel electrophoresis (Figure 4. 3).

Table 4. 2. NanoDrop measurement results of plasmids

	Plasmid 1	**Plasmid 3**
Concentration (ng/ µl)	142.3	162.3
260/230	2.578	2.417
260/280	1.924	1.918

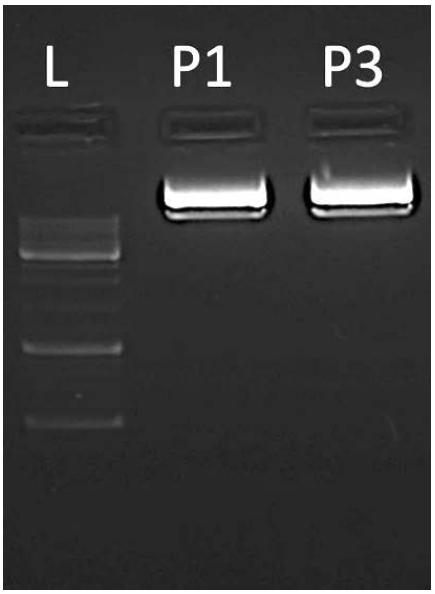

Figure 4. 3. Plasmids isolated from colony-1 and colony-3 containing pEAQ-HT vector. L: Ladder (SMO331), P: plasmid

A final PCR check was performed for the plasmids isolated from colony-1 and colony-3 and amplification products were visualized on agarose gel electrophoresis (Figure 4. 4).

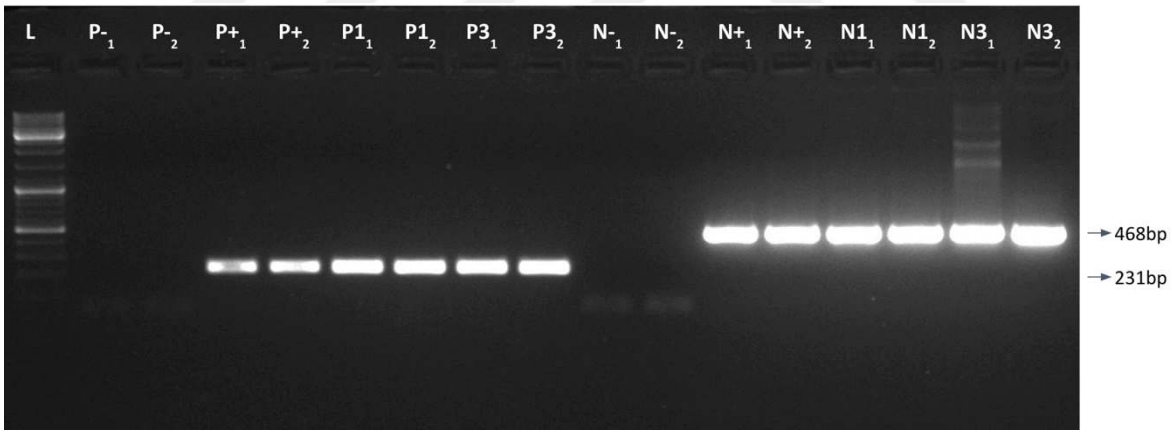

Figure 4. 4. PCR validation pEAQ-HT plasmids isolation from colony-1 and colony-3. L: Ladder (SMO331), +: positive control, -: negative control P: p19, N: nptII

pEAQ-HT-GFP was transferred to *E. coli* 10-Beta competent cells. The presence of the plasmid was validated by colony Polymerase Chain Reaction (PCR) by using primers p19 and nptII targeting on the backbone into pEAQ-HT vector. The colony-PCR result of 10 colonies grown on kanamycin selective medium was shown in Figure 4. 5. As a result of PCR performed with the p19 primer pair, the expected 231 bp size bands were observed for

the 1st and 3rd colonies. As a result of PCR performed with the nptII primer pair, the expected 468 bp size bands were observed in colonies 1, 3, 4, 6, 7, 8 and 10th.

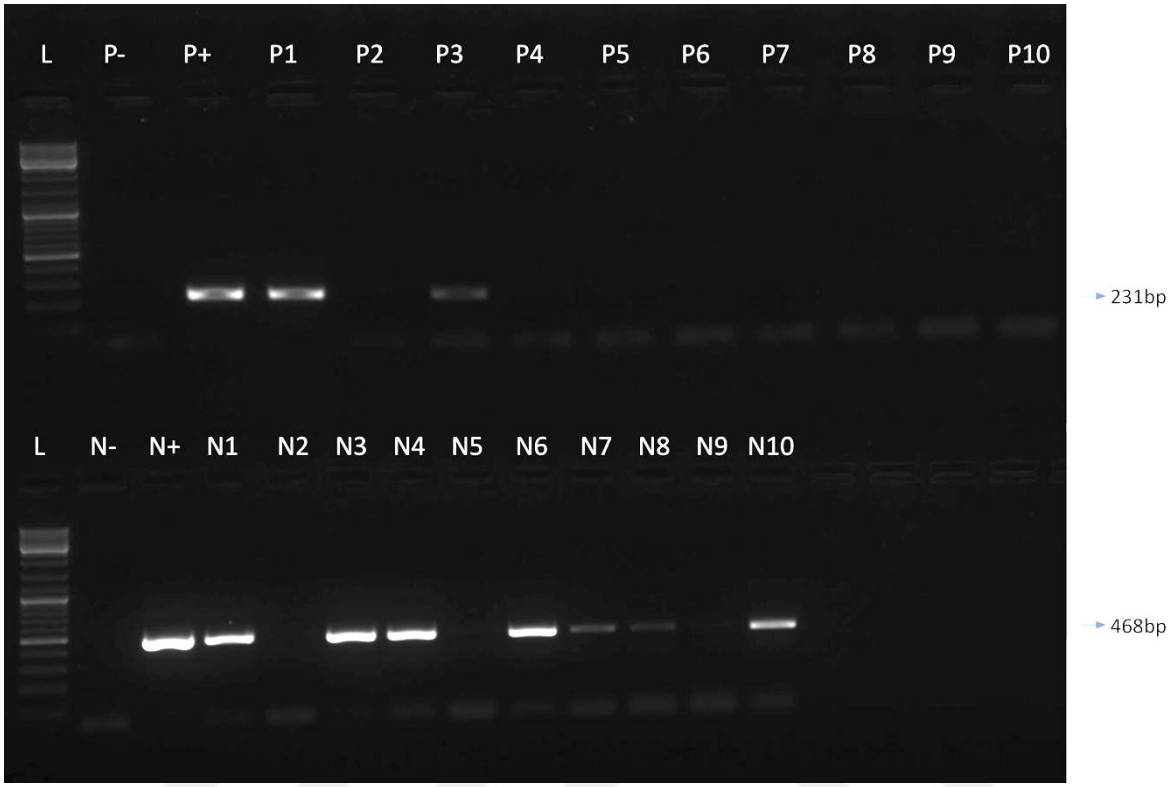

Figure 4. 5. Colony PCR results for pEAQ-HT-GFP vector L: Ladder (SMO331), +: positive control, -: negative control, P: p19, N: nptII

Colony-1 and colony-3 were selected for plasmid isolation and were grown in LB containing 50 mg/L kanamycin. Concentrations and purities of the plasmids were measured by NanoDrop (DeNovix, DS-11) (Table 4. 3) and integrities of the plasmids were visualized by agarose gel electrophoresis (Figure 4. 6).

Table 4. 3. NanoDrop measurement results of plasmids

	Plasmid 1	**Plasmid 3**
Concentration (ng/ µl)	163.2	128.0
260/230	2.550	2.557
260/280	1.901	1.892

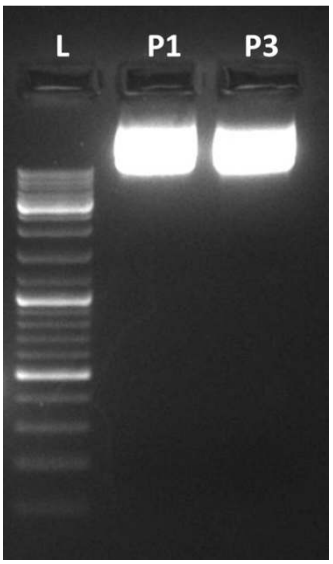

Figure 4. 6. Plasmids isolated from colony-1 and colony-3 containing pEAQ-HT-GFP vector. L: Ladder (SMO331), P: plasmid

A final PCR check was performed for the plasmids isolated from colony-1 and colony-3 and amplification products were visualized on agarose gel electrophoresis (Figure 4. 7).

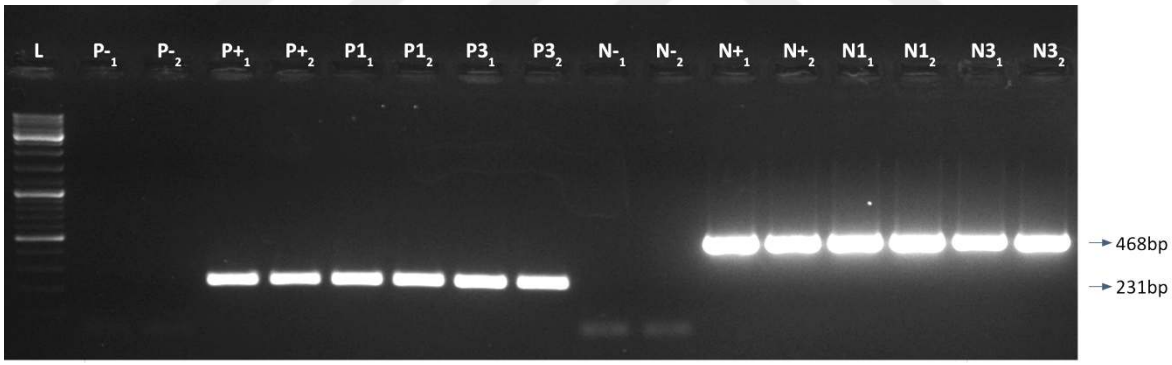

Figure 4. 7. PCR validation pEAQ-HT-GFP plasmids isolation from colony-1 and colony-3. L: Ladder (SMO331), +: positive control, -: negative control P: p19, N: nptII

4.3. Preparation of SARS-CoV-2 gene cassettes

The designed gene cassettes (Figure 4. 8, 4. 9, 4. 10, 4. 11, 4. 12) were translated into amino acid sequence and analyzed for target signal with the TargetP program. Accordingly, peaks were formed in the expected regions in the E, S, S-chl, and sequences. A signal was also observed in the expected region in the M sequence whereas no signal was observed for N (Figure 4. 10).

A

accggtATGGGATGGTCTTGTATTATTCTTTTTCTTGTTGCTACTGCTACTGGAGTTCATTCTTATTCTTTTGTTTCTGAAGAAATTGGAACTCT
TATTGTTAATTCTGTTCTTCTTTTTCTTGCTTTTGTTGTTTTTCTTCTTGTTACTCTTGCTATTCTTACTGCTCTTAGACTTTGTGCTTATTGTT
GTAATATTGTTAATGTTTCTCTTGTTAAGCCATCTTTTTATGTTTATTCTAGAGTTAAGAATCTTAATTCTTCTAGAGTTCCAGATCTTCTTGT
TTCTGAGAAGGATGAGCTTTAActcgag

B

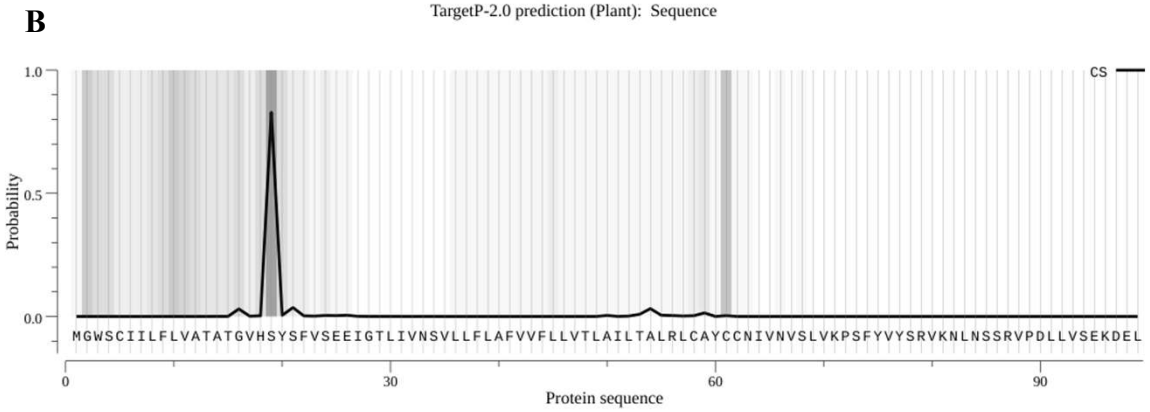

Figure 4. 8. A) E gene expression cassette design, B) E gene TargetP analysis result, Yellow: restriction enzyme recognition sites, Dark Green: Murine leader ER targeting signal, Pink: SEKDEL ER retention signal

A

accggtATGGGATGGTCTTGTATTATTCTTTTTCTTGTTGCTACTGCTACTGGAGTTCATTCTGCTGGATCTAATGGAACTATTACTGTTGAAGAACTTAAGAAGCTTCTTGAAGAAT
GGAATCTTGTTATTGGATTTCTTTTTCTTACTTGGATTTGTCTTCTTCAATTTGCTTATGCTAATAGAAATAGATTTCTTTATATTATTAAGCTTATTTTTCTTTGGCTTCTTTGGCCAGTTA
CTCTTACTTGTTTTGTTCTTGCTGCTGTTTATAGAATTAATTGGATTACTGGAGGAATTGCTATTGCTATGGCTTGTCTTGTTGGACTTATGTGGCTTTCTTATTTTATTGCTTCTTTTAG
ACTTTTTGCTAGAACTAGATCTATGTGGTCTTTTAATCCAGAAACTAATATTCTTCTTAATGTTCCACTTCATGGAACTATTCTTACTAGACCACTTCTTGAATCTGAACTTGTTATTGGA
GCTGTTATTCTTAGAGGACATCTTAGAATTGCTGGACATCATCTTGGAAGATGTGATATTAAGGATCTTCCAAAGGAAATTACTGTTGCTACTTCTAGAACTCTTTCTTATTATAAGCTT
GGAGCTTCTCAAAGAGTTGCTGGAGATTCTGGATTTGCTGCTTATTCTAGATATAGAATTGGAAATTATAAGCTTAATACTGATCATTCTTCTTCTTCTGATAATATTGCTCTTCTTGTTC
AATCTGAGAAGGATGAGCTTTAActcgag

B

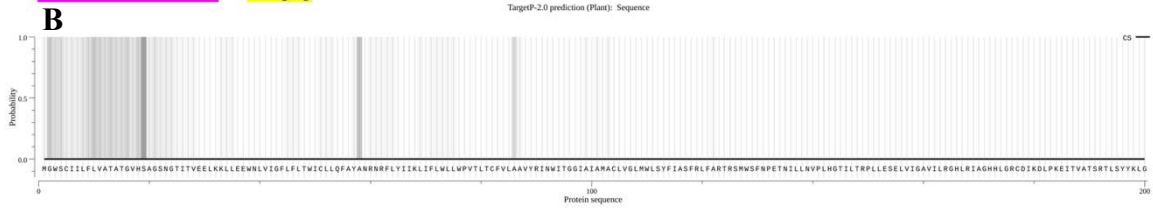

Figure 4. 9. A) M gene expression cassette design, B) M gene TargetP analysis result, Yellow: restriction enzyme recognition sites, Dark Green: Murine leader ER targeting signal, Pink: SEKDEL ER retention signal

A

accggtATGTCTGATAATGGACCACAAAATCAAAGAAATGCTCTTAGAATTACTTTTGGAGGACCATCTGATTCTACTGGATCTAATCAAAAT
GGAGGAGCTAGATCTAAGCAAAGAAGACCACAAGGACTTCCAAATAATACTGCTTCTTGGTTTACTGCTCTTACTCAACATGGAAAGGA
AGATCTTAAGTTTCCAAGAGGACAAGGAGTTCCAATTAATACTAATTCTTCTCCAGATGATCAAATTGGATATTATAGAAGAGCTACTAGA
AGAATTAGAGGAGGAGATGGAAAGATGAAGGATCTTTCTCCAAGATGGTATTTTTATTATCTTGGAACTGGACCAGAAGCTGGACTTCC
ATATGGAGCTAATAAGGATGGAATTATTTGGGTTGCTACTGAAGGAGCTCTTAATACTCCAAAGGATCATATTGGAACTAGAAATCCAGCT
AATAATGCTGCTATTGTTCTTCAACTTCCACAAGGAACTACTCTTCCAAAGGGATTTTATGCTGAAGGATCTAGAGGAGGATCTCAAGCT
TCTTCTAGATCTTCTTCTAGATCTAGAAATTCTTCTAGAAATTCTACTCCAGGATCTTCTAAGAGAACTTCTCCAGCTAGAATGGCTGGAA
ATGGAGGAGATGCTGCTCTTGCTCTTCTTCTTCTTGATAGACTTAATCAACTTGAATCTAAGATGTCTGGAAAGGGACAACAACAACAAG
GACAAACTGTTACTAAGAAGTCTGCTGCTGAAGCTTCTAAGAAGCCAAGACAAAAGAGAACTGCTACTAAGGCTTATAATGTTACTCAA
GCTTTTGGAAGAAGAGGACCAGAACAAACTCAAGGAAATTTTGGAGATCAAGAACTTATTAGACAAGGAACTGATTATAAGCATTGGCC
ACAAATTGCTCAATTTGCTCCATCTGCTTCTGCTTTTTTTGGAATGTCTAGAATTGGAATGGAAGTTACTCCATCTGGAACTTGGCTTACT
TATACTGGAGCTATTAAGCTTGATGATAAGGATCCAAATTTTAAGGATCAAGTTATTCTTCTTAATAAGCATATTGATGCTTATAAGACTTTT
CCACCAACTGAACCAAAGAAGGATAAGAAGAAGAAGGCTGATGAAACTCAAGCTCTTCCACAAAGACAAAAGAAGCAACAAACTGTT
ACTCTTCTTCCAGCTGCTGATCTTGATGATTTTTCTAAGCAACTTCAACAATCTATGTCTTCTGCTGATTCTACTCAAGCTTAActcgag

B

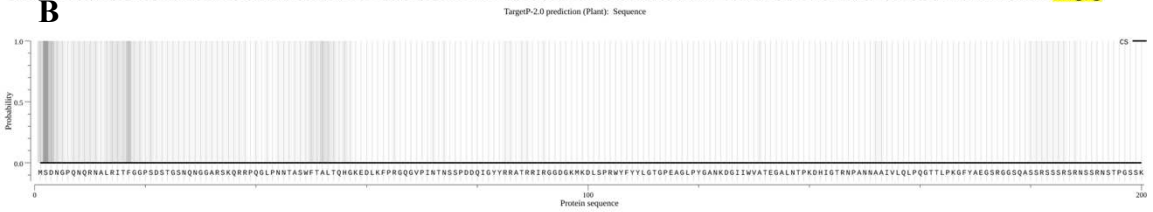

Figure 4. 10. A) N gene expression cassette design, B) N gene TargetP analysis result, Yellow: restriction enzyme recognition sites

A

accggtATGGGATGGTCTTGTATTATTCTTTTTCTTGTTGCTACTGCTACTGGAGTTCATTCTTCTCAATGTGTTAATCTTACTACTAGAACTCAACTTCCACCAGCATACACAAATTCTTTTACTAG
AGGTGTTTACTATCCAGATAAGGTTTTTAGATCATCAGTTTTGCATTCTACTCAAGATCTTTTCCTTCCTTTTTTTTCTAATGTTACTTGGTTTCATGTTATTTCAGGTACAAATGGTACAAAGAGATT
TGATAATCCAGTTCTTCCATTTAATGATGGAGTTTATTTTGCTTCTATTGAGAAATCAAATATTATTAGGGGTTGGATTTTTGGAACTACTTTGGATTCAAAGACACAGTCATTGCTTATTGTGAACA
ATGCTACTAATGTGGTGATTAAGGTTTGTGAATTTCAATTTTGTAATGATCCATTTCTTGATCATAAGAATAATAAGTCTTGGATGGAATCTGAATTTAGGGTTTACTCATCTGCTAATAATTGCACAT
TTGAATATGTTTCTCAACCATTTTTGATGGATTTGGAAGGAAAGCAAGGAAATTTCAAAAATCTTAGAGAATTTGTTTTTAAGAATATTGATGGATACTTCAAAATTTATTCTAAGCATACTCCAAT
TATTGTGAGGGAACCAGAGGATTTGCCACAAGGATTCTCAGCATTGGAACCATTGGTTGATTTGCCAATTGGTATTAATATTACAAGGTTTCAAACATTGTTGGCTCTTCATAGATCTTACTTGAC
ACCTGGTGATTCTTCATCAGGTTGGACAGCAGGTGCTGCAGCATATTATGTTGGATATCTTCAACCAAGAACTTTTCTTCTTAAGTATAATGAAAATGGTACAATTACAGATGCAGTTGATTGCGC
TTTGGATCCTCTTTCTGAAACTAAGTGTACTCTTAAGTCTTTTACTGTTGAAAAGGGTATTTACCAGACTTCTAATTTTAGAGTTCAACCAACAGAGTCAATTGTTAGATTTCCAAATATTACAAATT
TGTGTCCATTCGATGAGGTTTTTAATGCTACTAGATTTGCTTCAGTTTACGCATGGAATAGAAAGAGAATTTCTAATTGTGTTGCAGATTACTCAGTTTTGTACAATCTTGCTCCATTTTTTACTTTT
AAGTGCTACGGTGTTTCTCCAACTAAGCTTAATGATCTTTGTTTTACTAATGTTTATGCTGATTCTTTTGTTATTAGAGGAGATGAAGTTAGACAAATTGCTCCAGGACAAACTGGAAATATTGCA
GATTATAATTATAAGCTTCCAGATGATTTTACTGGATGTGTTATTGCTTGGAATTCAAACAAGCTTGATTCTAAGGTTTCAGGTAATTACAATTATCTTTATAGACTTTTTAGAAAGTCTAATCTTAAG
CCATTTGAAAGGGATATTTCAACTGAAATTTATCAAGCTGGAAATAAGCCATGTAATGGAGTTGCAGGTTTCAATTGTTATTTTCCACTTAGGTCATATTCTTTTAGACCAACTTATGGAGTTGGAC
ATCAACCATATAGAGTTGTTGTTCTTTCTTTTGAACTTCTTCATGCACCTGCAACTGTTTGTGGACCAAAGAAGTCTACTAATTTGGTTAAAAATAAGTGTGTGAATTTCAATTTTAATGGACTTAA
GGGAACAGGTGTTTTGACAGAATCTAATAAGAAGTTTCTTCCATTTCAACAATTTGGAAGAGATATTGCTGATACAACAGATGCTGTTAGAGATCCACAAACTCTTGAAATTCTTGATATTACACC
TTGTTCATTCGGTGGTGTTTCTGTTATTACTCCAGGAACTAATACTTCTAATCAAGTTGCTGTTCTTTATCAAGGAGTTAATTGTACTGAAGTTCCAGTTGCTATTCATGCTGATCAACTTACTCCAA
CTTGGAGAGTTTATTCTACTGGATCTAATGTTTTTCAAACTAGAGCTGGATGTCTTATTGGTGCAGAGTATGTTAATAATTCTTATGAATGTGATATTCCAATTGGTGCAGGTATTTGTGCTTCTTAT
CAAACTCAAACTAAGTCTCATGGATCTGCTTCATCAGTTGCATCTCAATCTATTATTGCTTATACTATGTCTCTTGGAGCTGAAAATTCTGTTGCTTATTCTAATAATTCAATTGCAATTCCAACTAATT
TCACAATTTCTGTTACAACAGAGATTCTTCCTGTTTCTATGACTAAGACTTCTGTTGATTGTACTATGTATATTTGTGGAGATTCTACTGAATGTTCTAATCTTCTTCTTCAATATGGATCTTTTGTAC
TCAACTTAAGAGAGCTCTTACTGGAATTGCTGTTGAACAAGATAAGAATACTCAAGAAGTTTTTGCTCAAGTTAAGCAAATTTATAAGACTCCACCAATTAAATACTTCGGAGGATTTAATTTTTC
TCAAATTCTTCCAGATCCATCTAAGCCTTCAAAAAGGTCTTTTATTGAAGATCTTCTTTTTAATAAGGTTACTCTTGCTGATGCAGGTTTCATTAAGCAATATGGAGATTGCTTGGGTGATATTGCT
GCTAGAGATCTTATTTGTGCTCAAAAGTTTAAGGGACTTACTGTTCTTCCACCACTTCTTACTGATGAAATGATTGCTCAATATACATCAGCACTTCTTGCTGGAACTATTACTTCTGGATGGACTTT
TGGAGCTGGAGCTGCTCTTCAAATTCCATTTGCTATGCAAATGGCTTATAGATTTAATGGAATTGGAGTTACACAGAATGTTCTTTATGAAAATCAAAAATTGATTGCTAATCAATTTAATTCTGCT
ATTGGAAAGATTCAAGATTCTTTGTCATCAACTGCTTCTGCTCTTGGAAAGCTTCAAGATGTGGTGAATCATAATGCTCAAGCTCTTAATACTCTTGTTAAGCAACTTTCTTCTAAGTTTGGAGCTA
TTTCTTCTGTTCTTAATGATATTTTTTCTAGACTTGATCCACCAGAAGCTGAAGTTCAGATTGATAGGTTGATTACTGGAAGACTTCAATCTCTTCAAACTTACGTTACACAGCAACTTATTAGAGC
TGCTGAAATTAGAGCTTCTGCTAATCTTGCTGCTACTAAGATGTCTGAATGTGTTCTTGGACAATCTAAGAGAGTTGATTTTTGTGGAAAGGGATATCATCTTATGTCTTTCCACAATCTGCTCCA
CATGGAGTTGTTTTTCTTCATGTTACTTATGTTCCAGCTCAAGAAAAGAATTTTACTACTGCTCCAGCTATTTGTCATGATGGAAAGGCTCATTTTCCAAGAGAAGGAGTTTTCGTTTCAAATGGA
ACTCATTGGTTTGTTACTCAAAGAAATTTTTATGAACCACAAATTATTACTACTGATAATACTTTTGTTTCTGGAAATTGTGATGTTGTTATTGGAATTGTTAATAATACTGTTTATGATCCACTTCAA
CCTGAGTTGGATTCTTTAAGGAAGAACTTGATAAGTATTTAAGAATCATACTTCTCCAGATGTTGATCTTGGAGATATTCTGGAATTAATGCTTCTGTTGTTAATATTCAAAAGGAAATTGATA
GACTTAATGAAGTTGCTAAGAATCTTAATGAATCTCTTATTGATCTTCAAGAACTTGGAAAGTATGAACAATATATTAAGTGGCCATGGTATATTTGGCTTGGATTATTGCTGGACTTATTGCTATT
GTTATGGTTACTATTATGCTTTGTTGTATGACTTCTTGCTGCTCTTGCCTTAAGGGATGTTGTTCTTGTGGATCTTGTTGTAAGTTTGATGAAGATGATTCTGAACCAGTTCTTAAGGGAGTTGAAA
ATCTTTATTTTCAATCTAGAATGAAGCAAATTGAAGATAAGATTGAAGAAATTCTTTCTAAGATTTATCATATTGAAAATGAAATTGCTAGAATTAAGAAGCTTATTGGAGAAAGATCTGAGAAGG
ATGAGCTTTAAccgctcgag

B

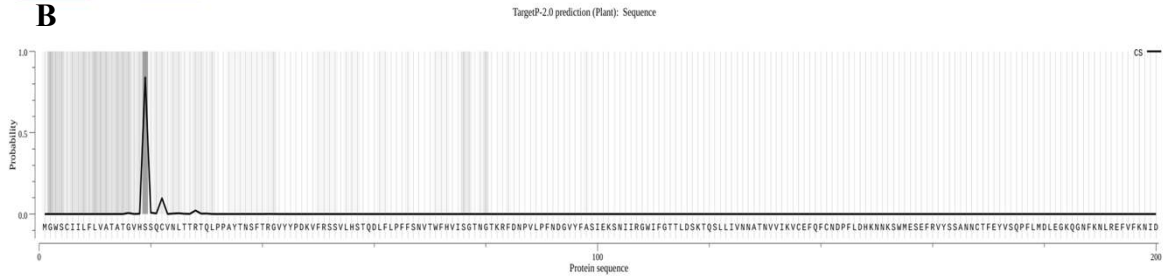

Figure 4. 11. A) S gene expression cassette design, B) S gene TargetP analysis result, Yellow: restriction enzyme recognition sites, Dark Green: Murine leader ER targeting signal, Blue: TEV protease cleavage site, Green: GCN4p-II trimerization domain, Pink: SEKDEL ER retention signal

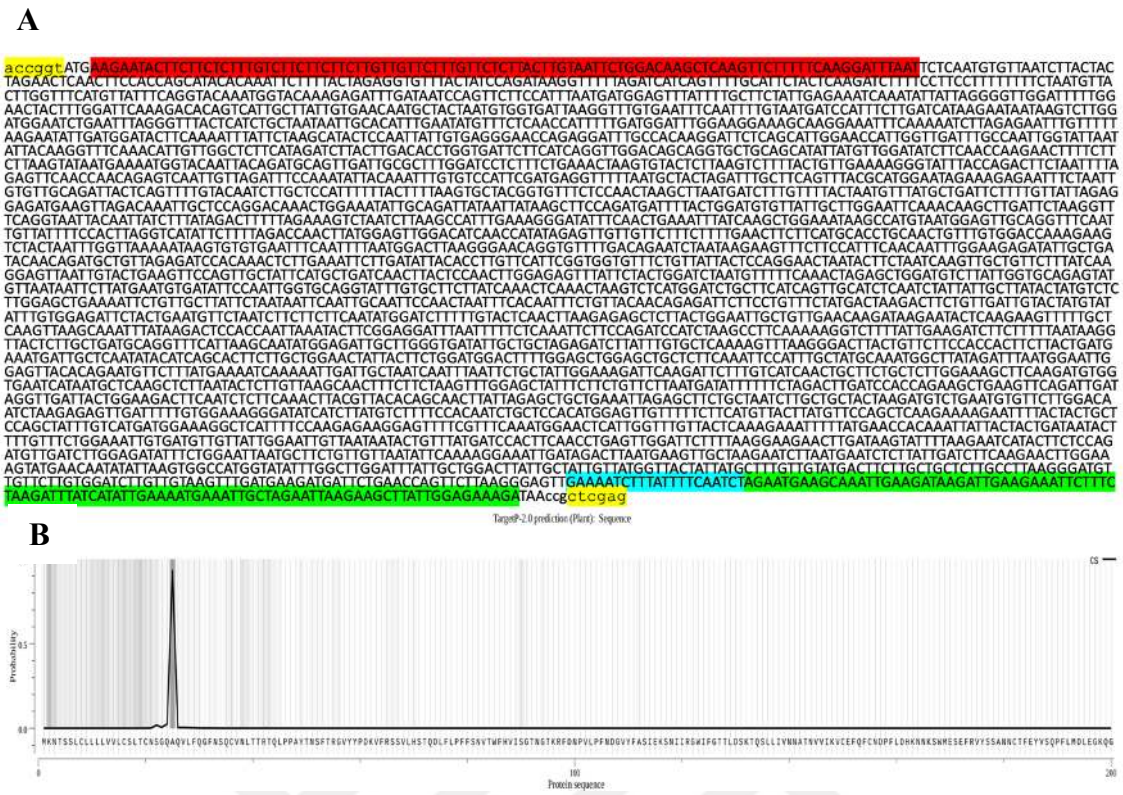

Figure 4. 12. A) S-chl gene expression cassette design, B) S-chl gene TargetP analysis result, Red: ER-chloroplast signal peptide alpha Amy-3, Blue: TEV protease cleavage site, Green: GCN4p-II trimerization domain.

4.3.1. Preparation of E gene cassette

E gene cassette was obtained in a plasmid pEX-A128-E which was transferred into *E. coli* 10-beta cells. The presence of the pEX-A128-E plasmid was confirmed by colony PCR with E_gene_F and E_gene_R primers. As a result, the expected 318 bp size bands were observed for 10 colonies. (Figure 4. 13)

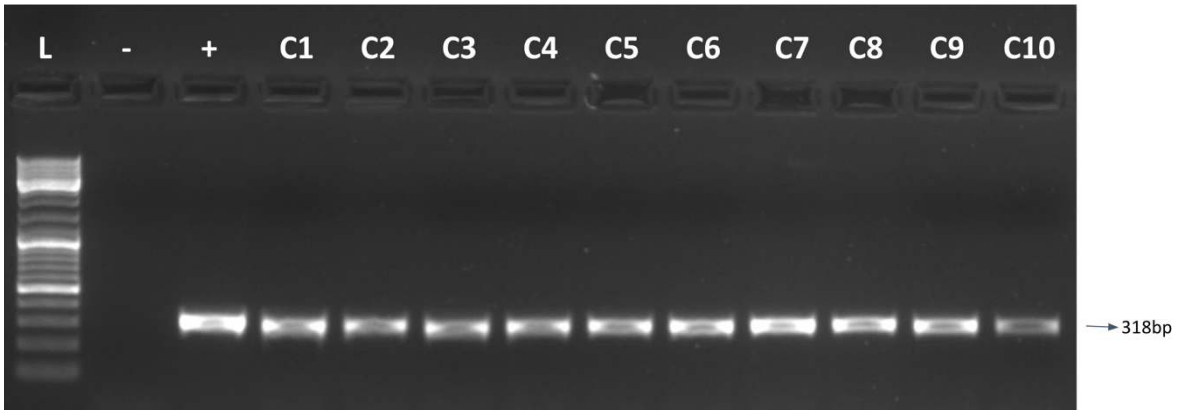

Figure 4. 13. Colony PCR result after transformation with pEX-A128-E plasmid. L: Ladder (SMO331), +: positive control (pEX-A128-E), -: negative control (water), C1-C10: colonies

Colony-7 and colony-8 were selected for plasmid isolation and were grown in LB containing 100 mg/L ampicillin. Concentrations and purities of the plasmids were measured by NanoDrop (DeNovix, DS-11) (Table 4. 4) and integrities of the plasmids were visualized by agarose gel electrophoresis (Figure 4. 14).

Table 4. 4. NanoDrop measurement results of plasmids

	Plasmid 7	**Plasmid 8**
Concentration (ng/ µl)	157.3	158.4
260/230	2.36	2.37
260/280	1.84	1.81

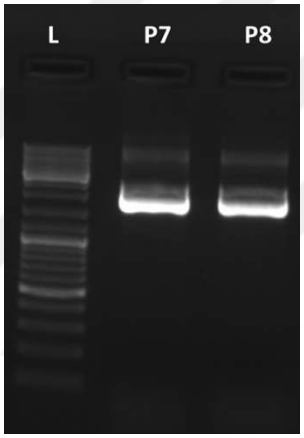

Figure 4. 14. Plasmids isolated from colony-7 and colony-8 containing pEX-A128-E plasmid. L: Ladder (SMO331), P: plasmid

A final PCR check was performed for the plasmids isolated from colony-7 and colony-8 and amplification products were visualized on agarose gel electrophoresis (Figure 4. 15).

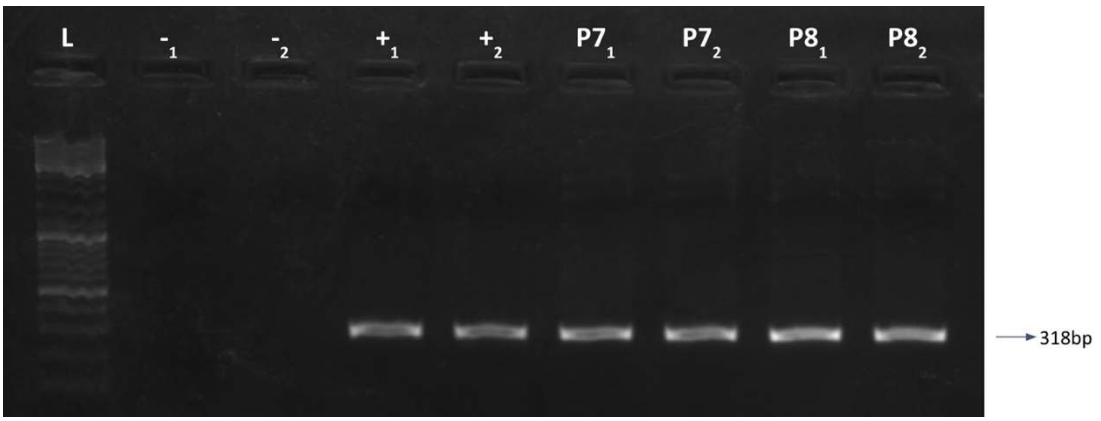

Figure 4. 15. PCR validation pEX-A128-E plasmids isolation from colony-7 and colony-8. L: Ladder (SMO331), +: positive control (pEX-A128-E), -: negative control (water), P: plasmid, P7-P8: plasmids isolated from colony 7 and colony 8

In order to clone E gene to pEAQ-HT vector was amplified with Q5 High-Fidelity DNA Polymerase by using gene specific primers (E-gene_F and E_gene_R) and the expected 323 bp amplification product was observed (Figure 4. 16). The PCR product was purified by using magnetic beads then its concentration was measured as 115 ng/µl by qubit.

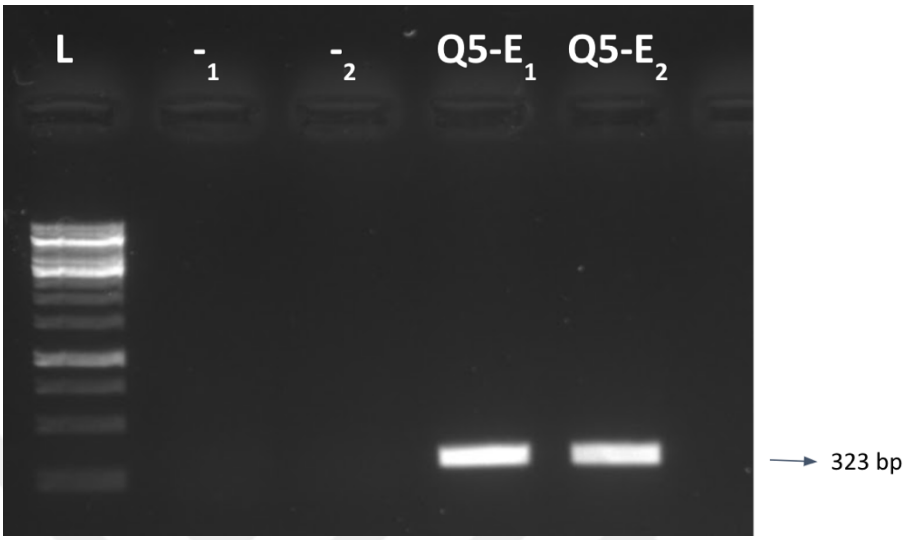

Figure 4. 16. Gel result of the Q5 amplification product of the E gene, L: Ladder (SMO331), -: negative control.

Purified E gene PCR product and pEAQ-HT plasmid were digested with AgeI-HF and XhoI restriction enzymes and ligated with T4 DNA ligase. The final plasmid was named as pEAQ-HT-E and transferred into *E. coli* 10-beta cells. The presence of pEAQ-HT-E was confirmed by colony PCR using E-in_F and E-in_R primers (Figure 4. 17).

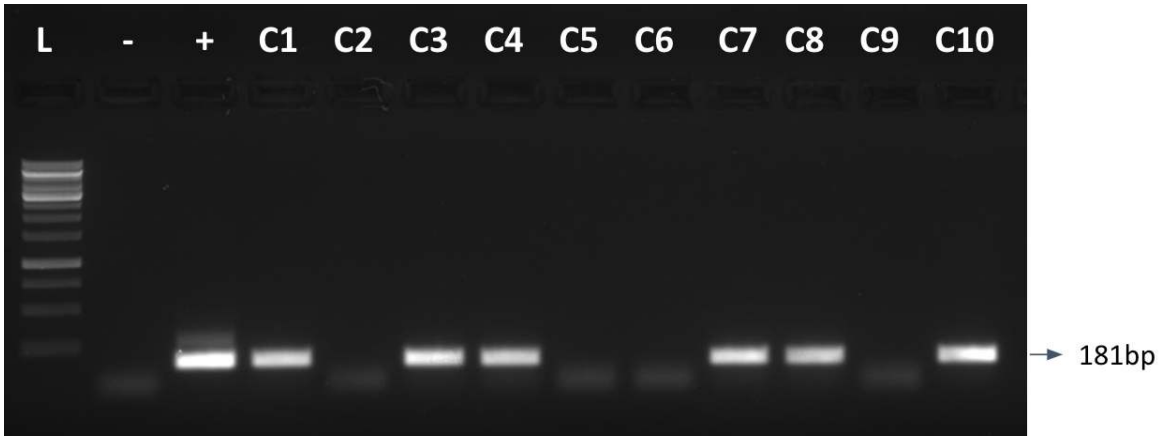

Figure 4. 17. Colony PCR result for pEAQ-HT-E plasmid. L: Ladder (SMO311), +: positive control (pEX-A128-E), -: negative control (water), C1-C10: colonies.

Colony-3 and colony-10 were selected for plasmid isolation and were grown in LB containing 50 mg/L kanamycin. Concentrations and purities of the plasmids were measured

by NanoDrop (DeNovix, DS-11) (Table 4. 5) and integrities of the plasmids were visualized by agarose gel electrophoresis (Figure 4. 18).

Table 4. 5. NanoDrop measurement results of plasmids

	Plasmid 3	**Plasmid 10**
Concentration (ng/ µl)	47.8	206.9
260/230	2.17	2.31
260/280	1.72	1.84

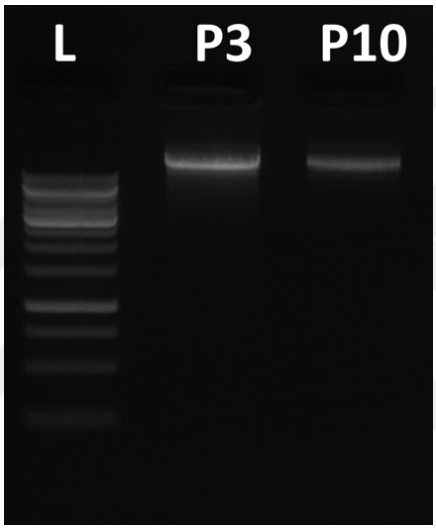

Figure 4. 18. Plasmids isolated from colony-3 and colony-10 containing pEAQ-HT-E plasmid. L: Ladder (SMO311), P3-P10: Plasmids isolated from colony-3 and colony-10.

A final PCR check was performed for the plasmids isolated from colony-3 and colony-10 and amplification products were visualized on agarose gel electrophoresis (Figure 4. 19).

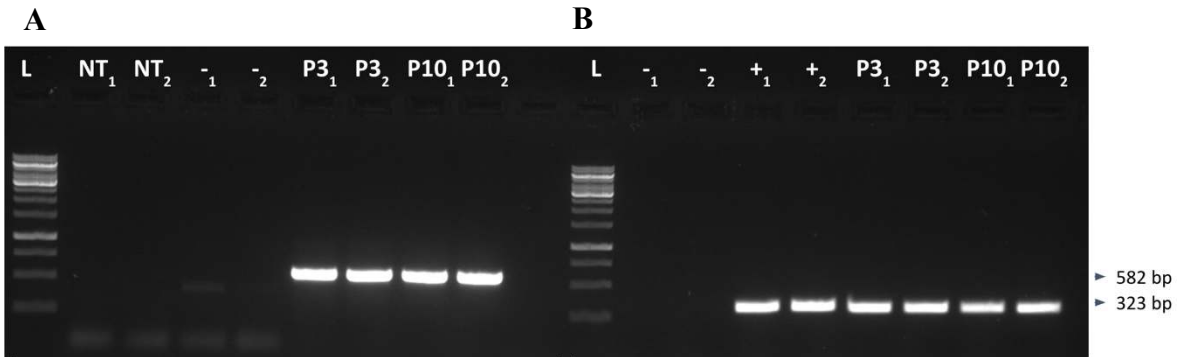

Figure 4. 19. PCR validation pEAQ-HT-E plasmids isolation from colony-3 and colony-10. A) PCR products prepared with orientation primers, B) PCR products prepared with insert specific primers. L: Ladder (SMO311), NT: No Template (water), +: positive control (pEAQ-HT), -: negative control (pEX-A128-E), P3-P10: plasmids isolated from colony 3 and colony 10.

Finally, the E gene insert in pEAQ-HT-E plasmid-10 was confirmed by INTERGEN Genetics and Rare Diseases Diagnostics Center via next generation sequencing (NGS). According to the alignment analysis by Cluster Omega, the sequence of cloned E gene was 100 % compatible with the original construct (Figure 4. 20).

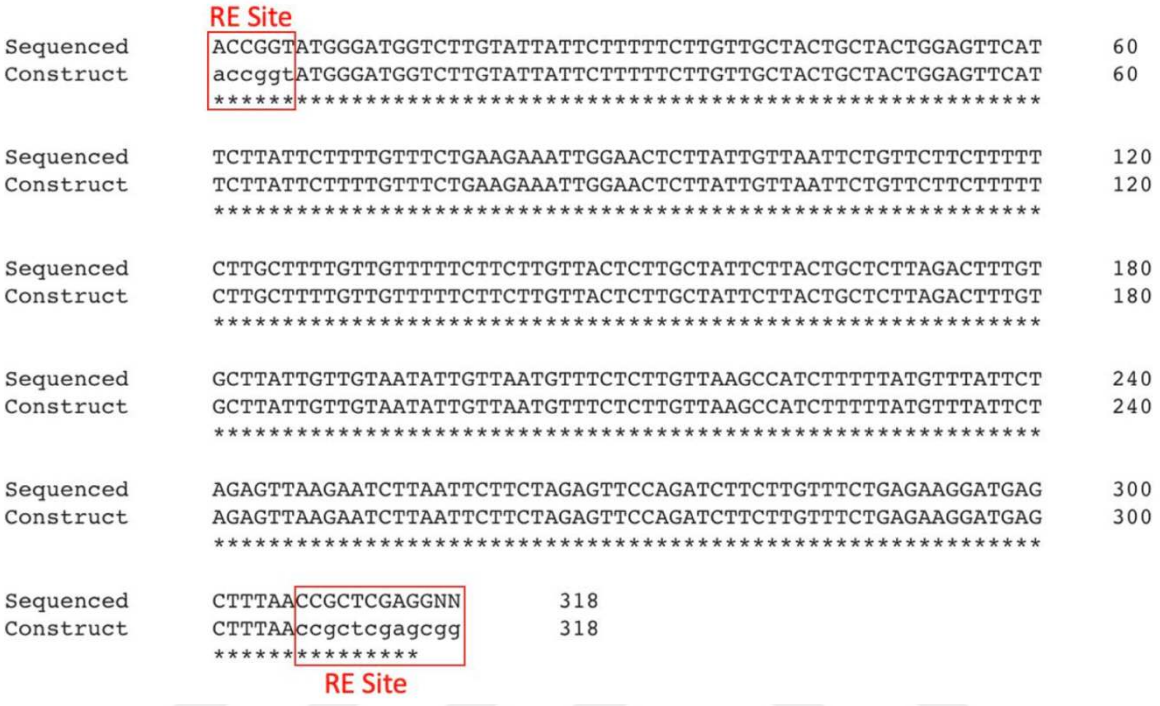

Figure 4. 20. Alignment result of cloned E gene and the original construct, RE Site: Restriction Enzyme site.

4.3.2. Preparation of N gene casssette

N gene cassette was obtained in a plasmid pEX-A128-N which was transferred into *E. coli* 10-beta cells. The presence of the pEX-A128-N plasmid was confirmed by colony PCR with N_gene_F and N_gene_R primers. As a result, the expected 1269 bp size bands were observed for 10 colonies. (Figure 4. 21)

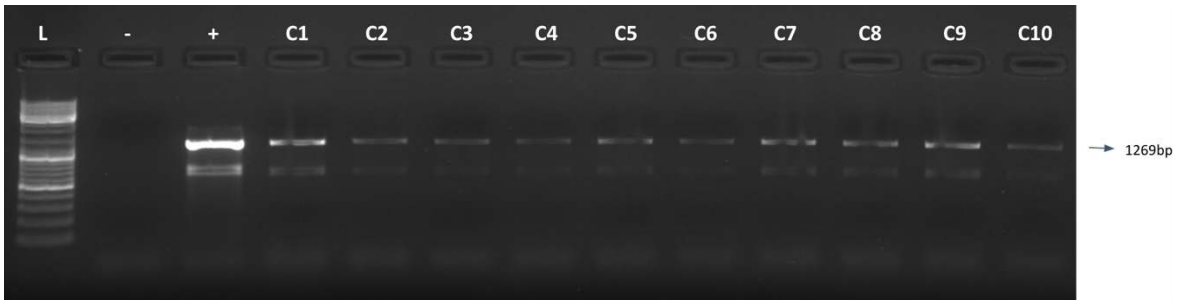

Figure 4. 21. Colony PCR result after transformation with pEX-A128-N plasmid. L: Ladder (SMO331), +: positive control (pEX-A128-N), -: negative control (water), C1-C10: colonies

Colony-1 and colony-9 were selected for plasmid isolation and were grown in LB containing 100 mg/L ampicillin. Concentrations and purities of the plasmids were measured by NanoDrop (DeNovix, DS-11) (Table 4. 6) and integrities of the plasmids were visualized by agarose gel electrophoresis (Figure 4. 22).

Table 4. 6. NanoDrop measurement results of plasmids

	Plasmid 1	**Plasmid 9**
Concentration (ng/ µl)	169.7	148.2
260/230	2.33	2.36
260/280	1.81	1.85

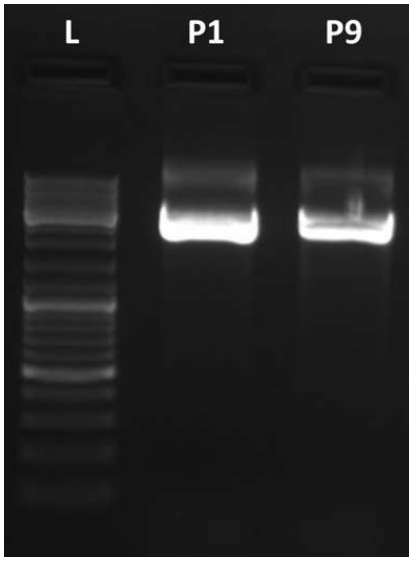

Figure 4. 22. Plasmids isolated from colony-1 and colony-9 containing pEX-A128-N plasmid. L: Ladder (SMO331), P: plasmid

A final PCR check was performed for the plasmids isolated from colony-1 and colony-9 and amplification products were visualized on agarose gel electrophoresis (Figure 4. 23).

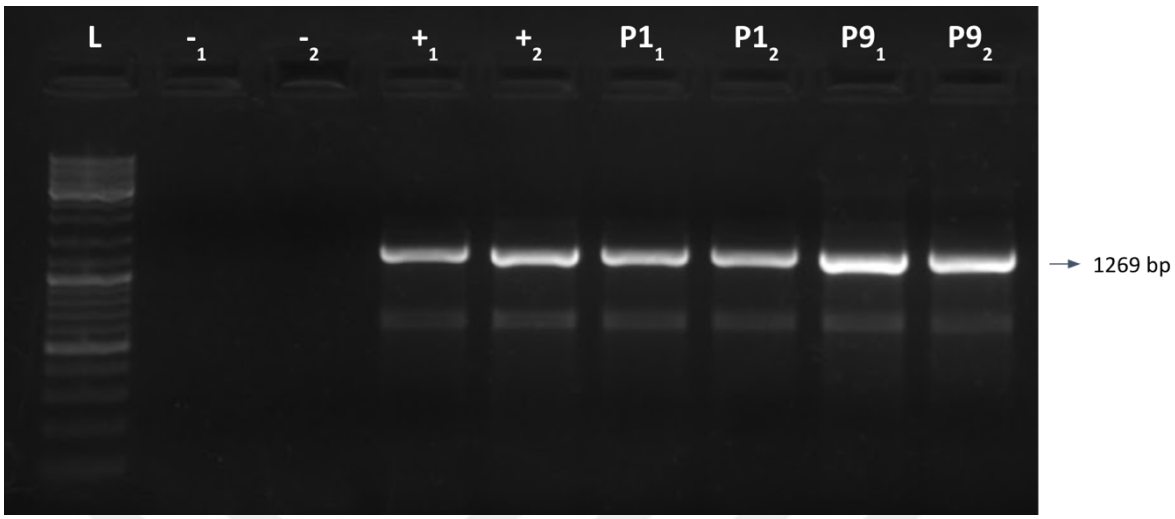

Figure 4. 23. PCR validation pEX-A128-N plasmids isolation from colony-1 and colony-9. L: Ladder (SMO331), +: positive control (pEX-A128-N), -: negative control (water), P: plasmid, P1-P9: plasmids isolated from colony-1 and colony-9.

In order to clone N gene to pEAQ-HT vector, it was amplified with Q5 High-Fidelity DNA Polymerase by using gene specific primers (N-gene_F and N_gene_R) and the expected 1269 bp amplification product was observed (Figure 4. 24). The PCR product was purified by using magnetic beads then its concentration was measured as 62.2 ng/µl by qubit.

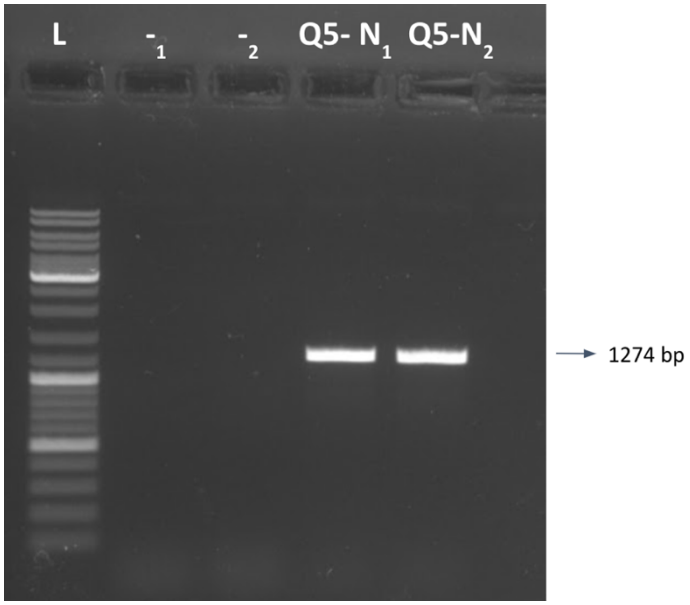

Figure 4. 24. Gel result of the Q5 amplification product of the N gene, L: Ladder (SMO331), -: negative control.

Purified N gene PCR product and pEAQ-HT plasmid were digested with AgeI-HF and XhoI restriction enzymes and ligated with T4 DNA ligase. The final plasmid was named as pEAQ-HT-N and transferred into *E. coli* 10-beta cells. The presence of pEAQ-HT-N was confirmed by colony PCR using N-in_F and N-in_R primers and 5UTR-F and N-in_R primers (Figure 4. 25).

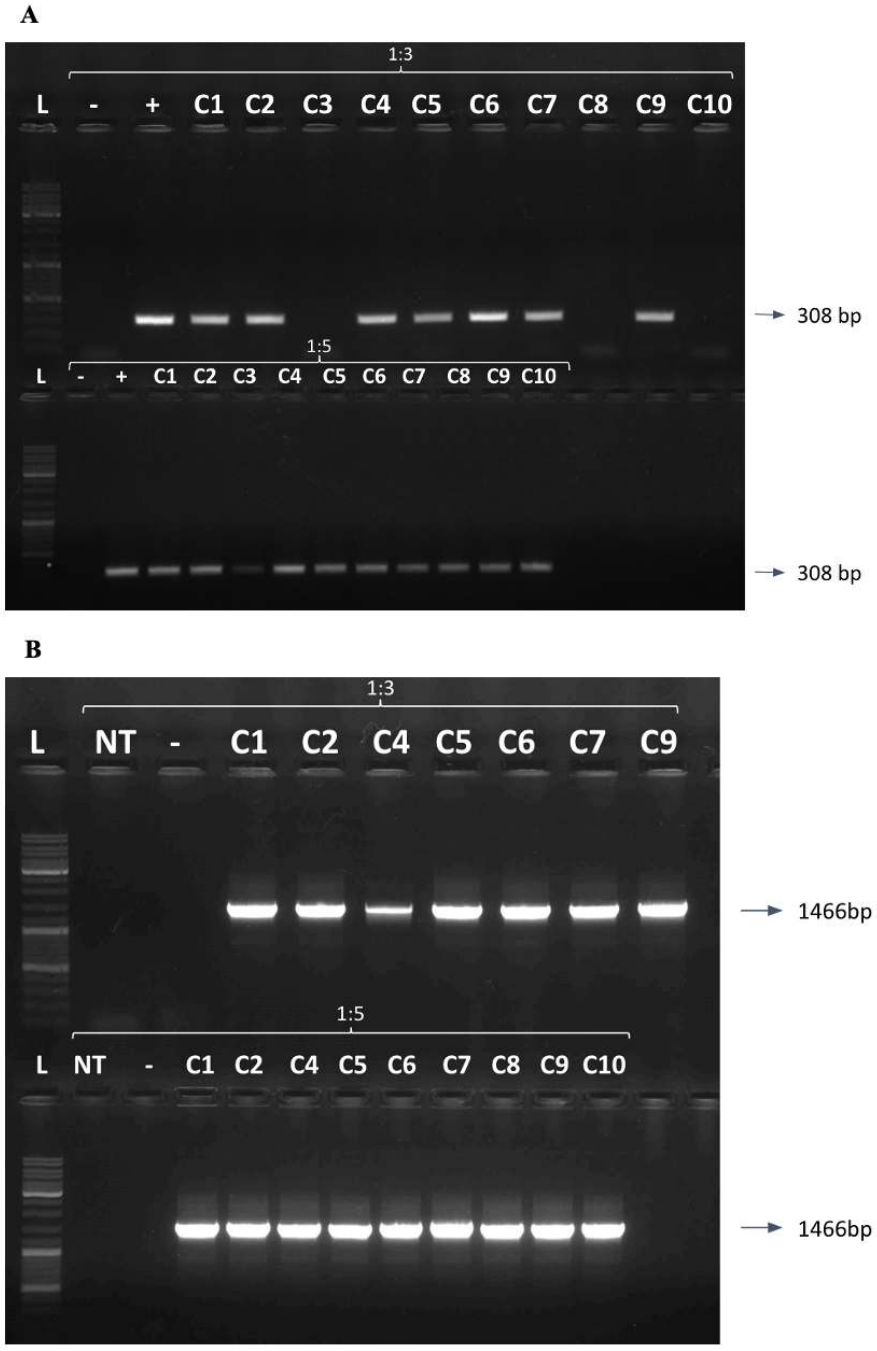

Figure 4. 25. Colony PCR result for pEAQ-HT-N plasmid. A) PCR result with specific primers, +: positive control (pEX-A128-N), -: negative control (water), C1-C10: colonies, B) PCR result with orientation primers, L: Ladder (SMO311), NT: No Template (water), -: negative control (pEAQ-HT), C1-C2-C4-C5-C5-C6-C7-C7-C8-C9-C10: colonies, ligation ratios 1:3 and 1:5.

Colony-6 which was taken from 1:3 ratio ligated transformants and colony-4 which taken from 1:5 ratio ligated transformants were selected for plasmid isolation and were grown in LB containing 50 mg/L kanamycin. Concentrations and purities of the plasmids were measured by NanoDrop (DeNovix, DS-11) (Table 4. 7) and integrities of the plasmids were visualized by agarose gel electrophoresis (Figure 4. 26).

Table 4. 7. NanoDrop measurement results of plasmids

	Plasmid 6	**Plasmid 4**
Concentration (ng/ µl)	120.398	149.025
260/230	2.36	2.27
260/280	1.82	1.81

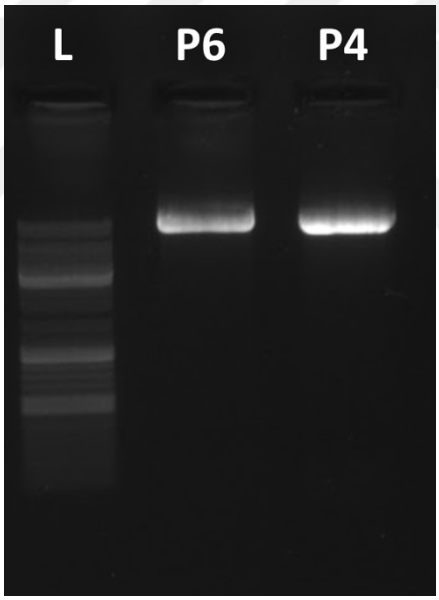

Figure 4. 26. Plasmids isolated from colony-6 and colony-4 containing pEAQ-HT-N plasmid. L: Ladder (SMO311), P6-P4: Plasmids isolated from colony-6 and colony-4.

A final PCR check was performed for the plasmids isolated from colony-6 and colony-4 and amplification products were visualized on agarose gel electrophoresis (Figure 4. 27).

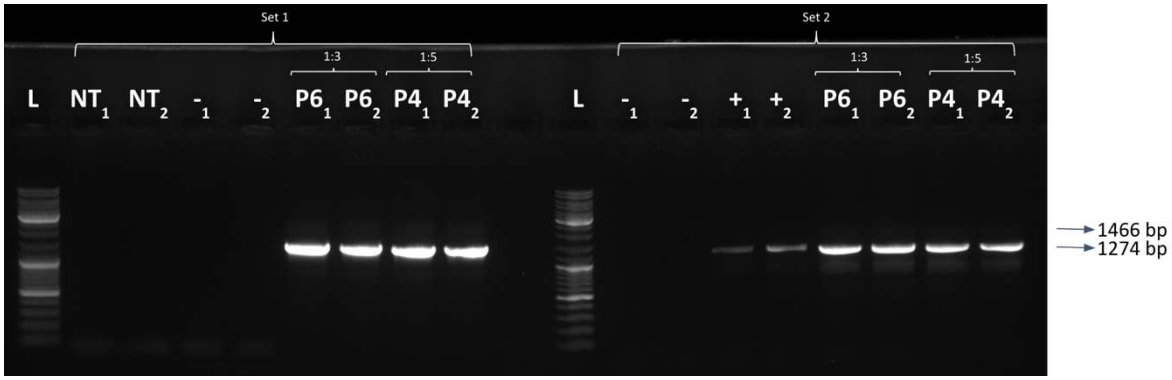

Figure 4. 27. PCR validation pEAQ-HT-N plasmids isolation from colony-6 and colony-4. A) PCR result with orientation primers, L: Ladder (SMO331), NT: No Template (water), -: negative control (pEAQ-HT), P6-P4: plasmids isolated from colony 6 and colony 4, B) PCR result with insert specific primers, L: Ladder (SMO331), -: Negative control (water), +: positive control (pEAQ-HT), P6-P4: plasmids isolated from colony 6 and colony 4, ligation ratios 1:3 and 1:5, set1: orientation primers, set2: insert specific primers

Finally, the N gene insert in pEAQ-HT-N plasmid-6 was confirmed by INTERGEN Genetics and Rare Diseases Diagnostics Center via NGS. According to the alignment analysis by Cluster Omega, the sequence of cloned N gene was 100 % compatible with the original construct (Figure 4. 28).

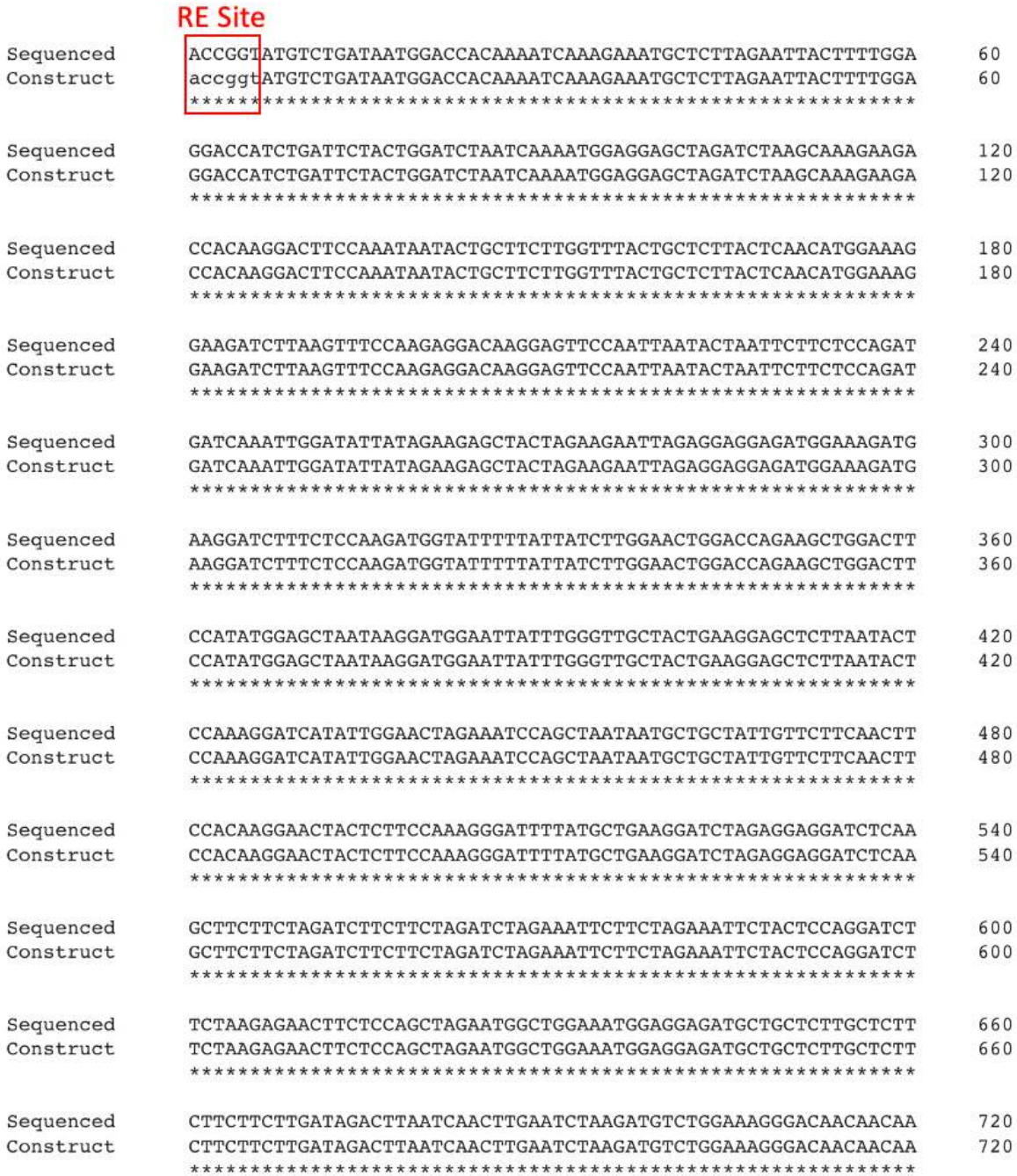

Figure 4. 28. Continued

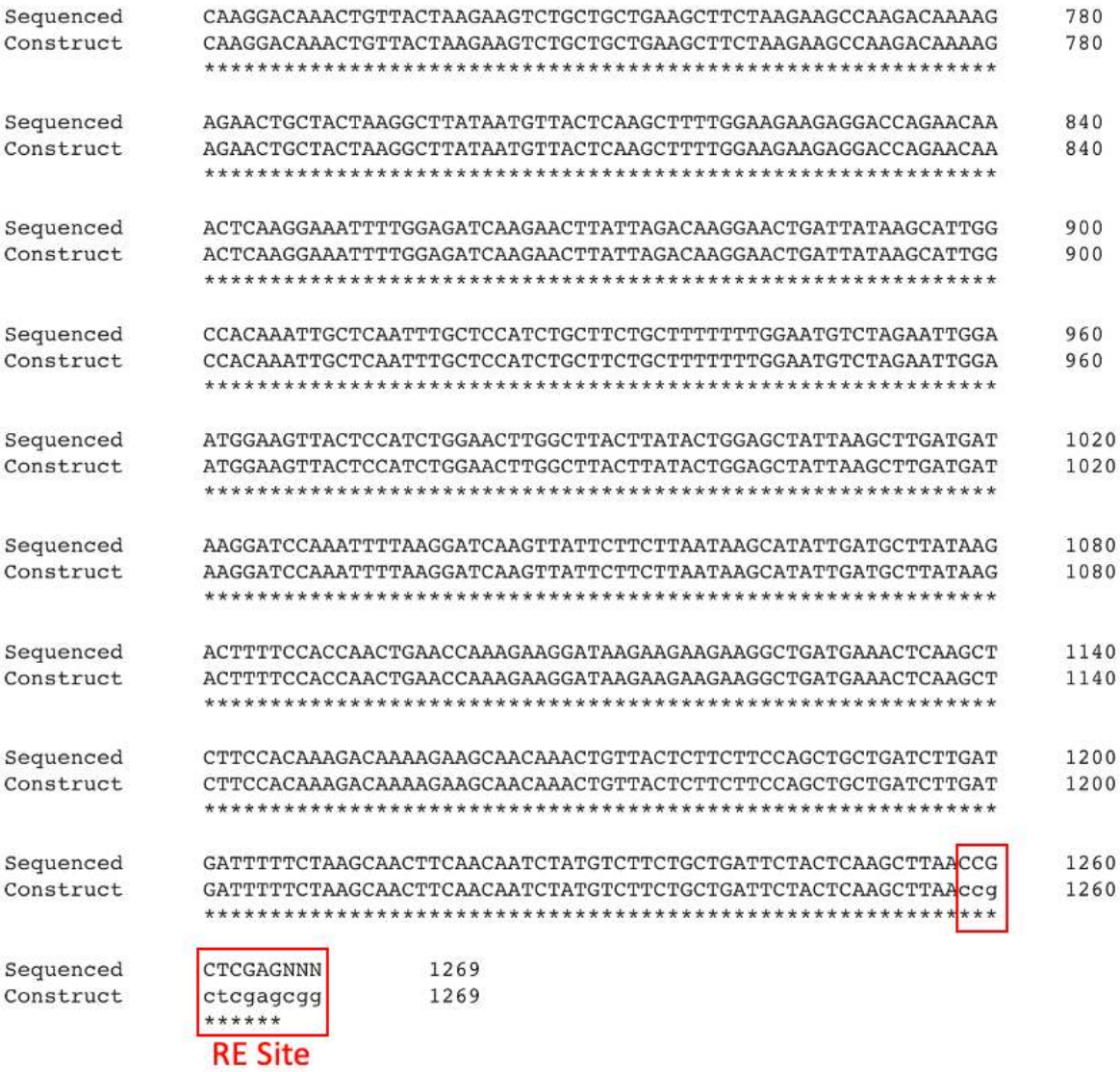

Figure 4. 28. Alignment result of cloned N gene and the original construct, RE Site: Restriction Enzyme site.

4.3.3. Preparation of M gene construct

The M gene cassette was obtained in a plasmid pEX-A128-M which was transferred into *E. coli* 10-beta cells. The presence of the pEX-A128-M plasmid was confirmed by colony PCR with M_gene_F and M_gene_R primers. As a result, the expected 759 bp size bands were observed for 10 colonies. (Figure 4. 29)

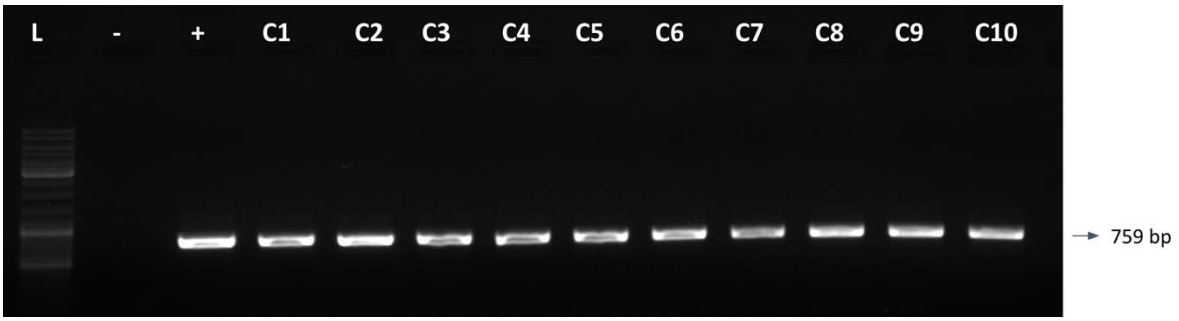

Figure 4. 29. Colony PCR result after transformation with pEX-A128-M plasmid. L: Ladder (SMO331), +: positive control (pEX-A128-M), -: negative control (water), C1-C10: colonies

Colony-2 and colony-8 were selected for plasmid isolation and were grown in LB containing 100 mg/L ampicilin. Concentrations and purities of the plasmids were measured by NanoDrop (DeNovix, DS-11) (Table 4. 8) and integrities of the plasmids were visualized by agarose gel electrophoresis (Figure 4. 30).

Table 4. 8. NanoDrop measurement results of plasmids

	Plasmid 2	**Plasmid 8**
Concentration (ng/ µl)	135.5	132.8
260/230	2.50	2.45
260/280	1.82	1.83

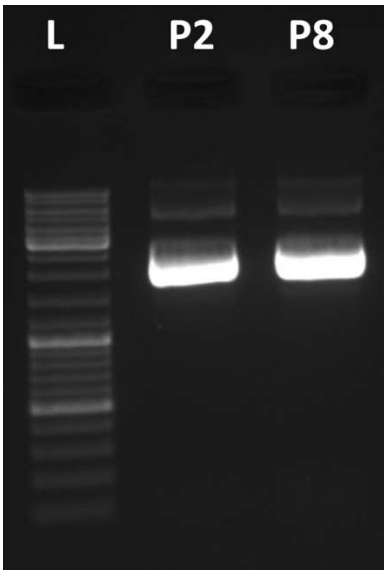

Figure 4. 30. Plasmids isolated from colony-2 and colony-8 containing pEX-A128-M plasmid. L: Ladder (SMO331), P: plasmid

A final PCR check was performed for the plasmids isolated from colony-2 and colony-8 and amplification products were visualized on agarose gel electrophoresis (Figure 4. 31).

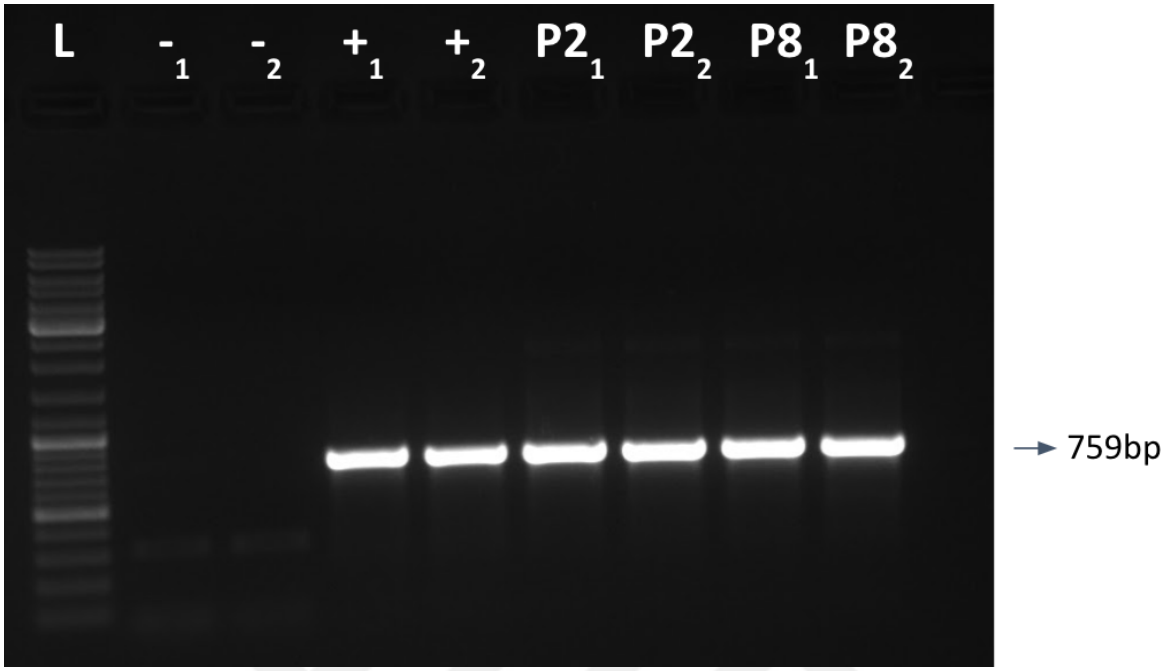

Figure 4. 31. PCR validation pEX-A128-M plasmids isolation from colony-2 and colony-8. L: Ladder (SMO331), +: positive control (pEX-A128-M), -: negative control (water), P: plasmid, P2-P8: plasmids isolated from colony-2 and colony-8.

In order to clone M gene to pEAQ-HT vector, it was amplified with Q5 High-Fidelity DNA Polymerase by using gene specific primers (M-gene_F and M_gene_R) and the expected 764 bp amplification product was observed (Figure 4. 32). The PCR product was purified by using magnetic beads then its concentration was measured as 115 ng/µl by qubit.

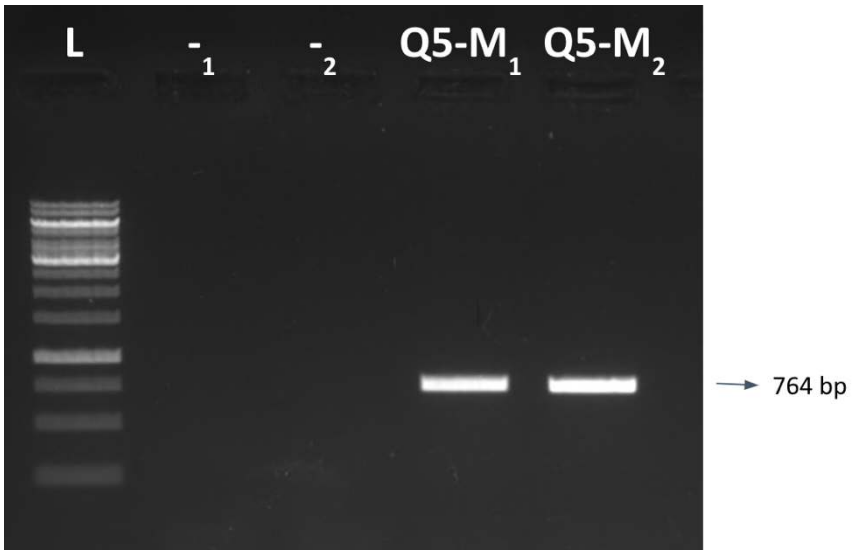

Figure 4. 32. Gel result of the Q5 amplification product of the M gene, L: Ladder (SMO331), -: negative control.

Purified M gene PCR product and pEAQ-HT plasmid were digested with AgeI-HF and XhoI restriction enzymes and ligated with T4 DNA ligase. The final plasmid was named as pEAQ-HT-M and transferred into *E. coli* 10-beta cells. The presence of pEAQ-HT-M was confirmed by colony PCR using M-in_F and M-in_R primers and HT-5UTR_F and M-in_R primers (Figure 4. 33).

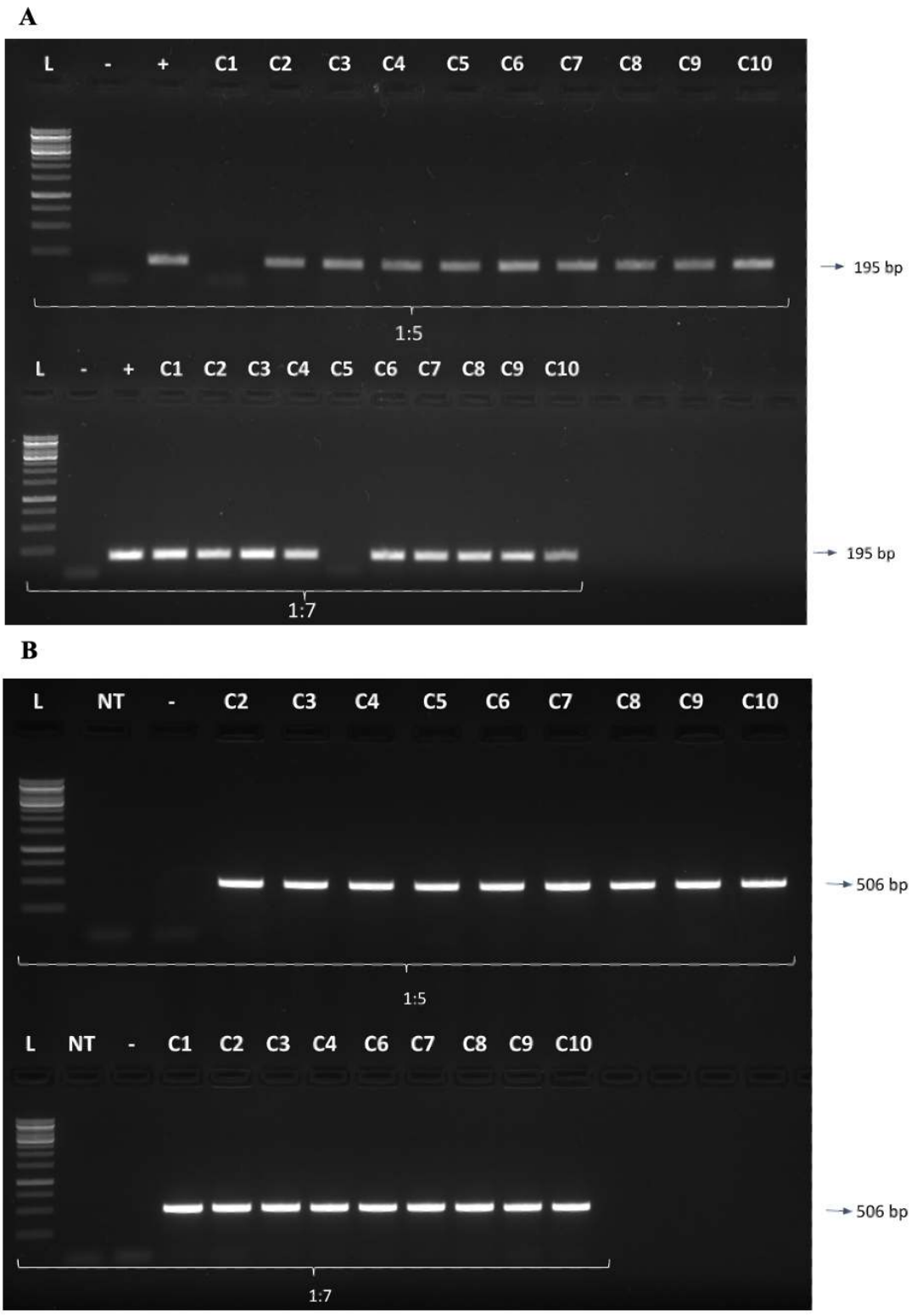

Figure 4. 33. Colony PCR result for pEAQ-HT-M plasmid. A) PCR result with specific primers, +: positive control (pEX-A128M), -: negative control (water), C1-C10: colonies, B) PCR result with orientation primers, L: Ladder (SMO311), NT: No Template (water), -: negative control (pEAQ-HT), ligation ratios 1:5 and 1:7.

Colony-3 which was taken from 1:5 ratio ligated transformants and colony-4 which was taken from 1:7 ratio ligated transformants were selected for plasmid isolation and were grown in LB containing 50 mg/L kanamycin. Concentrations and purities of the plasmids were measured by NanoDrop (DeNovix, DS-11) (Table 4. 9) and integrities of the plasmids were visualized by agarose gel electrophoresis (Figure 4. 34).

Table 4. 9. NanoDrop measurement results of plasmids

	Plasmid 3	**Plasmid 4**
Concentration (ng/ µl)	253.636	226.392
260/230	2.41	2.36
260/280	1.90	1.85

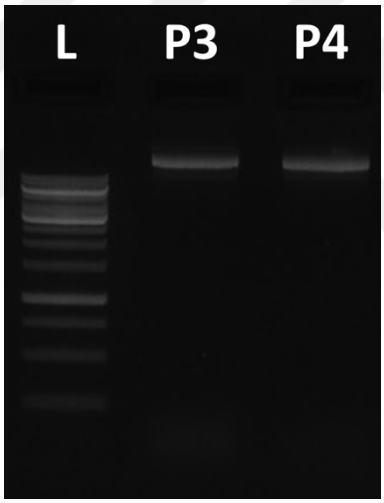

Figure 4. 34. Plasmids isolated from colony-3 and colony-4 containing pEAQ-HT-M plasmid. L: Ladder (SMO311), P3-P4: Plasmids isolated from colony-3 and colony-4.

A final PCR check was performed for the plasmids isolated from colony-3 and colony-4 and amplification products were visualized on agarose gel electrophoresis (Figure 4. 35).

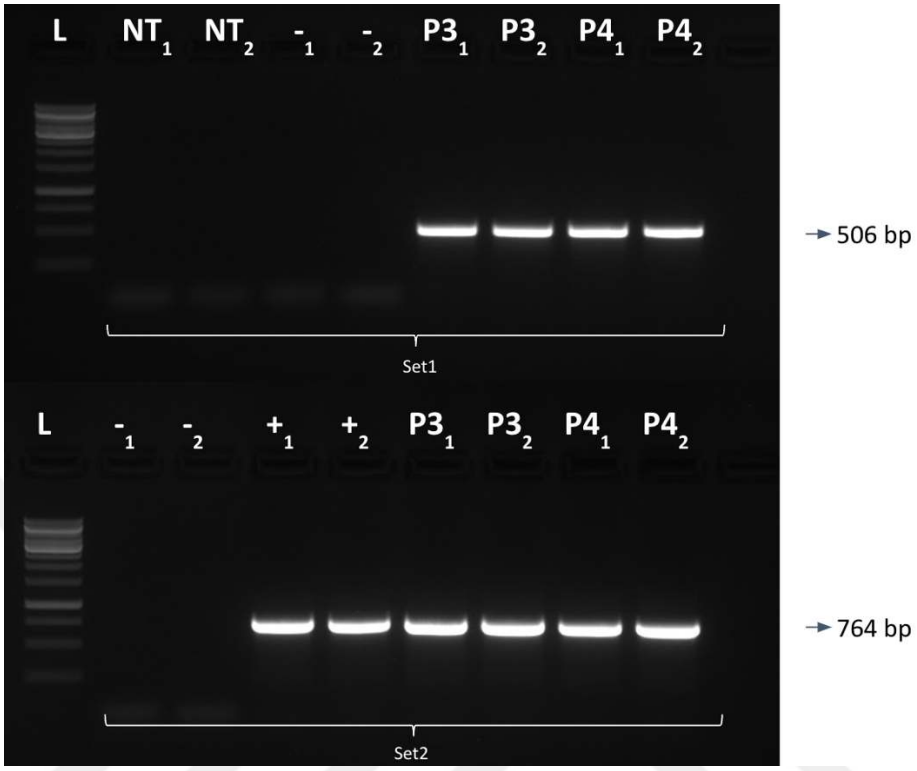

Figure 4. 35. PCR validation pEAQ-HT-M plasmids isolation from colony-3 and colony-4. L: Ladder (SMO331), NT: No Template (water), +: positive control (pEX-A158-M), -: negative control (pEAQ-HT colony 1 plasmid 1ng/ul), P: plasmid, P3-P4: plasmids isolated from colony 3 and colony 4

Finally, the N gene insert in pEAQ-HT-M plasmid-6 was confirmed by INTERGEN Genetics and Rare Diseases Diagnostics Center via NGS. According to the alignment analysis by Cluster Omega, the sequence of cloned M gene was 100 % compatible with the original construct (Figure 4. 36).

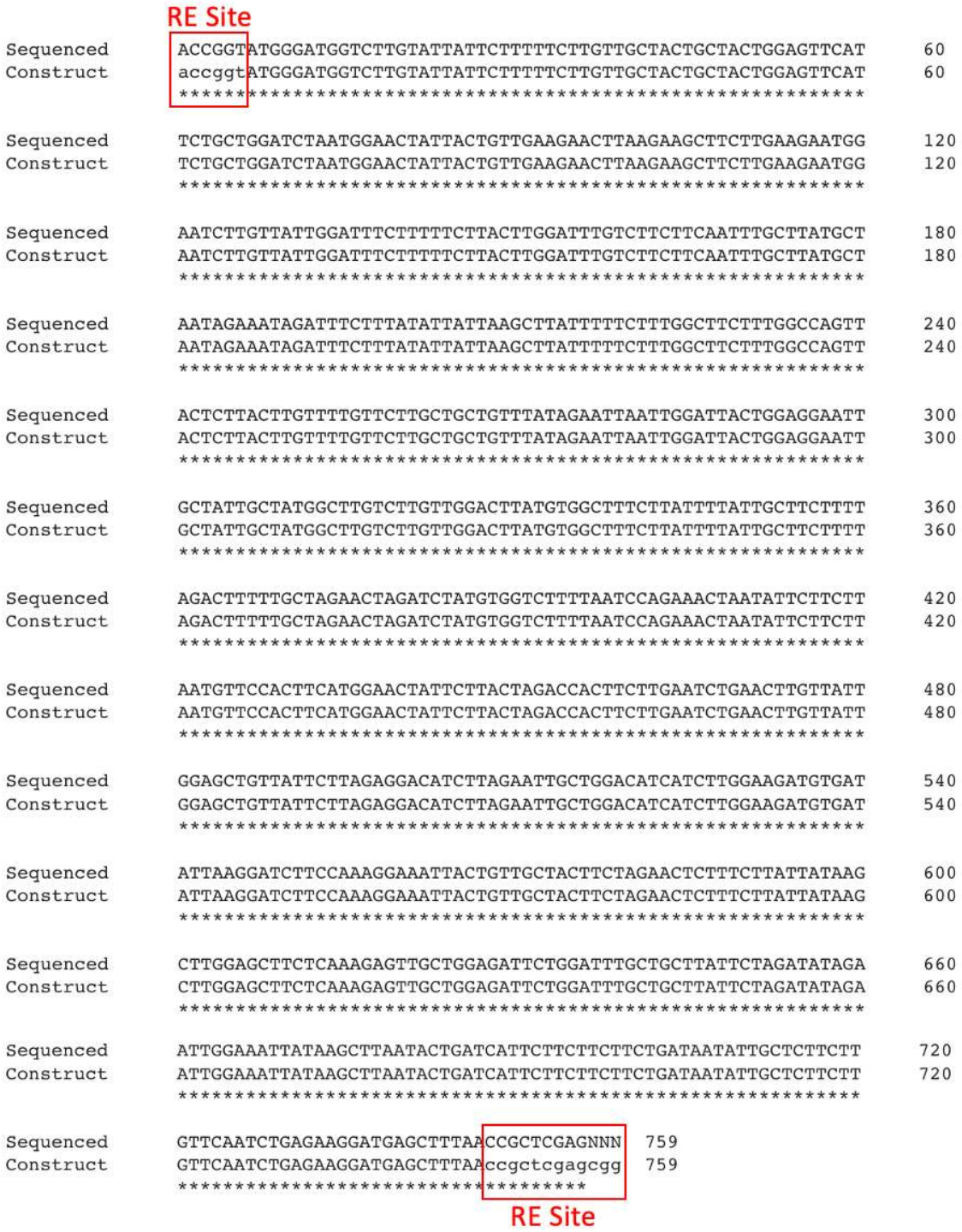

Figure 4. 36. Alignment result of cloned M gene and the original construct, RE Site: Restriction Enzyme site.

4.3.4. Preparation of S-ER gene construct

S gene cassette was obtained in a plasmid pUC57-Amp-S which was transferred into *E. coli* 10-beta cells. The presence of the pUC57-Amp-S plasmid was confirmed by colony PCR with S_gene_F and S_gene_R primers. As a result, the expected 3980 bp size bands were observed for 10 colonies (Figure 4. 37).

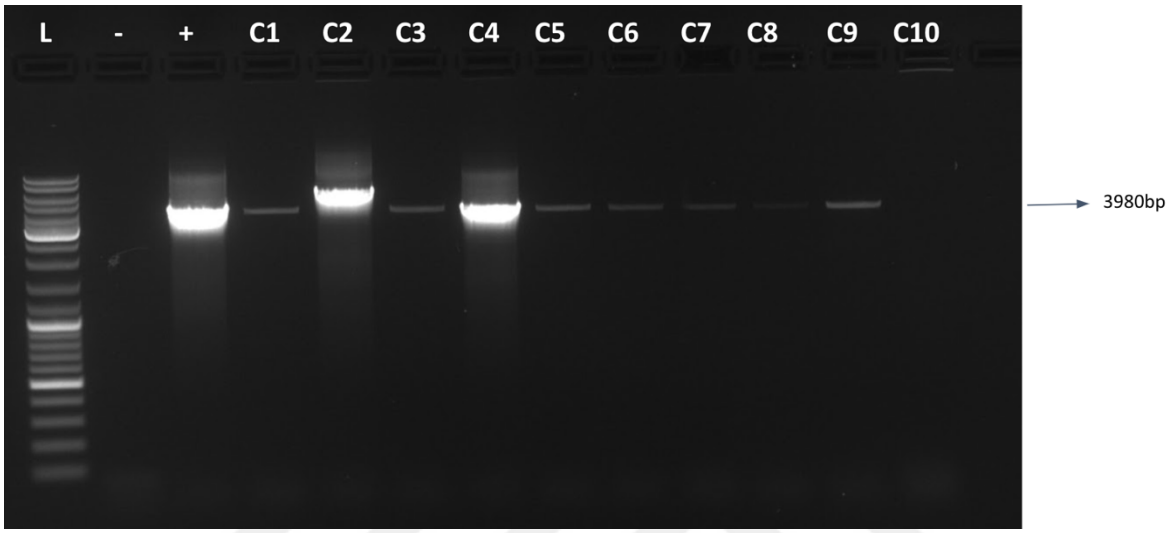

Figure 4. 37. Colony PCR result after transformation with pUC57-Amp-S plasmid. L: Ladder (SMO331), +: positive control (pUC57-Amp-S), -: negative control (water), C1-C10: colonies.

Colony-1 and colony-4 were selected for plasmid isolation and were grown in LB containing 100 mg/L ampicilin. Concentrations and purities of the plasmids were measured by NanoDrop (DeNovix, DS-11) (Table 4. 10) and integrities of the plasmids were visualized by agarose gel electrophoresis (Figure 4. 38).

Table 4. 10. NanoDrop measurement results of plasmids

	Plasmid 1	**Plasmid 4**
Concentration (ng/ µl)	109.550	149.143
260/230	2.20	2.90
260/280	1.89	1.89

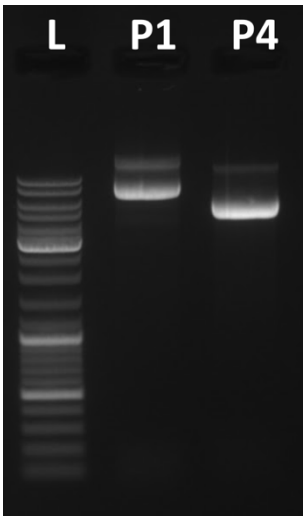

Figure 4. 38. Plasmids isolated from colony-1 and colony-4 containing pEAQ-HT-S plasmid. L: Ladder (SMO311), P1-P4: Plasmids isolated from colony-1 and colony-4.

A final PCR check was performed for the plasmids isolated from colony-1 and colony-4 and amplification products were visualized on agarose gel electrophoresis (Figure 4. 39).

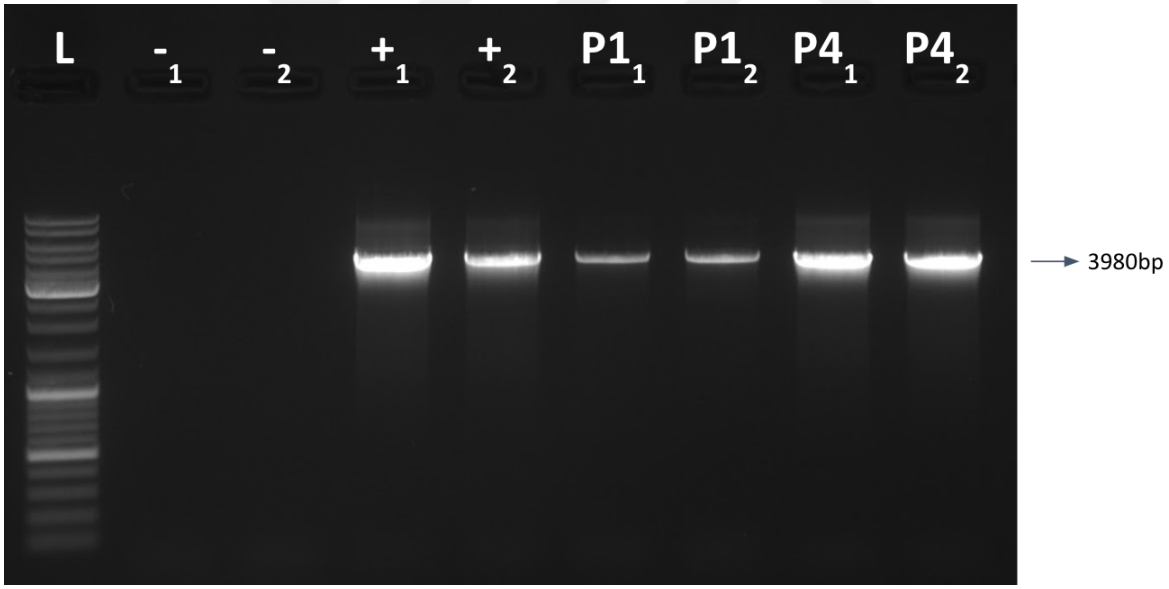

Figure 4. 39. PCR validation pUC57-Amp-S plasmids isolation from colony-1 and colony-4. L: Ladder (SMO331), +: positive control (pUC57-Amp-S), -: negative control (water), P: plasmid, P1-P4: plasmids isolated from colony-1 and colony-4.

In order to clone S gene to pEAQ-HT vector, it was amplified with Q5 High-Fidelity DNA Polymerase by using gene specific primers (S-gene_F and S_gene_R) and the expected 3890 bp amplification product was observed (Figure 4. 40). The PCR product was purified by using magnetic beads then its concentration was measured as 115 ng/µl by qubit.

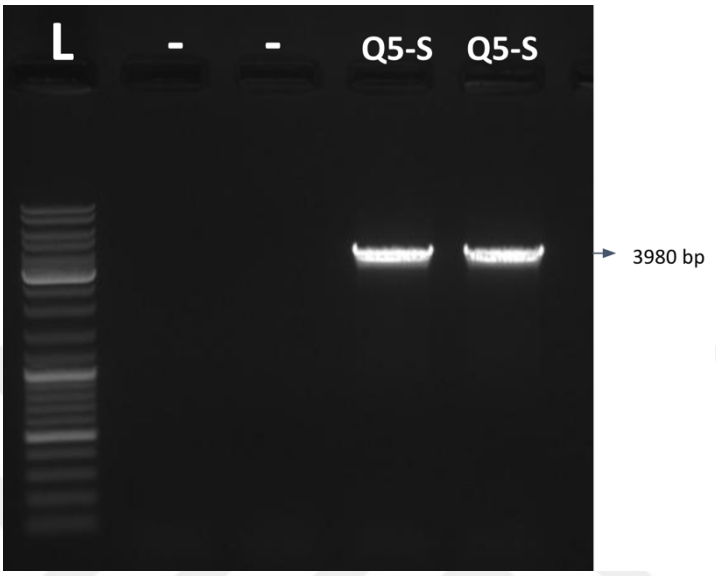

Figure 4. 40. Gel result of the Q5 amplification product of the S gene, L: Ladder (SMO311), -: negative control (water).

Purified S gene PCR product and pEAQ-HT plasmid were digested with AgeI-HF and XhoI restriction enzymes and ligated with T4 DNA ligase. The final plasmid was named as pEAQ-HT-S and transferred into *E. coli* 10-beta cells. The presence of pEAQ-HT-S was confirmed by colony PCR using S-gene_F and S-gene_R primers and HT-5UTR_F and S-in_R primers (Figure 4. 41).

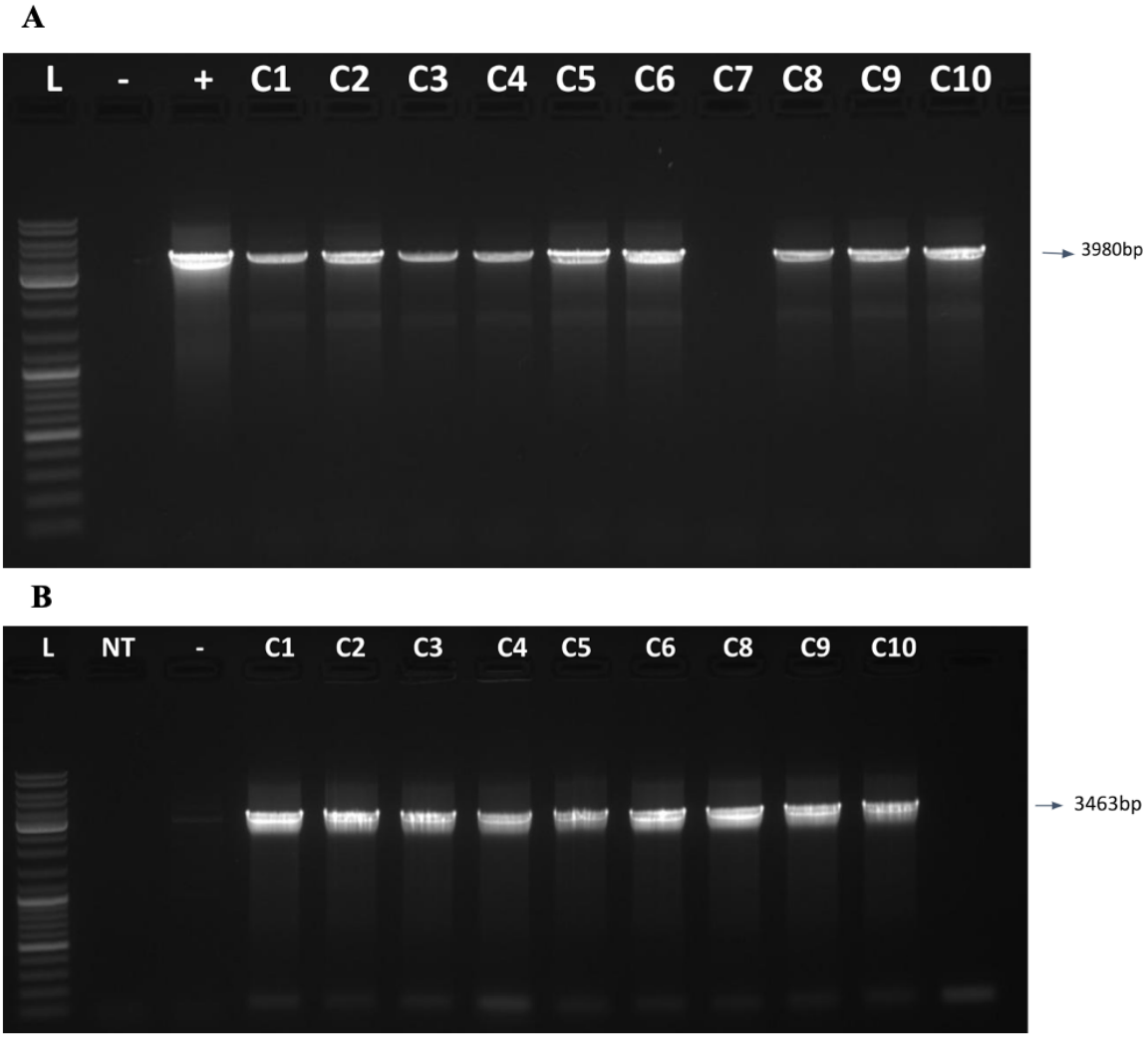

Figure 4. 41. Colony PCR result for pEAQ-HT-S plasmid. A) PCR result with gene specific primers, +: positive control (pUC57-Amp-S), -: negative control (water), C1-C10: colonies, B) PCR result with orientation primers, L: Ladder (SMO311), NT: No Template (water), -: negative control (pEAQ-HT).

Colony-4 and colony-8 were selected for plasmid isolation and were grown in LB containing 50 mg/L kanamycin. Concentrations and purities of the plasmids were measured by NanoDrop (DeNovix, DS-11) (Table 4. 11) and integrities of the plasmids were visualized by agarose gel electrophoresis (Figure 4. 42).

Table 4. 11. NanoDrop measurement results of plasmids

	Plasmid 4	**Plasmid 8**
Concentration (ng/ µl)	100.0	91.4
260/230	2.13	2.23
260/280	1.84	1.88

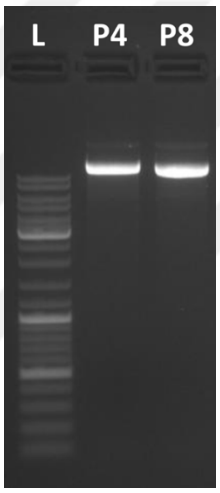

Figure 4. 42. Agarose gel images of pEAQ-HT-S plasmids isolated from colony-4 and colony-8. L: Ladder (SMO331), P4-P8: Plasmids isolated from colony 4 and colony 8.

A final PCR check was performed for the plasmids isolated from colony-1 and colony-4 and amplification products were visualized on agarose gel electrophoresis (Figure 4. 43).

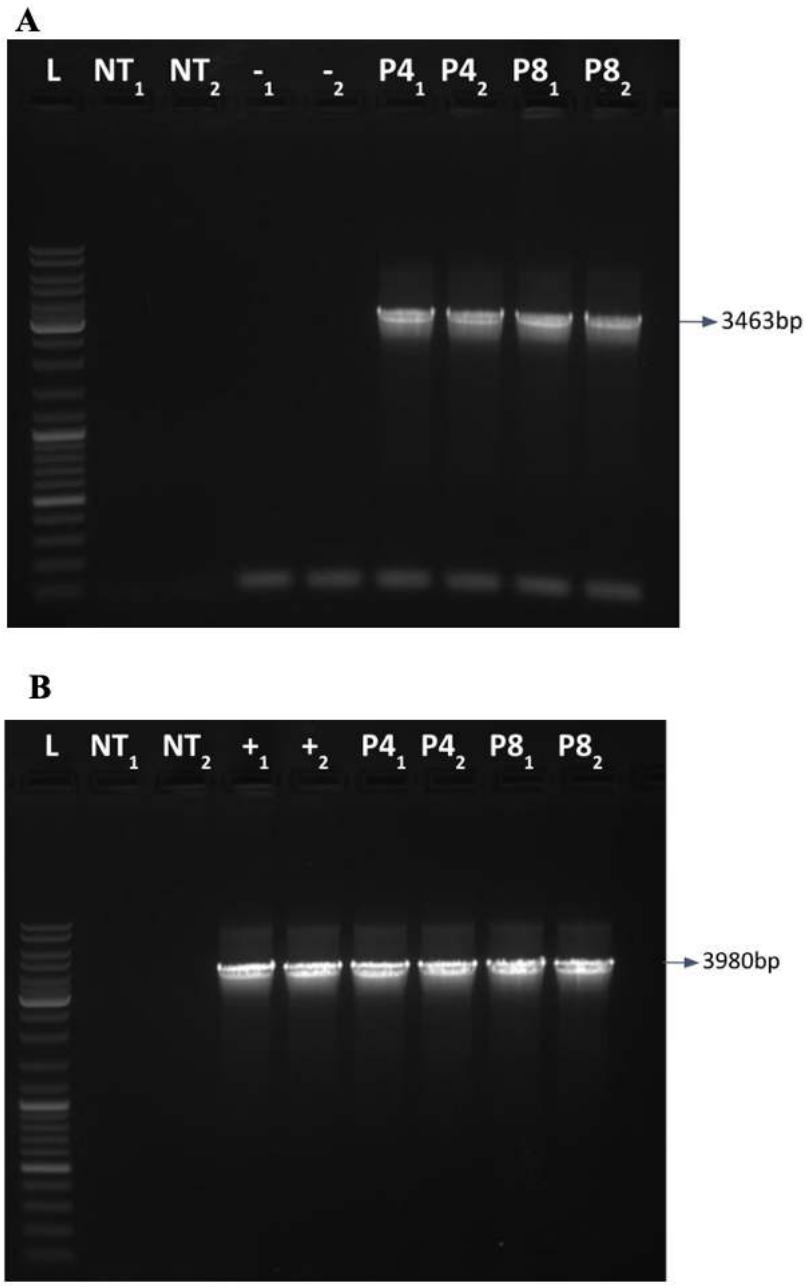

Figure 4. 43. PCR validation pEAQ-HT-S plasmids isolation from colony-1 and colony-4. L: Ladder (SMO331), NT: No Template (water), +: positive control (pUC57-Amp-S), -: negative control (pEAQ-HT colony 1 plasmid 1ng/ul), P: plasmid, P1-P4: plasmids isolated from colony-1 and colony-4.

Finally, the S gene insert in pEAQ-HT-S plasmid-4 was confirmed by INTERGEN Genetics and Rare Diseases Diagnostics Center via NGS. According to the alignment analysis by Cluster Omega, the sequence of cloned S gene was 100 % compatible with the original construct (Fgure 4. 44).

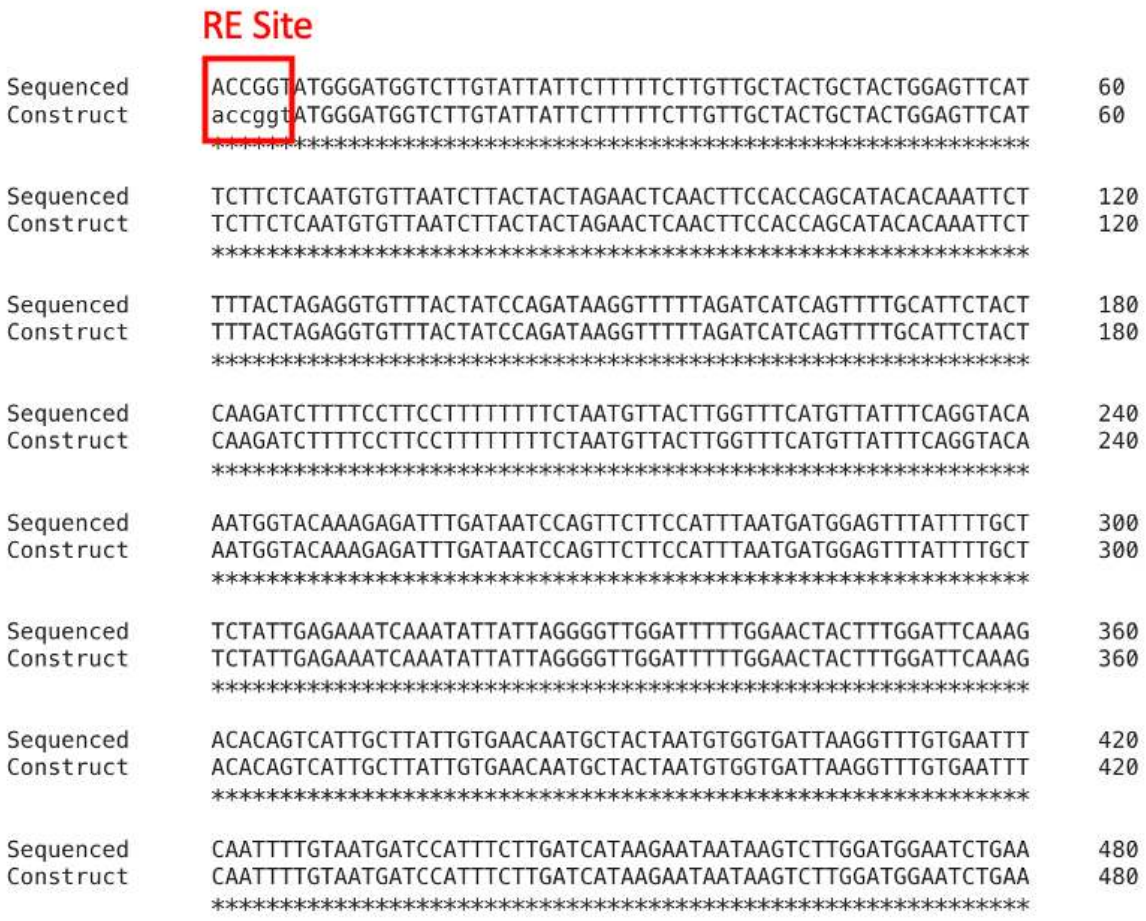

Figure 4. 44. Continued

```
Sequenced       TTTAGGGTTTACTCATCTGCTAATAATTGCACATTTGAATATGTTTCTCAACCATTTTTG     540
Construct       TTTAGGGTTTACTCATCTGCTAATAATTGCACATTTGAATATGTTTCTCAACCATTTTTG     540
                ************************************************************

Sequenced       ATGGATTTGGAAGGAAAGCAAGGAAATTTCAAAAATCTTAGAGAATTTGTTTTTAAGAAT     600
Construct       ATGGATTTGGAAGGAAAGCAAGGAAATTTCAAAAATCTTAGAGAATTTGTTTTTAAGAAT     600
                ************************************************************

Sequenced       ATTGATGGATACTTCAAAATTTATTCTAAGCATACTCCAATTATTGTGAGGGAACCAGAG     660
Construct       ATTGATGGATACTTCAAAATTTATTCTAAGCATACTCCAATTATTGTGAGGGAACCAGAG     660
                ************************************************************

Sequenced       GATTTGCCACAAGGATTCTCAGCATTGGAACCATTGGTTGATTTGCCAATTGGTATTAAT     720
Construct       GATTTGCCACAAGGATTCTCAGCATTGGAACCATTGGTTGATTTGCCAATTGGTATTAAT     720
                ************************************************************

Sequenced       ATTACAAGGTTTCAAACATTGTTGGCTCTTCATAGATCTTACTTGACACCTGGTGATTCT     780
Construct       ATTACAAGGTTTCAAACATTGTTGGCTCTTCATAGATCTTACTTGACACCTGGTGATTCT     780
                ************************************************************

Sequenced       TTTCTTCTTAAGTATAATGAAAATGGTACAATTACAGATGCAGTTGATTGCGCTTTGGAT     900
Construct       TTTCTTCTTAAGTATAATGAAAATGGTACAATTACAGATGCAGTTGATTGCGCTTTGGAT     900
                ************************************************************

Sequenced       CCTCTTTCTGAAACTAAGTGTACTCTTAAGTCTTTTACTGTTGAAAAGGGTATTTACCAG     960
Construct       CCTCTTTCTGAAACTAAGTGTACTCTTAAGTCTTTTACTGTTGAAAAGGGTATTTACCAG     960
                ************************************************************

Sequenced       ACTTCTAATTTTAGAGTTCAACCAACAGAGTCAATTGTTAGATTTCCAAATATTACAAAT    1020
Construct       ACTTCTAATTTTAGAGTTCAACCAACAGAGTCAATTGTTAGATTTCCAAATATTACAAAT    1020
                ************************************************************

Sequenced       TTGTGTCCATTCGATGAGGTTTTTAATGCTACTAGATTTGCTTCAGTTTACGCATGGAAT    1080
Construct       TTGTGTCCATTCGATGAGGTTTTTAATGCTACTAGATTTGCTTCAGTTTACGCATGGAAT    1080
                ************************************************************

Sequenced       AGAAAGAGAATTTCTAATTGTGTTGCAGATTACTCAGTTTTGTACAATCTTGCTCCATTT    1140
Construct       AGAAAGAGAATTTCTAATTGTGTTGCAGATTACTCAGTTTTGTACAATCTTGCTCCATTT    1140
                ************************************************************

Sequenced       TTTACTTTTAAGTGCTACGGTGTTTCTCCAACTAAGCTTAATGATCTTTGTTTTACTAAT    1200
Construct       TTTACTTTTAAGTGCTACGGTGTTTCTCCAACTAAGCTTAATGATCTTTGTTTTACTAAT    1200
                ************************************************************

Sequenced       GTTTATGCTGATTCTTTTGTTATTAGAGGAGATGAAGTTAGACAAATTGCTCCAGGACAA    1260
Construct       GTTTATGCTGATTCTTTTGTTATTAGAGGAGATGAAGTTAGACAAATTGCTCCAGGACAA    1260
                ************************************************************

Sequenced       ACTGGAAATATTGCAGATTATAATTATAAGCTTCCAGATGATTTTACTGGATGTGTTATT    1320
Construct       ACTGGAAATATTGCAGATTATAATTATAAGCTTCCAGATGATTTTACTGGATGTGTTATT    1320
                ************************************************************

Sequenced       GCTTGGAATTCAAACAAGCTTGATTCTAAGGTTTCAGGTAATTACAATTATCTTTATAGA    1380
Construct       GCTTGGAATTCAAACAAGCTTGATTCTAAGGTTTCAGGTAATTACAATTATCTTTATAGA    1380
                ************************************************************

Sequenced       CTTTTTAGAAAGTCTAATCTTAAGCCATTTGAAAGGGATATTTCAACTGAAATTTATCAA    1440
Construct       CTTTTTAGAAAGTCTAATCTTAAGCCATTTGAAAGGGATATTTCAACTGAAATTTATCAA    1440
                ************************************************************

Sequenced       GCTGGAAATAAGCCATGTAATGGAGTTGCAGGTTTCAATTGTTATTTTCCACTTAGGTCA    1500
Construct       GCTGGAAATAAGCCATGTAATGGAGTTGCAGGTTTCAATTGTTATTTTCCACTTAGGTCA    1500
                ************************************************************

Sequenced       TATTCTTTTAGACCAACTTATGGAGTTGGACATCAACCATATAGAGTTGTTGTTCTTTCT    1560
Construct       TATTCTTTTAGACCAACTTATGGAGTTGGACATCAACCATATAGAGTTGTTGTTCTTTCT    1560
                ************************************************************
```

Figure 4. 44. Continued.

```
Sequenced       TTTGAACTTCTTCATGCACCTGCAACTGTTTGTGGACCAAAGAAGTCTACTAATTTGGTT    1620
Construct       TTTGAACTTCTTCATGCACCTGCAACTGTTTGTGGACCAAAGAAGTCTACTAATTTGGTT    1620
                ************************************************************

Sequenced       AAAAATAAGTGTGTGAATTTCAATTTTAATGGACTTAAGGGAACAGGTGTTTTGACAGAA    1680
Construct       AAAAATAAGTGTGTGAATTTCAATTTTAATGGACTTAAGGGAACAGGTGTTTTGACAGAA    1680
                ************************************************************

Sequenced       TCTAATAAGAAGTTTCTTCCATTTCAACAATTTGGAAGAGATATTGCTGATACAACAGAT    1740
Construct       TCTAATAAGAAGTTTCTTCCATTTCAACAATTTGGAAGAGATATTGCTGATACAACAGAT    1740
                ************************************************************

Sequenced       GCTGTTAGAGATCCACAAACTCTTGAAATTCTTGATATTACACCTTGTTCATTCGGTGGT    1800
Construct       GCTGTTAGAGATCCACAAACTCTTGAAATTCTTGATATTACACCTTGTTCATTCGGTGGT    1800
                ************************************************************

Sequenced       GTTTCTGTTATTACTCCAGGAACTAATACTTCTAATCAAGTTGCTGTTCTTTATCAAGGA    1860
Construct       GTTTCTGTTATTACTCCAGGAACTAATACTTCTAATCAAGTTGCTGTTCTTTATCAAGGA    1860
                ************************************************************

Sequenced       GTTAATTGTACTGAAGTTCCAGTTGCTATTCATGCTGATCAACTTACTCCAACTTGGAGA    1920
Construct       GTTAATTGTACTGAAGTTCCAGTTGCTATTCATGCTGATCAACTTACTCCAACTTGGAGA    1920
                ************************************************************

Sequenced       GTTTATTCTACTGGATCTAATGTTTTTCAAACTAGAGCTGGATGTCTTATTGGTGCAGAG    1980
Construct       GTTTATTCTACTGGATCTAATGTTTTTCAAACTAGAGCTGGATGTCTTATTGGTGCAGAG    1980
                ************************************************************

Sequenced       TATGTTAATAATTCTTATGAATGTGATATTCCAATTGGTGCAGGTATTTGTGCTTCTTAT    2040
Construct       TATGTTAATAATTCTTATGAATGTGATATTCCAATTGGTGCAGGTATTTGTGCTTCTTAT    2040
                ************************************************************

Sequenced       CAAACTCAAACTAAGTCTCATGGATCTGCTTCATCAGTTGCATCTCAATCTATTATTGCT    2100
Construct       CAAACTCAAACTAAGTCTCATGGATCTGCTTCATCAGTTGCATCTCAATCTATTATTGCT    2100
                ************************************************************

Sequenced       TATACTATGTCTCTTGGAGCTGAAAATTCTGTTGCTTATTCTAATAATTCAATTGCAATT    2160
Construct       TATACTATGTCTCTTGGAGCTGAAAATTCTGTTGCTTATTCTAATAATTCAATTGCAATT    2160
                ************************************************************

Sequenced       CCAACTAATTTCACAATTTCTGTTACAACAGAGATTCTTCCTGTTTCTATGACTAAGACT    2220
Construct       CCAACTAATTTCACAATTTCTGTTACAACAGAGATTCTTCCTGTTTCTATGACTAAGACT    2220
                ************************************************************

Sequenced       TCTGTTGATTGTACTATGTATATTTGTGGAGATTCTACTGAATGTTCTAATCTTCTTCTT    2280
Construct       TCTGTTGATTGTACTATGTATATTTGTGGAGATTCTACTGAATGTTCTAATCTTCTTCTT    2280
                ************************************************************

Sequenced       CAATATGGATCTTTTTGTACTCAACTTAAGAGAGCTCTTACTGGAATTGCTGTTGAACAA    2340
Construct       CAATATGGATCTTTTTGTACTCAACTTAAGAGAGCTCTTACTGGAATTGCTGTTGAACAA    2340
                ************************************************************

Sequenced       GATAAGAATACTCAAGAAGTTTTTGCTCAAGTTAAGCAAATTTATAAGACTCCACCAATT    2400
Construct       GATAAGAATACTCAAGAAGTTTTTGCTCAAGTTAAGCAAATTTATAAGACTCCACCAATT    2400
                ************************************************************

Sequenced       AAATACTTCGGAGGATTTAATTTTTCTCAAATTCTTCCAGATCCATCTAAGCCTTCAAAA    2460
Construct       AAATACTTCGGAGGATTTAATTTTTCTCAAATTCTTCCAGATCCATCTAAGCCTTCAAAA    2460
                ************************************************************

Sequenced       AGGTCTTTTATTGAAGATCTTCTTTTTAATAAGGTTACTCTTGCTGATGCAGGTTTCATT    2520
Construct       AGGTCTTTTATTGAAGATCTTCTTTTTAATAAGGTTACTCTTGCTGATGCAGGTTTCATT    2520
                ************************************************************

Sequenced       AAGCAATATGGAGATTGCTTGGGTGATATTGCTGCTAGAGATCTTATTTGTGCTCAAAAG    2580
Construct       AAGCAATATGGAGATTGCTTGGGTGATATTGCTGCTAGAGATCTTATTTGTGCTCAAAAG    2580
                ************************************************************
```

Figure 4. 44. Continued

```
Sequenced       TTTAAGGGACTTACTGTTCTTCCACCACTTCTTACTGATGAAATGATTGCTCAATATACA     2640
Construct       TTTAAGGGACTTACTGTTCTTCCACCACTTCTTACTGATGAAATGATTGCTCAATATACA     2640
                ************************************************************

Sequenced       TCAGCACTTCTTGCTGGAACTATTACTTCTGGATGGACTTTTGGAGCTGGAGCTGCTCTT     2700
Construct       TCAGCACTTCTTGCTGGAACTATTACTTCTGGATGGACTTTTGGAGCTGGAGCTGCTCTT     2700
                ************************************************************

Sequenced       CAAATTCCATTTGCTATGCAAATGGCTTATAGATTTAATGGAATTGGAGTTACACAGAAT     2760
Construct       CAAATTCCATTTGCTATGCAAATGGCTTATAGATTTAATGGAATTGGAGTTACACAGAAT     2760
                ************************************************************

Sequenced       GTTCTTTATGAAAATCAAAAATTGATTGCTAATCAATTTAATTCTGCTATTGGAAAGATT     2820
Construct       GTTCTTTATGAAAATCAAAAATTGATTGCTAATCAATTTAATTCTGCTATTGGAAAGATT     2820
                ************************************************************

Sequenced       CAAGATTCTTTGTCATCAACTGCTTCTGCTCTTGGAAAGCTTCAAGATGTGGTGAATCAT     2880
Construct       CAAGATTCTTTGTCATCAACTGCTTCTGCTCTTGGAAAGCTTCAAGATGTGGTGAATCAT     2880
                ************************************************************

Sequenced       AATGCTCAAGCTCTTAATACTCTTGTTAAGCAACTTTCTTCTAAGTTTGGAGCTATTTCT     2940
Construct       AATGCTCAAGCTCTTAATACTCTTGTTAAGCAACTTTCTTCTAAGTTTGGAGCTATTTCT     2940
                ************************************************************

Sequenced       TCTGTTCTTAATGATATTTTTTCTAGACTTGATCCACCAGAAGCTGAAGTTCAGATTGAT     3000
Construct       TCTGTTCTTAATGATATTTTTTCTAGACTTGATCCACCAGAAGCTGAAGTTCAGATTGAT     3000
                ************************************************************

Sequenced       AGGTTGATTACTGGAAGACTTCAATCTCTTCAAACTTACGTTACACAGCAACTTATTAGA     3060
Construct       AGGTTGATTACTGGAAGACTTCAATCTCTTCAAACTTACGTTACACAGCAACTTATTAGA     3060
                ************************************************************

Sequenced       GCTGCTGAAATTAGAGCTTCTGCTAATCTTGCTGCTACTAAGATGTCTGAATGTGTTCTT     3120
Construct       GCTGCTGAAATTAGAGCTTCTGCTAATCTTGCTGCTACTAAGATGTCTGAATGTGTTCTT     3120
                ************************************************************

Sequenced       GGACAATCTAAGAGAGTTGATTTTTGTGGAAAGGGATATCATCTTATGTCTTTTCCACAA     3180
Construct       GGACAATCTAAGAGAGTTGATTTTTGTGGAAAGGGATATCATCTTATGTCTTTTCCACAA     3180
                ************************************************************

Sequenced       TCTGCTCCACATGGAGTTGTTTTTCTTCATGTTACTTATGTTCCAGCTCAAGAAAAGAAT     3240
Construct       TCTGCTCCACATGGAGTTGTTTTTCTTCATGTTACTTATGTTCCAGCTCAAGAAAAGAAT     3240
                ************************************************************

Sequenced       TTTACTACTGCTCCAGCTATTTGTCATGATGGAAAGGCTCATTTTCCAAGAGAAGGAGTT     3300
Construct       TTTACTACTGCTCCAGCTATTTGTCATGATGGAAAGGCTCATTTTCCAAGAGAAGGAGTT     3300
                ************************************************************

Sequenced       TTCGTTTCAAATGGAACTCATTGGTTTGTTACTCAAAGAAATTTTTATGAACCACAAATT     3360
Construct       TTCGTTTCAAATGGAACTCATTGGTTTGTTACTCAAAGAAATTTTTATGAACCACAAATT     3360
                ************************************************************

Sequenced       ATTACTACTGATAATACTTTTGTTTCTGGAAATTGTGATGTTGTTATTGGAATTGTTAAT     3420
Construct       ATTACTACTGATAATACTTTTGTTTCTGGAAATTGTGATGTTGTTATTGGAATTGTTAAT     3420
                ************************************************************

Sequenced       AATACTGTTTATGATCCACTTCAACCTGAGTTGGATTCTTTTAAGGAAGAACTTGATAAG     3480
Construct       AATACTGTTTATGATCCACTTCAACCTGAGTTGGATTCTTTTAAGGAAGAACTTGATAAG     3480
                ************************************************************
```

Figure 4. 44. Continued

Figure 4. 44. Alignment result of cloned S gene and the original construct, RE Site: Restriction Enzyme site.

4.3.5. Preparation of S-Chl gene construct

S-chl gene cassette was obtained in a plasmid pUC57-Amp-S-chl which was transferred into *E. coli* 10-beta cells. The presence of the pUC57-Amp-S-chl plasmid was confirmed by colony PCR with S_in_F and S_in_R primers. As a result, the expected 658 bp size bands were observed for 10 colonies (Figure 4. 45).

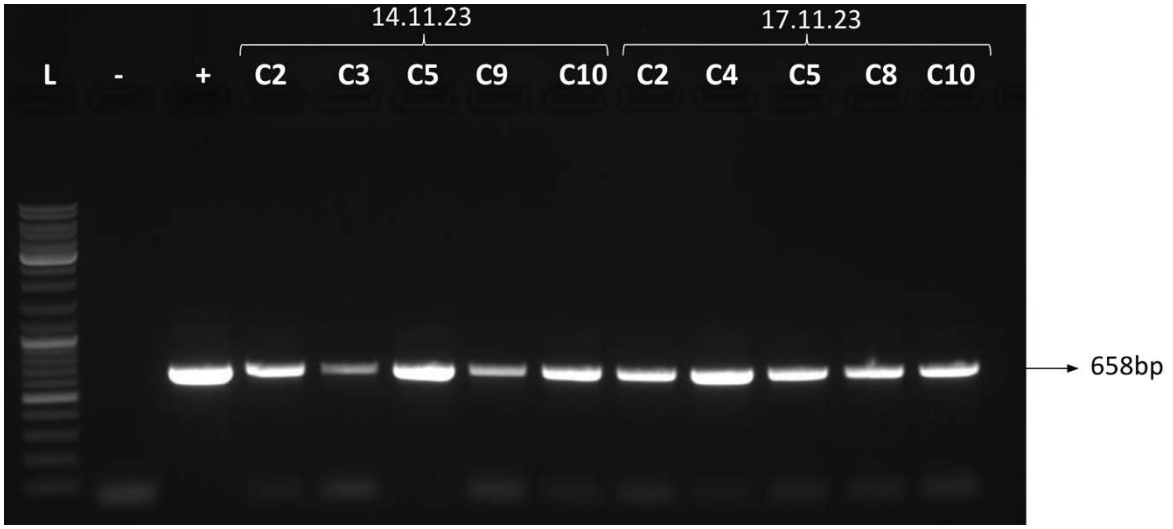

Figure 4. 45. Colony PCR result after transformation with pUC57-Amp-S-chl plasmid. L: Ladder (SMO331), +: positive control (pUC57-Amp-S-chl), -: negative control (water), C1-C10: colonies. 14.11.23: colonies selected on November 14, 17.11.23: colonies selected on November 17.

Colony-4 was selected for plasmid isolation and was grown in LB containing 100 mg/L ampicilin. Concentrations and purities of the plasmids were measured by NanoDrop (DeNovix, DS-11) (Table 4. 12) and integrities of the plasmids were visualized by agarose gel electrophoresis (Figure 4. 46).

Table 4. 12. Nanodrop measurement result of pUC57-S-chl plasmid

	Plasmid 4
Concentration (ng/ µl)	170.7
260/230	2.37
260/280	1.99

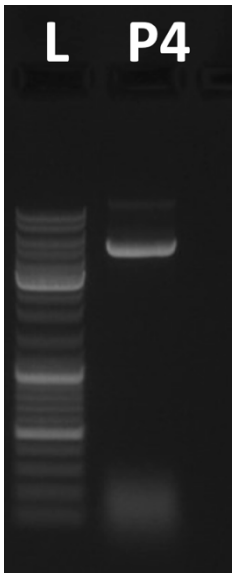

Figure 4. 46. Plasmid isolated from colony-4 containing pEAQ-HT-S plasmid. L: Ladder (SMO311), P4: Plasmid isolated from colony-4.

A final PCR check was performed for the plasmid isolated from colony-4 and amplification products were visualized on agarose gel electrophoresis (Figure 4. 47).

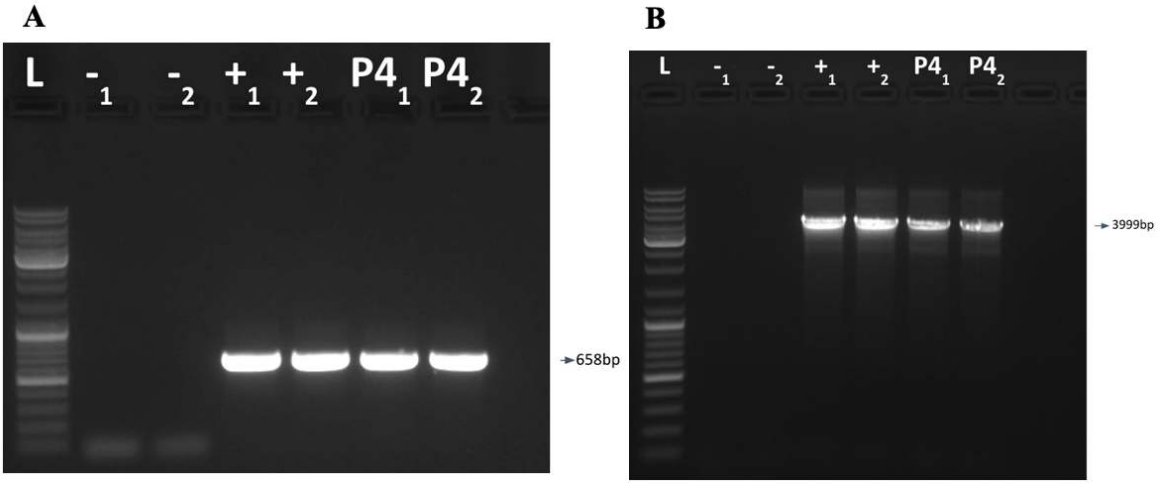

Figure 4. 47. PCR validation pUC57-Amp-S-chl plasmid isolation from colony-4. Agarose gel image of pUC57-S-chl plasmid after PCR. A) PCR result with insert specific primers, B) PCR result with gene specific primers, L: Ladder (SMO331), -: Negative control (water), +: positive control (pEAQ-HT), -: negative control (pUC57-S-chl), p4: plasmid isolated from colony-4

In order to clone S-chl gene to pEAQ-HT vector, it was amplified with Q5 High-Fidelity DNA Polymerase by using gene specific primers (S-chl-gene_F and S-chl_gene_R) and the expected 3999 bp amplification product was observed (Figure 4. 48). The PCR product was purified by using magnetic beads then its concentration was measured as 65.5 ng/µl by Qubit.

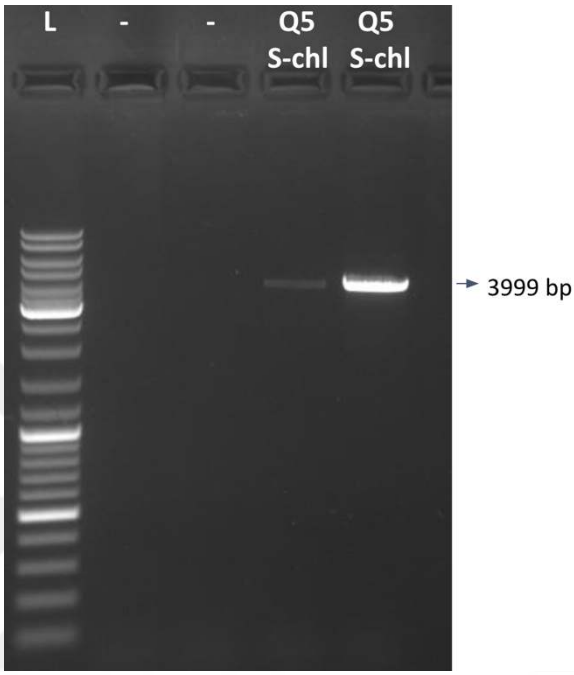

Figure 4. 48. Gel result of the Q5 amplification product of the S-chl gene, L: Ladder (SMO311), -: negative control (water).

Purified S-chl gene PCR product and pEAQ-HT plasmid were digested with AgeI-HF and XhoI restriction enzymes and ligated with T4 DNA ligase. Final plasmid was named pEAQ-HT-S-chl and transferred into *E. coli* 10-beta cells. The presence of pEAQ-HT-S-chl was confirmed by colony PCR using S-chl-gene_F and S-chl-gene_R primers and HT-5UTR_F and S-in_R primers (Figure 4. 49).

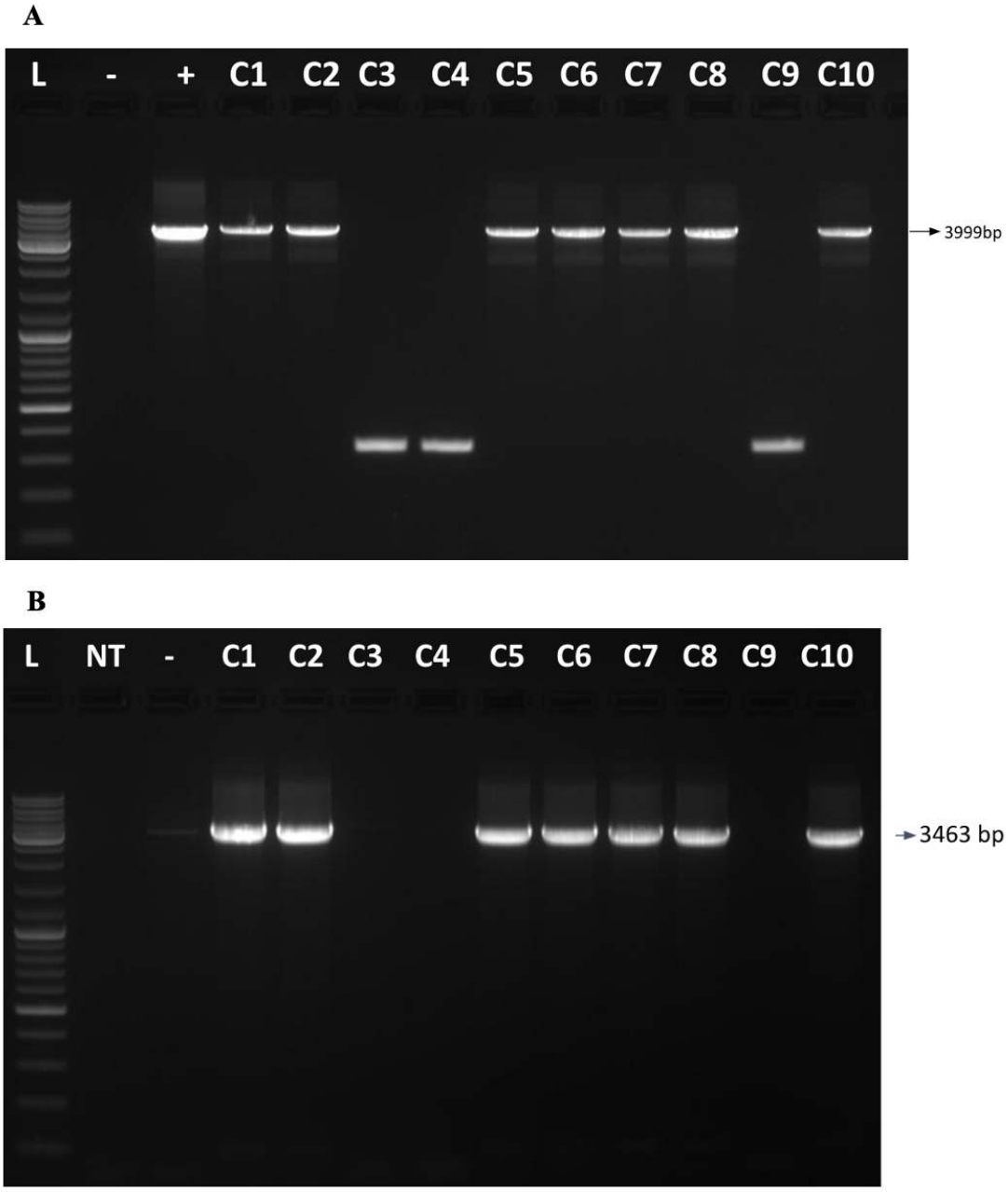

Figure 4. 49. Colony PCR result for pEAQ-HT-S-chl plasmid. A) PCR result with gene specific primers, +: positive control (pUC57-Amp-S-chl), -: negative control (water), C1-C10: colonies, B) PCR result with orientation primers, L: Ladder (SMO311), NT: No Template (water), -: negative control (pEAQ-HT).

Colony-2 and colony-5 were selected for plasmid isolation and were grown in LB containing 50 mg/L kanamycin. Concentrations and purities of the plasmids were measured by NanoDrop (DeNovix, DS-11) (Table 4. 13) and integrities of the plasmids were visualized by agarose gel electrophoresis (Figure 4. 50).

Table 4. 13. Nanodrop results of plasmids of pEAQ-HT-S-chl

	Plasmid 2	**Plasmid 5**
Concentration (ng/ µl)	191.1	136.9
260/230	2.36	2.28
260/280	1.85	1.84

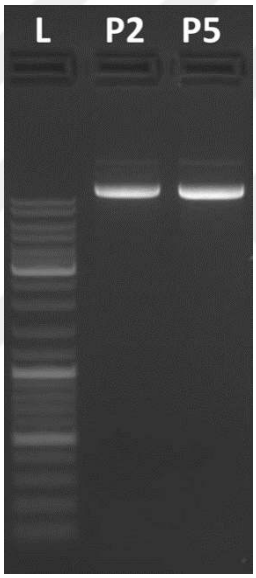

Figure 4. 50. Agarose gel result of pEAQ-HT-S-chl plasmids isolated from colony-2 and colony-5. L: Ladder (SMO331), P2-P5: Plasmids isolated from colony-2 and colony-5.

A final PCR check was performed for the plasmids isolated from colony-2 and colony-5 and amplification products were visualized on agarose gel electrophoresis (Figure 4. 51).

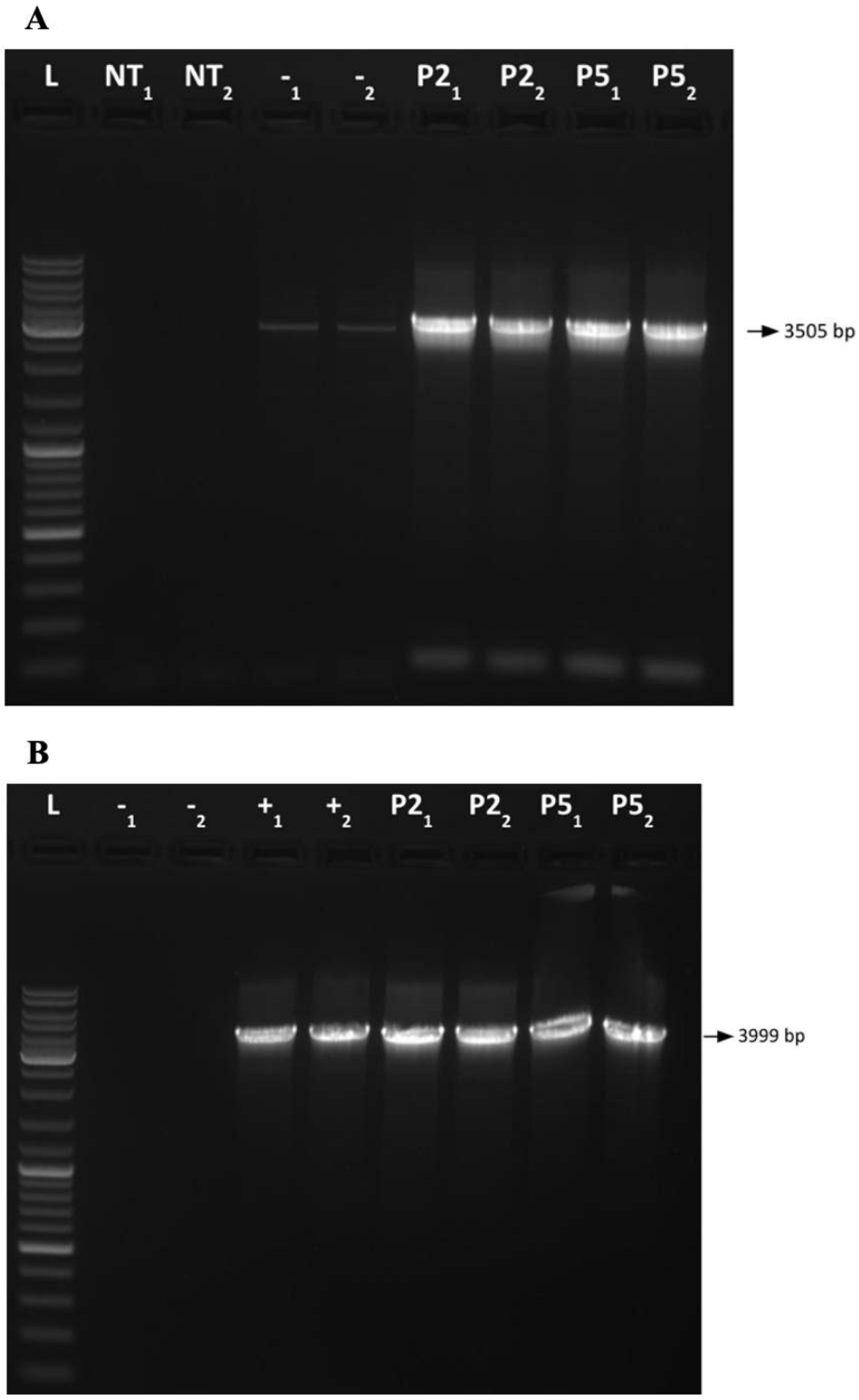

Figure 4. 51. PCR validation pEAQ-HT-S-chl plasmids isolation from colony-2 and colony-5. L: Ladder (SMO331), NT: No Template (water), +: positive control (pUC57-Amp-S-chl), -: negative control (pEAQ-HT colony 1 plasmid 1ng/ul), P: plasmid, P2-P5: plasmids isolated from colony-2 and colony-5.

Finally, S-chl gene insert in pEAQ-HT-S-chl plasmid-2 was confirmed by INTERGEN Genetics and Rare Diseases Diagnostics Center via NGS. According to the alignment analysis by Cluster Omega, the sequence of cloned S-chl gene was 100 % compatible with the original construct (Figure 4. 52).

Figure 4. 52. Continued

```
Sequenced       GCTAATAATTGCACATTTGAATATGTTTCTCAACCATTTTTGATGGATTTGGAAGGAAAG    600
Construct       GCTAATAATTGCACATTTGAATATGTTTCTCAACCATTTTTGATGGATTTGGAAGGAAAG    600
                ************************************************************

Sequenced       CAAGGAAATTTCAAAAATCTTAGAGAATTTGTTTTTAAGAATATTGATGGATACTTCAAA    660
Construct       CAAGGAAATTTCAAAAATCTTAGAGAATTTGTTTTTAAGAATATTGATGGATACTTCAAA    660
                ************************************************************

Sequenced       ATTTATTCTAAGCATACTCCAATTATTGTGAGGGAACCAGAGGATTTGCCACAAGGATTC    720
Construct       ATTTATTCTAAGCATACTCCAATTATTGTGAGGGAACCAGAGGATTTGCCACAAGGATTC    720
                ************************************************************

Sequenced       TCAGCATTGGAACCATTGGTTGATTTGCCAATTGGTATTAATATTACAAGGTTTCAAACA    780
Construct       TCAGCATTGGAACCATTGGTTGATTTGCCAATTGGTATTAATATTACAAGGTTTCAAACA    780
                ************************************************************

Sequenced       TTGTTGGCTCTTCATAGATCTTACTTGACACCTGGTGATTCTTCATCAGGTTGGACAGCA    840
Construct       TTGTTGGCTCTTCATAGATCTTACTTGACACCTGGTGATTCTTCATCAGGTTGGACAGCA    840
                ************************************************************

Sequenced       GGTGCTGCAGCATATTATGTTGGATATCTTCAACCAAGAACTTTTCTTCTTAAGTATAAT    900
Construct       GGTGCTGCAGCATATTATGTTGGATATCTTCAACCAAGAACTTTTCTTCTTAAGTATAAT    900
                ************************************************************

Sequenced       GAAAATGGTACAATTACAGATGCAGTTGATTGCGCTTTGGATCCTCTTTCTGAAACTAAG    960
Construct       GAAAATGGTACAATTACAGATGCAGTTGATTGCGCTTTGGATCCTCTTTCTGAAACTAAG    960
                ************************************************************

Sequenced       TGTACTCTTAAGTCTTTTACTGTTGAAAAGGGTATTTACCAGACTTCTAATTTTAGAGTT   1020
Construct       TGTACTCTTAAGTCTTTTACTGTTGAAAAGGGTATTTACCAGACTTCTAATTTTAGAGTT   1020
                ************************************************************

Sequenced       CAACCAACAGAGTCAATTGTTAGATTTCCAAATATTACAAATTTGTGTCCATTCGATGAG   1080
Construct       CAACCAACAGAGTCAATTGTTAGATTTCCAAATATTACAAATTTGTGTCCATTCGATGAG   1080
                ************************************************************

Sequenced       GTTTTTAATGCTACTAGATTTGCTTCAGTTTACGCATGGAATAGAAAGAGAATTTCTAAT   1140
Construct       GTTTTTAATGCTACTAGATTTGCTTCAGTTTACGCATGGAATAGAAAGAGAATTTCTAAT   1140
                ************************************************************

Sequenced       TGTGTTGCAGATTACTCAGTTTTGTACAATCTTGCTCCATTTTTTACTTTTAAGTGCTAC   1200
Construct       TGTGTTGCAGATTACTCAGTTTTGTACAATCTTGCTCCATTTTTTACTTTTAAGTGCTAC   1200
                ************************************************************

Sequenced       GGTGTTTCTCCAACTAAGCTTAATGATCTTTGTTTTACTAATGTTTATGCTGATTCTTTT   1260
Construct       GGTGTTTCTCCAACTAAGCTTAATGATCTTTGTTTTACTAATGTTTATGCTGATTCTTTT   1260
                ************************************************************

Sequenced       GTTATTAGAGGAGATGAAGTTAGACAAATTGCTCCAGGACAAACTGGAAATATTGCAGAT   1320
Construct       GTTATTAGAGGAGATGAAGTTAGACAAATTGCTCCAGGACAAACTGGAAATATTGCAGAT   1320
                ************************************************************

Sequenced       TATAATTATAAGCTTCCAGATGATTTTACTGGATGTGTTATTGCTTGGAATTCAAACAAG   1380
Construct       TATAATTATAAGCTTCCAGATGATTTTACTGGATGTGTTATTGCTTGGAATTCAAACAAG   1380
                ************************************************************

Sequenced       CTTGATTCTAAGGTTTCAGGTAATTACAATTATCTTTATAGACTTTTTAGAAAGTCTAAT   1440
Construct       CTTGATTCTAAGGTTTCAGGTAATTACAATTATCTTTATAGACTTTTTAGAAAGTCTAAT   1440
                ************************************************************
```

Figure 4. 52. Continued

```
Sequenced       CTTAAGCCATTTGAAAGGGATATTTCAACTGAAATTTATCAAGCTGGAAATAAGCCATGT     1500
Construct       CTTAAGCCATTTGAAAGGGATATTTCAACTGAAATTTATCAAGCTGGAAATAAGCCATGT     1500
                ************************************************************

Sequenced       AATGGAGTTGCAGGTTTCAATTGTTATTTTCCACTTAGGTCATATTCTTTTAGACCAACT     1560
Construct       AATGGAGTTGCAGGTTTCAATTGTTATTTTCCACTTAGGTCATATTCTTTTAGACCAACT     1560
                ************************************************************

Sequenced       TATGGAGTTGGACATCAACCATATAGAGTTGTTGTTCTTTCTTTTGAACTTCTTCATGCA     1620
Construct       TATGGAGTTGGACATCAACCATATAGAGTTGTTGTTCTTTCTTTTGAACTTCTTCATGCA     1620
                ************************************************************

Sequenced       CCTGCAACTGTTTGTGGACCAAAGAAGTCTACTAATTTGGTTAAAAATAAGTGTGTGAAT     1680
Construct       CCTGCAACTGTTTGTGGACCAAAGAAGTCTACTAATTTGGTTAAAAATAAGTGTGTGAAT     1680
                ************************************************************

Sequenced       TTCAATTTTAATGGACTTAAGGGAACAGGTGTTTTGACAGAATCTAATAAGAAGTTTCTT     1740
Construct       TTCAATTTTAATGGACTTAAGGGAACAGGTGTTTTGACAGAATCTAATAAGAAGTTTCTT     1740
                ************************************************************

Sequenced       CCATTTCAACAATTTGGAAGAGATATTGCTGATACAACAGATGCTGTTAGAGATCCACAA     1800
Construct       CCATTTCAACAATTTGGAAGAGATATTGCTGATACAACAGATGCTGTTAGAGATCCACAA     1800
                ************************************************************

Sequenced       ACTCTTGAAATTCTTGATATTACACCTTGTTCATTCGGTGGTGTTTCTGTTATTACTCCA     1860
Construct       ACTCTTGAAATTCTTGATATTACACCTTGTTCATTCGGTGGTGTTTCTGTTATTACTCCA     1860
                ************************************************************

Sequenced       GGAACTAATACTTCTAATCAAGTTGCTGTTCTTTATCAAGGAGTTAATTGTACTGAAGTT     1920
Construct       GGAACTAATACTTCTAATCAAGTTGCTGTTCTTTATCAAGGAGTTAATTGTACTGAAGTT     1920
                ************************************************************

Sequenced       CCAGTTGCTATTCATGCTGATCAACTTACTCCAACTTGGAGAGTTTATTCTACTGGATCT     1980
Construct       CCAGTTGCTATTCATGCTGATCAACTTACTCCAACTTGGAGAGTTTATTCTACTGGATCT     1980
                ************************************************************

Sequenced       AATGTTTTTCAAACTAGAGCTGGATGTCTTATTGGTGCAGAGTATGTTAATAATTCTTAT     2040
Construct       AATGTTTTTCAAACTAGAGCTGGATGTCTTATTGGTGCAGAGTATGTTAATAATTCTTAT     2040
                ************************************************************

Sequenced       GAATGTGATATTCCAATTGGTGCAGGTATTTGTGCTTCTTATCAAACTCAAACTAAGTCT     2100
Construct       GAATGTGATATTCCAATTGGTGCAGGTATTTGTGCTTCTTATCAAACTCAAACTAAGTCT     2100
                ************************************************************

Sequenced       CATGGATCTGCTTCATCAGTTGCATCTCAATCTATTATTGCTTATACTATGTCTCTTGGA     2160
Construct       CATGGATCTGCTTCATCAGTTGCATCTCAATCTATTATTGCTTATACTATGTCTCTTGGA     2160
                ************************************************************

Sequenced       GCTGAAAATTCTGTTGCTTATTCTAATAATTCAATTGCAATTCCAACTAATTTCACAATT     2220
Construct       GCTGAAAATTCTGTTGCTTATTCTAATAATTCAATTGCAATTCCAACTAATTTCACAATT     2220
                ************************************************************

Sequenced       TCTGTTACAACAGAGATTCTTCCTGTTTCTATGACTAAGACTTCTGTTGATTGTACTATG     2280
Construct       TCTGTTACAACAGAGATTCTTCCTGTTTCTATGACTAAGACTTCTGTTGATTGTACTATG     2280
                ************************************************************

Sequenced       TATATTTGTGGAGATTCTACTGAATGTTCTAATCTTCTTCTTCAATATGGATCTTTTTGT     2340
Construct       TATATTTGTGGAGATTCTACTGAATGTTCTAATCTTCTTCTTCAATATGGATCTTTTTGT     2340
                ************************************************************

Sequenced       ACTCAACTTAAGAGAGCTCTTACTGGAATTGCTGTTGAACAAGATAAGAATACTCAAGAA     2400
Construct       ACTCAACTTAAGAGAGCTCTTACTGGAATTGCTGTTGAACAAGATAAGAATACTCAAGAA     2400
                ************************************************************

Sequenced       GTTTTTGCTCAAGTTAAGCAAATTTATAAGACTCCACCAATTAAATACTTCGGAGGATTT     2460
Construct       GTTTTTGCTCAAGTTAAGCAAATTTATAAGACTCCACCAATTAAATACTTCGGAGGATTT     2460
                ************************************************************
```

Figure 4. 52. Continued

```
Sequenced       AATTTTTCTCAAATTCTTCCAGATCCATCTAAGCCTTCAAAAAGGTCTTTTATTGAAGAT     2520
Construct       AATTTTTCTCAAATTCTTCCAGATCCATCTAAGCCTTCAAAAAGGTCTTTTATTGAAGAT     2520
                ************************************************************

Sequenced       CTTCTTTTTAATAAGGTTACTCTTGCTGATGCAGGTTTCATTAAGCAATATGGAGATTGC     2580
Construct       CTTCTTTTTAATAAGGTTACTCTTGCTGATGCAGGTTTCATTAAGCAATATGGAGATTGC     2580
                ************************************************************

Sequenced       TTGGGTGATATTGCTGCTAGAGATCTTATTTGTGCTCAAAAGTTTAAGGGACTTACTGTT     2640
Construct       TTGGGTGATATTGCTGCTAGAGATCTTATTTGTGCTCAAAAGTTTAAGGGACTTACTGTT     2640
                ************************************************************

Sequenced       CTTCCACCACTTCTTACTGATGAAATGATTGCTCAATATACATCAGCACTTCTTGCTGGA     2700
Construct       CTTCCACCACTTCTTACTGATGAAATGATTGCTCAATATACATCAGCACTTCTTGCTGGA     2700
                ************************************************************

Sequenced       ACTATTACTTCTGGATGGACTTTTGGAGCTGGAGCTGCTCTTCAAATTCCATTTGCTATG     2760
Construct       ACTATTACTTCTGGATGGACTTTTGGAGCTGGAGCTGCTCTTCAAATTCCATTTGCTATG     2760
                ************************************************************

Sequenced       CAAATGGCTTATAGATTTAATGGAATTGGAGTTACACAGAATGTTCTTTATGAAAATCAA     2820
Construct       CAAATGGCTTATAGATTTAATGGAATTGGAGTTACACAGAATGTTCTTTATGAAAATCAA     2820
                ************************************************************

Sequenced       AAATTGATTGCTAATCAATTTAATTCTGCTATTGGAAAGATTCAAGATTCTTTGTCATCA     2880
Construct       AAATTGATTGCTAATCAATTTAATTCTGCTATTGGAAAGATTCAAGATTCTTTGTCATCA     2880
                ************************************************************

Sequenced       ACTGCTTCTGCTCTTGGAAAGCTTCAAGATGTGGTGAATCATAATGCTCAAGCTCTTAAT     2940
Construct       ACTGCTTCTGCTCTTGGAAAGCTTCAAGATGTGGTGAATCATAATGCTCAAGCTCTTAAT     2940
                ************************************************************

Sequenced       ACTCTTGTTAAGCAACTTTCTTCTAAGTTTGGAGCTATTTCTTCTGTTCTTAATGATATT     3000
Construct       ACTCTTGTTAAGCAACTTTCTTCTAAGTTTGGAGCTATTTCTTCTGTTCTTAATGATATT     3000
                ************************************************************

Sequenced       TTTTCTAGACTTGATCCACCAGAAGCTGAAGTTCAGATTGATAGGTTGATTACTGGAAGA     3060
Construct       TTTTCTAGACTTGATCCACCAGAAGCTGAAGTTCAGATTGATAGGTTGATTACTGGAAGA     3060
                ************************************************************

Sequenced       CTTCAATCTCTTCAAACTTACGTTACACAGCAACTTATTAGAGCTGCTGAAATTAGAGCT     3120
Construct       CTTCAATCTCTTCAAACTTACGTTACACAGCAACTTATTAGAGCTGCTGAAATTAGAGCT     3120
                ************************************************************

Sequenced       TCTGCTAATCTTGCTGCTACTAAGATGTCTGAATGTGTTCTTGGACAATCTAAGAGAGTT     3180
Construct       TCTGCTAATCTTGCTGCTACTAAGATGTCTGAATGTGTTCTTGGACAATCTAAGAGAGTT     3180
                ************************************************************

Sequenced       GATTTTTGTGGAAAGGGATATCATCTTATGTCTTTTCCACAATCTGCTCCACATGGAGTT     3240
Construct       GATTTTTGTGGAAAGGGATATCATCTTATGTCTTTTCCACAATCTGCTCCACATGGAGTT     3240
                ************************************************************

Sequenced       GTTTTTCTTCATGTTACTTATGTTCCAGCTCAAGAAAAGAATTTTACTACTGCTCCAGCT     3300
Construct       GTTTTTCTTCATGTTACTTATGTTCCAGCTCAAGAAAAGAATTTTACTACTGCTCCAGCT     3300
                ************************************************************

Sequenced       ATTTGTCATGATGGAAAGGCTCATTTTCCAAGAGAAGGAGTTTTCGTTTCAAATGGAACT     3360
Construct       ATTTGTCATGATGGAAAGGCTCATTTTCCAAGAGAAGGAGTTTTCGTTTCAAATGGAACT     3360
                ************************************************************

Sequenced       CATTGGTTTGTTACTCAAAGAAATTTTTATGAACCACAAATTATTACTACTGATAATACT     3420
Construct       CATTGGTTTGTTACTCAAAGAAATTTTTATGAACCACAAATTATTACTACTGATAATACT     3420
                ************************************************************

Sequenced       TTTGTTTCTGGAAATTGTGATGTTGTTATTGGAATTGTTAATAATACTGTTTATGATCCA     3480
Construct       TTTGTTTCTGGAAATTGTGATGTTGTTATTGGAATTGTTAATAATACTGTTTATGATCCA     3480
                ************************************************************
```

Figure 4. 52. Continued

Figure 4. 52. Alignment result of cloned S-chl gene and the original construct, RE Site: Restriction Enzyme site.

4.4. Preparation of *Agrobacterium* transformation systems

4.4.1. Transformation of *Agrobacterium* with pEAQ-HT

Empty vector pEAQ-HT P1 was transformed to *A. tumefaciens* LBA4404 by electroporation. The expected 231 bp amplification product was observed using p19_F and p19_R primers which was confirmed by colony PCR (Figure 4. 53).

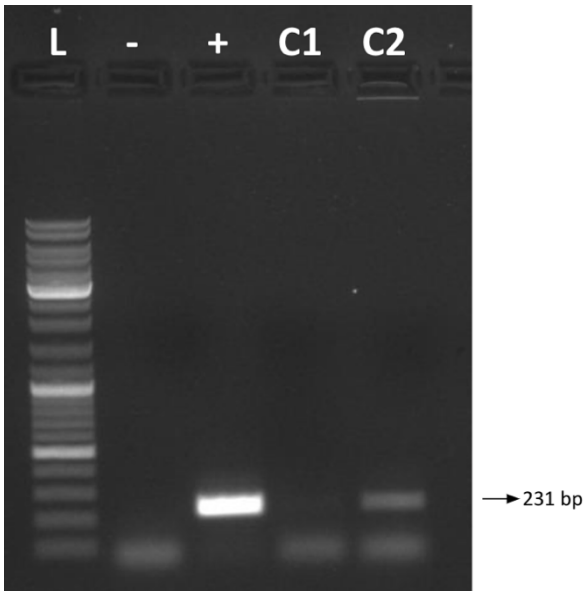

Figure 4. 53. Colony PCR result after transformation of *Agrobacterium* with pEAQ-HT plasmid. L: Ladder (SMO331), +: positive control, -: negative control, C1-C2: colonies.

The integrity and purity of the plasmid isolated from colony-2 were demonstrated by agarose gel electrophoresis (Figure 4. 54) and NanoDrop (DeNovix, DS-11) (Table 4. 14).

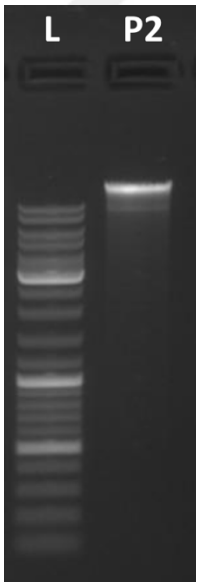

Figure 4. 54. Agarose gel result of pEAQ-HT plasmid isolated from *Agrobacterium* colony 2. L: Ladder (SMO331), P2: plasmid isolated from Colony-2.

Table 4. 14. Nanodrop result of pEAQ-HT plasmid isolated from *Agrobacterium* Colony-2.

	Plasmid 2
Concentration (ng/ µl)	**29.784**
260/230	**26.9**
260/280	**1.87**

A final PCR check was performed to validate the plasmid isolated from *Agrobacteirum* using the orientation primers HT-5UTR_F and p19_R, and the expected PCR product of 1585 bp was observed on agarose gel (Figure 4. 55).

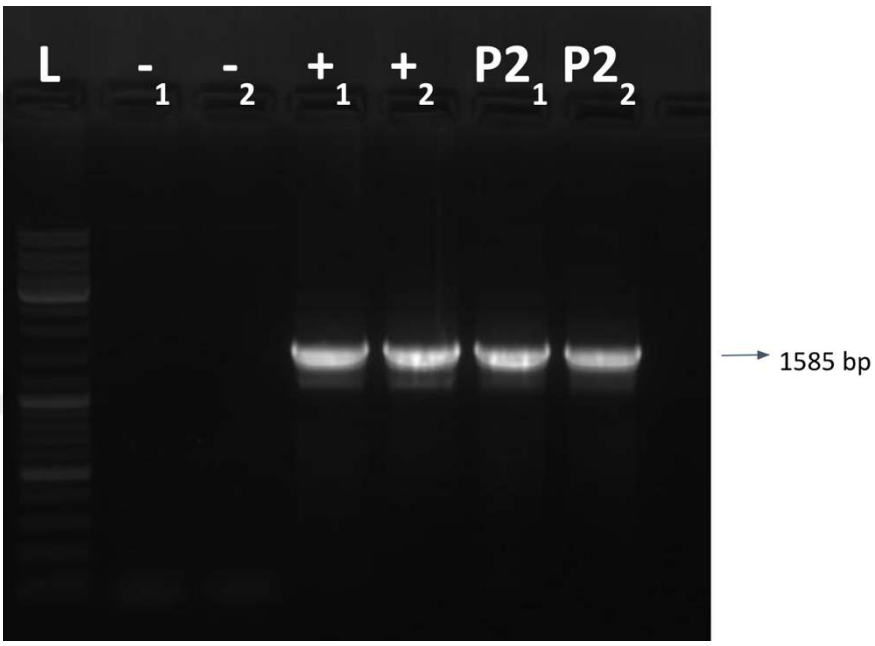

Figure 4. 55. PCR validation of pEAQ-HT isolated from *Agrobacterium* colony-2. L: Ladder (SMO331), +: positive control, -: negative control, P2: plasmid isolated from colony-2.

4.4.2. Transformation of *Agrobacterium* with pEAQ-HT-GFP

pEAQ-HT-GFP P1 was transformed to *A. tumefaciens* LBA4404 by electroporation. The expected 231 bp amplification product was observed using p19_F and p19_R primers which was confirmed by colony PCR (Figure 4. 56).

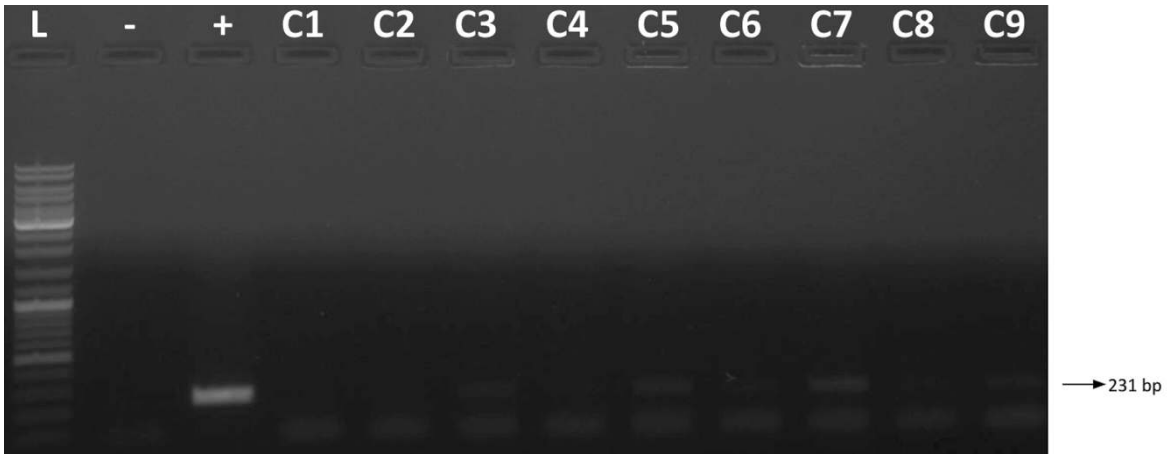

Figure 4. 56. Colony PCR result after transformation of *Agrobacterium* with pEAQ-HT-GFP plasmid. L: Ladder (SMO331), +: positive control, -: negative control, C1-C9: colonies.

The integrity and purity of the plasmid isolated from colony-7 were demonstrated by agarose gel electrophoresis (Figure 4. 57) and NanoDrop (DeNovix, DS-11) (Table 4. 15).

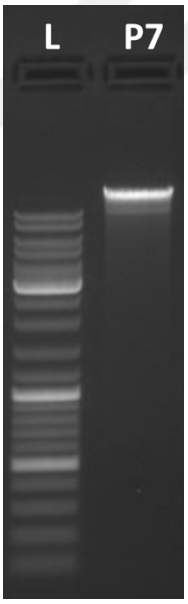

Figure 4. 57. Agarose gel result of pEAQ-HT-GFP plasmid isolated from *Agrobacterium* colony-7. L: Ladder (SMO331), P7: plasmid isolated from Colony-7.

Table 4. 15. Nanodrop result of pEAQ-HT-GFP plasmid isolated from *Agrobacterium* Colony-2.

	Plasmid 7
Concentration (ng/ µl)	**31.061**
260/230	**220.79**
260/280	**1.82**

A final PCR check was performed to validate the plasmid isolated from *Agrobacterium* using the orientation primers HT-5UTR_F and p19_R, and the expected PCR product of between 2000 and 2500 bp was observed on agarose gel (Figure 4. 58).

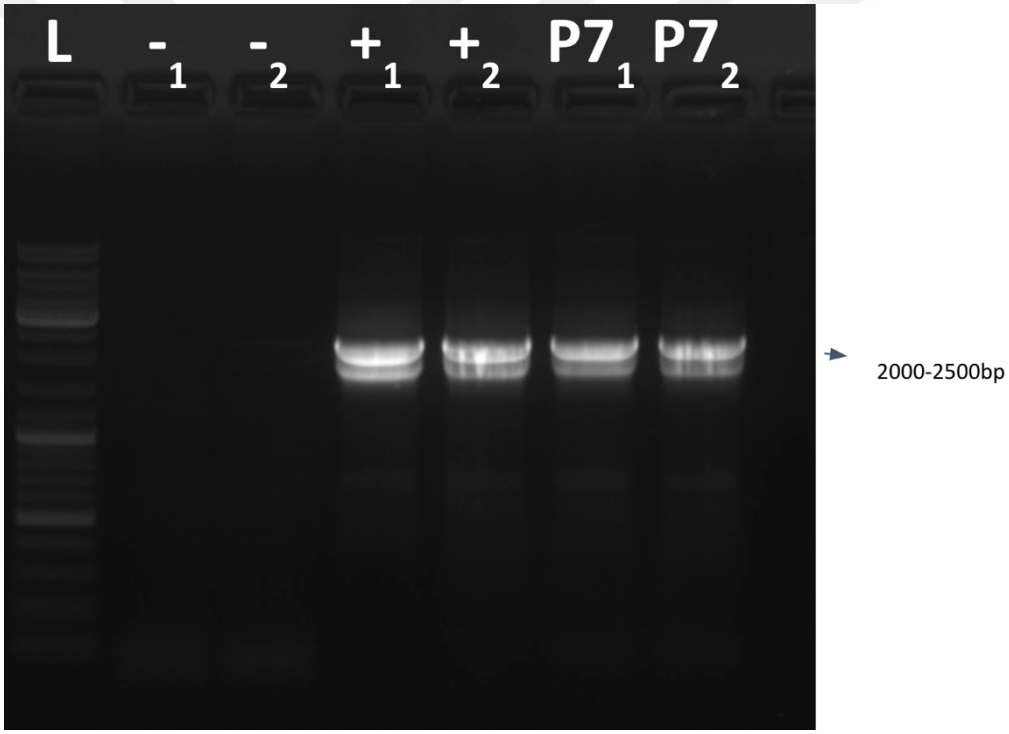

Figure 4. 58. PCR validation of pEAQ-HT-GFP isolated from *Agrobacterium* colony-7. L: Ladder (SMO331), +: positive control, -: negative control, P7: plasmid isolated from colony-7.

4.4.3. Transformation of *Agrobacterium* with pEAQ-HT-E

pEAQ-HT-E P3 was transformed to *A. tumefaciens* LBA4404 by electroporation. The expected 181 bp amplification product was observed using E-in_F and E-in_R primers which was confirmed by colony PCR (Figure 4. 59).

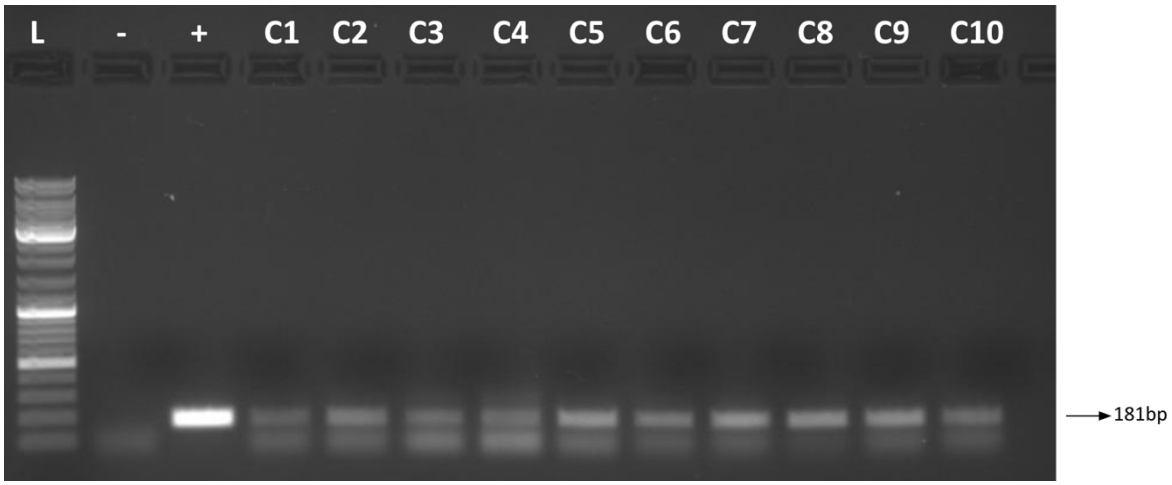

Figure 4. 59. Colony PCR result after transformation of *Agrobacterium* with pEAQ-HT-E plasmid. L: Ladder (SMO331), +: positive control, -: negative control, C1-C10: colonies.

The integrity and purity of the plasmid isolated from colony-8 were demonstrated by agarose gel electrophoresis (Figure 4. 60) and NanoDrop (DeNovix, DS-11) (Table 4. 16).

Figure 4. 60. Agarose gel result of pEAQ-HT-E plasmid isolated from *Agrobacterium* colony-8. L: Ladder (SMO331), P8: plasmid isolated from Colony-8.

Table 4. 16. Nanodrop result of pEAQ-HT-E plasmid isolated from *Agrobacterium* Colony-8.

	Plasmid 8
Concentration (ng/ µl)	39.839
260/230	6.56
260/280	1.81

A final PCR check was performed to validate the plasmid isolated from *Agrobacterium* using the orientation primers HT-5UTR_F and E-in_R, and the expected PCR product of 582 bp was observed on agarose gel (Figure 4. 61).

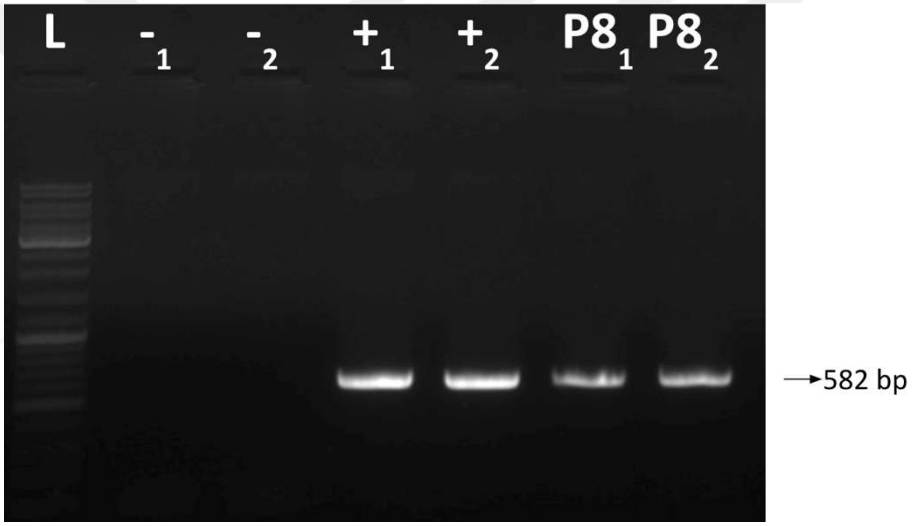

Figure 4. 61. PCR validation of pEAQ-HT-E isolated from *Agrobacterium* colony-8. L: Ladder (SMO331), +: positive control, -: negative control, P8: plasmid isolated from colony-8.

4.4.4. Transformation of *Agrobacterium* with pEAQ-HT-N

pEAQ-HT-N P6 was transformed to *A. tumefaciens* LBA4404 by electroporation. The expected 306 bp amplification product was observed using N-in_F and N-in_R primers which was confirmed by colony PCR (Figure 4. 62).

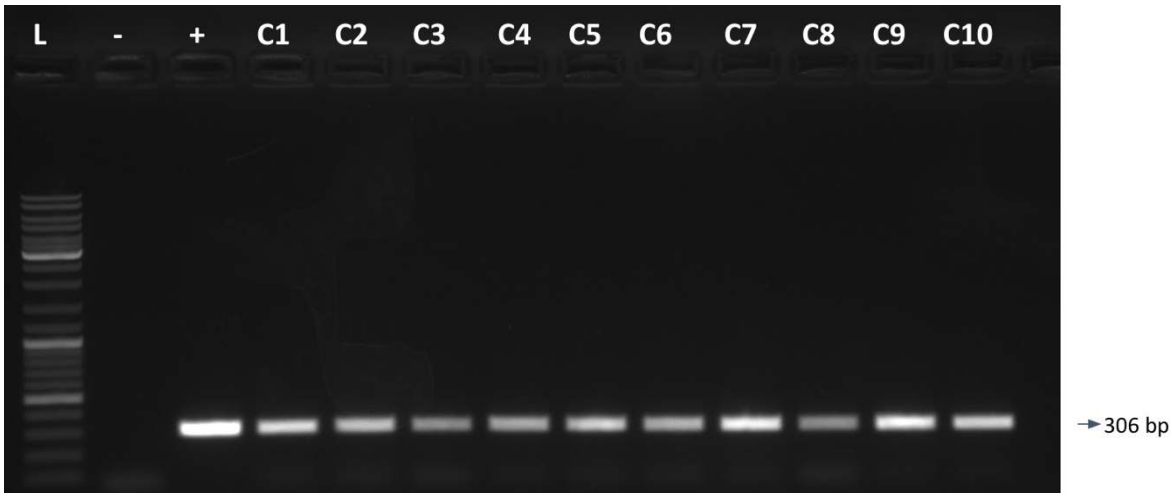

Figure 4. 62. Colony PCR result after transformation of *Agrobacterium* with pEAQ-HT-N plasmid. L: Ladder (SMO331), +: positive control, -: negative control, C1-C10: colonies.

The integrity and purity of the plasmid isolated from colony-1 and colony-7 were demonstrated by agarose gel electrophoresis (Figure 4. 63) and NanoDrop (DeNovix, DS-11) (Table 4. 17).

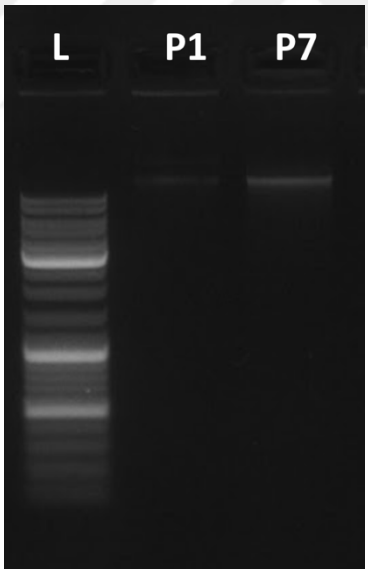

Figure 4. 63. Agarose gel result of pEAQ-HT-N plasmid isolated from *Agrobacterium* colony-1 and colony-7. L: Ladder (SMO331), P1: plasmid isolated from colony-1, P7: plasmid isolated from colony-7.

Table 4. 17. Nanodrop result of pEAQ-HT-N plasmidS isolated from *Agrobacterium* Colony-1 and Colony-7.

	Plasmid 1	**Plasmid 7**
Concentration (ng/ µl)	29.149	9.290
260/230	1.18	1.30
260/280	1.85	1.99

A final PCR check was performed to validate the plasmid isolated from *Agrobacterium* using the orientation primers HT-5UTR_F and N-in_R, and the expected PCR product of 1466 bp was observed on agarose gel (Figure 4. 64).

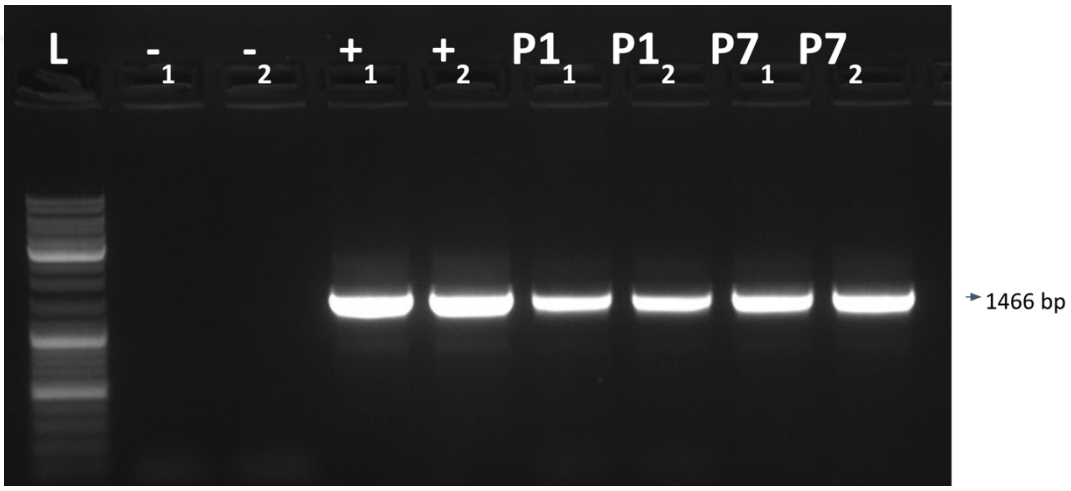

Figure 4. 64. PCR validation of pEAQ-HT-N isolated from *Agrobacterium* colony-1 and colony-7. L: Ladder (SMO331), -: negative control, +: positive control (pEAQ-HT-N (plasmid 6: Sequenced plasmid)), P1-P7: plasmid isolated from colony-1 and colony-7,

4.4.5. Transformation of *Agrobacterium* with pEAQ-HT-M

pEAQ-HT-M P3 was transformed to *A. tumefaciens* LBA4404 by electroporation. The expected 195 bp amplification product was observed using M-in_F and M-in_R primers which was confirmed by colony PCR (Figure 4. 65).

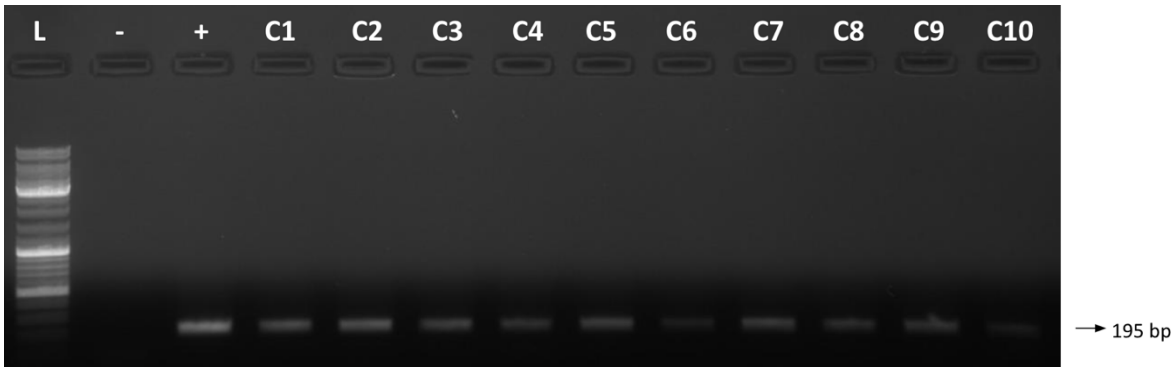

Figure 4. 65. Colony PCR result after transformation of *Agrobacterium* with pEAQ-HT-M plasmid. L: Ladder (SMO331), +: positive control, -: negative control, C1-C10: colonies.: *Agrobacterium* strains.

The integrity and purity of the plasmid isolated from colony-2 was demonstrated by agarose gel electrophoresis (Figure 4. 66) and NanoDrop (DeNovix, DS-11) (Table 4. 18).

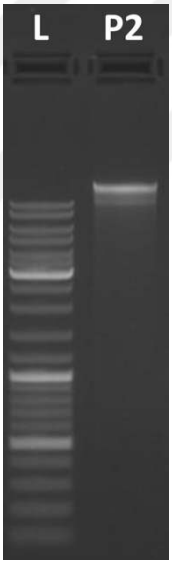

Figure 4. 66. Agarose gel result of pEAQ-HT-M plasmid isolated from colony-2. L: Ladder (SMO331), P2: plasmid isolated from Colony 2.

Table 4. 18. Nanodrop result of pEAQ-HT-M plasmid isolated from *Agrobacterium* Colony-2.

	Plasmid 2
Concentration (ng/ µl)	16.401
260/230	1.72
260/280	1.67

A final PCR check was performed to validate the plasmid isolated from *Agrobacterium* using the orientation primers HT-5UTR_F and M-in_R, and the expected PCR product of 506 bp was observed on agarose gel (Figure 4. 67).

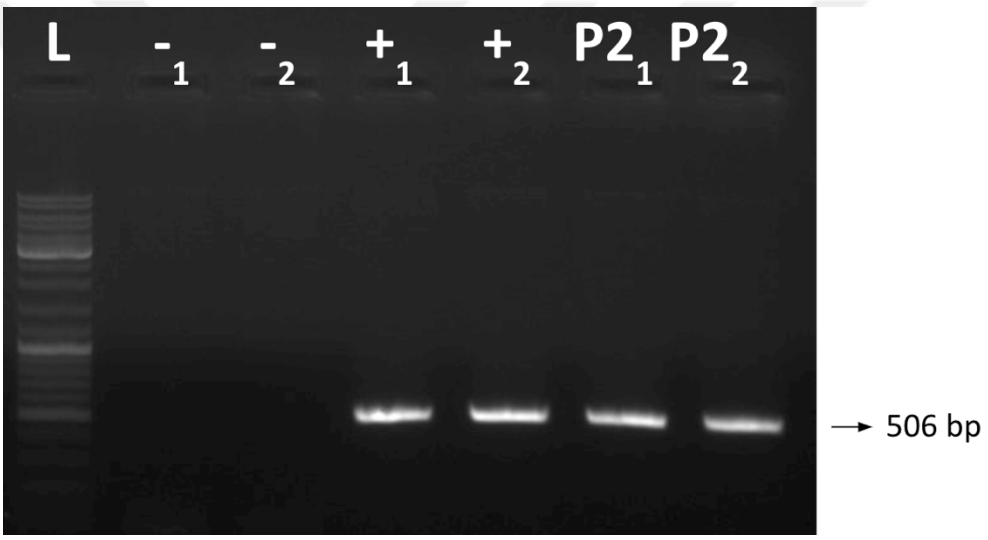

Figure 4. 67. PCR validation of pEAQ-HT-M isolated from *Agrobacterium* colony-2. L: Ladder (SMO331), +: positive control, -: negative control, P2: plasmid isolated from colony-2.

4.4.6. Transformation of *Agrobacterium* with pEAQ-HT-S

pEAQ-HT-S P4 was transformed to *A. tumefaciens* LBA4404 by electroporation. The expected 658 bp amplification product was observed using S-in_F and S-in_R primers which was confirmed by colony PCR (Figure 4. 68).

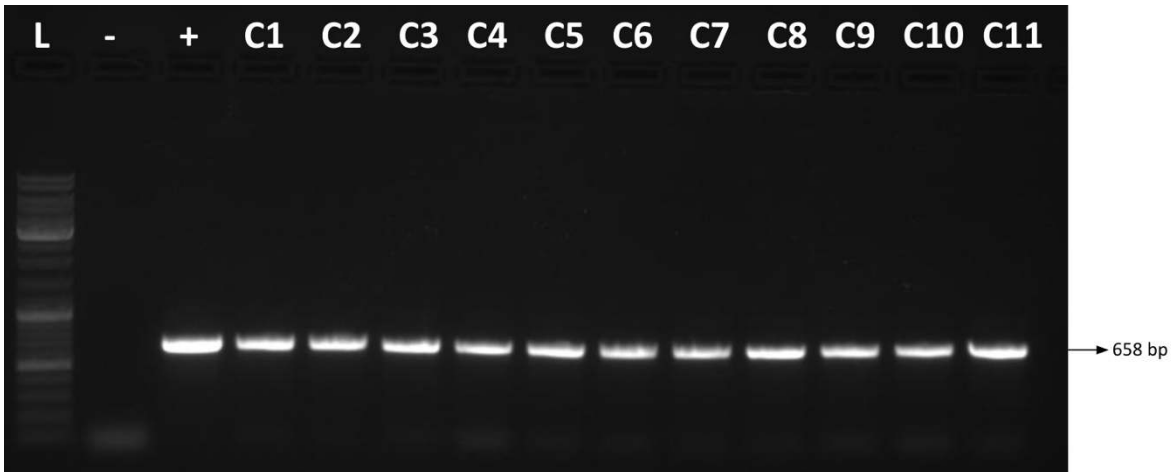

Figure 4. 68. Colony PCR result after transformation of *Agrobacterium* with pEAQ-HT-S plasmid. L: Ladder (SMO331), +: positive control, -: negative control, C1-C11: colonies.

The integrity and purity of the plasmid isolated from colony-1 was demonstrated by agarose gel electrophoresis (Figure 4. 69) and NanoDrop (DeNovix, DS-11) (Table 4. 19).

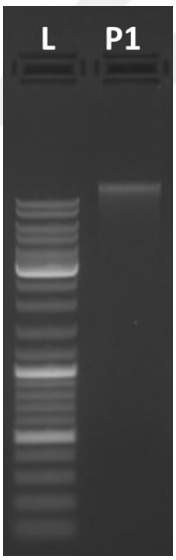

Figure 4. 69. Agarose gel result of pEAQ-HT-S plasmid isolated from colony-1. L: Ladder (SMO331), P1: plasmid isolated from Colony-1.

Table 4. 19. Nanodrop result of pEAQ-HT-S plasmid isolated from *Agrobacterium* Colony-1.

	Plasmid 1
Concentration (ng/ µl)	8.562
260/230	-1.00
260/280	2.06

A final PCR check was performed to validate the plasmid isolated from *Agrobacterium* using the orientation primers HT-5UTR_F and S-in_R, and the expected PCR product of 4236 bp was observed on agarose gel (Figure 4. 70).

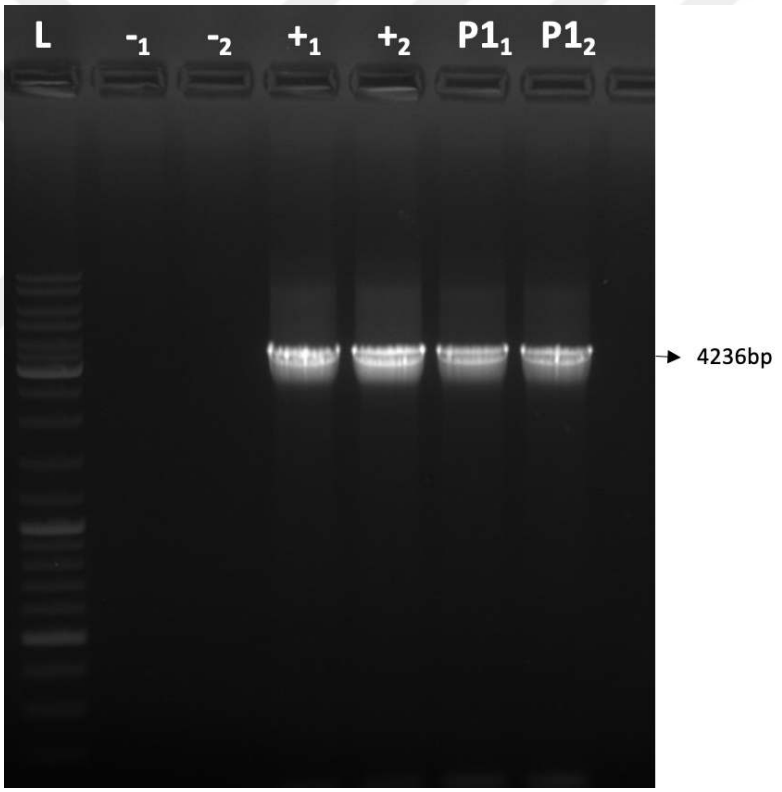

Figure 4. 70. PCR validation of pEAQ-HT-S isolated from *Agrobacterium* colony-1. L: Ladder (SMO331), +: positive control, -: negative control, P1: plasmid isolated from colony-1.

4.4.7. Transformation of *Agrobacterium* with S-chl

pEAQ-HT-S-chl P4 was transformed to *A. tumefaciens* LBA4404 by electroporation. The expected 658 bp amplification product was observed using S-in_F and S-in_R primers which was confirmed by colony PCR (Figure 4. 71).

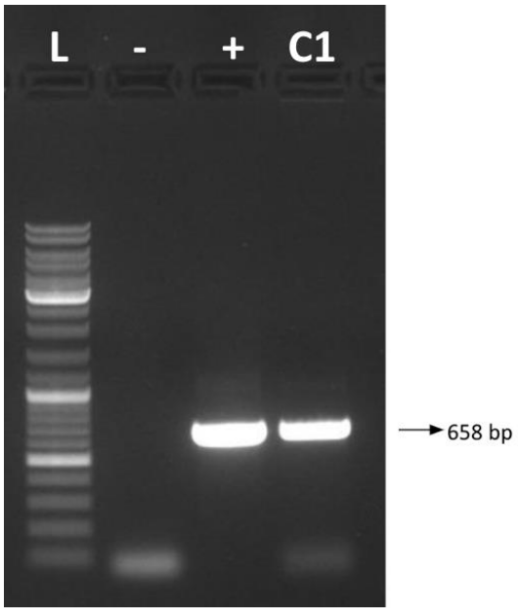

Figure 4. 71. Colony PCR result after transformation of *Agrobacterium* with pEAQ-HT-S-chl plasmid. L: Ladder (SMO331), +: positive control, -: negative control, C1: colony

The integrity and purity of the plasmid isolated from colony-1 was demonstrated by agarose gel electrophoresis (Figure 4. 72) and NanoDrop (DeNovix, DS-11) (Table 4. 20).

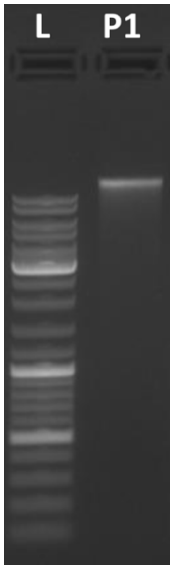

Figure 4. 72. Agarose gel result of pEAQ-HT-S-chl plasmid isolated from colony-1. L: Ladder (SMO331), P1: plasmid isolated from Colony-1.

Table 4. 20. Nanodrop result of pEAQ-HT-S-chl plasmid isolated from *Agrobacterium* Colony-1.

	Plasmid 1
Concentration (ng/ µl)	20.826
260/230	-9.79
260/280	1.77

A final PCR check was performed to validate the plasmid isolated from *Agrobacterium* using the orientation primers HT-5UTR_F and S-in_R, and the expected PCR product of 4270 bp was observed on agarose gel (Figure 4. 73).

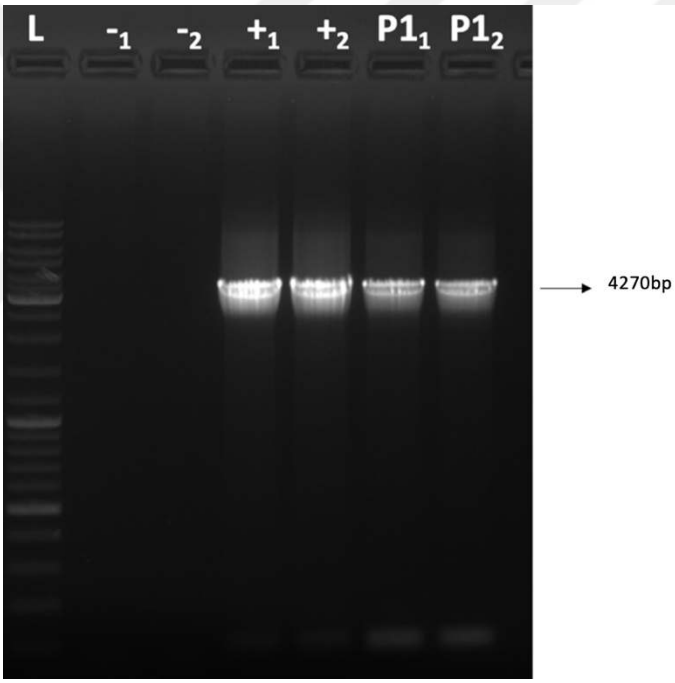

Figure 4. 73. PCR validation of pEAQ-HT-S-chl isolated from *Agrobacterium* colony-1. L: Ladder (SMO331), +: positive control, -: negative control, P1: plasmid isolated from colony-1.

4.5. Agro-infiltration of *N.benthamiana* leaves

Agrobacterium co-infiltration was prepared in two different combinations targeting two different compartmentalization of VLPs, endoplasmic reticulum and chloroplast. Endoplasmic reticulum-targeted VLP (VLP-ER), consisted of E, M, N and S gene cassettes, whereas chloroplast-targeted VLP (VLP-Chl) consisted of E, M, N and S-chl gene cassettes.

4.5.1. Phenotypic views of infiltrated leaves

In order to assess if infiltration process of constructs led to any extra negative effect, leaf samples were photographed 3-5-7 dpi (Figure 4. 74). Accordingly, necrotic zones were observed in the infiltrated leaves only in the infiltration application areas due to mechanical stress. On the other hand, a slight chlorosis was observed in all Agro-infiltrated leaves, regardless of which *Agrobacterium* was employed. In other words, our constructs did not cause any significant (S or S-chl alone and VLP-ER or VLP-Chl) phenotypic effect when compared to leaves infiltrated with *Agrobacterium* containing empty vector (pEAQ-HT).

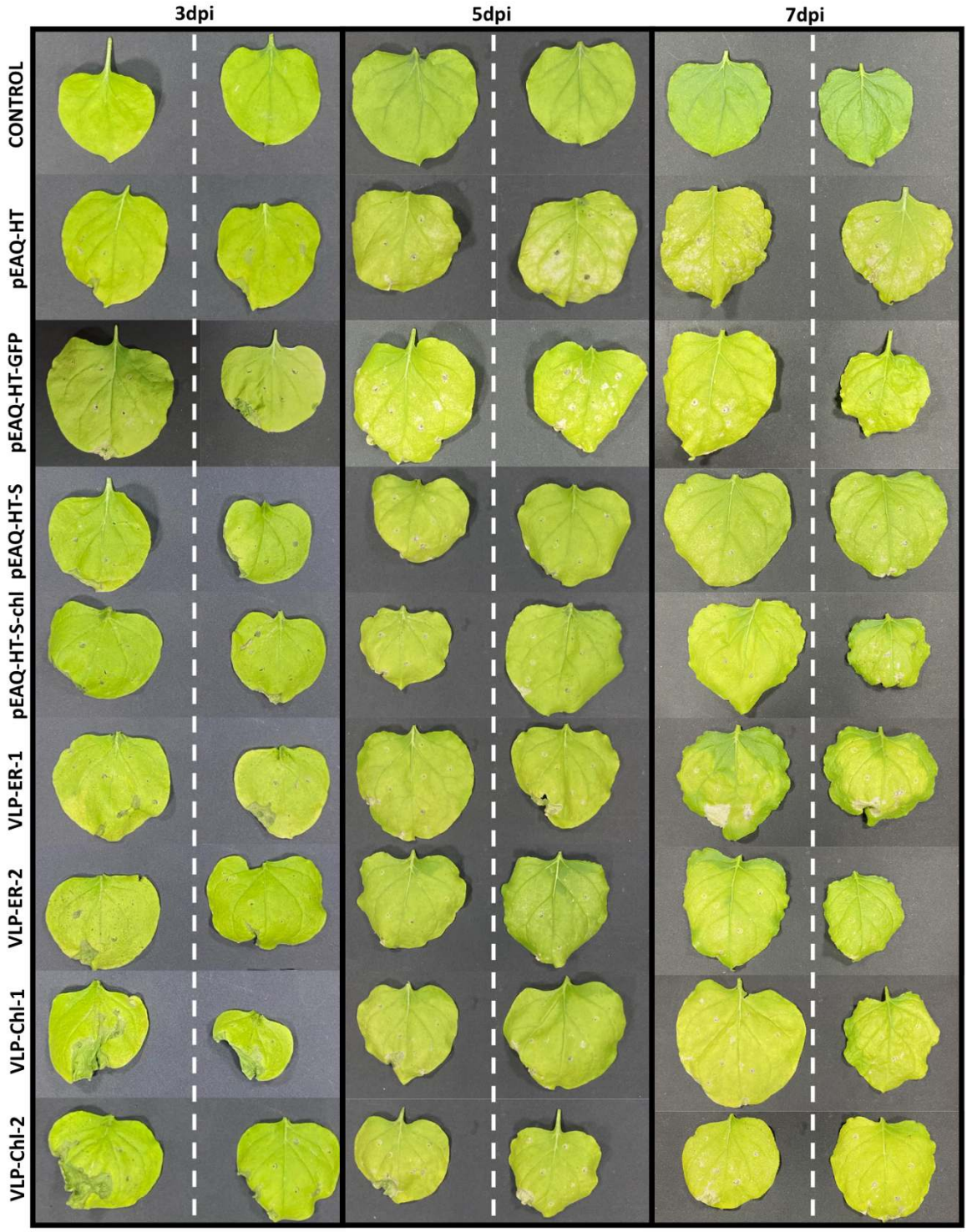

Figure 4. 74. Photographs of agro-infiltrated *N. benthamiana* leaves infiltrated with Agrobacterium 3-5-7 dpi. 3-5-7 dpi: days 3, 5 and 7 after infiltration. Control: Non-infiltrated leaves, pEAQ-HT: leaves infiltrated with Agrobacterium containing empty vector, pEAQ-HT-GFP: leaves infiltrated with Agrobacterium containing GFP gene, pEAQ-HT-S: leaves infiltrated with Agrobacterium containing S gene, pEAQ-HT-S-chl: Leaves infiltrated with *Agrobacterium* containing the S-chl gene, VLP-ER: Leaves co-infiltrated with *Agrobacterium* bacteria containing pEAQ-HT-E, pEAQ-HT-M, pEAQ-HT-N, pEAQ-HT-S vectors (VLP-ER-1 and VLP-ER-2: replica plants), VLP-Chl: leaves co-infiltrated with *Agrobacterium* bacteria containing the vectors pEAQ-HT-E, pEAQ-HT-M, pEAQ-HT-N, pEAQ-HT-S-chl (VLP-Chl-1 and VLP-Chl-2: replica plants).

4.5.2. GFP Expression in agro-infiltrated *N.benthamiana* leaves

As a control in each Agro-infiltration experiment, *Agrobacterium* containing pEAQ-HT-GFP was included and GFP luminescence was visualized 3-5-7 dpi under UV light. Accordingly, it was observed that the level of GFP expression was higher on 5dpi and 7dpi compared to 3 dpi, and there was no significant difference between 5 dpi and 7 dpi (Figure 4. 75).

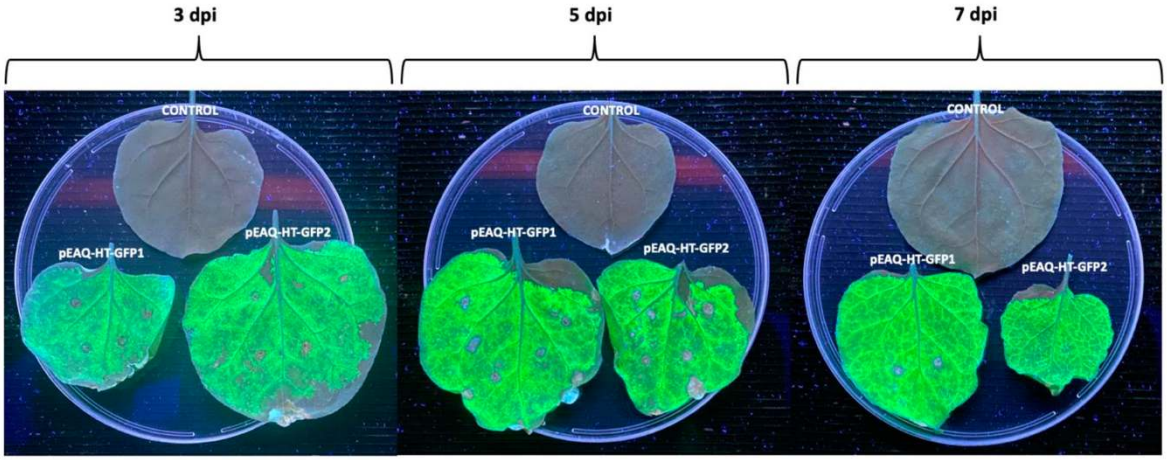

Figure 4. 75. *N. benthamiana* leaves 3-5-7 dpi with *Agrobacterium* containing pEAQ-HT-GFP under UV light. dpi: day-post infiltration, 1-2: replicate number.

4.6. Expression analysis at mRNA level

In order to validate the expression of GOIs at mRNA level, RT-PCR was conducted with RNAs isolated from infiltrated leaves. Concentration and purities of the total RNAs were given in Table 4. 21. Furthermore, integrities of total RNAs were visualized on agarose gel (Figure 4. 76).

Table 4. 21. Nanodrop results of RNAs isolated from agroinfiltrated samples.

Sample	Concentration (ng/µl)	260/280	260/230
WT	152.225	1.918	0.834
E2-3d	664.319	1.981	2.105
E2-5d	836.548	2.009	2.269
N2-5d	304.535	1.897	1.839
M2-5d	141.775	1.862	0.406

EV	47.231	1.694	0.557
VLP-ER	95.375	1.688	1.990
VLP-Chl	66.173	1.581	1.404

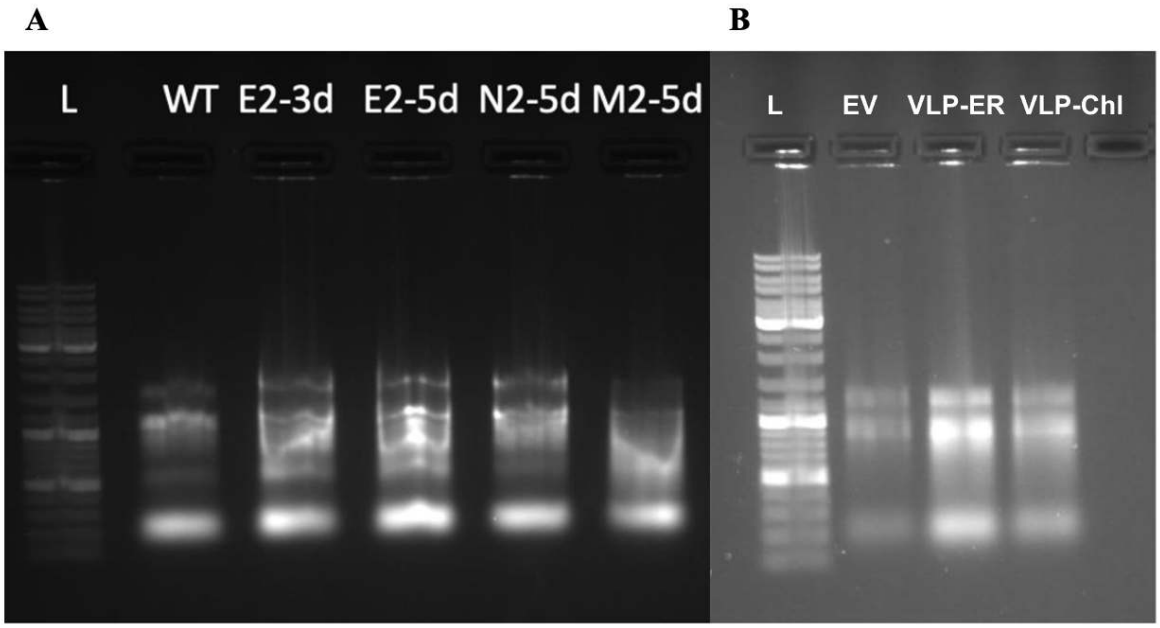

Figure 4. 76. A) RNA images of C2-5d (WT), E2-3d, E2-5d, N2-5d, M2-5d, B) RNA images of VLP-ER and VLP-Chl samples on agarose gel, L: Ladder (SMO331)

At the end of RT-PCR, the expected amplicons (318 bp) were obtained (Figure 4. 77).

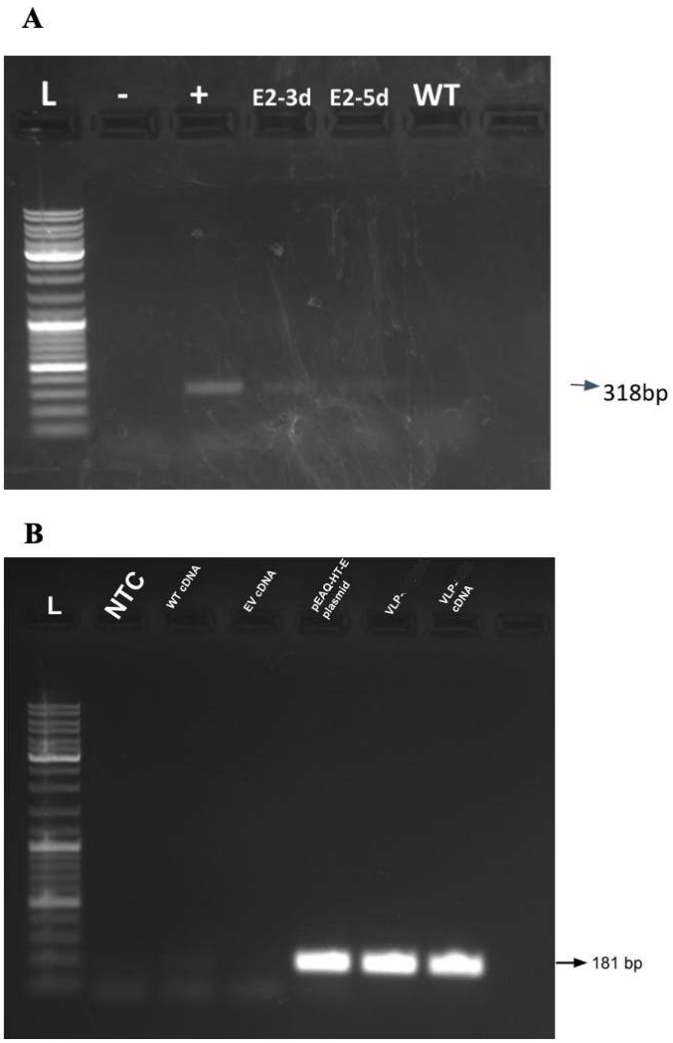

Figure 4. 77. RT-PCR result of RNAs isolated from leaves infiltrated with *Agrobacterium* containing pEAQ-HT-E A) Results of RT-PCR conducted with E gene specific primers by using Taq polymerase, L: Ladder (SMO331), +: positive control (pEAQ-HT-E), -: negative control, E2-3d; E2-5d: cDNAs isolated from leaf samples infiltrated with Agro-pEAQ-HT-E on day 3 and day 5, WT: Wild Type, B) Results of RT-PCR conducted with insert specific primers by using Q5 polymerase, NTC: No Template, WT: Wild Type, EV: Empty Vector, pEAQ-HT-E: Plasmid isolated from *Agrobacterium*, VLP-ER, VLP-Chl

At the end of RT-PCR, the expected amplicons (195 bp) were obtained (Figure 4. 78).

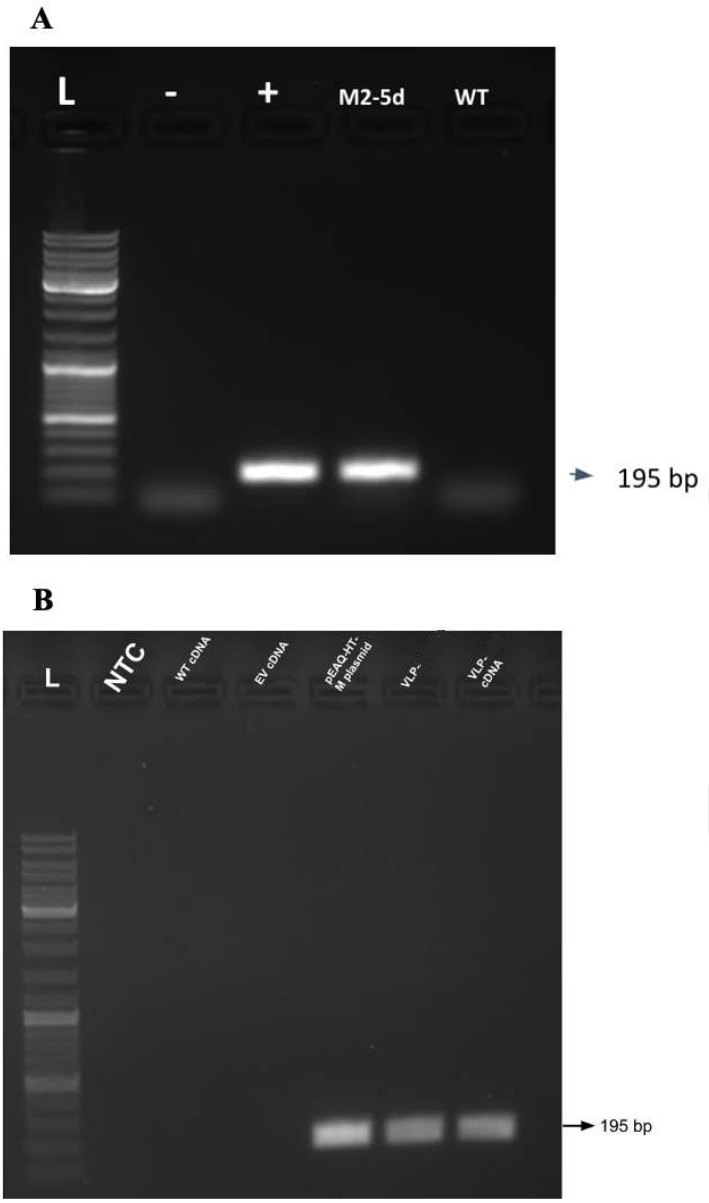

Figure 4. 78. RT-PCR result of RNAs isolated from leaves infiltrated with Agrobacterium containing pEAQ-HT-M A) Results of RT-PCR conducted with M insert specific primers by using Taq polymerase, L: Ladder (SMO331), +: positive control (pEAQ-HT-M), -: negative control, M2-5d: cDNA isolated from leaf sample infiltrated with Agro-pEAQ-HT-M on day 5, WT: Wild Type, B) Results of RT-PCR conducted with insert specific primers by using Q5 polymerase, NTC: No Template, WT: Wild Type, EV: Empty Vector, pEAQ-HT-M: Plasmid isolated from *Agrobacterium*, VLP-ER, VLP-Chl

At the end of RT-PCR, the expected amplicons (306 bp) were obtained (Figure 4. 79).

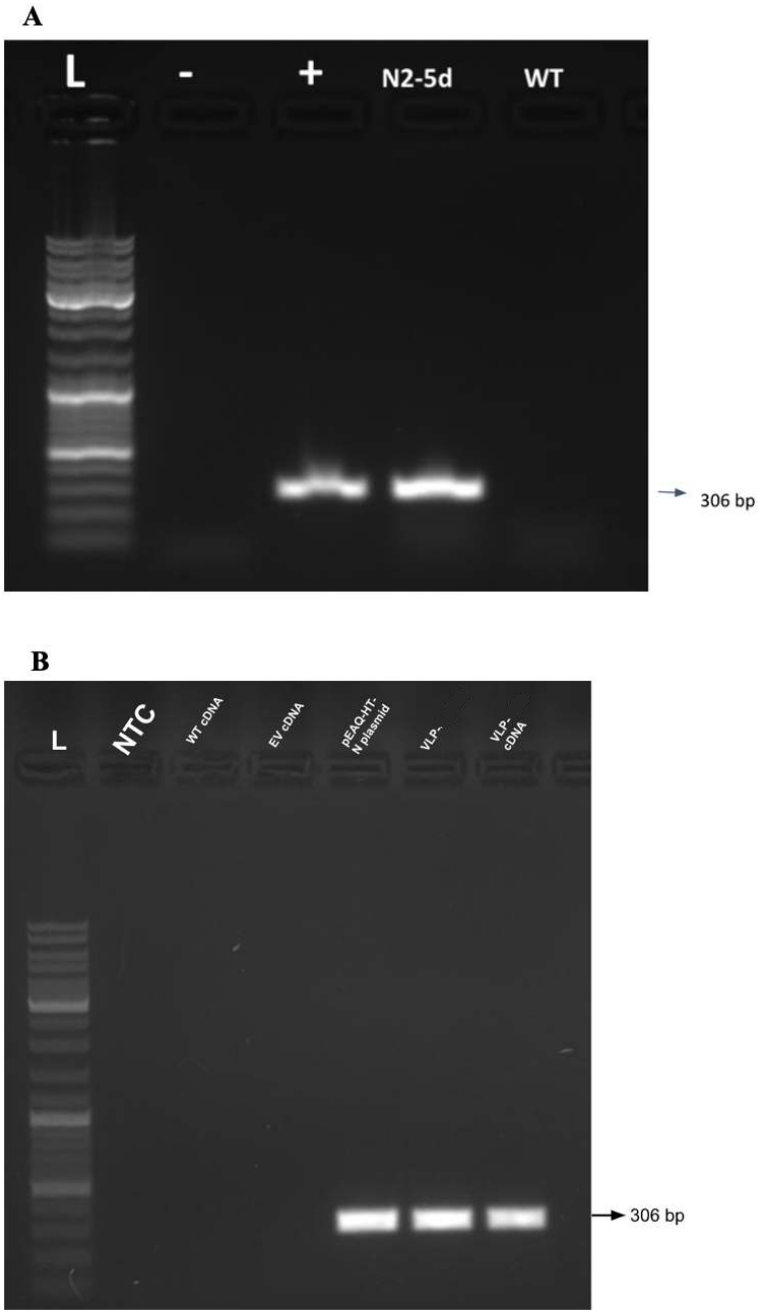

Figure 4. 79. RT-PCR result of RNAs isolated from leaves infiltrated with *Agrobacterium* containing pEAQ-HT-N A) Results of RT-PCR conducted with N insert specific primers by using Taq polymerase, L: Ladder (SMO331), +: positive control (pEAQ-HT-N), -: negative control, N2-5d: cDNA isolated from leaf sample infiltrated with Agro-pEAQ-HT-N on day 5, WT: Wild Type, B) Results of RT-PCR conducted with insert specific primers by using Q5 polymerase, NTC: No Template, WT: Wild Type, EV: Empty Vector, pEAQ-HT-N: Plasmid isolated from *Agrobacterium*, VLP-ER, VLP-Chl

At the end of RT-PCR, the expected amplicons (658 bp) were obtained (Figure 4. 80).

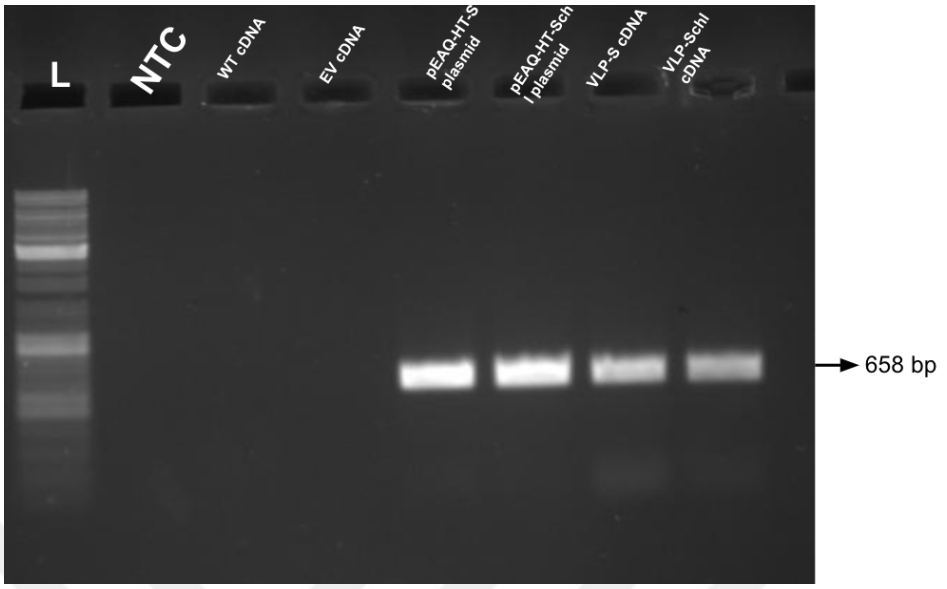

Figure 4. 80. RT-PCR result of RNAs isolated from leaves infiltrated with *Agrobacterium* containing pEAQ-HT-S and pEAQ-HT-S-chl. Result of RT-PCR conducted with insert specific primers by using Q5 polymerase, L: Ladder (SMO331), NTC: No Template, WT: Wild Type, EV: Empty Vector, pEAQ-HT-S: Plasmid isolated from *Agrobacterium*, pEAQ-HT-S-chl: Plasmid isolated from *Agrobacterium*, VLP-ER, VLP-Chl

4.7. Protein Quantification

Total soluble proteins (TSP) were isolated from agro-infiltrated leaves 3, 5 and 7 dpi. Extracted proteins concentration were measured by BCA assay (Table 4. 22).

Table 4. 22. TSP concentrations of agro-infiltrated leaves.

Samples		Absorbance Value Measured on the Device (mg/ml)	DF	Sample Concentration (µg/ml)	Fresh Weight of leave (g)
Wild Type	Control-3d-1	0,395	10	3950	0.34
	Control-3d-2	0,407	10	4070	0.36
	Control-5d-1	0,415	10	4150	0.50
	Control-5d-2	0,453	10	4530	0.38
	Control-7d-1	0,602	10	6020	0.25
	Control-7d-2	0,845	10	8450	0.24
Envelope	E1-3d	1,488	3	4464	0.50
	E1-5d	1,856	3	5568	0.40
	E1-7d	1,651	3	4953	0.50
Membrane	M1-3d	0,439	10	4390	0.38

Nucleocapsid	M1-5d	0,284	10	2840	0.38
	M1-7d	0,541	10	5410	0.41
	N1-3d	0,425	10	4250	0.20
	N1-5d	0,4	10	4000	0.41
	N1-7d	0,521	10	5210	0.38
Spike	S-3d-1	0,304	10	3040	0.36
	S-3d-2	0,252	10	2520	0.27
	S-5d-1	0,567	10	5670	0.41
	S-5d-2	0,485	10	4850	0.51
	S-7d-1	1,143	10	11430	0.47
	S-7d-2	0,605	10	6050	0.41
Spike-chl	S-chl-3d-1	0,271	10	2710	0.42
	S-chl-3d-2	0,176	10	1760	0.31
	S-chl-5d-1	0,437	10	4370	0.41
	S-chl-5d-2	0,449	10	4490	0.50
	S-chl-7d-1	0,510	10	5100	0.44
	S-chl-7d-2	0,623	10	6230	0.31
Empty Vector	HT-3d-1	0,431	10	4310	0.36
	HT-3d-2	0,458	10	4580	0.28
	HT-5d-1	0,544	10	5440	0.32
	HT-5d-2	0,422	10	4220	0.35
	HT-7d-1	0,864	10	8640	0.40
	HT-7d-2	0,558	10	5580	0.32
VLP-ER	VLP-ER-1-3d-1	0,252	10	2520	0.53
	VLP-ER-1-3d-2	0,206	10	2060	0.27
	VLP-ER-2-3d-1	0,297	10	2970	0.45
	VLP-ER-2-3d-2	0,437	10	4370	0.52
	VLP-ER-1-5d-1	0,381	10	3810	0.50
	VLP-ER-1-5d-2	0,415	10	4150	0.50
	VLP-ER-2-5d-1	0,395	10	3950	0.55
	VLP-ER-2-5d-2	0,431	10	4310	0.45
	VLP-ER-1-7d-1	1,593	10	15930	0.45
	VLP-ER-1-7d-2	0,979	10	9790	0.40
	VLP-ER-2-7d-1	1,926	10	19260	0.55
	VLP-ER-2-7d-2	1,767	10	17670	0.41
VLP-Chl	VLP-Chl-1-3d-1	0,293	10	2930	0.31
	VLP-Chl-1-3d-2	0,29	10	2900	0.18
	VLP-Chl-2-3d-1	0,259	10	2590	0.30
	VLP-Chl-2-3d-2	0,303	10	3030	0.37
	VLP-Chl-1-5d-1	0,379	10	3790	0.52
	VLP-Chl-1-5d-2	0,441	10	4410	0.55
	VLP-Chl-2-5d-1	0,47	10	4700	0.36
	VLP-Chl-2-5d-2	0,562	10	5620	0.36

	VLP-Chl-1-7d-1	1,497	10	14970	0.56
	VLP-Chl-1-7d-2	1,153	10	11530	0.48
	VLP-Chl-2-7d-1	1,859	10	18590	0.38
	VLP-Chl-2-7d-2	0,337	20	6740	0.36

4.8. Large-Scale Protein Purification and Detection of VLPs

In order to purify VLPs, double layer sucrose cushion was conducted by ultracentrifugation. After ultracentrifugation, 25% sucrose and 70 % sucrose layers were observed (Figure 4. 81).

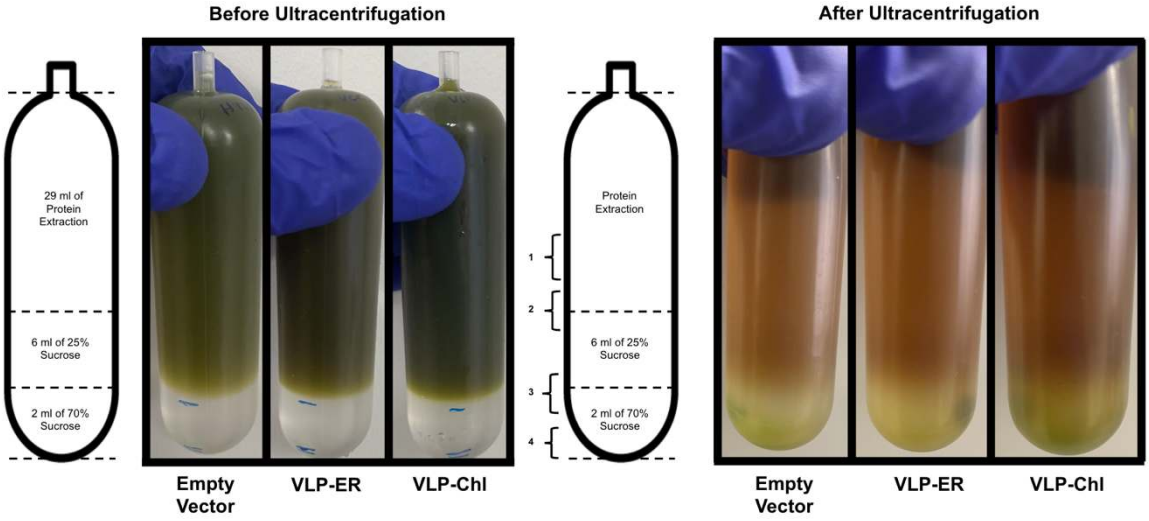

Figure 4. 81. Photographs before and after ultracentrifugation. Empty vector, VLP-ER and VLP-Chl of sucrose cushion samples. 1: sample taken from protein extraction, 2: from interface between protein extraction and 25% sucrose, 3: from interface between 25% sucrose and 70% sucrose, 4: taken from 70% sucrose.

The concentrations of the collected samples were measured by BCA Assay (Table 4. 23).

Table 4. 23. Protein concentrations of samples after sucrose cushion.

Sample	Absorbance Value Measured on the Device (mg/ml)	DF	Sample Concentration (µg/ml)
HT-1	0,143	40	5720
HT-2	0,08	40	3200
HT-3	0,436	1	436
HT-4	0,562	1	562
VLP-ER-1	0,087	40	3480
VLP-ER-2	0,082	40	3280
VLP-ER-3	0,569	1	569
VLP-ER-4	0,632	1	632
VLP-Chl-1	0,126	40	5040
VLP-Chl-2	0,097	40	3880
VLP-Chl-3	1,123	1	1123
VLP-Chl-4	1,102	1	1102

Figure 4. 82 demonstrates the western blot result of TSPs of VLP-ER and VLP-Chl samples by using N antibody, which showed an expected 50 kDa protein detection.

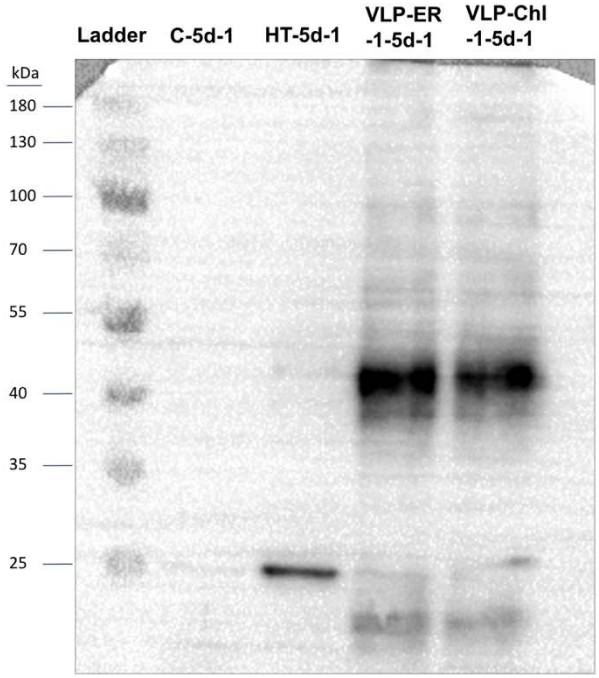

Figure 4. 82. Western-blot result of proteins isolated from leaves infiltrated with Agro-pEAQ-HT, VLP-ER, VLP-Chl using primary N antibody (ProteinTech, 28769-1-AP), C: wild type, Ladder 26616

The western blot result of the samples collected after sucrose cushion was shown in Figure 4. 83. VLP-ER and VLP-Chl samples collected from regions 3 and 4 were shown to contain nucleocapsid (N) protein.

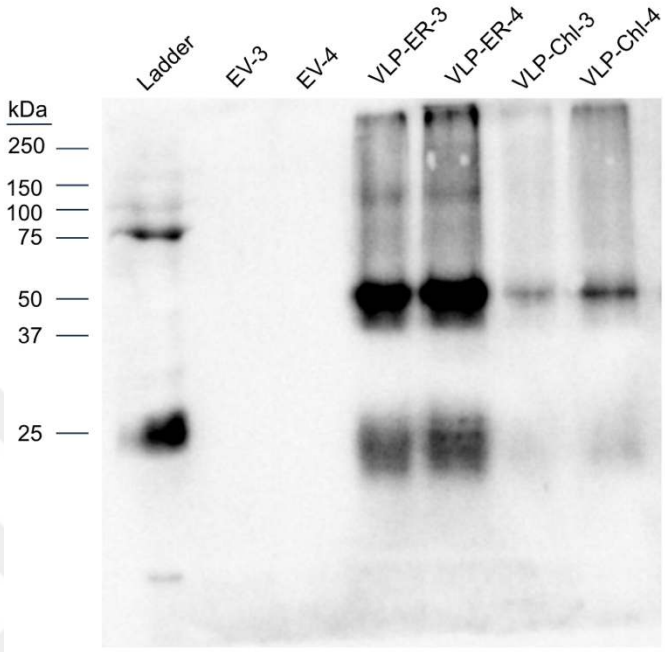

Figure 4. 83. Western-blot result of proteins after sucrose cushion protocol by ultracentrifugation. EV-3, VLP-ER-3 and VLP-Chl-3: collected samples from interface between 25 % sucrose and 75 % sucrose, EV-4, VLP-ER-4 and VLP-Chl-4: collected samples from 75 % sucrose, EV: Empty Vector, VLP-ER, VLP-Chl using primary N antibody (ProteinTech, 28769-1-AP), Ladder: BioRad, 1610374

The ELISA result of TSPs and the samples collected after sucrose cushion is shown in Figure 4. 84. VLP-ER and VLP-Chl samples collected from regions 3 were shown to contain N protein.

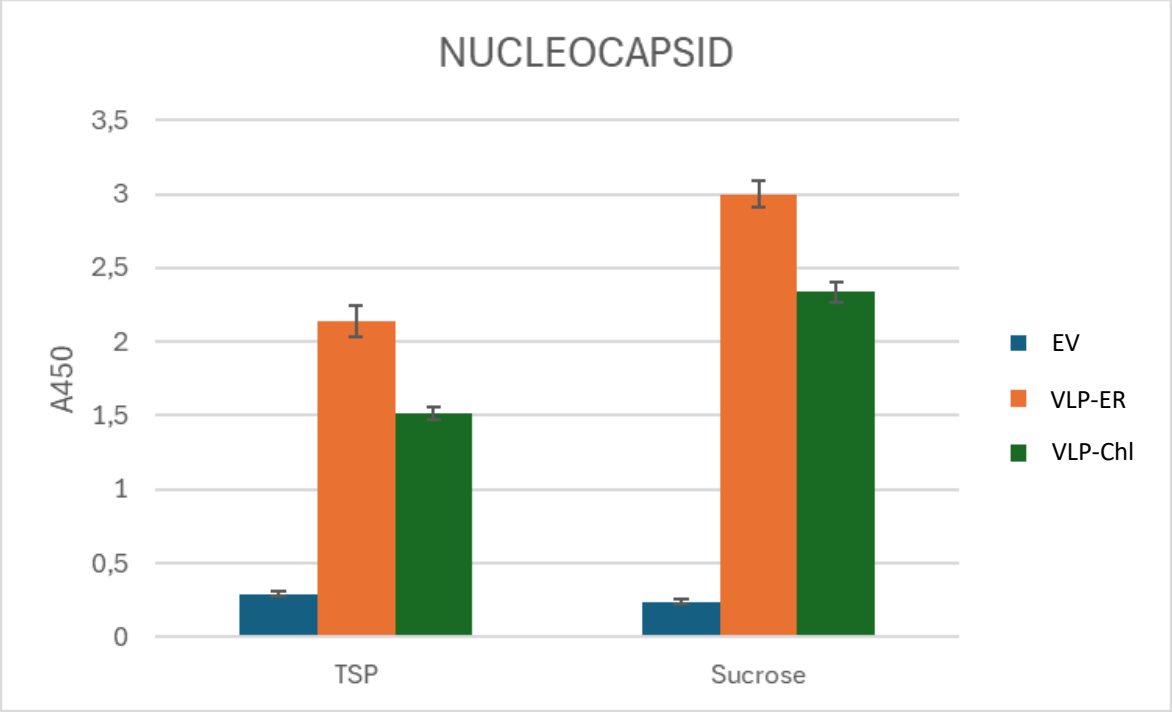

Figure 4. 84. ELISA graph of proteins isolated from leaves infiltrated with Agro-pEAQ-HT, VLP-ER, VLP-Chl using primary N antibody (ProteinTech, 28769-1-AP), the ELISA procedure was performed at 2 replicates for each sample, EV (empty vector): protein taken from *N.benthamiana* leaf infiltrated with pEAQ-HT, VLP-ER: protein taken from *N.benthamiana* leaf co-infiltrated with combination of pEAQ-HT-E, pEAQ-HT-M, pEAQ-HT-Nand pEAQ-HT-S, VLP-Chl: protein taken from *N.benthamiana* leaf co-infiltrated with combination of pEAQ-HT-E, pEAQ-HT-M, pEAQ-HT-Nand pEAQ-HT-S-chl.

The ELISA result of TSPs was shown in Figure 4. 85. VLP-ER and VLP-Chl samples were shown to contain the N protein.

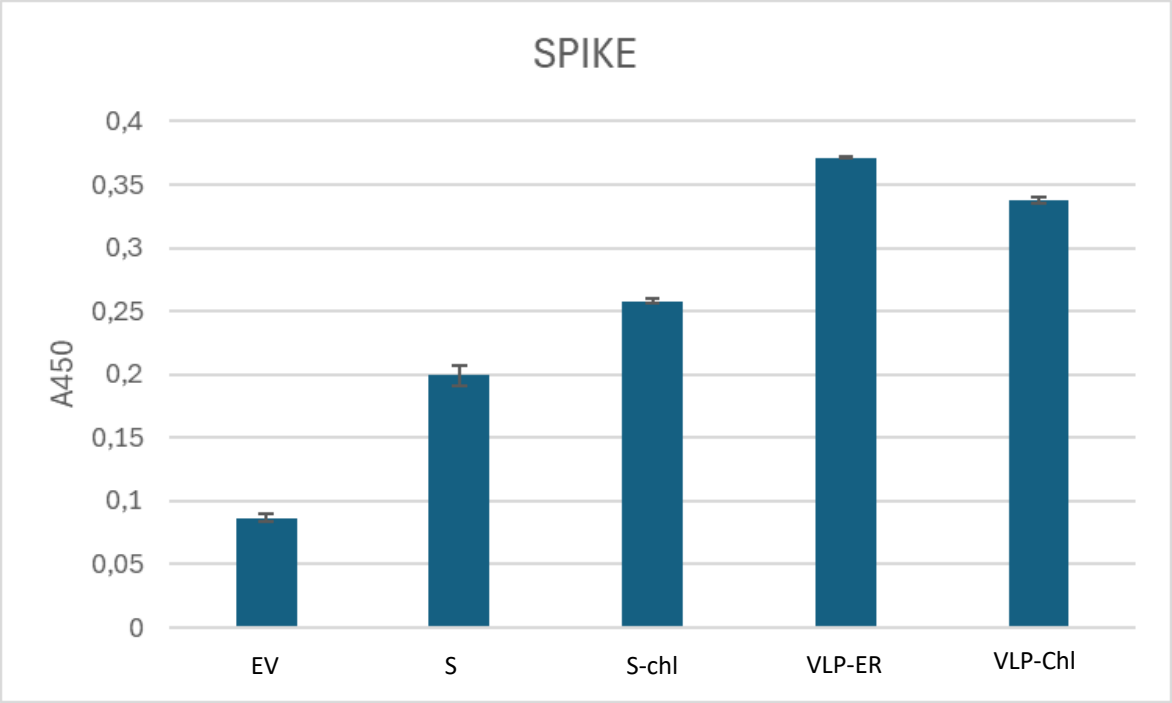

Figure 4. 85. ELISA graph of proteins isolated from leaves infiltrated with Agro-pEAQ-HT, pEAQ-HT-S, pEAQ-HT-S-chl, VLP-ER, VLP-Chl using primary S antibody (TUBITAK MAM), the ELISA procedure was performed at 2 replicates for each sample, EV (empty vector): protein taken from *N.benthamiana* leaf infiltrated with pEAQ-HT, S: protein taken from *N.benthamiana* leaf infiltrated with pEAQ-HT-S, S-chl: protein taken from *N.benthamiana* leaf infiltrated with pEAQ-HT-S-chl, VLP-ER: protein taken from *N.benthamiana* leaf co-infiltrated with combination of pEAQ-HT-E, pEAQ-HT-M, pEAQ-HT-Nand pEAQ-HT-S, VLP-Chl: protein taken from *N.benthamiana* leaf co-infiltrated with combination of pEAQ-HT-E, pEAQ-HT-M, pEAQ-HT-N and pEAQ-HT-S-chl.

5. DISCUSSION

SARS-CoV-2 belongs to the Coronaviridae virus family and is a positive-sense single-stranded RNA virus. Several vaccination programs have been implemented globally to alleviate the severe consequences of the COVID-19 pandemic, which was brought on by the SARS-CoV-2 virus [14]. Equal COVID-19 vaccination distribution is still difficult, nevertheless, particularly in emerging or impoverished nations. Even with the tremendous efforts made thus far in the development and delivery of COVID-19 vaccinations against SARS-CoV-2, the creation of a vaccine that is widely available and capable of cross-neutralizing newly developing variations is still crucial [14]. Various platforms can be used to develop a group of vaccines. One of the most advanced vaccination strategies is VLPs, which are created spontaneously by the assembly of one or more distinct molecules of viral origin [14, 168]. Although they resemble viruses in size and structure, they lack genetic material and cannot infect host cells.

In this study, structural proteins of SARS-CoV-2 virus were specifically designed with appropriate signals and restriction enzymes recognition sites for cloning into the pEAQ-HT plant expression vector. Each construct was first transformed into competent *E. coli* and this plasmid was isolated. The purity and integration of the isolated plasmids belonging to pEAQ vectors (pEAQ-HT and pEAQ-HT-GFP) and each gene construct (E, M, N, S and S-chl) were demonstrated on nanodrop and agarose gel. The 260/280 ratio of the plasmids was around 1.8, indicating that their purity was sufficient. Purities and integrities of every plasmid were adequately observed according to 260/280 ratio and agarose gel electrophoresis. After their integration and purities were checked, isolated gene construct was cloned into pEAQ-HT vector individually and isolated each plasmid including desired gene from *E. coli*. After checking whether desired genes into vector via PCR, these plasmids were sequenced via NGS.

The confirmed plasmids and pEAQ vectors were transferred into *Agrobacterium tumefaciens* LBA4404 strain. Then, *Agrobacterium* containing pEAQ-HT and pEAQ-HT-GFP vectors were infiltrated into 6-week old *N.benthamiana* leaves via syringe. Further, *Agrobacterium* cells containing each plasmid were co-infiltrated in two different combinations (*Agrobacterium* cells containing pEAQ-HT-E, pEAQ-HT-M, pEAQ-HT-N, pEAQ-HT-S were combinated for VLP-ER and *Agrobacterium* cells containing pEAQ-HT-

E, pEAQ-HT-M, pEAQ-HT-N, pEAQ-HT-S-Chl were combinated for VLP-Chl). Agro-infiltration results demonstrated that each leaf had slight chlorosis and necrosis on the infiltrated area because of mechanical stress. In the research paper of Jung et. al [169], *N. benthamiana* leaves infiltrated with pEAQ-HT-M alone showed lower amounts of chlorosis than leaves co-infiltrated with combination of pEAQ-HT-S, pEAQ-HT-E and pEAQ-HT-M plasmids. It was stated that co-infiltration alleviated necrosis caused by infiltration of M gene. On the contrary, we did not find any significant phenotypic difference between co-infiltrated leaves and the leaves infiltrated with *Agrobacterium* containing S or S-chl alone. Tissue injury is caused by the three TM domains present in the native M gene sequence [143]. The reason why the TM domain does not cause tissue damage in this study may be due to the signal peptides incorporated into the M protein during cassette design.

In order to determine the highest expression level post infiltration, pEAQ-HT-GFP plasmid was visualized 3-5-7 dpi under UV light. The highest expression of GFP was observed at 5 dpi and 7 dpi compatible with suggested by Saxena et. al [159].

Total RNA was isolated from 5 dpi samples as there was no significant difference between 5 dpi and 7 dpi according to GFP expression results and high expression level in a shorter time. cDNAs obtained by reverse transcriptase enzyme were generated from total RNA samples whose purity and integrity were confirmed by nanodrop and agarose gel electrophoresis. Using these cDNAs as template, RNA expression was demonstrated using gene-specific primers for each construct.

To compare two different compartmentalization (VLP-ER and VLP-Chl) proteins were isolated from co-infiltrated *N. benthamiana* leaves on 3-5-7 dpi and protein amounts were measured. Western blot analysis was performed on 5 dpi samples. The major band of N protein was obtained in TSPs of VLP-ER and VLP-Chl at approximately 50 kDa. According to the results of Meyers et. al [170] and Yanez et. al [171] studies, it was determined that the amount of target protein in the chloroplast was higher compared to the cytoplasmic localization of protein expression. It is suggested that the reason for this may be that the number of proteases or cellular toxicity is lower in these regions than in the cytoplasm and thus proteins may be less affected by plant physiology and better protected from degradation [155, 172]. On the contrary, in this thesis, the expression of N protein was higher in VLP-ER samples than in VLP-Chl samples according to both the western blot and

ELISA results for TSPs and purified proteins after sucrose cushion. Compatible with that, in a study examining subcellular targeting of the antigen to cytosolic, endomembrane/apoplast and chloroplast sites, the maximal expression level was achieved with cytosolic targeting [173]. ER and chloroplast are the preferred cellular organelles for high level expression and protein folding. However, it was mentioned by Song et. al [174] that the reasons for not achieving high level expression results in the chloroplast are the PTM of the target protein and resistance to degradation. According to this article, compatible with our findings, it was shown that the amount of fluorescence accumulated in the ER was slightly higher than in the chloroplast.

The expression of S protein in VLPs seems to be higher than its individual expression. This situation may be due to the prevention of the protein from degradation when it is assembled in the VLP structure. Since individual proteins might be degraded when expressed alone, the protein level in VLPs appeared to be higher. Pêra et al. [175] reported the VLP vaccine candidate in plant platform for human rotavirus. They confirmed the expression of VP2 and VP6 which are two capsid proteins of rotaviruses by co-expressing them in a VLP structure. They hypothesized that their assembled proteins in the VLP structure were protected from degradation by assembling similar to the natural virion morphogenesis [175].

As a first demonstration of plant-based production of VLPs containing all structural proteins of SARS-CoV-2, this thesis is considered an important step towards the development of a low-cost and scalable COVID-19 vaccine candidate.

6. CONCLUSION

Using conventional cloning method, genes encoding structural proteins of SARS-CoV-2 were cloned into pEAQ-HT expression vector in order to utilize *Agrobacterium*-mediated transient expression in *N. benthamiana* leaves. Two cellular compartments, ER (VLP-ER) and chloroplast (VLP-Chl) were targeted. The expression of N protein in plant was confirmed by both Western and ELISA methods. Higher protein expression level of N was determined by the expression system where VLPs accumulated in ER compared to chloroplast targeted VLPs. Although expressions of the other structural genes (E, M, S, S-chl) were confirmed at mRNA level, respective protein products need to be confirmed. Additionally, visualization of VLP assembly of these proteins remained to be validated.

In further pre-clinical studies, mouse immunization and virus challenge experiments will be performed to determine the dosage of VLP-based vaccines. This study is the first attempt in the world, to produce a COVID-19 vaccine candidate in VLP structure containing all structural proteins of SARS-CoV-2 virus by a plant expression system and is considered an important step towards the development of a low-cost and scalable COVID-19 vaccine.

REFERENCES

[1] N. Zhu *et al.*, “A Novel Coronavirus from Patients with Pneumonia in China, 2019,” *New England Journal of Medicine*, vol. 382, no. 8, pp. 727–733, Feb. 2020, doi: 10.1056/nejmoa2001017.

[2] V. D. Menachery *et al.*, “A SARS-like cluster of circulating bat coronaviruses shows potential for human emergence,” *Nature Medicine*, vol. 21, no. 12, pp. 1508–1513, Nov. 2015, doi: 10.1038/nm.3985.

[3] J. Pallesen *et al.*, “Immunogenicity and structures of a rationally designed prefusion MERS-CoV spike antigen,” *Proceedings of the National Academy of Sciences*, vol. 114, no. 35, Aug. 2017, doi: 10.1073/pnas.1707304114.

[4] R. N. Kirchdoerfer *et al.*, “Pre-fusion structure of a human coronavirus spike protein,” *Nature*, vol. 531, no. 7592, pp. 118–121, Mar. 2016, doi: 10.1038/nature17200.

[5] M. Letko, A. Marzi, and V. Munster, “Functional assessment of cell entry and receptor usage for SARS-CoV-2 and other lineage B betacoronaviruses,” *Nature Microbiology*, vol. 5, no. 4, pp. 562–569, Feb. 2020, doi: 10.1038/s41564-020-0688-y.

[6] H. Berreiros-Hortala, G. Vilchez-Pinto, A. Diaz-Perales, M. Garrido-Arandia, and J. Tome-Amat, “Virus-like Particles as Vaccines for Allergen-Specific Therapy: An Overview of Current Developments,” *International Journal of Molecular Sciences*, vol. 25, no. 13, p. 7429, Jul. 2024, doi: 10.3390/ijms25137429.

[7] M. O. Mohsen and M. F. Bachmann, “Virus-like particle vaccinology, from bench to bedside,” *Cellular and Molecular Immunology*, vol. 19, no. 9, pp. 993–1011, Aug. 2022, doi: 10.1038/s41423-022-00897-8.

[8] W. Wang *et al.*, “A virus-like particle candidate vaccine based on CRISPR/Cas9 gene editing technology elicits broad-spectrum protection against SARS-CoV-2,” *Antiviral Research*, vol. 225, p. 105854, May 2024, doi: 10.1016/j.antiviral.2024.105854.

[9] B. J. Ward *et al.*, “Phase 1 randomized trial of a plant-derived virus-like particle vaccine for COVID-19,” *Nature Medicine*, vol. 27, no. 6, pp. 1071–1078, May 2021, doi: 10.1038/s41591-021-01370-1.

[10] H. Tariq, S. Batool, S. Asif, M. Ali, and B. H. Abbasi, “Virus-Like Particles: Revolutionary Platforms for Developing Vaccines Against Emerging Infectious Diseases,” *Frontiers in Microbiology*, vol. 12, Jan. 2022, doi: 10.3389/fmicb.2021.790121.

[11] H. Peyret and G. P. Lomonossoff, “When plant virology met Agrobacterium: the rise of the deconstructed clones,” *Plant Biotechnology Journal*, vol. 13, no. 8, pp. 1121–1135, Jun. 2015, doi: 10.1111/pbi.12412.

[12] B. J. Ward *et al.*, “Phase 1 randomized trial of a plant-derived virus-like particle vaccine for COVID-19,” *Nature Medicine*, vol. 27, no. 6, pp. 1071–1078, May 2021, doi: 10.1038/s41591-021-01370-1.

[13] D. Calina *et al.*, “Towards effective COVID-19 vaccines: Updates, perspectives and challenges (Review),” *International Journal of Molecular Medicine*, vol. 46, no. 1, pp. 3–16, May 2020, doi: 10.3892/ijmm.2020.4596.

[14] R. Xu, M. Shi, J. Li, P. Song, and N. Li, “Construction of SARS-CoV-2 Virus-Like Particles by Mammalian Expression System,” *Frontiers in Bioengineering and Biotechnology*, vol. 8, Jul. 2020, doi: 10.3389/fbioe.2020.00862.

[15] I. C. Yilmaz *et al.*, “Development and preclinical evaluation of virus-like particle vaccine against COVID-19 infection,” *Allergy*, vol. 77, no. 1, pp. 258–270, Sep. 2021, doi: 10.1111/all.15091.

[16] N. Pogrebnyak *et al.*, “Severe acute respiratory syndrome (SARS) S protein production in plants: Development of recombinant vaccine,” *Proceedings of the National Academy of Sciences*, vol. 102, no. 25, pp. 9062–9067, Jun. 2005, doi: 10.1073/pnas.0503760102.

[17] H.-Y. Li, S. Ramalingam, and M.-L. Chye, “Accumulation of Recombinant SARS-CoV Spike Protein in Plant Cytosol and Chloroplasts Indicate Potential for Development of Plant-Derived Oral Vaccines,” *Experimental Biology and Medicine*, vol. 231, no. 8, pp. 1346–1352, Sep. 2006, doi: 10.1177/153537020623100808.

[18] H. S. Mason, D. M. Lam, and C. J. Arntzen, “Expression of hepatitis B surface antigen in transgenic plants.,” *Proceedings of the National Academy of Sciences*, vol. 89, no. 24, pp. 11745–11749, Dec. 1992, doi: 10.1073/pnas.89.24.11745.

[19] P. M. Maharjan and S. Choe, “Plant-Based COVID-19 Vaccines: Current Status, Design, and Development Strategies of Candidate Vaccines,” *Vaccines*, vol. 9, no. 9, p. 992, Sep. 2021, doi: 10.3390/vaccines9090992.

[20] S. Nooraei *et al.*, “Virus-like particles: preparation, immunogenicity and their roles as nanovaccines and drug nanocarriers,” *Journal of Nanobiotechnology*, vol. 19, no. 1, Feb. 2021, doi: 10.1186/s12951-021-00806-7.

[21] S. Rosales-Mendoza, “Will plant-made biopharmaceuticals play a role in the fight against COVID-19?,” *Expert Opinion on Biological Therapy*, vol. 20, no. 6, pp. 545–548, Apr. 2020, doi: 10.1080/14712598.2020.1752177.

[22] L. Derevnina, S. Kamoun, and C. Wu, “Dude, where is my mutant? Nicotiana benthamiana meets forward genetics,” *New Phytologist*, vol. 221, no. 2, pp. 607–610, Dec. 2018, doi: 10.1111/nph.15521.

[23] J. Bally *et al.*, “The Rise and Rise of Nicotiana benthamiana: A Plant for All Reasons,” *Annual Review of Phytopathology*, vol. 56, no. 1, pp. 405–426, Aug. 2018, doi: 10.1146/annurev-phyto-080417-050141.

[24] L. J. Kelly, A. R. Leitch, J. J. Clarkson, S. Knapp, and M. W. Chase, “RECONSTRUCTING THE COMPLEX EVOLUTIONARY ORIGIN OF WILD

ALLOPOLYPLOID TOBACCOS (NICOTIANASECTIONSUAVEOLENTES),” *Evolution*, vol. 67, no. 1, pp. 80–94, Aug. 2012, doi: 10.1111/j.1558-5646.2012.01748.x.

[25] A. C. VelÁsquez, S. Chakravarthy, and G. B. Martin, “Virus-induced Gene Silencing (VIGS) in Nicotiana benthamiana and Tomato,” *Journal of Visualized Experiments*, no. 28, Jun. 2009, doi: 10.3791/1292.

[26] M. M. Goodin, D. Zaitlin, R. A. Naidu, and S. A. Lommel, “Nicotiana benthamiana: Its History and Future as a Model for Plant–Pathogen Interactions,” *Molecular Plant-Microbe Interactions*, vol. 21, no. 8, pp. 1015–1026, Aug. 2008, doi: 10.1094/mpmi-21-8-1015.

[27] M.-C. Goulet *et al.*, “Production of Biopharmaceuticals in Nicotiana benthamiana—Axillary Stem Growth as a Key Determinant of Total Protein Yield,” *Frontiers in Plant Science*, vol. 10, Jun. 2019, doi: 10.3389/fpls.2019.00735.

[28] “Coronavirus disease (COVID-19) – World Health Organization,” Jul. 12, 2024. https//who.int/emergencies/diseases/novel-coronavirus-2019

[29] “T.C. Sağlık Bakanlığı COVID-19 Bilgilendirme Platformu.” https//covid19.saglik.gov.tr/ (accessed Aug. 22, 2024).

[30] R. Arya *et al.*, “Structural insights into SARS-CoV-2 proteins,” *Journal of Molecular Biology*, vol. 433, no. 2, p. 166725, Jan. 2021, doi: 10.1016/j.jmb.2020.11.024.

[31] H. Wade, Q. Duan, and Q. Su, “Interaction between Sars-CoV-2 structural proteins and host cellular receptors: From basic mechanisms to clinical perspectives,” *Advances in Protein Chemistry and Structural Biology*, pp. 243–277, Jan. 2022, doi: 10.1016/bs.apcsb.2022.05.010.

[32] R. Gorkhali, P. Koirala, S. Rijal, A. Mainali, A. Baral, and H. K. Bhattarai, “Structure and Function of Major SARS-CoV-2 and SARS-CoV Proteins,” *Bioinformatics and Biology Insights*, vol. 15, p. 117793222110258, Jan. 2021, doi: 10.1177/11779322211025876.

[33] C. Huang, K. G. Lokugamage, J. M. Rozovics, K. Narayanan, B. L. Semler, and S. Makino, “SARS Coronavirus nsp1 Protein Induces Template-Dependent Endonucleolytic Cleavage of mRNAs: Viral mRNAs Are Resistant to nsp1-Induced RNA Cleavage,” *PLoS Pathogens*, vol. 7, no. 12, p. e1002433, Dec. 2011, doi: 10.1371/journal.ppat.1002433.

[34] Y. Sakai, K. Kawachi, Y. Terada, H. Omori, Y. Matsuura, and W. Kamitani, “Two-amino acids change in the nsp4 of SARS coronavirus abolishes viral replication,” *Virology*, vol. 510, pp. 165–174, Oct. 2017, doi: 10.1016/j.virol.2017.07.019.

[35] R. Yadav *et al.*, “Role of Structural and Non-Structural Proteins and Therapeutic Targets of SARS-CoV-2 for COVID-19,” *Cells*, vol. 10, no. 4, p. 821, Apr. 2021, doi: 10.3390/cells10040821.

[36] A. Nikolaou, “Functions of SARS-CoV-2 accessory proteins: Contribution to viral pathogenicity and potential role for the development of novel therapeutics and immunodiagnostics,” Nov. 2023.

[37] J. Chai *et al.*, “Structural basis for SARS-CoV-2 envelope protein recognition of human cell junction protein PALS1,” *Nature Communications*, vol. 12, no. 1, Jun. 2021, doi: 10.1038/s41467-021-23533-x.

[38] D. Schoeman and B. C. Fielding, “Is There a Link Between the Pathogenic Human Coronavirus Envelope Protein and Immunopathology? A Review of the Literature,” *Frontiers in Microbiology*, vol. 11, Sep. 2020, doi: 10.3389/fmicb.2020.02086.

[39] J. L. Nieto-Torres *et al.*, “Severe acute respiratory syndrome coronavirus E protein transports calcium ions and activates the NLRP3 inflammasome,” *Virology*, vol. 485, pp. 330–339, Nov. 2015, doi: 10.1016/j.virol.2015.08.010.

[40] D. Schoeman and B. C. Fielding, “Coronavirus envelope protein: current knowledge,” *Virology Journal*, vol. 16, no. 1, May 2019, doi: 10.1186/s12985-019-1182-0.

[41] V. S. Mandala, M. J. McKay, A. A. Shcherbakov, A. J. Dregni, A. Kolocouris, and M. Hong, “Structure and drug binding of the SARS-CoV-2 envelope protein transmembrane domain in lipid bilayers,” *Nature Structural & Molecular Biology*, vol. 27, no. 12, pp. 1202–1208, Nov. 2020, doi: 10.1038/s41594-020-00536-8.

[42] Y. Zheng *et al.*, “Severe acute respiratory syndrome coronavirus 2 (SARS-CoV-2) membrane (M) protein inhibits type I and III interferon production by targeting RIG-I/MDA-5 signaling,” *Signal Transduction and Targeted Therapy*, vol. 5, no. 1, Dec. 2020, doi: 10.1038/s41392-020-00438-7.

[43] B. Boson *et al.*, “The SARS-CoV-2 envelope and membrane proteins modulate maturation and retention of the spike protein, allowing assembly of virus-like particles,” *Journal of Biological Chemistry*, vol. 296, p. 100111, Jan. 2021, doi: 10.1074/jbc.ra120.016175.

[44] C.-K. Chang, M.-H. Hou, C.-F. Chang, C.-D. Hsiao, and T.-H. Huang, “The SARS coronavirus nucleocapsid protein – Forms and functions,” *Antiviral Research*, vol. 103, pp. 39–50, Mar. 2014, doi: 10.1016/j.antiviral.2013.12.009.

[45] Y. Peng *et al.*, “Structures of the SARS -CoV-2 nucleocapsid and their perspectives for drug design,” *The EMBO Journal*, vol. 39, no. 20, Sep. 2020, doi: 10.15252/embj.2020105938.

[46] R. McBride, M. Van Zyl, and B. Fielding, “The Coronavirus Nucleocapsid Is a Multifunctional Protein,” *Viruses*, vol. 6, no. 8, pp. 2991–3018, Aug. 2014, doi: 10.3390/v6082991.

[47] B. Shang *et al.*, “Characterization and application of monoclonal antibodies against N protein of SARS-coronavirus,” *Biochemical and Biophysical Research Communications*, vol. 336, no. 1, pp. 110–117, Oct. 2005, doi: 10.1016/j.bbrc.2005.08.032.

[48] S. Liu *et al.*, “Immunological characterizations of the nucleocapsid protein based SARS vaccine candidates,” *Vaccine*, vol. 24, no. 16, pp. 3100–3108, Apr. 2006, doi: 10.1016/j.vaccine.2006.01.058.

[49] S. Xia *et al.*, “Fusion mechanism of 2019-nCoV and fusion inhibitors targeting HR1 domain in spike protein,” *Cellular and Molecular Immunology*, vol. 17, no. 7, pp. 765–767, Feb. 2020, doi: 10.1038/s41423-020-0374-2.

[50] R. Yan, Y. Zhang, Y. Li, L. Xia, Y. Guo, and Q. Zhou, “Structural basis for the recognition of SARS-CoV-2 by full-length human ACE2,” *Science*, vol. 367, no. 6485, pp. 1444–1448, Mar. 2020, doi: 10.1126/science.abb2762.

[51] Q. Wang *et al.*, “Structural and Functional Basis of SARS-CoV-2 Entry by Using Human ACE2,” *Cell*, vol. 181, no. 4, pp. 894-904.e9, May 2020, doi: 10.1016/j.cell.2020.03.045.

[52] V. R. Flores-Vega, J. V. Monroy-Molina, L. E. Jiménez-Hernández, A. G. Torres, J. I. Santos-Preciado, and R. Rosales-Reyes, “SARS-CoV-2: Evolution and Emergence of New Viral Variants,” *Viruses*, vol. 14, no. 4, p. 653, Mar. 2022, doi: 10.3390/v14040653.

[53] T. N. Starr *et al.*, “Deep Mutational Scanning of SARS-CoV-2 Receptor Binding Domain Reveals Constraints on Folding and ACE2 Binding,” *Cell*, vol. 182, no. 5, pp. 1295-1310.e20, Sep. 2020, doi: 10.1016/j.cell.2020.08.012.

[54] S. A. Kemp *et al.*, “SARS-CoV-2 evolution during treatment of chronic infection,” *Nature*, vol. 592, no. 7853, pp. 277–282, Feb. 2021, doi: 10.1038/s41586-021-03291-y.

[55] L. J. Abu-Raddad *et al.*, “Pfizer-BioNTech mRNA BNT162b2 Covid-19 vaccine protection against variants of concern after one versus two doses,” *Journal of Travel Medicine*, vol. 28, no. 7, May 2021, doi: 10.1093/jtm/taab083.

[56] H. Tegally *et al.*, “Detection of a SARS-CoV-2 variant of concern in South Africa,” *Nature*, vol. 592, no. 7854, pp. 438–443, Mar. 2021, doi: 10.1038/s41586-021-03402-9.

[57] C. Liu *et al.*, “The antibody response to SARS-CoV-2 Beta underscores the antigenic distance to other variants,” *Cell Host & Microbe*, vol. 30, no. 1, pp. 53-68.e12, Jan. 2022, doi: 10.1016/j.chom.2021.11.013.

[58] S. A. Madhi *et al.*, “Efficacy of the ChAdOx1 nCoV-19 Covid-19 Vaccine against the B.1.351 Variant,” *New England Journal of Medicine*, vol. 384, no. 20, pp. 1885–1898, May 2021, doi: 10.1056/nejmoa2102214.

[59] S. Martin *et al.*, “SARS-CoV-2 integral membrane proteins shape the serological responses of patients with COVID-19,” *iScience*, vol. 24, no. 10, p. 103185, Oct. 2021, doi: 10.1016/j.isci.2021.103185.

[60] “Tracking SARS-CoV-2 variants,” Mar. 27, 2024. https//who.int/en/activities/tracking-SARS-CoV-2-variants/

[61] “SARS-CoV-2 variants ~ ViralZone.” https//viralzone.expasy.org/9556

[62] F. Maggi *et al.*, “Imported SARS-CoV-2 Variant P.1 in Traveler Returning from Brazil to Italy,” *Emerging Infectious Diseases*, vol. 27, no. 4, pp. 1249–1251, Apr. 2021, doi: 10.3201/eid2704.210183.

[63] K. Hayawi, S. Shahriar, M. A. Serhani, H. Alashwal, and M. M. Masud, “Vaccine versus Variants (3Vs): Are the COVID-19 Vaccines Effective against the Variants? A Systematic Review,” *Vaccines*, vol. 9, no. 11, p. 1305, Nov. 2021, doi: 10.3390/vaccines9111305.

[64] D. M. Skowronski *et al.*, “Single-dose mRNA Vaccine Effectiveness Against Severe Acute Respiratory Syndrome Coronavirus 2 (SARS-CoV-2), Including Alpha and Gamma Variants: A Test-negative Design in Adults 70 Years and Older in British Columbia, Canada,” *Clinical Infectious Diseases*, vol. 74, no. 7, pp. 1158–1165, Jul. 2021, doi: 10.1093/cid/ciab616.

[65] M. McCallum *et al.*, “Molecular basis of immune evasion by the Delta and Kappa SARS-CoV-2 variants,” *Science*, vol. 374, no. 6575, pp. 1621–1626, Dec. 2021, doi: 10.1126/science.abl8506.

[66] T. Mamedov *et al.*, “Plant-Produced Glycosylated and In Vivo Deglycosylated Receptor Binding Domain Proteins of SARS-CoV-2 Induce Potent Neutralizing Responses in Mice,” *Viruses*, vol. 13, no. 8, p. 1595, Aug. 2021, doi: 10.3390/v13081595.

[67] J. L. Bernal *et al.*, “Effectiveness of the Pfizer-BioNTech and Oxford-AstraZeneca vaccines on covid-19 related symptoms, hospital admissions, and mortality in older adults in England: test negative case-control study,” *BMJ*, p. n1088, May 2021, doi: 10.1136/bmj.n1088.

[68] X. Deng *et al.*, “Transmission, infectivity, and neutralization of a spike L452R SARS-CoV-2 variant,” *Cell*, vol. 184, no. 13, pp. 3426-3437.e8, Jun. 2021, doi: 10.1016/j.cell.2021.04.025.

[69] J. Chen, R. Wang, M. Wang, and G.-W. Wei, “Mutations Strengthened SARS-CoV-2 Infectivity,” *Journal of Molecular Biology*, vol. 432, no. 19, pp. 5212–5226, Sep. 2020, doi: 10.1016/j.jmb.2020.07.009.

[70] D. A. Collier *et al.*, “Sensitivity of SARS-CoV-2 B.1.1.7 to mRNA vaccine-elicited antibodies,” *Nature*, vol. 593, no. 7857, pp. 136–141, Mar. 2021, doi: 10.1038/s41586-021-03412-7.

[71] L. Zhang *et al.*, “Ten emerging SARS-CoV-2 spike variants exhibit variable infectivity, animal tropism, and antibody neutralization,” *Communications Biology*, vol. 4, no. 1, Oct. 2021, doi: 10.1038/s42003-021-02728-4.

[72] A. J. Wozney *et al.*, “Evolution of Stronger SARS-CoV-2 Variants as Revealed Through the Lens of Molecular Dynamics Simulations,” *The Protein Journal*, vol. 41, no. 4–5, pp. 444–456, Aug. 2022, doi: 10.1007/s10930-022-10065-6.

[73] M. I. Barton, S. A. MacGowan, M. A. Kutuzov, O. Dushek, G. J. Barton, and P. A. Van Der Merwe, “Effects of common mutations in the SARS-CoV-2 Spike RBD and its ligand, the human ACE2 receptor on binding affinity and kinetics,” *eLife*, vol. 10, Aug. 2021, doi: 10.7554/elife.70658

[74] P. Mlcochova *et al.*, “SARS-CoV-2 B.1.617.2 Delta variant replication and immune evasion,” *Nature*, vol. 599, no. 7883, pp. 114–119, Sep. 2021, doi: 10.1038/s41586-021-03944-y.

[75] C. Liu *et al.*, “Reduced neutralization of SARS-CoV-2 B.1.617 by vaccine and convalescent serum,” *Cell*, vol. 184, no. 16, pp. 4220-4236.e13, Aug. 2021, doi: 10.1016/j.cell.2021.06.020.

[76] T. Tada, H. Zhou, B. M. Dcosta, M. I. Samanovic, M. J. Mulligan, and N. R. Landau, “SARS-CoV-2 Lambda Variant Remains Susceptible to Neutralization by mRNA Vaccine-elicited Antibodies and Convalescent Serum,” *bioRxiv (Cold Spring Harbor Laboratory)*, Jul. 2021, doi: 10.1101/2021.07.02.450959.

[77] K. Uriu *et al.*, “Neutralization of the SARS-CoV-2 Mu Variant by Convalescent and Vaccine Serum,” *New England Journal of Medicine*, vol. 385, no. 25, pp. 2397–2399, Dec. 2021, doi: 10.1056/nejmc2114706.

[78] S. A. Buchan *et al.*, “Estimated Effectiveness of COVID-19 Vaccines Against Omicron or Delta Symptomatic Infection and Severe Outcomes,” *JAMA Network Open*, vol. 5, no. 9, p. e2232760, Sep. 2022, doi: 10.1001/jamanetworkopen.2022.32760.

[79] European Medicine Agency (EMA) EMA recommends Nuvaxovid for authorisation in the EU,” Dec. 20, 2021. https//ema.europa.eu/en/news/ema-recommends-nuvaxovid-authorisation-eu. (accessed Aug. 23, 2024).

[80] J. H. Tian *et al.*, “SARS-CoV-2 spike glycoprotein vaccine candidate NVX-CoV2373 immunogenicity in baboons and protection in mice,” *Nature Communications*, vol. 12, no. 1, Jan. 2021, doi: 10.1038/s41467-020-20653-8.

[81] “WHO – COVID19 Vaccine Tracker.” https//covid19.trackvaccines.org/agency/who/

[82] W. B. Park, Y. H. Hwang, and H. J. Cheong, “COVID-19 Vaccination in Korea,” *Infection and Chemotherapy*, vol. 55, no. 1, p. 135, Jan. 2023, doi: 10.3947/ic.2023.0023.

[83] L. R. Baden *et al.*, “Efficacy and Safety of the mRNA-1273 SARS-CoV-2 Vaccine,” *New England Journal of Medicine*, vol. 384, no. 5, pp. 403–416, Feb. 2021, doi: 10.1056/nejmoa2035389.

[84] “Yahoo is part of the Yahoo family of brands.” https//finance.yahoo.com/news/moderna-announces-clinical-bivalent-covid-105000561.html?guccounter=1&guce_referrer=aHR0cHM6Ly93d3cuZ29vZ2xlLmNvbS8&guce_referrer_sig=AQAAACigneNUT8tgdQTa6y-DKZtYEJX-uj8o5nCK96XvUfXE5FGb2ODEZOqMlALW6MhnK52VzWQtOr1U9zwVyLg82jC-GfBfAc_2uX872EVXrcX1pNBoR0QhMJyW-3hTVOBbZAcmijx6_rH161YKIRQ6W_eB6EquT95g3z62XPRCEExn

[85] "First bivalent COVID-19 booster vaccine approved by UK medicines regulator," *GOV.UK*, Aug. 15, 2022. [Online]. Available: https//gov.uk/government/news/first-bivalent-covid-19-booster-vaccine-approved-by-uk-medicines-regulator#:~:text=An%20updated%20version%20of%20the,regulator's%20standards%20of%20safety%2C%20quality

[86] E. E. Walsh *et al.*, "Safety and Immunogenicity of Two RNA-Based Covid-19 Vaccine Candidates," *New England Journal of Medicine*, vol. 383, no. 25, pp. 2439–2450, Dec. 2020, doi: 10.1056/nejmoa2027906.

[87] M. T. Mascellino, F. Di Timoteo, M. De Angelis, and A. Oliva, "Overview of the Main Anti-SARS-CoV-2 Vaccines: Mechanism of Action, Efficacy and Safety," *Infection and Drug Resistance*, vol. Volume 14, pp. 3459–3476, Aug. 2021, doi: 10.2147/idr.s315727.

[88] "Comirnaty Original/Omicron BA.4-5 (15/15 micrograms)/dose dispersion for injection COVID-19 mRNA Vaccine - Summary of Product Characteristics (SmPC) - (emc)." https//medicines.org.uk/emc/product/14457/smpc#gref

[89] V. Chavda *et al.*, "Adenoviral Vector-Based Vaccine Platform for COVID-19: Current Status," *Vaccines*, vol. 11, no. 2, p. 432, Feb. 2023, doi: 10.3390/vaccines11020432.

[90] S. Wu *et al.*, "A single dose of an adenovirus-vectored vaccine provides protection against SARS-CoV-2 challenge," *Nature Communications*, vol. 11, no. 1, Aug. 2020, doi: 10.1038/s41467-020-17972-1.

[91] R. Patel, M. Kaki, V. S. Potluri, P. Kahar, and D. Khanna, "A comprehensive review of SARS-CoV-2 vaccines: Pfizer, Moderna & Johnson & Johnson," *Human Vaccines & Immunotherapeutics*, vol. 18, no. 1, Jan. 2022, doi: 10.1080/21645515.2021.2002083.

[92] S. Banerjee, M. Sandhu, E. Tonzi, A. Tambe, and H. S. Gambhir, "Immune-Mediated Thrombocytopenia Associated With Ad26.COV2.S (Janssen; Johnson & Johnson) Vaccine," *American Journal of Therapeutics*, vol. 28, no. 5, pp. e604–e606, Aug. 2021, doi: 10.1097/mjt.0000000000001431.

[93] "Department of Error," *The Lancet*, vol. 396, no. 10266, p. 1884, Dec. 2020, doi: 10.1016/s0140-6736(20)32597-6.

[94] M. Kishimoto, T. Ishikawa, and M. Odawara, "Subacute thyroiditis with liver dysfunction following coronavirus disease 2019 (COVID-19) vaccination: report of two cases and a literature review," *Endocrine Journal*, vol. 69, no. 8, pp. 947–957, Jan. 2022, doi: 10.1507/endocrj.ej21-0629.

[95] R. Ella *et al.*, "Safety and immunogenicity of an inactivated SARS-CoV-2 vaccine, BBV152: a double-blind, randomised, phase 1 trial," *The Lancet Infectious Diseases*, vol. 21, no. 5, pp. 637–646, May 2021, doi: 10.1016/s1473-3099(20)30942-7.

[96] P. J. Hotez and M. E. Bottazzi, "Whole Inactivated Virus and Protein-Based COVID-19 Vaccines," *Annual Review of Medicine*, vol. 73, no. 1, pp. 55–64, Jan. 2022, doi: 10.1146/annurev-med-042420-113212.

[97] Q. Gao *et al.*, “Development of an inactivated vaccine candidate for SARS-CoV-2,” *Science*, vol. 369, no. 6499, pp. 77–81, Jul. 2020, doi: 10.1126/science.abc1932.

[98] T. T. Le *et al.*, “The COVID-19 vaccine development landscape,” *Nature Reviews Drug Discovery*, vol. 19, no. 5, pp. 305–306, Apr. 2020, doi: 10.1038/d41573-020-00073-5.

[99] R. S. De Queiroz Simões and D. Rodríguez-Lázaro, “Classical and Next-Generation Vaccine Platforms to SARS-CoV-2: Biotechnological Strategies and Genomic Variants,” *International Journal of Environmental Research and Public Health*, vol. 19, no. 4, p. 2392, Feb. 2022, doi: 10.3390/ijerph19042392.

[100] J. Louten, “Vaccines, Antivirals, and the Beneficial Uses of Viruses,” in *Elsevier eBooks*, 2016, pp. 133–154. doi: 10.1016/b978-0-12-800947-5.00008-9.

[101] P. D. Minor, “Live attenuated vaccines: Historical successes and current challenges,” *Virology*, vol. 479–480, pp. 379–392, May 2015, doi: 10.1016/j.virol.2015.03.032.

[102] Y. Dong, T. Dai, Y. Wei, L. Zhang, M. Zheng, and F. Zhou, “A systematic review of SARS-CoV-2 vaccine candidates,” *Signal Transduction and Targeted Therapy*, vol. 5, no. 1, Oct. 2020, doi: 10.1038/s41392-020-00352-y.

[103] F. Bayani *et al.*, “An overview of the vaccine platforms to combat COVID-19 with a focus on the subunit vaccines,” *Progress in Biophysics and Molecular Biology*, vol. 178, pp. 32–49, Mar. 2023, doi: 10.1016/j.pbiomolbio.2023.02.004.

[104] S. Rauch, E. Jasny, K. E. Schmidt, and B. Petsch, “New Vaccine Technologies to Combat Outbreak Situations,” *Frontiers in Immunology*, vol. 9, Sep. 2018, doi: 10.3389/fimmu.2018.01963.

[105] N. Liu, “A Comparison of Plasmid DNA and mRNA as Vaccine Technologies,” *Vaccines*, vol. 7, no. 2, p. 37, Apr. 2019, doi: 10.3390/vaccines7020037.

[106] S. Liu, S. Wang, and S. Lu, “DNA immunization as a technology platform for monoclonal antibody induction,” *Emerging Microbes & Infections*, vol. 5, no. 1, pp. 1–12, Jan. 2016, doi: 10.1038/emi.2016.27.

[107] U. Sahin, K. Karikó, and Ö. Türeci, “mRNA-based therapeutics — developing a new class of drugs,” *Nature Reviews Drug Discovery*, vol. 13, no. 10, pp. 759–780, Sep. 2014, doi: 10.1038/nrd4278.

[108] C. Vellozzi, D. R. Burwen, A. Dobardzic, R. Ball, K. Walton, and P. Haber, “Safety of trivalent inactivated influenza vaccines in adults: Background for pandemic influenza vaccine safety monitoring,” *Vaccine*, vol. 27, no. 15, pp. 2114–2120, Mar. 2009, doi: 10.1016/j.vaccine.2009.01.125.

[109] Q. Chen and H. Lai, “Plant-derived virus-like particles as vaccines,” *Human Vaccines & Immunotherapeutics*, vol. 9, no. 1, pp. 26–49, Jan. 2013, doi: 10.4161/hv.22218.

[110] J. Zepeda-Cervantes, J. O. Ramírez-Jarquín, and L. Vaca, “Interaction Between Virus-Like Particles (VLPs) and Pattern Recognition Receptors (PRRs) From

Dendritic Cells (DCs): Toward Better Engineering of VLPs," *Frontiers in Immunology*, vol. 11, Jun. 2020, doi: 10.3389/fimmu.2020.01100.

[111] J. Fuenmayor, F. Gòdia, and L. Cervera, "Production of virus-like particles for vaccines," *New Biotechnology*, vol. 39, pp. 174–180, Oct. 2017, doi: 10.1016/j.nbt.2017.07.010.

[112] X. Huang, X. Wang, J. Zhang, N. Xia, and Q. Zhao, "Escherichia coli-derived virus-like particles in vaccine development," *Npj Vaccines*, vol. 2, no. 1, Feb. 2017, doi: 10.1038/s41541-017-0006-8.

[113] B. Donaldson, F. Al-Barwani, V. Young, S. Scullion, V. Ward, and S. Young, "Virus-Like Particles, a Versatile Subunit Vaccine Platform," in *Advances in delivery science and technology*, 2014, pp. 159–180. doi: 10.1007/978-1-4939-1417-3_9.

[114] B. Şerefoğlu *et al.*, "SARS-CoV-2'YE KARŞI GELİŞTİRİLEN AŞILAR VE ÜRETİM METOTLARI," Aug. 31, 2021. https//dergipark.org.tr/tr/pub/tusebdergisi/issue/64741/983430

[115] Y. Gleba, V. Klimyuk, and S. Marillonnet, "Magnifection?a new platform for expressing recombinant vaccines in plants," *Vaccine*, vol. 23, no. 17–18, pp. 2042–2048, Mar. 2005, doi: 10.1016/j.vaccine.2005.01.006.

[116] N. Charland, "Plant-Made Influenza Virus-Like Particles: for Pandemic and Beyond," Jan. 2012, [Online]. Available: http//dc.engconfintl.org/cgi/viewcontent.cgi?article=1042&context=vaccine_iv

[117] E. P. Rybicki, "Plant molecular farming of virus-like nanoparticles as vaccines and reagents," *Wiley Interdisciplinary Reviews Nanomedicine and Nanobiotechnology*, vol. 12, no. 2, Sep. 2019, doi: 10.1002/wnan.1587.

[118] M. D'Aoust *et al.*, "The production of hemagglutinin-based virus-like particles in plants: a rapid, efficient and safe response to pandemic influenza," *Plant Biotechnology Journal*, vol. 8, no. 5, pp. 607–619, May 2010, doi: 10.1111/j.1467-7652.2009.00496.x.

[119] Q. Chen and H. Lai, "Plant-derived virus-like particles as vaccines," *Human Vaccines & Immunotherapeutics*, vol. 9, no. 1, pp. 26–49, Jan. 2013, doi: 10.4161/hv.22218.

[120] K. Kashima *et al.*, "Good manufacturing practices production of a purification-free oral cholera vaccine expressed in transgenic rice plants," *Plant Cell Reports*, vol. 35, no. 3, pp. 667–679, Dec. 2015, doi: 10.1007/s00299-015-1911-9.

[121] Y. Thanavala *et al.*, "Immunogenicity in humans of an edible vaccine for hepatitis B," *Proceedings of the National Academy of Sciences*, vol. 102, no. 9, pp. 3378–3382, Feb. 2005, doi: 10.1073/pnas.0409899102.

[122] J. Kapusta *et al.*, "A plant-derived edible vaccine against hepatitis B virus," *The FASEB Journal*, vol. 13, no. 13, pp. 1796–1799, Oct. 1999, doi: 10.1096/fasebj.13.13.1796.

[123] H. Mason and M. M. Herbst-Kralovetz, “Plant-Derived Antigens as Mucosal Vaccines,” *Current Topics in Microbiology and Immunology*, pp. 101–120, Jan. 2011, doi: 10.1007/82_2011_158.

[124] M. A. Escobar and A. M. Dandekar, “Agrobacterium tumefaciens as an agent of disease,” *Trends in Plant Science*, vol. 8, no. 8, pp. 380–386, Aug. 2003, doi: 10.1016/s1360-1385(03)00162-6.

[125] D. J. Garfinkel and E. W. Nester, “Agrobacterium tumefaciens mutants affected in crown gall tumorigenesis and octopine catabolism,” *Journal of Bacteriology*, vol. 144, no. 2, pp. 732–743, Nov. 1980, doi: 10.1128/jb.144.2.732-743.1980.

[126] S. E. Stachel, E. Messens, M. Van Montagu, and P. Zambryski, “Identification of the signal molecules produced by wounded plant cells that activate T-DNA transfer in Agrobacterium tumefaciens,” *Nature*, vol. 318, no. 6047, pp. 624–629, Dec. 1985, doi: 10.1038/318624a0.

[127] G. W. Bolton, E. W. Nester, and M. P. Gordon, “Plant Phenolic Compounds Induce Expression of the Agrobacterium tumefaciens Loci Needed for Virulence,” *Science*, vol. 232, no. 4753, pp. 983–985, May 1986, doi: 10.1126/science.3085219.

[128] L. S. Melchers, A. J. Regensburg-Tuïnk, R. A. Schilperoort, and P. J. Hooykaas, “Specificity of signal molecules in the activation of Agrobacterium virulence gene expression,” *Molecular Microbiology*, vol. 3, no. 7, pp. 969–977, Jul. 1989, doi: 10.1111/j.1365-2958.1989.tb00246.x.

[129] A. Brencic and S. C. Winans, “Detection of and Response to Signals Involved in Host-Microbe Interactions by Plant-Associated Bacteria,” *Microbiology and Molecular Biology Reviews*, vol. 69, no. 1, pp. 155–194, Mar. 2005, doi: 10.1128/mmbr.69.1.155-194.2005.

[130] G. A. Cangelosi, R. G. Ankenbauer, and E. W. Nester, “Sugars induce the Agrobacterium virulence genes through a periplasmic binding protein and a transmembrane signal protein.,” *Proceedings of the National Academy of Sciences*, vol. 87, no. 17, pp. 6708–6712, Sep. 1990, doi: 10.1073/pnas.87.17.6708.

[131] N. Shimoda *et al.*, “Control of expression of Agrobacterium vir genes by synergistic actions of phenolic signal molecules and monosaccharides.,” *Proceedings of the National Academy of Sciences*, vol. 87, no. 17, pp. 6684–6688, Sep. 1990, doi: 10.1073/pnas.87.17.6684.

[132] K. Lee, M. W. Dudley, K. M. Hess, D. G. Lynn, R. D. Joerger, and A. N. Binns, “Mechanism of activation of Agrobacterium virulence genes: identification of phenol-binding proteins.,” *Proceedings of the National Academy of Sciences*, vol. 89, no. 18, pp. 8666–8670, Sep. 1992, doi: 10.1073/pnas.89.18.8666.

[133] N. Shimoda, A. Toyoda-Yamamoto, S. Aoki, and Y. Machida, “Genetic evidence for an interaction between the VirA sensor protein and the ChvE sugar-binding protein of Agrobacterium.,” *Journal of Biological Chemistry*, vol. 268, no. 35, pp. 26552–26558, Dec. 1993, doi: 10.1016/s0021-9258(19)74348-8.

[134] A. D. Tomlinson and C. Fuqua, “Mechanisms and regulation of polar surface attachment in Agrobacterium tumefaciens,” *Current Opinion in Microbiology*, vol. 12, no. 6, pp. 708–714, Dec. 2009, doi: 10.1016/j.mib.2009.09.014.

[135] A. G. Matthysse, “Role of bacterial cellulose fibrils in Agrobacterium tumefaciens infection,” *Journal of Bacteriology*, vol. 154, no. 2, pp. 906–915, May 1983, doi: 10.1128/jb.154.2.906-915.1983.

[136] S. Backert, R. Fronzes, and G. Waksman, “VirB2 and VirB5 proteins: specialized adhesins in bacterial type-IV secretion systems?,” *Trends in Microbiology*, vol. 16, no. 9, pp. 409–413, Sep. 2008, doi: 10.1016/j.tim.2008.07.001.

[137] C. I. Kado, “The role of the T-pilus in horizontal gene transfer and tumorigenesis,” *Current Opinion in Microbiology*, vol. 3, no. 6, pp. 643–648, Dec. 2000, doi: 10.1016/s1369-5274(00)00154-5.

[138] C. Young and E. W. Nester, “Association of the virD2 protein with the 5’ end of T strands in Agrobacterium tumefaciens,” *Journal of Bacteriology*, vol. 170, no. 8, pp. 3367–3374, Aug. 1988, doi: 10.1128/jb.170.8.3367-3374.1988.

[139] C. Young and E. W. Nester, “Association of the virD2 protein with the 5’ end of T strands in Agrobacterium tumefaciens,” *Journal of Bacteriology*, vol. 170, no. 8, pp. 3367–3374, Aug. 1988, doi: 10.1128/jb.170.8.3367-3374.1988.

[140] A. Herrera-Estrella, M. Van Montagu, and K. Wang, “A bacterial peptide acting as a plant nuclear targeting signal: the amino-terminal portion of Agrobacterium VirD2 protein directs a beta-galactosidase fusion protein into tobacco nuclei.,” *Proceedings of the National Academy of Sciences*, vol. 87, no. 24, pp. 9534–9537, Dec. 1990, doi: 10.1073/pnas.87.24.9534.

[141] A. Ziemienowicz, T. Merkle, F. Schoumacher, B. Hohn, and L. Rossi, “Import of Agrobacterium T-DNA into Plant Nuclei: Two Distinct Functions of VirD2 and VirE2 Proteins,” *The Plant Cell*, vol. 13, no. 2, pp. 369–383, Feb. 2001, doi: 10.1105/tpc.13.2.369.

[142] V. Citovsky *et al.*, “Protein Interactions Involved in Nuclear Import of the Agrobacterium VirE2 Protein in Vivo and in Vitro,” *Journal of Biological Chemistry*, vol. 279, no. 28, pp. 29528–29533, Jul. 2004, doi: 10.1074/jbc.m403159200.

[143] T. Tzfira, M. Vaidya, and V. Citovsky, “VIP1, an Arabidopsis protein that interacts with Agrobacterium VirE2, is involved in VirE2 nuclear import and Agrobacterium infectivity,” *The EMBO Journal*, vol. 20, no. 13, pp. 3596–3607, Jul. 2001, doi: 10.1093/emboj/20.13.3596.

[144] H.-H. Hwang, M. Yu, and E.-M. Lai, “Agrobacterium-Mediated Plant Transformation: Biology and Applications,” *The Arabidopsis Book*, vol. 15, p. e0186, Jan. 2017, doi: 10.1199/tab.0186.

[145] T. Tzfira and V. Citovsky, *Agrobacterium: From Biology to Biotechnology*. 2008. doi: 10.1007/978-0-387-72290-0.

[146] D. Valvekens, M. Van Montagu, and M. Van Lijsebettens, “Agrobacterium tumefaciens -mediated transformation of Arabidopsis thaliana root explants by using kanamycin selection,” *Proceedings of the National Academy of Sciences*, vol. 85, no. 15, pp. 5536–5540, Aug. 1988, doi: 10.1073/pnas.85.15.5536.

[147] J. R. Kikkert, J. R. Vidal, and B. I. Reisch, “Stable Transformation of Plant Cells by Particle Bombardment/Biolistics,” *Humana Press eBooks*, pp. 061–078, Aug. 2004, doi: 10.1385/1-59259-827-7:061.

[148] C. A. Newell, “Plant Transformation Technology: Developments and Applications,” *Molecular Biotechnology*, vol. 16, no. 1, pp. 53–66, Jan. 2000, doi: 10.1385/mb:16:1:53.

[149] D. Verma, N. P. Samson, V. Koya, and H. Daniell, “A protocol for expression of foreign genes in chloroplasts,” *Nature Protocols*, vol. 3, no. 4, pp. 739–758, Apr. 2008, doi: 10.1038/nprot.2007.522.

[150] H. Daniell, C.-S. Lin, M. Yu, and W.-J. Chang, “Chloroplast genomes: diversity, evolution, and applications in genetic engineering,” *Genome Biology*, vol. 17, no. 1, Jun. 2016, doi: 10.1186/s13059-016-1004-2.

[151] T. Yamamoto *et al.*, “Improvement of the transient expression system for production of recombinant proteins in plants,” *Scientific Reports*, vol. 8, no. 1, Mar. 2018, doi: 10.1038/s41598-018-23024-y.

[152] A. Sánchez-Álvarez, N. Ruíz-López, A. J. Moreno-Pérez, E. Martínez-Force, R. Garcés, and J. J. Salas, “Agrobacterium-Mediated Transient Gene Expression in Developing Ricinus communis Seeds: A First Step in Making the Castor Oil Plant a Chemical Biofactory,” *Frontiers in Plant Science*, vol. 10, Oct. 2019, doi: 10.3389/fpls.2019.01410.

[153] S. Guan, X. Kang, J. Ge, R. Fei, S. Duan, and X. Sun, “An efficient Agrobacterium-mediated transient transformation system and its application in gene function elucidation in Paeonia lactiflora Pall,” *Frontiers in Plant Science*, vol. 13, Oct. 2022, doi: 10.3389/fpls.2022.999433.

[154] N. Scotti and E. P. Rybicki, “Virus-like particles produced in plants as potential vaccines,” *Expert Review of Vaccines*, vol. 12, no. 2, pp. 211–224, Feb. 2013, doi: 10.1586/erv.12.147.

[155] J. Maclean *et al.*, “Optimization of human papillomavirus type 16 (HPV-16) L1 expression in plants: comparison of the suitability of different HPV-16 L1 gene variants and different cell-compartment localization,” *Journal of General Virology*, vol. 88, no. 5, pp. 1460–1469, May 2007, doi: 10.1099/vir.0.82718-0.

[156] M. Zahin *et al.*, “Scalable Production of HPV16 L1 Protein and VLPs from Tobacco Leaves,” *PLoS ONE*, vol. 11, no. 8, p. e0160995, Aug. 2016, doi: 10.1371/journal.pone.0160995.

[157] M. Pyrski *et al.*, “Parenteral–Oral Immunization with Plant-Derived HBcAg as a Potential Therapeutic Vaccine against Chronic Hepatitis B,” *Vaccines*, vol. 7, no. 4, p. 211, Dec. 2019, doi: 10.3390/vaccines7040211.

[158] F. Sainsbury and G. P. Lomonossoff, “Extremely High-Level and Rapid Transient Protein Production in Plants without the Use of Viral Replication,” *PLANT PHYSIOLOGY*, vol. 148, no. 3, pp. 1212–1218, Sep. 2008, doi: 10.1104/pp.108.126284.

[159] P. Saxena, E. C. Thuenemann, F. Sainsbury, and G. P. Lomonossoff, “Virus-Derived Vectors for the Expression of Multiple Proteins in Plants,” *Methods in Molecular Biology*, pp. 39–54, Jan. 2016, doi: 10.1007/978-1-4939-3289-4_3.

[160] M. C. Cañizares, L. Liu, Y. Perrin, E. Tsakiris, and G. P. Lomonossoff, “A bipartite system for the constitutive and inducible expression of high levels of foreign proteins in plants,” *Plant Biotechnology Journal*, vol. 4, no. 2, pp. 183–193, Nov. 2005, doi: 10.1111/j.1467-7652.2005.00170.x.

[161] J. B. Rohll, C. L. Holness, G. P. Lomonossoff, and A. J. Maule, “3′-Terminal Nucleotide Sequences Important for the Accumulation of Cowpea Mosaic Virus M-RNA,” *Virology*, vol. 193, no. 2, pp. 672–679, Apr. 1993, doi: 10.1006/viro.1993.1175.

[162] L. Liu, J. Grainger, M. C. Cañizares, S. M. Angell, and G. P. Lomonossoff, “Cowpea mosaic virus RNA-1 acts as an amplicon whose effects can be counteracted by a RNA-2-encoded suppressor of silencing,” *Virology*, vol. 323, no. 1, pp. 37–48, May 2004, doi: 10.1016/j.virol.2004.02.013.

[163] “Replication of positive-strand RNA viruses in plants: contact points between plant and virus components.” https//ouci.dntb.gov.ua/en/works/4NAYMVY7/

[164] P. Rice, I. Longden, and A. Bleasby, “EMBOSS: The European Molecular Biology Open Software Suite,” *Trends in Genetics*, vol. 16, no. 6, pp. 276–277, Jun. 2000, doi: 10.1016/s0168-9525(00)02024-2.

[165] H. Spiegel *et al.*, “Application of a Scalable Plant Transient Gene Expression Platform for Malaria Vaccine Development,” *Frontiers in Plant Science*, vol. 6, Dec. 2015, doi: 10.3389/fpls.2015.01169.

[166] K. S. Corbett *et al.*, “SARS-CoV-2 mRNA vaccine design enabled by prototype pathogen preparedness,” *Nature*, vol. 586, no. 7830, pp. 567–571, Aug. 2020, doi: 10.1038/s41586-020-2622-0.

[167] M. Chen, L. Liu, Y. Chen, H. Wu, and S. Yu, “Expression of α-amylases, carbohydrate metabolism, and autophagy in cultured rice cells is coordinately regulated by sugar nutrient,” *The Plant Journal*, vol. 6, no. 5, pp. 625–636, Nov. 1994, doi: 10.1046/j.1365-313x.1994.6050625.x.

[168] J. A. Malik, A. H. Mulla, T. Farooqi, F. H. Pottoo, S. Anwar, and K. R. R. Rengasamy, “Targets and strategies for vaccine development against SARS-CoV-2,” *Biomedicine & Pharmacotherapy*, vol. 137, p. 111254, May 2021, doi: 10.1016/j.biopha.2021.111254.

[169] J. Jung, G. Zahmanova, I. Minkov, and G. P. Lomonossoff, “Plant-based expression and characterization of SARS-CoV-2 virus-like particles presenting a native spike

protein," *Plant Biotechnology Journal*, vol. 20, no. 7, pp. 1363–1372, Apr. 2022, doi: 10.1111/pbi.13813.

[170] A. Meyers *et al.*, "Expression of HIV-1 antigens in plants as potential subunit vaccines," *BMC Biotechnology*, vol. 8, no. 1, Jun. 2008, doi: 10.1186/1472-6750-8-53.

[171] R. J. R. Yanez *et al.*, "Expression optimization of a cell membrane-penetrating human papillomavirus type 16 therapeutic vaccine candidate in Nicotiana benthamiana," *PLoS ONE*, vol. 12, no. 8, p. e0183177, Aug. 2017, doi: 10.1371/journal.pone.0183177.

[172] M. T. Waheed, H. Ismail, J. Gottschamel, B. Mirza, and A. G. Lössl, "Plastids: The Green Frontiers for Vaccine Production," *Frontiers in Plant Science*, vol. 6, Nov. 2015, doi: 10.3389/fpls.2015.01005.

[173] L. Santi *et al.*, "An efficient plant viral expression system generating orally immunogenic Norwalk virus-like particles," *Vaccine*, vol. 26, no. 15, pp. 1846–1854, Mar. 2008, doi: 10.1016/j.vaccine.2008.01.053.

[174] S.-J. Song, H.-P. Diao, Y.-F. Guo, and I. Hwang, "Advances in Subcellular Accumulation Design for Recombinant Protein Production in Tobacco," *BioDesign Research*, Aug. 2024, doi: 10.34133/bdr.0047.

[175] F. F. P. G. Pêra *et al.*, "Engineering and expression of a human rotavirus candidate vaccine in Nicotiana benthamiana," *Virology Journal*, vol. 12, no. 1, Dec. 2015, doi: 10.1186/s12985-015-0436-8.

[176] J.-M. Claverie, "A Putative Role of de-Mono-ADP-Ribosylation of STAT1 by the SARS-CoV-2 Nsp3 Protein in the Cytokine Storm Syndrome of COVID-19," *Viruses*, vol. 12, no. 6, p. 646, Jun. 2020, doi: 10.3390/v12060646.